THE UNIVERSITY
of EDINBURGH

Mechanistic investigations into pro-survival and pro-death neuronal Ca^{2+} signalling pathways

By

Nóra M. Márkus BSc (Hons)

A thesis submitted for the degree of Doctor of Philosophy

at The University of Edinburgh

September 2016

College of Medicine and Veterinary Medicine

The University of Edinburgh

Supervisor: Prof. Giles Hardingham

2nd Supervisor: Prof. Matthew Nolan

Declaration

I declare that the majority of the work presented in this thesis is my own, except where otherwise clearly indicated in the text. I also declare that this thesis was composed by me, and has not been submitted for any other degree or professional qualification.

Nóra M. Márkus

Abstract

Ca^{2+} is an important second messenger which modulates a variety of signalling pathways in both excitable and non-excitable cells. In the CNS, Ca^{2+} plays an important role in neurons both physiologically and pathologically. Ca^{2+} influx following synaptic activity, is important in development, plasticity, redox balance, as well as in neuroprotection, largely through activation of pro-survival pathways downstream of synaptic NMDAR activation, including upregulation of antioxidant defences. However, excessive Ca^{2+} influx in neurons leads to neuronal damage and excitotoxicity, in which mitochondrial Ca^{2+} uptake through the mitochondrial Ca^{2+} uniporter (Mcu) resulting in mitochondrial dysfunction is a key player. Excitotoxicity occurs due to glutamate efflux from astrocytes following stroke, traumatic brain injury and in chronic neurodegenerative diseases, leading to excessive neuronal NMDAR activation and triggering of its downstream pro-death pathways. This thesis focuses on understanding the pro-survival and pro-death effects of signalling pathways activated by Ca^{2+} in neurons, as well as the potential effect of neuronal synaptic activity on influencing neuroprotective gene transcription in astrocytes.

I investigated the role of AMPK, a master regulator of metabolism, in NMDA excitotoxicity in cortical neurons as a potential downstream effector of Mcu-dependent excitotoxic death; and found the deletion of AMPKα1/2 to be neuroprotective against NMDA-mediated excitotoxicity, however I found AMPK activation to be independent of Mcu. I also investigated the expression pattern of Mcu and other mitochondrial calcium regulatory genes (MCRGs), and found MCRGs to be differentially expressed in different neural cells (primary neurons vs astrocytes), and neuronal subtypes (CA1 vs CA3 region of the hippocampus), suggesting differing dependence on the various MCRGs in mitochondrial Ca^{2+} handling in these cell types. A better functional understanding of these genes will allow for investigation of their importance in mitochondrial Ca^{2+} handling, including their potential role in excitotoxicity.

I next investigated the neuroprotective effects of synaptic activity induced Ca^{2+} influx, focusing on antioxidant target genes of Nrf2, a transcription factor and major regulator of antioxidant genes. I found that unlike astrocytes, neurons express very low levels of Nrf2. However, synaptic activity increased the expression of several Nrf2 target genes in neurons, independently of astrocytes and Nrf2. Additionally, I found no effect of synaptic activity on increasing Nrf2 protein levels, despite previous reports in literature of Nrf2 pathway activation following synaptic activity. Finally, using RNA-seq I identified a list of genes strongly upregulated by a known Nrf2 activator in astrocytes, and found no evidence that neuronal

activity triggers expression of these genes independently of neurons, providing further evidence that neuronal activity does not activate the Nrf2 pathway in astrocytes. This suggests that synaptic activity via pathways activated by Ca^{2+} signalling provides neurons with cell-autonomous antioxidant defences, independently of Nrf2; thus providing a distinct pathway for antioxidant defences in neurons from the Nrf2 pathway, which is activated in astrocytes providing neurons with non-cell autonomous antioxidant support.

These results give us further insight into the mechanisms that underlie synaptic and non-synaptic Ca^{2+} signalling pathways mediating neuronal survival and death, which could help in identifying therapeutic targets to combat excitotoxicity and oxidative stress in various neurological diseases.

Lay Summary

Stroke, traumatic brain injury and neurodegenerative diseases, such as Alzheimer's disease, involve the death of neurons, a type of brain cell. Neurons can take up excessive amounts of calcium due to their over activation in these diseases, leading to their death. This is partly due to too much calcium entering mitochondria, which are responsible for providing cells with energy, disrupting their function and leading to the death of neurons. I looked at the machinery responsible for the calcium content of mitochondria, which control the amount of calcium going in and out of mitochondria, in different brain cells. I also looked at the possible role of AMPK, a molecule responsible for promoting energy production in cells, in conveying cell death messages from mitochondria which are overloaded with calcium. Additionally, I looked at whether antioxidants produced after increasing normal brain activity were made by neurons or astrocytes, which are supporting brain cells. I found that mitochondrial calcium machinery varied in neurons and astrocytes, as well as in different types of neurons. I found that AMPK was important in the cell death of neurons after too much calcium uptake, but was not connected to cell death due to excessive calcium uptake by mitochondria. I found that although astrocytes are able to make antioxidants themselves with the help of Nrf2, the master regulator of antioxidants in the brain, antioxidants are also made by neurons themselves after increasing normal brain activity, although these are not made with the help of Nrf2. Thus, antioxidants are made in both neurons and astrocytes to prevent neuronal death, but by different mechanisms.

The results show the importance of these molecules in causing or preventing cell death following calcium uptake by neurons. AMPK encourages cell death following too much calcium uptake by neurons, whilst normal brain activity increases antioxidant production in neurons, providing them with protection against oxidative stress. Thus, stopping the effects of excessive calcium uptake into neurons by blocking AMPK activity or manipulating mitochondrial calcium machinery to reduce mitochondrial calcium uptake, as well as enhancing antioxidants production by increasing normal brain activity, would make good therapeutic targets for dugs which promote the survival of neurons in different brain diseases involving calcium overload, such as stroke and neurodegenerative diseases.

Table of Contents

List of Figures

Abbreviations

Aβ	Amyloid β peptide
AD	Alzheimer's disease
AICAR	5-Aminoimidazole-4-carboxamide ribonucleotide
ALS	Amyotrophic lateral sclerosis
AMPK	5' adenosine monophosphate-activated protein kinase
AP	Action potential
ARE	Antioxidant response element
ATP	Adenosine triphosphate
Bic/4-AP	Bicuculline/4-aminopyridine
CaMKKβ	Ca^{2+}/calmodulin dependent kinase kinase β
$CDDO^{MA}$	1[2-Cyano-3,12-dioxool-eana-1,9(11)-dien-28-oyl] methylamine
$CDDO^{(TF)EA}$	1[2-Cyano-3,12-dioxool-eana-1,9(11)-dien-28-oyl] (trifluoro)ethylamide
CREB	c-AMP response element binding protein
CNS	Central nervous system
CSF	Cerebrospinal fluid
DAPI	4',6-diamidino-2-phenylindole
DIV	Days in vitro
DMF	Dimethyl fumarate
EAAT	Excitatory amino acid transporter
EE	Environmental enrichment
Emre	Essential Mcu regulator
ETC	Electron transport chain
FOXO	Forkhead box subgroup O
Gclc	Glutamate cysteine ligase, catalytic subunit
GFAP	Glial fibrillary acidic protein

GSH	Glutathione
HD	Huntington's disease
Hmox1	Haem-oxygenase 1
IMM	Inner mitochondrial membrane
IMS	Mitochondrial intermembrane space
JNK	c-Jun N-terminal kinase
KD	Knock-down
Keap1	Kelch-like ECH-associated protein 1
KO	Knock-out
Letm1	Leucine Zipper and EF-hand containing transmembrane protein 1
LKB1	Liver kinase B1
MCAO	Middle cerebral artery occlusion
MCRGs	Mitochondrial calcium regulatory genes
Mcu	Mitochondrial calcium uniporter
Mcub	Mcu dominant negative beta subunit
Mcur1	Mcu regulator 1
Micu1/2/3	Mitochondrial calcium uptake 1/2/3
MK-801	5-Methyl-10,11-dihydro-5*H*-dibenzo[*a*,*d*]cyclohepten-5,10-imine
MPTP	1-methyl-4-phenyl-1,2,3,6-tetrahydropyridine
MS	Multiple sclerosis
NAD(P)H	Nicotinamide adenine dinucleotide (phosphate)
Nclx	Sodium/lithium/calcium exchanger
ND	Neurodegenerative
NMDA	N-methyl-D-aspartate
NMDAR	NMDA receptor
Nqo-1	NAD(P)H Quinone Dehydrogenase 1

nNOS	Neuronal nitric oxide synthase
Nrf2	Nuclear factor erythroid 2 like 2
OE	Overexpression
OMM	Outer mitochondrial membrane
OGD	Oxygen-glucose deprivation
PARP-1	Poly (ADP-ribose) polymerase 1
PD	Parkinson’s disease
Prx	Peroxiredoxin
ROS	Reactive oxygen species
RNS	Reactive nitrogen species
Ryr	Ryanodine receptor
Slc25a23	Solute Carrier Family 25 Member 23
SLF	Sulforaphane
SOD	Superoxide dismutase
Srxn1	Sulfiredoxin 1
tBHQ	tert-Butylhydroquinone
TBI	Traumatic brain injury
TMD	Transmembrane domain
Trpc3	Transient receptor potential channel 3
Trx	Thioredoxin
Txnip	Trx inhibitor protein
Ucp2/3	Uncoupling protein 2/3
VDAC	Voltage-dependent anion channel
VGCC	Voltage-gated calcium channel
xCT	Amino Acid Transport System Xc^-

Acknowledgments

First and foremost, I would like to thank my supervisor, Prof. Giles Hardingham, for all of his guidance and support throughout my PhD, without which the completion of this thesis would not have been possible. I would also like to thank the other members of my thesis committee, my second supervisor Prof. Matthew Nolan and my thesis chair, Prof. Mark Evans. Additionally, I would like to thank the University of Edinburgh and the Medical Research Council for funding me throughout my degree, making this PhD possible. Furthermore, I would like to thank Dr. Karen Bell and Dr. Jing Qiu for teaching me the initial techniques I required for the completion of my PhD, as well as the other members of the Hardingham lab throughout the years, Sean, Marc-André, Katie, Jamie, Philip, Paul, Allison, Zoeb, Nicola and Ruth, for all of their help and advice about science, creating a friendly work environment, and especially for putting up with my endless questions! And last, but not least, I would like to give a very special thank you to all of my close family and friends (whether you live in Edinburgh or on the other side of the world), for being there for me throughout the highs and lows of the last four years, I couldn't have done it without you.

Chapter 1: Introduction

Most neurons in the CNS are post-mitotic and cannot regenerate, thus it is essential for neurons to be highly adaptive to their environment to ensure their survival throughout the lifetime of the organism. Neurons have high metabolic activity and rely heavily on oxidative phosphorylation as their source of ATP, for which correct functioning of mitochondria is essential (Fernandez-Fernandez et al. 2012; Harris et al. 2012; Kann & Kovács 2007). Despite their high metabolic activity, neurons have low endogenous antioxidant defences making them vulnerable to oxidative stress (Fernandez-Fernandez et al. 2012).

Ca^{2+} is an important second messenger in the CNS, and neurons are dynamically regulated by increases in intracellular Ca^{2+} levels following their activation, which is important in development, plasticity, redox balance and neuroprotection (Hardingham 2009; Hardingham & Bading 2003; Tashiro et al. 2006; Paoletti et al. 2013). Neuronal activity places an increased demand on neuronal metabolism to produce ATP to restore ionic gradients through the activation of ATPases (Kann & Kovács 2007). Increased metabolism leads to increased ROS production, which needs to be eliminated to avoid mitochondrial dysfunction and cell death; thus it makes biological sense for neuronal activity-mediated Ca^{2+} uptake, largely mediated by NMDA receptors, to be essential in adapting neurons to their changing environment and protecting them from various intrinsic and extrinsic insults via the upregulation of neuroprotective pathways, including strengthening of endogenous antioxidant defences (Hardingham & Bading 2010; Papadia et al. 2008; Baxter et al. 2015). Astrocytes also play a role in neuroprotection, largely through their superior antioxidant defences compared to neurons, helping to reduce oxidative stress (Fernandez-Fernandez et al. 2012; Shih et al. 2003). Although physiological Ca^{2+} uptake is essential for neuronal survival, excessive amounts of Ca^{2+} uptake leads to neuronal damage and excitotoxicity (Hardingham 2009). Excitotoxicity occurs in response to excessive neuronal NMDAR activation leading to excessive Ca^{2+} uptake by neurons following glutamate efflux from astrocytes (Hardingham & Bading 2010). Ca^{2+} handling by mitochondria in neurons plays an essential role in both neuronal survival and death (Kann & Kovács 2007; Qiu et al. 2013).

Both oxidative stress and excitotoxicity have been implicated in acute and chronic neurodegenerative disorders (Parsons & Raymond 2014; Gan & Johnson 2014). Thus, understanding how neurons are dynamically regulated by Ca^{2+}, and which pathways and molecules are responsible for mediating cell death and survival is essential for development of novel therapeutic treatments.

This thesis aims to uncover the potential role of astrocytes in increased antioxidant gene transcription following neuronal activity, as well as to investigate a possible pathway downstream of mitochondrial dysfunction mediated cell death following excitotoxicity, and to uncover the neural specificity of genes involved in mitochondrial Ca^{2+} handling.

This introduction provides a summary of the current knowledge about oxidative stress and antioxidant pathways, including the role of transcription factor Nrf2 in upregulating antioxidant gene transcription, as well as the pro-survival and pro-death effect of NMDAR-mediated Ca^{2+} uptake in neurons, and the importance and function of the genes involved in mitochondrial Ca^{2+} handling in neurons.

1.1. Oxidative stress and antioxidant pathways

1.1.1. Oxidative stress and reactive oxygen species

Reactive oxygen species (ROS) are oxygen radicals containing unpaired electrons such as superoxide (O_2^-), or non-radical oxygen species such as hydrogen peroxide (H_2O_2), which can oxidise molecules in the cell (Halliwell 2006). Reactive nitrogen species (RNS) are ROS containing nitrogen, such as nitric oxide (NO).

Neurons have a high metabolism and thus consume large amounts of oxygen for ATP production to supply energy through aerobic respiration. Most oxygen is reduced to water by the mitochondrial cytochrome oxidase, but some oxygen can form ROS, such as superoxide, as the by-product of the mitochondrial electron transport chain (ETC) complexes I and III, or NADPH oxidase in the cytoplasm (Halliwell 2006; Kann & Kovács 2007). ROS have several biological functions in neurons, such as for cell signalling and fighting inflammation, but excess ROS need to be detoxified by antioxidant mechanisms in the cell (Halliwell 2006). If this does not occur, or the amount of ROS overwhelms the antioxidant capacity of the cell, oxidative stress occurs leading to ROS-mediated posttranslational modifications of various molecules, such as DNA, proteins and lipids, leading to cellular damage and eventually cell death (Popa-Wagner et al. 2013; Halliwell 2006). Thus, dynamic regulation of antioxidant defences to maintain redox balance is essential for neuronal survival.

The “free radical theory of ageing” states that oxidative damage caused by ROS in cells can accumulate over time contributing to the aging process, increasing neuronal susceptibility to insults and disease in the process (Patenaude et al. 2005). Indeed, excessive amounts of ROS and oxidative stress have been implicated in several different neurological disorders, not just acute conditions such as stroke, but also chronic neurodegenerative (ND) disorders, such as Alzheimer’s disease (AD), Parkinson’s disease (PD) and amyotrophic lateral sclerosis (ALS), which usually appear later in life and exhibit signs of oxidative stress-induced damage (Halliwell 2006; Patenaude et al. 2005). Furthermore, oxidative stress can cause cell damage and promote excitotoxicity. The importance of oxidative stress in ageing and various diseases makes antioxidant pathways attractive candidates for therapeutic targeting.

Preventing oxidative stress and subsequent cell death is crucial in neurons, due to their post-mitotic nature and thus the lack of neurogenesis in most brain regions following development, leading neurons to require protection for the lifetime of the organism.

1.1.2. Antioxidant pathways in neural cells

Neurons have high metabolic activity, especially during physiological neuronal activity, but have low antioxidant defences leaving them vulnerable to oxidative stress (Fernandez-Fernandez et al. 2012; Harris et al. 2012; Kann & Kovács 2007). Neurons have low levels of catalase, which reduces H_2O_2 to H_2O and O_2 (Bell et al. 2015; Fernandez-Fernandez et al. 2012; Shih et al. 2003), and much lower levels of glutathione than astrocytes (Dringen et al. 1999). In addition to their own antioxidant defences, neurons receive non cell-autonomous antioxidant support from neighbouring astrocytes through the Nrf2 pathway, which is further discussed in the next section.

Superoxide dismutases (SODs) are responsible for the elimination of superoxide by forming H_2O_2 and O_2 from two O_2^- (Findlay et al. 2005; Patenaude et al. 2005). H_2O_2 can be further converted to the hydroxyl radical ($OH^·$) through the Fenton reaction (Aoyama et al. 2008). Furthermore, excess superoxide can react with NO to form peroxynitrite ($ONOO^-$), which is also toxic for cells (Halliwell 2006).

H_2O_2 and other ROS can be eliminated by a number of other antioxidants in neurons and astrocytes, such as by the thioredoxin-peroxiredoxin system, glutathione catalysed by glutathione peroxidase and ascorbate, which are some of the major antioxidant systems in the brain described further below, along with SODs.

1.1.2.1. Superoxide dismutases

SODs are ubiquitously expressed enzymes with metals in their active site which can dismutate superoxide into O_2 and H_2O_2 (Sheng et al. 2014).

There are three different types of human SOD: SOD1 is a CuZnSOD mainly found in the cytosol with some SOD1 in the mitochondrial intermembrane space, whilst SOD2 is a MnSOD localised to the mitochondrial matrix, and SOD3 is found extracellularly and is also bound to Cu and Zn (Aoyama & Nakaki 2015; Fernandez-Fernandez et al. 2012; Sheng et al. 2014). SOD1 is a homodimer, whilst SOD2 and 3 have a tetrameric structure (Sheng et al. 2014; Kaur et al. 2016).

The importance of SOD2 is demonstrated by its KO leading to perinatal death in mice (Li et al. 1995). SOD2 is thought to be a tumour suppressor, and indeed its epigenetic silencing has been observed in some forms of cancer (Archer 2016).

SOD1 KO on the other hand is not lethal, but does lead to increased susceptibility of motor neurons to cell death following injury (Reaume et al. 1996), and has been shown to slightly

decrease the lifespan of mice due to increased chances of developing some diseases (Edrey & Salmon 2014; Sheng et al. 2014).

SODs are especially important in neurons, where superoxide is one of the major ROS produced. Dismutation of superoxide by SOD is essential in preventing peroxynitrite formation by superoxide and NO, which causes oxidative damage to cells. Moreover, peroxynitrite can nitrate SOD2, inhibiting its function (Yamakura et al. 1998). Nitrated SOD2 levels are increased in some patients with neurodegenerative diseases, such as amyotrophic lateral sclerosis (ALS) (Aoyama et al. 2000; Yamakura et al. 1998).

Various mutations in SOD1 have been identified which cause familial forms of ALS, a lethal neurodegenerative disease involving motor neuron degeneration (Rosen et al. 1993; Sheng et al. 2014; Kaur et al. 2016). The mechanism by which SOD1 mutation causes ALS has been debated. A mouse model overexpressing a human SOD1 mutant ($SOD1^{G93A}$) showed impairment in anterograde axonal transport of mitochondria, leading to a reduction of mitochondria in axons, thought to be a consequence of increased levels of ROS (De vos et al. 2007). Furthermore, SOD1 mutations are also linked to increases in mitochondrial dysfunction (Kaur et al. 2016). Moreover, SOD1 mRNA is thought to be stabilised in neurons, a function which seems to be lost due to SOD1 mutations linked to ALS, decreasing the half-life of the protein (Ge et al. 2006). Most SOD1 mutations are thought to make the protein more unstable, promoting SOD1 aggregates which can be found in intracellular inclusions (Kaur et al. 2016). Additionally, mutant SOD1 has been thought to be able to act in a prion-like manner, triggering the misfolding of mutant and WT SOD1 (Bunton-Stasyshyn et al. 2014). Although, inclusions with WT SOD1 have also been found in sporadic ALS cases, suggesting that SOD1 may be generally involved in all types of ALS (Bunton-Stasyshyn et al. 2014). Moreover, Graffmo *et al.* showed that overexpression of human WT SOD1 in mice, similar to levels of expression in $SOD1^{G93A}$ mice, led to an ALS-like phenotype including cell death and development of SOD1 aggregates (Graffmo et al. 2013).

SOD1 mutations have also been found to affect glia, such as astrocytes and microglia, which are activated following neuronal damage and release toxic factors (and potentially mutant SOD1), increasing inflammation and further damaging neurons (Boillée et al. 2006; Bunton-Stasyshyn et al. 2014).

1.1.2.2. The thioredoxin-peroxiredoxin pathway

The thioredoxin-peroxiredoxin (Trx-Prx) system reduces peroxides using NADPH in neurons and astrocytes, and is thus an important antioxidant defence system in neural cells.

There are six different types of peroxiredoxins, which are grouped into typical or atypical 2-Cys, or 1-Cys Prxs (Findlay et al. 2005; Halliwell 2006). The most common types of Prxs in the CNS are the typical 2-Cys Prxs which consist of Prxs I-IV, with Prx III being mitochondrial, and contain both a catalytic and resolving cysteine (Papadia et al. 2008). Some Prxs have cell-type specific expression patterns, for example Prx I is astrocytic, whilst Prx II is neuronal (Patenaude et al. 2005).

Prxs reduce H_2O_2 to H_2O using their cysteine thiol group (-SH), which gets oxidised to -SOH (Figure 1.1; Halliwell 2006). In 2-Cys Prxs the -SOH group reacts with the resolving cysteine on another Prx and they form a disulphide bridge releasing H_2O in the process, which can be reduced back to Prx-SH by Trx, an antioxidant enzyme which can reduce disulphide bonds such as those between cysteines of Prxs, resulting in the oxidation of its catalytic cysteines (Patenaude et al. 2005). Both cytoplasmic Trx1 and mitochondrial Trx2 are expressed in the brain, both in neurons and astrocytes (Patenaude et al. 2005). The oxidised form of Trx is reduced using NADPH as an electron donor, catalysed by Trx reductase (Bell & Hardingham 2011a; Patenaude et al. 2005). Trx can be inhibited by thioredoxin inhibitor protein (Txnip), which is induced following NMDAR blockade (Papadia et al. 2008). Trx has various other biological functions, such as inhibiting apoptosis through inhibition of apoptosis signal-regulating kinase I (ASK1) (Patenaude et al. 2005).

Prx can be oxidised further to form Prx-SO_2H or -SO_3H following insults such as oxidative stress, H_2O_2 exposure, middle cerebral artery occlusion (MCAO) mimicking stroke, bath application of glutamate or NMDAR blockade (Papadia et al. 2008; Léveillé et al. 2009; Bell & Hardingham 2011a). Hyperoxidised Prxs cannot be reduced using the resolving cysteine of Prx, but instead are reduced back to Prx-SH catalysed by sulfiredoxin 1 (Srxn1) or sestrin 2 (Sesn2) in an ATP-dependent process, preventing Prx inactivation and its eventual degradation (Soriano et al. 2009; Findlay et al. 2005; Bell & Hardingham 2011a). Although the role of Sesn2 in this process has been debated (Bell & Hardingham 2011a). However, the overexpression of Srxn1 and Sesn2 in primary neuronal culture is protective against H_2O_2-mediated cell death (Papadia et al. 2008). In addition to reducing cytosolic Prxs, Srxn1 can translocate to the mitochondria upon oxidative stress and reduce hyperoxidised Prx III, thus preventing mitochondrial depolarisation (Noh et al. 2009; Léveillé et al. 2009).

Since the Trx-Prx system is active in both neurons and astrocytes, it is likely to play an important antioxidant role in neurodegenerative disorders and stroke, which involve oxidative damage. Prxs have been shown to be neuroprotective following H_2O_2 and excitotoxic insults to neurons (Bell & Hardingham 2011a). Additionally, Trx1 has been shown to be

neuroprotective in models of stroke (Patenaude et al. 2005). Mitochondrial Prx III has also been demonstrated to provide protection following an ischaemic or excitotoxic insult, suggesting a role for it in the clearance of accumulated ROS (Bell & Hardingham 2011a). The Trx-Prx system may be especially important in neurons, due to their low expression of other H_2O_2 detoxifying antioxidants such as GSH and catalase. Neuronal Prx II decreases with age, whilst Txnip is upregulated, causing greater inhibition of Trx, and there is an increase in hyperoxidised Prxs which may increase neuronal susceptibility to oxidative stress in disease (Patenaude et al. 2005; Papadia et al. 2008). In line with this, Prx II has been shown to be important in preventing mitochondrial dysfunction in aged mice (Bell & Hardingham 2011a). Additionally, Prxs undergo inactivating modifications in AD as well as PD, whilst Prx OE was shown to be protective against MPTP-induced PD-like symptoms (Bell & Hardingham 2011a).

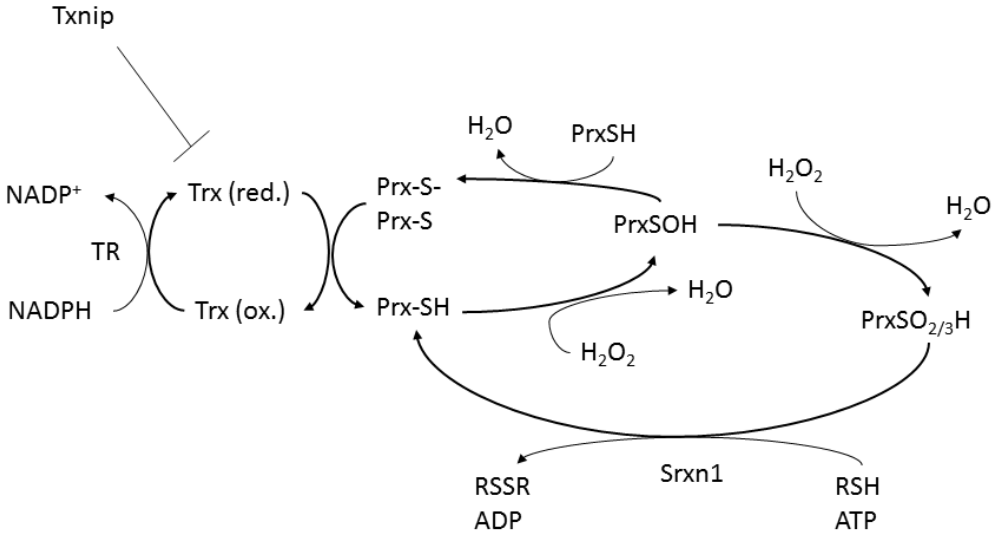

Figure 1.1. The Trx-Prx system. Diagram showing the reduction of H_2O_2 to H_2O by 2 Cys Prxs, the reduction of oxidised Prxs by Trx, and the reduction of hyperoxidised Prxs by Srxn1. Prx – peroxiredoxin, Srxn1 – sulfiredoxin 1, Trx – thioredoxin, TR – Trx reductase, Txnip – thioredoxin inhibitory protein

1.1.2.3. Glutathione

Glutathione (GSH) is a tripeptide thiol, and is one of the major antioxidants in the brain. GSH reacts non-enzymatically with free radicals to eliminate them, is a co-factor for the reduction of peroxides, and can conjugate with proteins to protect them from oxidative damage by hyperoxidising their thiol groups termed glutathionylation (Bridges et al. 2012; Findlay et al. 2005; Aoyama et al. 2008). Srxn1 has been suggested to catalyse the deglutathionylation of proteins (Findlay et al. 2005).

Glutathione peroxidase catalyses the reduction of H_2O_2 to H_2O using GSH as a co-factor, oxidising it to GSH disulphide (GSSG), which is reduced back to GSH catalysed by glutathione reductase using NADPH (Figure 1.2; Halliwell 2006; Dringen et al. 2015). GSH can be conjugated to xenobiotics using GSH S-transferase (GST), the product of which is then exported to the extracellular space, to help detoxify xenobiotics in the cell (Dringen et al. 2015). Furthermore, GSH can modulate NMDAR function, and possibly functions as a neurotransmitter itself (Janáky et al. 1999). GSH is present at millimolar concentrations intracellularly and the GSH:GSSG ratio can be used as a redox sensor (Findlay et al. 2005). Whilst most GSH is found in the cytoplasm, some GSH is located in mitochondria and other cell compartments (Vargas & Johnson 2009; Dringen et al. 2015).

GSH is synthesised from cysteine which binds to glutamate, catalysed by glutamate cysteine ligase (Gcl) (made of a modulatory (Gclm) and catalytic subunit (Gclc)), γGluCys is then attached to glycine catalysed by GSH synthase (GS) to form GSH; with all reaction steps requiring ATP (Figure 1.2; Aoyama et al. 2008; Vargas & Johnson 2009). Once synthesised, GSH inhibits Gcl activity to stop further γGluCys synthesis (Aoyama et al. 2008).

GSH levels are higher in astrocytes than neurons, thus astrocytes release GSH to provide neurons with the necessary precursors for GSH synthesis, and help detoxify the extracellular space of ROS (Figure 1.2; Halliwell 2006; Vargas & Johnson 2009). Indeed, culturing rat primary cortical neurons with astrocytes increases neurons' GSH content, whilst culturing them with astrocytes lacking GSH has no effect on neuronal GSH content, leaving neurons susceptible to damage of the ETC by NO (Gegg et al. 2005). Astrocytes release GSH through the multidrug resistance-associated protein 1 (MRP1) into the extracellular space, where it is broken down to Cys-Gly by gamma-glutamate-transpeptidase (gGT) and cysteine and glycine by aminopeptidase-N, thus supplying neurons with a source of cysteine, which is rate-limiting for GSH synthesis (Dringen et al. 1999; Shih et al. 2003; Bridges et al. 2012). Astrocytes also convert glutamate to glutamine which is transported to neurons for converting back to glutamate for GSH synthesis (Robert et al. 2014). Cysteine is often taken up by astrocytes in its oxidised dimer form, cystine, through system Xc^- (xCT), a cystine/glutamate antiporter (Bridges et al. 2012). Cystine can be taken up by developing cortical neurons through xCT, but cysteine is taken up by more mature neurons instead through other transporters such as the excitatory amino acid transporter 3 (EAAT3, aka EAAC1) (Bridges et al. 2012; Robert et al. 2014; Aoyama & Nakaki 2015). Excessive activation of xCT can cause glutamate overspill extracellularly activating extrasynaptic NMDARs leading to excitotoxicity, and thus xCT has been implicated in several neurological conditions such as epilepsy and neurodegenerative

diseases (Massie et al. 2015; Thorn et al. 2015; Lewerenz et al. 2014). Interestingly, both xCT and EAAT3 can be upregulated by the Nrf2 pathway (Lewerenz et al. 2014; Escartin et al. 2011).

Since GSH is essential for maintaining cellular redox balance as well as eliminating xenobiotics, it is not surprising that GSH and genes involved in its use, synthesis and recycling have been implicated in a number of neurological disorders involving oxidative stress. GSH is thought to decrease with age, a decline which is more pronounced in neurodegenerative diseases such as AD and PD (Aoyama et al. 2008). Thus, pharmacologically increasing GSH, or delivering its precursors to the brain could potentially have therapeutic effects in some ND diseases.

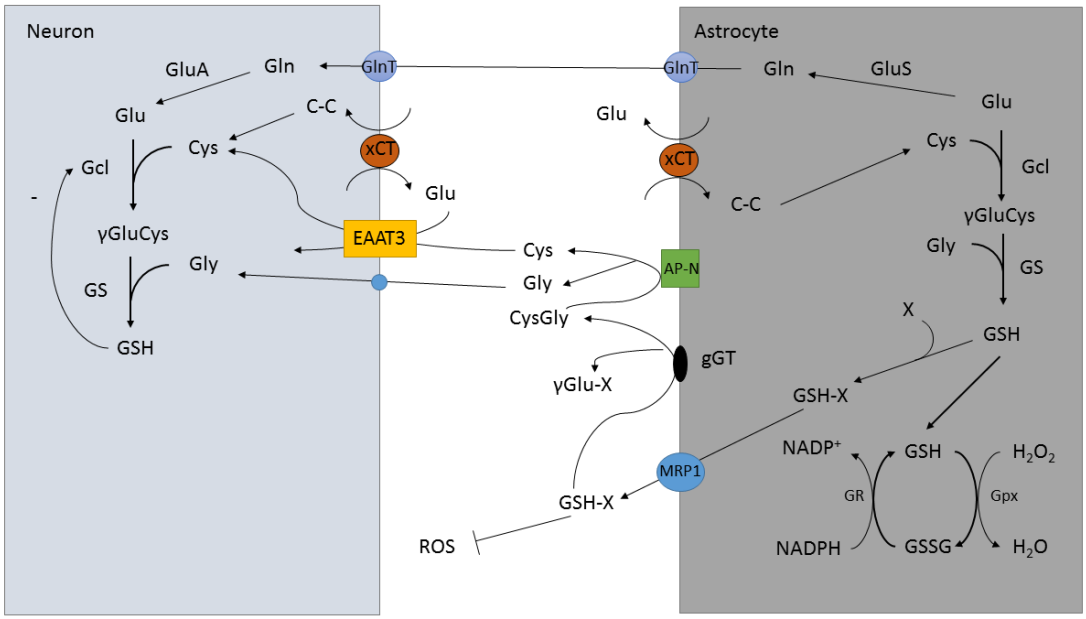

Figure 1.2. Glutathione synthesis, use and recycling in neurons and astrocytes. GSH is synthesised in astrocytes and is exported to the extracellular space through MRP1. Here, it is broken down to γGlu and CysGly, which is further broken down into Cys and Gly by AP-N. Neurons can take up GSH precursors Cys and Gly, as well as Gln (which is subsequently converted to Glu) to synthesise their own GSH. This is crucial since neurons have lower levels of GSH and Cys, which is the rate-limiting factor in GSH synthesis. Once synthesised, GSH can be used as a co-factor for Gpx to reduce H_2O_2 in neurons, decreasing oxidative stress. AP-N – aminopeptidase N, EAAT3 – excitatory amino acid transporter 3, Cys – cysteine, C-C – cystine, Glu – glutamate, Gln – glutamine, Gly – glycine, GPx – glutathione peroxidase, GR – glutathione reductase, Gcl – glutamyl cysteine ligase, GS – glutathione synthase, GSH – glutathione, GSSG – glutathione disulphide, GluS – glutamine synthase, GluA – glutaminase, GlnT – glutamine transporter, gGT – gamma-glutamyltransferase, xCT – system Xc^-, X – xenobiotics which can conjugate to GSH

1.1.2.4. Ascorbate

The brain contains high levels of the antioxidant ascorbate, with higher levels in neurons than astrocytes, where it exerts its neuroprotective effects through its ability to detoxify ROS acting as an electron donor (Halliwell 2006). Ascorbate is the anionic form of ascorbic acid (vitamin C) acquired through diet, arriving to the brain via cerebrospinal fluid (CSF) (Rice 2000). Ascorbate is taken up into neurons through the Na^+-dependent vitamin C transporter 2 (SVCT2) (Qiu et al. 2007). During elimination of ROS, ascorbate is oxidised to dehydroascorbate, which can be transported into astrocytes via glutamate transporters (GLUTs), which is also thought to be a possible route of entry for dehydroascorbate through the blood-brain barrier (Figueroa-Méndez & Rivas-Arancibia 2015). The efflux mechanism of ascorbate has been debated, but is thought to possibly occur through the activation of volume sensitive anion channels (VSACs) (Figueroa-Méndez & Rivas-Arancibia 2015). Dehydroascorbate and other oxidised forms of ascorbate can be reduced back to ascorbate by thiol-containing molecules such as GSH and Trx inside neurons and astrocytes, as well as by ascorbyl-free radical reductase (Rice 2000; Figueroa-Méndez & Rivas-Arancibia 2015).

Additionally, ascorbate can act as an enzyme co-factor, for example in the synthesis of noradrenaline and dopamine, and as a neuromodulator, inhibiting the binding of glutamate to NMDA receptors (Majewska et al. 1990; Rice 2000). Ascorbate has also been found to be important in neuronal maturation and myelination of axons (Rice 2000; Figueroa-Méndez & Rivas-Arancibia 2015; Qiu et al. 2007).

Ascorbate is important in neuronal survival following excitotoxicity, which is not surprising given its antioxidant effects, such as eliminating superoxide produced during an excitotoxic insult, and its ability to modulate NMDAR activity (Rice 2000; Figueroa-Méndez & Rivas-Arancibia 2015). Primary hippocampal culture from SVCT2 KO mice at DIV14 caused an increase in cell death in response to excitotoxic doses of NMDA, as well as high doses of H_2O_2 (Qiu et al. 2007). The importance of ascorbate was also demonstrated in human dopaminergic neurons against oxidative stress during glutamate excitotoxicity by Ballaz *et al*., showing increased cell survival against glutamate addition in the presence of ascorbate compared to its absence (Ballaz et al. 2013).

1.2. Nrf2

1.2.1. The Nrf2 pathway and its regulation

Nuclear factor erythroid 2 like 2 (Nrf2) is a transcription factor belonging to the Cap 'n' Collar basic leucine zipper family, which controls the transcription of several antioxidant and phase II detoxification genes in response to oxidative stress, providing antioxidant defence in various organs, from the kidney to the liver and the brain (Lee et al. 2005).

Nrf2 is basally bound to the cysteines of Kelch-like ECH-associated protein 1 (Keap1) in the cytoplasm through one of its 6 Neh domains, Neh3 at its N-terminus, and is ubiquitylated and targeted for 26S proteasomal degradation, with a half-life of 20 minutes; thus basal levels of Nrf2 activity are low (Loboda et al. 2016; Nguyen et al. 2004; McMahon et al. 2003). Nrf2 is well conserved throughout the animal kingdom, and its homologues are found in zebrafish, nematodes and *Drosophila*, amongst other organisms (Loboda et al. 2016). Oxidative stress, small molecule activators of Nrf2 or microRNAs alter the cysteine residues on Keap1 binding to Nrf2, thus dissociating Nrf2 from Keap1 and promoting its translocation to the nucleus using its nuclear localisation signal, where together with the help of small Maf proteins binding to its Neh1 domain, it binds to the antioxidant response element (ARE), initiating the transcription of phase II detoxification and antioxidant genes which contain the ARE in their promoter region (Figure 1.3; Loboda et al. 2016; Itoh et al. 1997; Jain et al. 2005).

Some protein kinases, such as PKC are known to phosphorylate Nrf2, initiating its dissociation from Keap1 (Vargas & Johnson 2009; Nguyen et al. 2004). Anchoring of Nrf2 in the cytosol by Keap1 is necessary, since too much Nrf2 activation can lead to reductive stress; supported by Keap1 KO being lethal (Wakabayashi et al. 2003). Whilst, glycogen synthase kinase 3β (GSK3β) has been shown to be able to phosphorylate Nrf2 and target it for degradation, independently of Keap-1 (Rada et al. 2011).

Nrf2 controls a battery of antioxidant genes which contain ARE in their promoter regions, such as catalase, genes involved in glutathione use, synthesis and recycling, such as Gclc, as well as components of the Trx-Prx system, such as Srxn1 (Singh et al. 2009; Soriano et al. 2009). Nrf2 also activates haem-oxygenase 1 (Hmox1) which breaks down haem into carbon monoxide, iron and biliverdin, which is later converted to bilirubin by biliverdin reductase (Vargas & Johnson 2009; Loboda et al. 2016). The products of haem cleavage not only protect against oxidative stress, but also possess anti-inflammatory and anti-apoptotic properties (Loboda et al. 2016). Hmox1 increases iron levels which can be damaging to cells, but it also increases ferritin synthesis which eliminates iron to stop its involvement in the Fenton reaction (Loboda et al. 2016). Moreover, Hmox1 KO is known to be embryonically lethal (Loboda et

al. 2016). SOD1 is also an Nrf2 target gene (Lacher et al. 2015). Nrf2 also activates a battery of other genes, such as genes involved in glucose metabolism (Lacher et al. 2015).

Nrf2 has also been suggested to autoregulate its own transcription, since AREs can be found in its promoter region (Kensler et al. 2007). Although AREs are also thought to be found in the promoter region of Keap1, suggesting that Nrf2 may also negatively regulate itself (Jiang et al. 2016).

Nrf2 activators such as tert-butylhydroquinone (tBHQ), a phenolic antioxidant, and sulforaphane (SLF) do not affect Nrf2 mRNA levels, instead they stabilise Nrf2 by its phosphorylation or target Keap1's cysteines to promote Nrf2 release, prolonging its half-life and allowing its nuclear translocation and binding to the ARE (Nguyen et al. 2004; Li et al. 2005; Kraft et al. 2004; Shih et al. 2005; Kensler et al. 2013; McMahon et al. 2003). A proteasomal inhibitor, MG-132, is often used experimentally to cause Nrf2 accumulation (Nguyen et al. 2004), but is not Nrf2 specific and does not have physiological relevance.

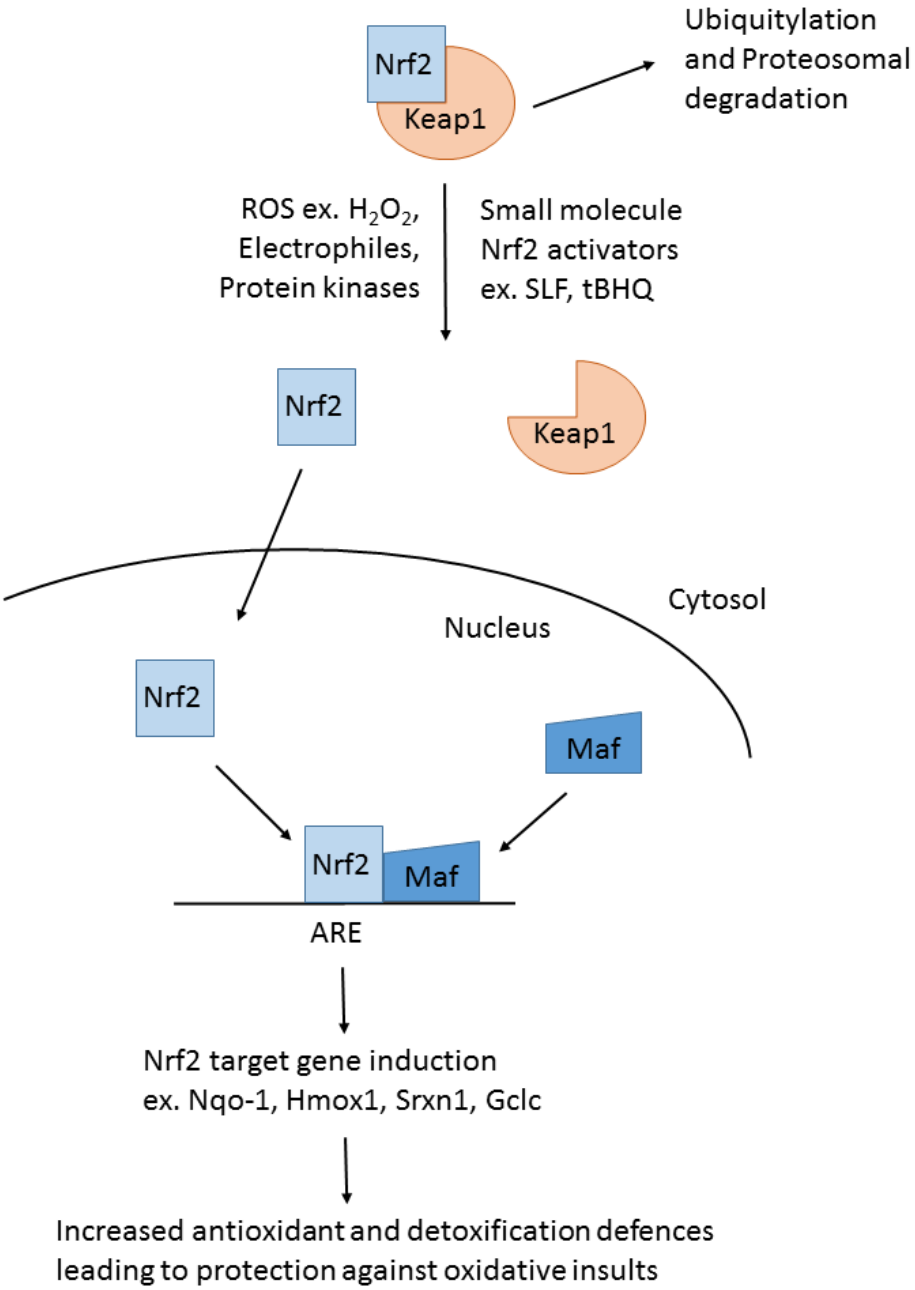

Figure 1.3. The Nrf2-ARE pathway. Nrf2 is basally bound to Keap1, but when it gets activated by oxidative stress, small molecule activators or other activators of Nrf2, it translocates to the nucleus and binds to the ARE to initiate transcription of antioxidant genes. The consensus sequence for the ARE is: 5'-puGTGACnnnGC-3', where pu is a purine and n is any nucleotide (Rushmore et al. 1991). ARE – antioxidant response element, Keap 1 – kelch-like ECH-associated protein, Maf – small Maf proteins, Nrf2 – nuclear factor erythroid 2 like 2

1.2.2. Nrf2 function in the brain and its potential as a therapeutic target in neurological diseases

1.2.2.1. The expression of Nrf2 in neural cells

Activation of the Nrf2 pathway is well documented in astrocytes (Vargas & Johnson 2009). In neurons on the other hand there have been conflicting accounts, with reports of the Nrf2 pathway being active primarily in astrocytes over neurons in mixed cultures by some (Kraft et al. 2004; Bell, Al-Mubarak, et al. 2011; Shih et al. 2003; Jimenez-Blasco et al. 2015), and the Nrf2 pathway being active in neurons themselves by others (Satoh et al. 2006; Yin et al. 2010; Zhang et al. 2009a). Many of the studies claiming that Nrf2 is activated in neurons carried out their experiments in mixed neuronal cultures containing astrocytes. The results in Ch.5 of this thesis demonstrate that Nrf2 is present at very low levels in neurons, and that Nrf2 levels observed in mixed culture are primarily due to the presence of astrocytes. Furthermore, our group demonstrated that low levels of Nrf2 in neurons are due to epigenetic repression of Nrf2 early in development, silencing the Nrf2 pathway in neurons (Bell et al. 2015).

Nrf2 has also been shown to be expressed in other neural cells. For instance, Nrf2 activators SLF and D3T have been shown to induce the transcription of various Nrf2 target genes in microglia (Konwinski et al. 2004). Furthermore, Nrf2 activation by a number of its activators has been shown to be protective in microglia (Jiang et al. 2016).

1.2.2.2. The role of Nrf2 in diseases involving oxidative stress

Since Nrf2 is activated by oxidative stress and regulates the transcription of antioxidant genes, it's involvement in neurological diseases in which oxidative stress plays a role, such as stroke and neurodegenerative diseases, is not surprising.

Nrf2 pathway activity is known to decrease during ageing, with lower levels of Nrf2 and its target genes, which may be due to the increase of Keap1 levels with age, leaving neurons vulnerable to oxidative stress (Loboda et al. 2016). Naked mole rats, which are known to live long, have higher levels of Nrf2 target genes and lower Keap1 levels compared to other rodents species, showing the importance of Nrf2 in longevity (Lewis et al. 2015). Although, Nrf2 target genes as well as Nrf2 have been found to be overexpressed in several neurological disorders, but this may be a compensatory mechanism following increased oxidative stress in these disorders.

Nrf2 activation in astrocytes provides neuroprotection, both *in vitro* and *in vivo*, mainly through the upregulation of GSH in astrocytes, providing the necessary precursors for neurons to synthesise their own GSH (Shih et al. 2003).

1.2.2.3. Nrf2 activation in neurodegenerative diseases is neuroprotective

Misfolded proteins and inclusions formed by them are characteristic pathological features in many chronic neurodegenerative diseases, such as α-synuclein forming intracellular Lewy bodies in Parkinson's disease (PD), tau forming intracellular neurofibrillary tangles and amyloid-β peptide (Aβ) aggregating into extracellular senile plaques in Alzheimer's disease (AD), mutant huntingtin causing intracellular inclusions in Huntington's disease (HD) or mutated SOD1 or TDP-43 forming inclusions in amyotrophic lateral sclerosis (ALS) (Gan & Johnson 2014). Mitochondrial dysfunction and oxidative stress are also characteristic signs in these diseases. Oxidative damage to many of these proteins is thought to promote their eventual misfolding and aggregation into protein inclusions, the formation of which induces further oxidative stress and toxicity in neurons. Thus, it is not surprising that Nrf2 pathway activation has been found to have a neuroprotective effect in several chronic neurodegenerative conditions.

Nrf2 overexpression (OE) has been found to have neuroprotective effects in animal models of ND diseases, such as AD, ALS and PD. For instance, Nrf2 OE was shown to correct the movement impairment caused by α-synuclein expression in dopaminergic neurons of *Drosophila* (Barone et al. 2011). Whilst viral injection of human Nrf2 into the hippocampus of an AD mouse model was shown to increase insoluble Aβ levels compared to soluble Aβ, which is thought to be the more toxic form, and to decrease memory impairment (Kanninen et al. 2009). Crossing of an Nrf2 KO mouse with this mouse model was found to exacerbate neuroinflammation and accumulate intracellular Aβ, possibly due to loss of autophagy regulation by Nrf2 (Joshi et al. 2015). In addition, transfection of Nrf2 into striatal neurons reduced cell death induced by mutant huntingtin protein, showing that Nrf2 OE is also beneficial in Huntington's disease (HD) (Tsvetkov et al. 2013). Furthermore, Nrf2 OE was also protective in a mouse model of Alexander disease, another type of ND disease (LaPash Daniels et al. 2012).

Mitochondrial dysfunction is also prevalent in ND diseases, and inhibition of the mitochondrial ETC has been shown to lead to excessive ROS production and oxidative stress. Interestingly, Nrf2 activation in astrocytes provides neuroprotection against ETC complex I and complex II inhibitors (Lee et al. 2003; Calkins et al. 2005). Furthermore, Nrf2 KO primary cortical neurons were shown to be more vulnerable to the toxicity caused by complex II inhibitors (Calkins et al. 2005).

Nrf2 OE in astrocytes has neuroprotective effects in various ND disorders, which has been demonstrated using a mouse line (Nrf2-GFAP mice), in which Nrf2 is bound to the GFAP promoter, thus selectively overexpressing Nrf2 in astrocytes (Vargas et al. 2008).

Co-culturing Nrf2-GFAP astrocytes with motor neurons expressing a human SOD1 mutant ($SOD1^{G93A}$) was shown to decrease neuronal death *in vitro*, due to secretion of GSH by astrocytes (Vargas et al. 2008). Additionally, crossing the Nrf2-GFAP to an ALS mouse model, expressing neurotoxic human $SOD1^{G93A}$, lead to an increased lifespan of these mice (Vargas et al. 2008).

Gan *et al.* demonstrated that Nrf2 OE in astrocytes is neuroprotective against the toxic effects of mutated α-synuclein, by crossing the Nrf2-GFAP mouse with a mouse line with a human α-synuclein mutation (Syn^{A53T}) (Gan et al. 2012). Nrf2 OE in astrocytes decreased oxidative stress, reduced the formation of Syn^{A53T} and phosphorylated Syn^{A53T} aggregates in the CNS *in vivo*, thought to be due to Nrf2 activation reversing the impairment of macroautophagy in the mouse model, thus promoting clearance of Syn^{A53T}, and increased the survival of motor neurons in the spinal cord, prolonging the life of these mice (Gan et al. 2012).

Additionally, the Nrf2-GFAP mouse was shown to block toxicity caused by MPTP, used to induce PD-like symptoms, in mice with and without Nrf2, suggesting that Nrf2 OE is only required in astrocytes for neuroprotection (Chen et al. 2009).

Thus, the neuroprotective effects of Nrf2 OE against protein misfolding are thought to be largely due to attenuation of oxidative stress in neurons themselves, by increased production and secretion of GSH, providing neurons with precursors for GSH synthesis; as well as Nrf2 modulating autophagy through its control of p62 (Fujita et al. 2011; Gan et al. 2012; Vargas et al. 2008; Shih et al. 2003). These results suggest that Nrf2 OE, specifically in astrocytes, could be a viable therapeutic treatment in several neurodegenerative diseases.

Interestingly, Nrf2 activator CDDO and its analogues have been shown to provide neuroprotection in a number of ND diseases. $CDDO^{TFEA}$ and $CDDO^{EA}$ were shown to provide neuroprotection in mouse models of ALS and HD, by upregulating the Nrf2 pathway, combating oxidative stress and increasing the lifespan of mice (Stack et al. 2010; Neymotin et al. 2011). Furthermore, $CDDO^{MA}$ reduced amyloid plaque formation and oxidative stress in a mouse model of AD (Dumont et al. 2009), and was neuroprotective against MPTP-induced neuronal death (Yang et al. 2009).

Another Nrf2 activator, dimethyl fumarate (DMF), which modifies the cysteines of Keap1 to promote Nrf2 activity, has been approved for the treatment of multiple sclerosis (MS)

(Brennan et al. 2015; Linker et al. 2011). It may be possible that DMF or other activators of Nrf2 may be a possible therapeutic for a number of other ND diseases.

1.2.2.4. Nrf2 activation in stroke and traumatic brain injury is neuroprotective

Oxidative stress is also an important contributor to the neuronal damage caused by stroke. Both mild oxidative stress (H_2O_2) and oxygen glucose deprivation (OGD) activate Nrf2 and its target genes, preconditioning neurons against later ischemic insults (Bell, Al-Mubarak, et al. 2011; Bell, Fowler, et al. 2011). Although there have also been reports of an Nrf2-independent mechanism for mild H_2O_2 mediated neuroprotection (Haskew-Layton et al. 2010). Nevertheless, application of Nrf2 activator plumbagin to cortical neurons *in vitro* was shown to reduce cell death following OGD (Son et al. 2010).

Injection of Nrf2 activators SLF and tBHQ into rodents had neuroprotective effects against middle cerebral artery occlusion (MCAO), used to mimic ischaemic stroke, in various experiments (Jiang et al. 2016). For instance, Shih *et al.* demonstrated that pre-treatment of rats with tBHQ for 3 days attenuated damage caused by MCAO even one month after the insult, whilst in Nrf2 KO mice the infarct volume in the cortex was increased following permanent focal ischaemia compared to wild-type mice (Shih et al. 2005).

Moreover, a tat-peptide was recently shown to activate the Nrf2 pathway, by dissociating Nrf2 from Keap1, and to provide neuroprotection against global cerebral ischaemia in the CA1 region of the hippocampus in rats (Tu et al. 2015).

Nrf2 activator SLF decreased neuronal death and oxidative stress due to TBI in rodents, in an Nrf2 dependent manner (Hong et al. 2010). Additionally, hypoxic preconditioning was shown to upregulate Nrf2 and its target gene Hmox1, providing protection against TBI in a rat model (Shu et al. 2016).

These results suggest that Nrf2 OE or activation prior to stroke or TBI may also be neuroprotective, although due to the acute nature of the diseases the therapeutic capacity of Nrf2 activation is uncertain.

1.3. The NMDA receptor

N-methyl D-aspartate receptors (NMDARs) are ionotropic glutamate receptors found in the central nervous system. Other glutamate receptors include ionotropic AMPA (α-amino-3-hydroxy-5-methyl-isoxazole propionate) and kainate receptors, and metabotropic glutamate receptors.

Binding of glutamate with glycine as a co-agonist leads to the opening of the NMDAR channel pore, but NMDARs are not only ligand, but also voltage gated, thus membrane depolarisation is required to remove the Mg^{+} block from the channel pore to allow Ca^{2+} influx into neurons (Regan et al. 2015; Wyllie et al. 2013; Papadia & Hardingham 2007).

NMDARs are mostly located post-synaptically on neurons as well as extrasynaptically, but can also be located peri- or pre-synaptically (Paoletti et al. 2013). NMDARs can also be found on glia, including astrocytes, as well as in other tissue, where they carry out several different functions, for which the reader is referred to a recent review (Hogan-Cann & Anderson 2016). Here, the effects of post-synaptic NMDAR activation in neurons will be discussed.

1.3.1. NMDAR structure and expression in the brain

NMDARs are heterotetramers made up of two Glun1 and two Glun2 subunits, with 4 transmembrane domains (TMDs), an extracellular N terminus and an intracellular C terminus to which many intracellular proteins bind via the PDZ domain (Wyllie et al. 2013; Kim & Sheng 2004). GluN1 subunits contain the glycine binding site, whilst GluN2 subunits contain the binding site for glutamate and NMDA (Regan et al. 2015). GluN1 is encoded by Grin1 which has 8 different splicing variants, Glun1-1a-d and Glun1-2a-d (Regan et al. 2015). GluN2 subunits have 4 subtypes: GluN2A, B, C and D, encoded by Grin2A-D; of which 2A and 2B are the most expressed in the forebrain, whilst C and D are largely expressed in other areas of the brain such as the cerebellum (Paoletti et al. 2013; Regan et al. 2015). GluN2 subunit composition changes throughout development, with a developmental switch from GluN2B to GluN2A shortly after birth (Paoletti et al. 2013). GluN2 subtype expression determines the biophysical properties of NMDARs, such as its sensitivity to Mg^{+} and its Ca^{2+} permeability, as well as the proteins coupling to its C termini (Wyllie et al. 2013; Paoletti et al. 2013).

Additionally, two GluN3 subunits, Glun3A and B also exist, which contain a glycine binding site and can be incorporated into NMDARs, either with both GluN1 and 2 subunits present in a triheteromeric receptor, or supposedly with GluN1 only forming excitatory glycine receptors (Pachernegg et al. 2012; Paoletti et al. 2013). GluN3 subunits were initially thought to be dominant-negative regulators of NMDAR activity, and have since been suggested to be

involved in synaptic plasticity and development amongst others functions (Pachernegg et al. 2012).

Moreover, NMDARs have recently been suggested to also be able to function in a non-ionotropic fashion, through conformational changes following agonist binding (Gray et al. 2016).

1.3.2. NMDAR function

NMDARs play a large role in synaptic plasticity, and mediating the slow-phase of excitatory post-synaptic potentials, and are thus implicated in learning and memory and help in facilitating long-term potentiation along with metabotropic glutamate receptors; and are also important in mediating cell survival and death (Hardingham 2009; Hardingham & Bading 2003; Tashiro et al. 2006; Paoletti et al. 2013).

Activation of NMDARs causes Ca^{2+} influx into post-synaptic neurons activating various downstream signalling cascades, the outcome of which can have protective or destructive effects, depending on several different factors, such as the intensity and duration of Ca^{2+} influx, as well as the site of entry (Hardingham 2009; Hardingham & Bading 2010). Blockade of NMDARs leads to cell death, as does excessive activation of NMDARs which causes excitotoxicity, whilst physiological activation of NMDARs has neuroprotective effects (Hardingham 2009; Hardingham & Bading 2010; Ikonomidou 1999). Excitotoxicity has been implicated in several different neurological disorders, such as chronic neurodegenerative diseases, stroke and TBI (Parsons & Raymond 2014; Lipton 2006). NMDAR dysfunction and mutations have also been implicated in some neurodevelopmental disorders, such as schizophrenia (Burnashev & Szepetowski 2015; Cohen et al. 2015).

The location of Ca^{2+} signalling within neurons is also important, with cytoplasmic, nuclear and mitochondrial Ca^{2+} activating different signalling cascades (Hardingham 2009; Hardingham & Bading 2010). The subunit composition of NMDARs can also influence downstream cascades activated, due to the differential binding of proteins to the C-terminal domains of the NMDAR subunits (Wyllie et al. 2013; Paoletti et al. 2013).

The site of Ca^{2+} entry is an important contributing factor to the outcome of NMDAR-mediated Ca^{2+} influx. NMDARs are located both synaptically and extrasynaptically on neurons. Synaptic NMDARs get activated following normal physiological synaptic activity, whilst extrasynaptic receptors are activated following chronic activation resulting in glutamate spillover, such as during pathological conditions or bath application of glutamate (Hardingham 2009; Hardingham & Bading 2010). Spontaneous neuronal activity causes action potential

(AP) firing, activating synaptic, but not extrasynaptic NMDARs. Thus, synaptic activity is thought to be linked with beneficial effects of NMDAR activity, promoting neuronal survival, whilst extrasynaptic NMDARs are thought to have destructive effects, promoting excitotoxic cell death (Hardingham 2009; Hardingham & Bading 2010; Bell & Hardingham 2011b).

Below the major pro-survival and pro-death pathways activated by NMDAR activity in neurons will be discussed.

1.3.3. Neuroprotective signalling mediated by the NMDAR and the role of neuronal activity

1.3.3.1. Neuronal activity and the NMDAR

Lack of spontaneous neuronal activity in the CNS during development leads to apoptotic neuronal death, such as after prolonged blockade of activity with tetrodotoxin (ttx), a sodium channel blocker, or after eliminating neuronal input (Mennerick & Zorumski 2001).

Thus, neuronal activity leading to AP firing is essential for neuronal health and survival in developing as well as mature neurons, and is known to protect neurons against subsequent oxidative, excitotoxic and apoptotic insults (Bell & Hardingham 2011b). Physiological neuronal activity is largely mediated by synaptic NMDARs through the activation of downstream cascades following Ca^{2+} influx, causing upregulation of anti-apoptotic genes and antioxidant systems and the inhibition of pro-apoptotic gene transcription, discussed in more detail below. Although other routes of cytosolic Ca^{2+} increase following neuronal activity exist and are known to promote neuronal survival, such as activation of L-type voltage gated Ca^{2+} channels, which can be mimicked *in vitro* by applying high K^+ extracellularly to depolarise neurons, and release of Ca^{2+} from intracellular stores (Mennerick & Zorumski 2001).

Consumption of alcohol during pregnancy can lead to apoptotic neuronal death and development of fetal alcohol syndrome in humans, largely due to the inhibitory effects of ethanol on NMDARs, demonstrating the harmful effects of NMDAR blockade *in vivo* during development (Olney et al. 2000; Wirkner et al. 1999). NMDAR inhibitors other than ethanol, such as MK-801, have been utilised in rodents to show the importance of NMDAR in apoptotic cell death during development (Olney et al. 2002). Injection of MK-801 to block NMDAR activity caused cell death by apoptosis in the cortex of P6 mice (Papadia et al. 2008). Ikonomidou demonstrated that even a few hours of NMDAR blockade with MK-801 triggers apoptosis during development in rats (Ikonomidou 1999). Blockade of NMDARs is also detrimental for mature neurons especially during injury, demonstrated by the failure of NMDAR antagonists as a treatment for stroke and TBI in clinical trials (Ikonomidou et al.

2000; Ikonomidou & Turski 2002). Synaptic activity through NMDARs is also essential for the survival of newly formed neurons in the adult mouse dentate gyrus (Tashiro et al. 2006).

Synaptic NMDAR activation has been mimicked *in vitro* by the addition of $GABA_A$ receptor antagonist bicuculline and K^+ channel antagonist 4-aminopyridine (Bic/4-AP) leading to an increase in synaptic activity, action potential firing and activation of synaptic NMDARs, to study the effects of synaptic NMDAR activation (Papadia et al. 2008). Bic/4-AP activity also induces Ca^{2+} influx through voltage-gated Ca^{2+} channels and Ca^{2+} release from internal stores, but is thought to mainly act through synaptic NMDARs (Papadia et al. 2008).

Preconditioning neurons *in vitro* with Bic/4-AP stimulation provides neurons with long-term protection against oxidative and excitotoxic insults (Bell & Hardingham 2011b; Papadia et al. 2008; Qiu et al. 2013). Preconditioning hippocampal neurons with subtoxic doses of NMDA also has neuroprotective effects against subsequent apoptotic and excitotoxic insults, activating both synaptic and extrasynaptic NMDARs, although synaptic receptors dominate the outcome due to induction of AP firing (Soriano et al. 2006). Thus, the neuroprotective effects of NMDARs are mostly due to synaptic NMDAR activity, but mild activation of extrasynaptic receptors along with strong synaptic activation still promotes neuroprotective signalling.

Environmental enrichment (EE) in rodents, such as increasing novel objects within their housing, leads to neuronal activity *in vivo*, and has been shown to have neuroprotective effects against excitotoxicity and spontaneous apoptotic cell death (Young et al. 1999). EE is thought to induce glutamatergic signalling in rats, thus NMDARs are likely to play a role (Nichols et al. 2007). EE also improves learning and memory and has been shown to delay disease onset in mouse models of HD and decrease oxidative stress in a model of AD (Spires & Hannan 2005; Herring et al. 2010). Additionally a cognitively active lifestyle has been shown to reduce the risk of developing AD in humans (Spires & Hannan 2005). Increased neuronal activity throughout the lifetime of an organism will likely result in less oxidative damage due to increased ROS elimination, thus decreasing susceptibility to age-related diseases. Memantine, a weak NMDAR antagonist, is thought to block extrasynaptic NMDAR activity, but not synaptic NMDAR activity, and has been licenced for treatment of AD (Xia et al. 2010; Lipton 2006). The success of memantine as opposed to other NMDAR antagonists lies in its selective allowance of physiological synaptic NMDAR activity including the upregulation of antioxidant defences in neurons (Papadia et al. 2008). This further implicates synaptic NMDAR activity as an important mediator of the neuroprotective effects of neuronal activity.

The protection provided by neuronal activity is largely due to downstream effects of synaptic NMDAR activation, inducing the transcription of anti-apoptotic genes, suppressing pro-apoptotic gene transcription and increasing the neurons own antioxidant defences, which are discussed below.

1.3.3.2. Neuroprotective pathways mediated by the NMDAR

1.3.3.2.1. Synaptic NMDAR activation leads to the expression of anti-apoptotic genes

Synaptic NMDAR activity is known to activate the transcription factor CREB (cAMP response element-binding protein), which binds to the cAMP response element (CRE) in the promoter region of several anti-apoptotic genes inducing their transcription (Figure 1.4; Hardingham et al. 2001b). CREB is phosphorylated and activated by nuclear calcium/calmodulin dependent protein kinase IV (CaMKIV) and the Ras-Erk1/2 pathway (Hardingham et al. 2001b; Hardingham et al. 2001a; Papadia et al. 2005). Nuclear Ca^{2+} resulting from release of Ca^{2+} from intracellular stores activates CREB which binds to its co-activator CBP (CREB binding protein) and induces transcription of many pro-survival genes, via CaMKIV in the absence of CaM (Hardingham et al. 2001b; Zhang et al. 2009b). Activation of CREB by synaptic activity is responsible for inducing the long-lasting phase of synaptic NMDAR activation mediated neuroprotection (Papadia et al. 2005). CREB activation also takes place following application of low doses of NMDA in vitro, which induce AP firing, favouring synaptic NMDAR activation (Soriano et al. 2006).

Brain derived neurotrophic factor (Bdnf), a CREB target gene, is upregulated following synaptic NMDAR activation, dependent on neuronal firing, and is known to be important in neuronal survival (Soriano et al. 2006). Bdnf was shown to have a large role in the neuroprotective effects of NMDA preconditioning against a subsequent excitotoxic insult in hippocampal neurons (Jiang et al. 2005). Moreover, Bdnf has been shown to be upregulated following EE (Young et al. 1999).

CREB has also been found to induce the transcription of Npas4 following neuronal activity, inhibiting the transcription of Mcu, preventing mitochondrial Ca^{2+} overload and the resulting mitochondrial dysfunction and excitotoxic cell death (Qiu et al. 2013). Npas4 belongs to the neuroprotective activity-regulated inhibitor of death (AID) family of genes, which can be upregulated by nuclear Ca^{2+} signalling following neuronal activity and many of which are involved in preventing mitochondrial dysfunction (Zhang et al. 2009b).

Another AID gene, Btg2, was found to be induced by synaptic activity in hippocampal neurons, providing neuroprotection against mitochondrial permeability transition induced by

NMDA excitotoxicity, which involves the opening of the mitochondrial permeability transition pore (mPTP), mitochondrial depolarisation and the release of cytochrome c from mitochondria which induces apoptosis (Lau & Bading 2009; Zhang et al. 2007). CREB-target gene Bcl6 has also been implicated in providing neuroprotection against apoptosis (Zhang et al. 2007).

NMDAR-mediated Ca^{2+} influx also activates other transcription factors, such as nuclear factor of activator T cells (NFAT) and nuclear factor I subtype A (NFI-A), which play important roles in NMDAR-mediated neuroprotection (Vashishta et al. 2009; Zheng et al. 2010).

1.3.3.2.2. Synaptic NMDAR activity suppresses several pro-apoptotic pathways

Synaptic NMDAR activation has been shown to inhibit the expression of pro-apoptotic BH3-only gene Puma (p53 upregulated modulator of apoptosis) in cortical neurons (Léveillé et al. 2010; Baxter et al. 2015). Puma through its interactions with pro-apoptotic genes Bax and Bak activates the release of cytochrome c from mitochondria, which together with apoptosis protease activating factor (Apaf1) forms the apoptosome, triggering apoptosis via the activation of procaspase 9 and its downstream target caspase 3 (Léveillé et al. 2010). Interestingly, synaptic activity was found to supress the transcription of Apaf1, procaspase 9 and caspase 3, inhibiting neuronal apoptosis in cortical neurons (Léveillé et al. 2010). Activation of transcription factor p53 and its target genes, including Puma, were found to be inhibited following neuronal activity in hippocampal neurons, preventing mitochondrial permeability transition and resulting apoptosis due to oxidative stress or following an excitotoxic insults (Lau & Bading 2009). Activation of Puma in cortical neurons has also been reported to occur independently of tumor suppressor p53 activation following some insults (Fricker et al. 2010).

Activation of the PI3K-Akt pathway by synaptic NMDAR activation leads to phosphorylation and nuclear export of FOXOs (FOXO1 and 3 in neurons), a family of transcription factors which promote transcription of pro-apoptotic genes, such as FasL and Bim (Figure 1.4; Hardingham & Bading 2010). Since FOXO1 is a FOXO target gene, inhibition of FOXO activity causes a reduction in FOXO1 transcription, leading to prolonged neuroprotection by FOXO target gene suppression, even after activation of PI3K has ceased (Al-Mubarak et al. 2009). Neuronal activity also inhibits glycogen synthase kinase 3β (GSK3β) and Bcl2 family member Bad, via activation of the PI3K-Akt or Ras-Erk1/2 pathways (Hardingham 2006b).

Thus, synaptic NMDAR activity provides neuroprotection against apoptotic insults by suppressing pro-death pathways.

1.3.3.2.3. Synaptic NMDAR activity enhances neuronal antioxidant defences

Neuronal activity places an increased metabolic demand on neurons, upregulating oxidative phosphorylation to produce ATP and thereby ROS production, enhancing the requirement for antioxidant defences to prevent oxidative stress. Indeed, synaptic NMDAR activity has been linked to the upregulation of intrinsic antioxidant defences (Figure 1.4).

Activation of synaptic NMDARs by Bic/4-AP upregulates Srxn1 and Sesn2 mRNA in cortical rat neurons, which catalyse the reduction of hyperoxidised Prxs following a H_2O_2 insult (Papadia et al. 2008). Activation of Srxn1 is through transcription factor activator protein 1 (AP-1), whilst Sesn2 is upregulated by C/EBPβ, both of which are CREB target genes, and the induction of which is dependent on neuronal firing (Papadia et al. 2008).

Additionally, synaptic activity triggers phosphorylation and nuclear export of the FOXO family of transcription factors through PI3K activation, inhibiting the transcriptional upregulation of its target gene thioredoxin interacting protein (Txnip), thereby increasing Trx activity in neurons (Papadia et al. 2008). Thus, synaptic activity upregulates the activity of the Trx-Prx system, increasing endogenous neuronal antioxidant defences helping to prevent ROS accumulation and development of oxidative stress, and providing long lasting neuroprotection against oxidative insults, such as H_2O_2 (Papadia et al. 2008). These antioxidant pathways may also play a role in reducing cytochrome c, which is thought to prevent neuronal apoptotic death (Brown & Borutaite 2008). Interestingly, memantine has been shown to preferentially allow synaptic NMDAR activation, and was found not to upregulate Txnip or promote nuclear translocation of FOXOs (Papadia et al. 2008).

Applying subtoxic amounts of NMDA is known to preferentially activate synaptic NMDARs due to induction of AP firing (Soriano et al. 2006). When bath applying subtoxic doses of glutamate in the presence of ttx to block firing activity, activating both synaptic and extrasynaptic receptors, the neuroprotective antioxidant effects of NMDARs were abolished, suggesting that activation of synaptic, but not extrasynaptic NMDARs provides protection against subsequent oxidative insults (Papadia et al. 2008). Even very brief synaptic NMDAR activity (5 min) was enough to provide the cell with increased antioxidant defences, and was not specific to NMDAR subunit composition (Papadia et al. 2008).

More recently, neuronal activity through activation of synaptic NMDARs was found to induce the transcription of genes involved in the GSH system. Neuronal activity increases GSH activity in primary rat cortical neurons through upregulation of GSH peroxidase and GSH reductase activity and induces Gclc transcription and translation increasing use of Gcl in an NMDAR-dependent manner, independently of the presence of astrocytes (Baxter et al. 2015).

Preconditioning of primary rat cortical neurons with Bic/4-AP stimulation was protective against Puma-dependent apoptosis following H_2O_2 application, in a GSH dependent and astrocyte independent manner (Baxter et al. 2015). In contrast, blockade of NMDAR activity using MK-801, lead to a decrease in Gclc and thus GSH activity *in vivo* (Baxter et al. 2015). Thus, neuroprotection provided by neuronal activity seems to be intrinsic to neurons and independent of astrocytes. Transcription of xCT, a glutamate/cystine exchanger, has also been shown to be induced following neuronal activity, by activating transcription factor 4 (ATF-4) downstream of the PI3K-Akt pathways inhibition of GSK-3β leading to phosphorylation of eukaryotic initiation factor 2α (eIF2α), which may contribute to the neuroprotective effects of synaptic NMDAR activity (Lewerenz et al. 2014).

Thus, neuronal activity can activate endogenous antioxidant defences in neurons, involved in boosting the activity of both GSH and the Trx-Prx system. This upregulation of intrinsic neuronal antioxidant systems is required to help detoxify ROS following increases in metabolism, as well as to provide long-lasting protection against future oxidative, apoptotic and excitotoxic insults.

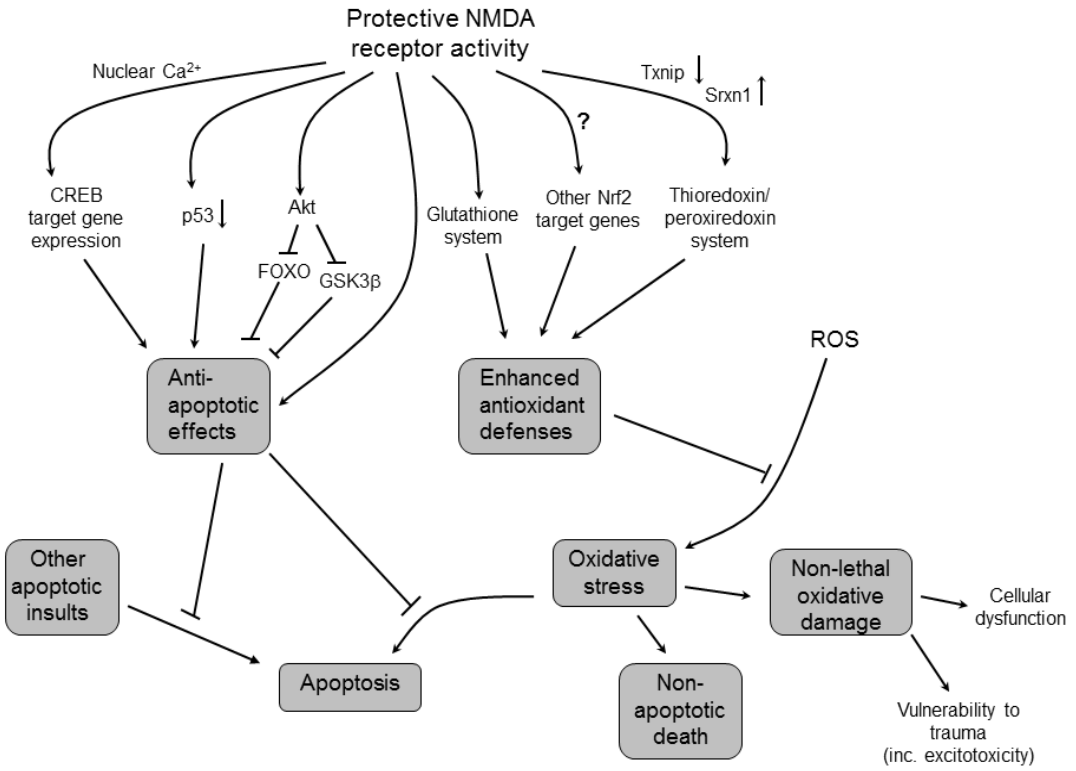

Figure 1.4. Pro-survival effects of NMDAR signalling. Figure modified from (Hardingham 2009). Physiological NMDAR activity leads to the upregulation of anti-apoptotic genes and the suppression of pro-apoptotic genes, leading to anti-apoptotic effects, and leads to enhanced endogenous antioxidant defences, which provides protection against various insults.

Recently Habas *et al.* showed activation of Nrf2 and upregulation of Nrf2 target genes following neuronal activity, suggesting that neuronal activity signals through the tripartite synapse to astrocytes activating the Nrf2 pathway (Habas et al. 2013). As demonstrated above, several antioxidant genes are upregulated by neuronal activity itself, some of which are Nrf2 target genes, such as Srxn1. Thus, in chapter 5 I address whether the induction of Nrf2 target genes by neuronal activity is dependent on Nrf2 or astrocytes.

1.3.4. Pro-death signalling from the NMDAR

1.3.4.1. The role of NMDARs in excitotoxicity

The toxic effects of glutamate on neurons was first observed around 50 years ago. Olney demonstrated that administration of glutamate caused neuronal death in the mouse brain, including the hippocampus and hypothalamus (Olney 1969; Olney & Ho 1970). Since this type of cell death resulted from the excessive activation of excitatory glutamate receptors and the downstream consequences of Ca^{2+} influx, the resulting cell death was termed excitotoxicity (Aarts & Tymianski 2003). Although glutamate application activates several routes of Ca^{2+} entry, NMDARs were found to be the predominant mediators of excitotoxicity (Choi 1988). Excitotoxicity has since been observed in many animal models, as well as in human pluripotent stem cell-derived neurons (Gupta et al. 2013b). Furthermore, excitotoxicity has been implicated as a major mechanism of cell death in several acute and chronic disorders, such as stroke and ND diseases, such as HD and AD, as well as in TBI (Hardingham & Bading 2010; Foster et al. 2016; Zhang et al. 2016; Prentice et al. 2015).

Excitotoxic cell death occurs through the activation of various signalling pathways by increased cytosolic Ca^{2+} in neurons, the activation of which can depend on various factors such as the cell type, developmental stage, NMDAR subunit composition, the site of Ca^{2+} entry as well as stimulus intensity and duration (Hardingham & Bading 2010; Wyllie et al. 2013; Hardingham 2006a). Excitotoxicity can be induced by bath application of high concentrations of NMDA or glutamate, or by recreating ischaemic conditions, such as with oxygen-glucose deprivation (OGD) *in vitro* or by middle cerebral artery occlusion (MCAO) *in vivo*. Ischaemic conditions lead to the reversal of glutamate transporters and the overactivation of neuronal glutamatergic receptors (Hardingham & Bading 2010).

Some of the signalling cascades activated during excitotoxicity are thought to be mediated preferentially by extrasynaptic receptors (Hardingham & Bading 2010; Hardingham 2006a; Hardingham et al. 2002; Parsons & Raymond 2014). Bath application of toxic doses of NMDA to hippocampal neurons *in vitro* leads to preferential activation of extrasynaptic NMDARs, due to suppression of AP firing, leading to neurodestructive effects (Soriano et al. 2006).

Nevertheless, the involvement of synaptic NMDARs in mediating pro-death signalling during excitotoxicity cannot be ruled out, due to technical difficulties in activating extrasynaptic receptors. NMDAR channel blocker MK-801 is often used to preferentially block synaptic NMDARs, but it has recently been shown that in contrast to previous findings, MK-801 can be washed out, bringing into question the validity of these experiments (McKay et al. 2013). Although synaptic NMDARs mediate neuronal survival following subtoxic doses of NMDA, toxic doses of NMDA are thought to activate both synaptic and extrasynaptic NMDARs, thus synaptic NMDARs may also contribute to cell-death signalling during bath activation of NMDARs (Zhou et al. 2015a).

The severity of excitotoxic death can also be influenced by the subtype of NMDAR activated at some stimulus intensities, due to the differential interactions of the C termini of GluN2 subunits with intracellular proteins, which activate different intracellular cascades mediating excitotoxicity. The preferential activation of excitotoxicity by GluN2B due to its C terminal domain coupling to PSD-95 and nNOS was demonstrated using mouse models in which the GluN2A C terminal was switched with that of GluN2B and vice versa (Martel et al. 2012). PSD-95 and nNOS have previously been proven to be important effectors of NMDAR-mediated excitotoxicity (Cui et al. 2007). The coupling of PSD-95 to the NMDAR is thought to underlie the importance of the preferential toxicity of Ca^{2+} entry through NMDARs as opposed to other receptors/channels, agreeing with the "source specificity hypothesis" which states that not just the amount, but the route of Ca^{2+} entry is important in the consequences of Ca^{2+} influx into neurons (Aarts & Tymianski 2003).

Due to the deleterious effects of NMDAR blockade, and the pro-survival effects of physiological NMDAR activation, the blockade of NMDARs therapeutically is not a viable option. Thus, it is important to understand the pro-death pathways mediated by NMDARs to find potential therapeutic targets downstream of NMDAR activation.

1.3.4.2. Pro-death signalling pathways activated by excitotoxicity

Extrasynaptic NMDAR-mediated Ca^{2+} influx following an excitotoxic insult activates calpains, a family of cysteine proteases, which cleave NCX3, the Na^{+}/Ca^{2+} exchanger in the plasma membrane which is the main route of Ca^{2+} efflux from neurons, leading to delayed Ca^{2+} deregulation and eventual cell death (Figure 1.5; Bano et al. 2005). Calpains also cleave striatal enriched tyrosine phosphatase (STEP), ceasing its inhibition of p38 mitogen activated (MAP) kinase, which induces cell death independently of caspase activation following excitotoxic insults as well as ischaemia (Xu et al. 2009). Furthermore, calpain activation leads

to mGlur1α cleavage, which ceases its activation of Akt, thus decreasing the anti-apoptotic defences of neurons leading to cell death (Xu et al. 2007).

Inhibition of pro-survival signalling by pathological NMDAR activation through the inactivation of CREB via inhibition of the Ras-ERK1/2 pathway or activation of Jacob, has been suggested to preferentially occur through extrasynaptic NMDAR activation (Hardingham & Bading 2010). This blocks the transcription of several anti-apoptotic and pro-survival genes induced by CREB. Inhibition of the Ras-ERK1/2 pathway also eliminates inhibition of GSK3β and Bad, promoting cell death (Hardingham 2009).

Activation of extrasynaptic NMDARs is also known to promote the nuclear import of FOXOs, leading to transcriptional upregulation of pro-apoptotic genes (Hardingham & Bading 2010). In addition, excitotoxicity increases hyperoxidised Prxs in neurons (Léveillé et al. 2009), most likely due to ceasing of Srxn1 and Sesn2 transcription. Thus, excitotoxicity decreases some of neurons intrinsic antioxidant defences.

Bath application of toxic NMDA doses leads to activation of extrasynaptic NMDARs, causing prolonged increases in Ca^{2+}, leading to mitochondrial Ca^{2+} uptake through the mitochondrial calcium uniporter (Mcu) and loss of the mitochondrial membrane potential, causing mitochondrial dysfunction and cell death (Soriano et al. 2006). Mcu KD in primary cortical cultures decreased mitochondrial Ca^{2+} uptake and depolarisation following NMDA application, preventing excitotoxic cell death; whilst Mcu OE rendered neurons more prone to excitotoxic cell death (Qiu et al. 2013). This demonstrates that mitochondrial Ca^{2+} uptake via Mcu is an essential mediator of excitotoxicity.

Excessive NMDAR signalling by glutamate activates neuronal nitric oxide synthase (nNOS), which along with mitochondrial Ca^{2+} uptake is an important mediator of mitochondrial dysfunction and excitotoxic cell death, by producing NO and activating p38-induced cell death, and is preferentially coupled to the GluN2B through PSD-95 (Keelan et al. 1999; Soriano et al. 2008b; Martel et al. 2012; Cao et al. 2005). Indeed, inhibition of nNOS was found to stop the loss of mitochondrial membrane potential and subsequent depletion of ATP in rat cortical neurons (Almeida et al. 1999). Excessive glutamate activation of NMDARs also activates phospholipase A_2 (PLA_2) which enhances ROS production leading to excitotoxic cell death (Bonventre 1997).

Along with p38, c-Jun N-terminal kinase (JNK) also helps to mediate excitotoxic cell death, but independently of the subtype of NMDAR (Martel et al. 2009). JNK is activated following

pathological NMDAR signalling, by ROS formed, and is therefore a possible downstream effector of Mcu-mediated Ca^{2+} uptake (Soriano et al. 2008b).

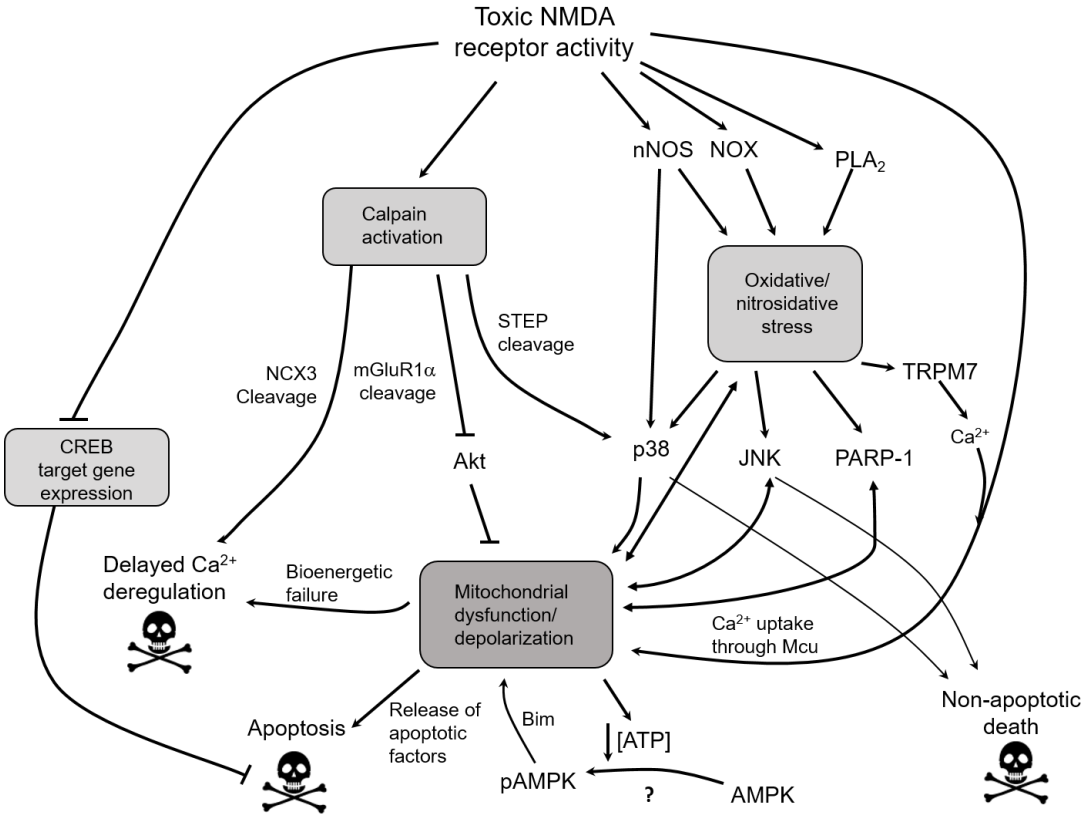

Figure 1.5. Pro-death effects of NMDAR signalling. Figure modified from (Hardingham 2009). Excessive NMDAR activation leads to inhibition of pro-survival genes, calpain activation, oxidative stress, mitochondrial dysfunction and eventually cell death.

NO produced by nNOS and superoxide produced due to an excitotoxic insult can form peroxynitrite, which can damage DNA by causing single-strand breaks, activating nuclear enzyme poly (ADP-ribose) polymerase 1 (PARP-1) (Duan et al. 2007). Peroxynitrite also activates TRPM7, which increases Ca^{2+} influx, leading to further cellular dysfunction and death (Aarts & Tymianski 2003; Hardingham 2009). During excitotoxicity, PAR polymers formed by PARP-1 leave the nucleus and bind to the apoptosis inducing factor (AIF) to promote its release from mitochondria, to mediate PARP-1 dependent cell death in the nucleus (Wang et al. 2011; Wang et al. 2009). PARP-1 has been shown to be activated by excitotoxicity, but only when mediated by NMDARs, implicating NO produced by nNOS to contribute to its activation due to its co-localisation with NMDARs (Mandir et al. 2000). PARP-1 was also suggested to be downstream of mitochondrial superoxide production (Duan et al. 2007), thus it may function as a downstream mediator of Mcu-mediated mitochondrial

Ca^{2+} uptake. Although superoxide produced by NADPH oxidase (NOX) following excessive Ca^{2+} influx may also contribute to peroxynitrite formation (Brennan et al. 2009). The involvement of PARP-1 in excitotoxicity is further supported by PARP-1 inhibitors decreasing necrosis following OGD in cortical cultures (Moroni et al. 2001).

Another possible downstream mediator of cell death following Mcu-mediated mitochondrial Ca^{2+} uptake is 5'AMP-activated protein kinase (AMPK), discussed in more detail below.

1.3.4.3. The potential role of AMPK in excitotoxicity

1.3.4.3.1. AMPK structure and function

AMPK is a serine threonine kinase which is the major cellular energy sensor, maintaining energy homeostasis in a number of different tissues through its activation of ATP producing pathways, such as glycolysis and mitochondrial biogenesis, and inhibition of ATP consuming pathways, such as protein synthesis (Carling 2004; Carling et al. 2008; Hardie 2007). AMPK is essential for energy homeostasis on the whole-body level, for instance in the hypothalamus AMPK is inhibited by leptin, and activated by ghrelin and low glucose concentrations, helping to regulate food intake (Minokoshi et al. 2004; Hardie 2007). Possibly through AMPK activation by its upstream kinase, Ca^{2+}/calmodulin dependent kinase kinase β (CaMKKβ), the pharmacological inhibition or KD of which reduces food intake (Anderson et al. 2008).

AMPK consists of a catalytic α and regulatory β and γ subunits making a triheteromeric protein. There are two types of AMPK α and β subunits, α1 and 2, and β1 and 2 and three types of γ subunits, γ1, 2 and 3 (Carling 2004; Hardie 2007). The expression pattern of AMPK subunits differs amongst tissues (Carling 2004). The most expressed subunits of AMPK in the embryonic and adult rat brain were found to be α1 and 2, β1 and 2 and γ1, although expression levels of α2 and β2 change throughout development (Turnley et al. 1999; Culmsee et al. 2001). Interestingly, although AMPK was found to be expressed throughout the brain, the expression of AMPK subunits in the cortex was predominantly neuronal, with α2 having higher expression than α1 (Turnley et al. 1999).

AMPK gets activated by a number of upstream kinases, which allow AMPK to exert its effect through phosphorylation of its downstream effectors. AMP binds to AMPK on Bateman domains on its γ subunit and allosterically activates the protein promoting the phosphorylation of Thr172 in the activation loop of its α subunit by LKB1 (Figure 1.6; Carling et al. 2008; Hardie 2007). The binding of AMP to the γ subunit has also been suggested to inhibit the dephosphorylation of AMPK by protein phosphatase 2Cα (Sanders et al. 2007; Fogarty et al. 2010). Alternatively, AMPK can form a complex with and be phosphorylated by CaMKKβ

following elevations in intracellular Ca^{2+} (Figure 1.6; Woods et al. 2005; Hawley et al. 1996; Carling et al. 2008; Green et al. 2011). Another kinase, transforming growth factorβ-activated kinase 1 (TAK-1) has been suggested to phosphorylate AMPK in yeast, but whether it is present in the mammalian CNS and what its roles are have not been extensively studied (Momcilovic et al. 2006). Some cells do not express all of these kinases, such as HeLa cells which lack LKB1 and require CaMKKβ for AMPK activation; but it is likely that in many cell types both kinases are activated in parallel (Hawley et al. 2005).

Due to AMPK controlling cell metabolism, it can be assumed that it will play a role in metabolic diseases and could be targeted therapeutically. Indeed, many anti-diabetic drugs for the treatment of Type II diabetes have been found to activate AMPK, such as rosiglitazone and metformin (Fryer et al. 2002). Resveratrol has been shown to promote the phosphorylation of AMPK by LKB1 in neurons, which increases mitochondrial biogenesis (Dasgupta & Milbrandt 2007). AICAR is often used to activate AMPK experimentally, due to its product formed in cells, ZMP, mimicking the actions of AMP. Furthermore, AMPK modulates the late phase of LTP, by inhibiting mTOR and plays a role in epilepsy (Potter et al. 2010). Moreover, AMPK has been suggested to be involved in cancer formation due to its ability to regulate the cell cycle and metabolic pathways in cells, and its upstream kinase LKB1 is mutated in a type of cancer, suggesting that AMPK may be important to suppress this type of cancer; thus AMPK could be targeted in the treatment of certain cancers (Luo et al. 2010). AMPK has been shown to be activated by various insults in neurons, such as hypoxia, ischaemia and glucose deprivation, and is implicated in stroke and chronic neurodegenerative diseases (Mairet-Coello et al. 2013; Thornton et al. 2011; Cai et al. 2012; Manwani & McCullough 2013; McCullough et al. 2005; Ju et al. 2012).

1.3.4.3.2. The role of AMPK in excitotoxicity

Activation of AMPK is thought to have a dual role in neurons during excitotoxicity, mediating both pro-death and pro-survival effects.

Brief activation of AMPK has been shown to have pro-survival effects. AMPK was activated independently of CaMKKβ following a brief glutamate exposure of cerebellar granule neurons (CGNs), promoting the translocation of glucose transporter 3 (GLUT3) to the cell membrane, increasing glucose uptake, thus upregulating neuronal metabolism leading to elevated levels of ATP and hyperpolarisation of the mitochondrial membrane potential (Figure 1.6; Weisova et al. 2009). The expression of GLUT3 provided neurons with tolerance against excitotoxicity, demonstrated by GLUT3 KD increasing neuronal death (Weisova et al. 2009). Activation of AMPK has also been found to mediate the protective effect of preconditioning with FCCP,

which causes mild mitochondrial uncoupling, in CGNs against subsequent glutamate-induced excitotoxicity, also by upregulating GLUT3 expression (Weisová et al. 2012). Pharmacological activation of AMPK with low concentrations of AICAR was shown to be neuroprotective against metabolic, oxidative and excitotoxic insults in rat hippocampal neurons, when applied 1 hour before the insult (Culmsee et al. 2001). Preconditioning with AICAR also transiently activated AMPK in mouse cortical neurons, providing protection against a subsequent excitotoxic insult; thought to be mediated by the transcriptional upregulation of a Bcl-2 family anti-apoptotic gene, Mcl-1, by AMPK (Anilkumar et al. 2013).

In contrast, prolonged activation of AMPK with higher AICAR concentrations was found to promote cell death following ischaemia, while inhibition of AMPK with compound C had neuroprotective effects (McCullough et al. 2005). Interestingly, phosphorylation of AMPK following ischaemia was found to be abolished in nNOS KO mice, suggesting that AMPK activation may be downstream of nNOS (McCullough et al. 2005). nNOS produces NO which together with superoxide forms peroxynitrite, which has been shown to activate AMPK in bovine aortic endothelial cells (Zou et al. 2003).

AMPK has also been shown to phosphorylate and activate mammalian FOXO3, resulting in the increase of various genes including Txnip in mouse embryonic fibroblasts (Greer et al. 2007). FOXOs are known to upregulate pro-apoptotic genes such as Bcl2 homology domain 3 (BH3)-only gene Bim in neurons, thus the activation of FOXO3 by AMPK may be a possible mechanism by which AMPK induces neuronal death. Indeed, Concannon *et al.* observed that upregulation of Bim following an excitotoxic insult by glutamate in CGNs or NMDA in cortical neurons, leads to caspase-independent apoptotic cell death through delayed Ca^{2+} deregulation and release of the apoptosis inducing factor (AIF) from mitochondria (Concannon et al. 2010). Bim activation was found to be dependent on AMPK activation following a transient decrease in mitochondrial membrane potential and loss of ATP levels due to an excitotoxic insult (Concannon et al. 2010). The transcriptional induction of Bim by AMPK was shown to take place via its activation of FOXO3 in CGNs in a proposed two-step process: firstly AMPK inhibits Akt in the cytoplasm promoting dephosphorylation and nuclear translocation of FOXO3, and secondly it phosphorylates FOXO3 in the nucleus to induce gene transcription, which only takes place upon prolonged AMPK activation (>100 min) (Figure 1.6; Davila et al. 2012). AMPK has also been shown to activate other BH3-only family members in different tissues, such as Bmf in INS-1 cells (Kilbride et al. 2010). PARP-1 activation leads to AIF dissociation from mitochondria, thus it is tempting to speculate that AMPK activation may also induce PARP-1 mediated cell death (Wang et al. 2011). Indeed, a

link between AMPK and PARP-1 has been described in human endothelial cells (Gongol et al. 2013).

Thus, transient AMPK activation is thought to have neuroprotective effects, whilst prolonged activation of AMPK is thought to be neurodestructive following an excitotoxic insult through Bim-induced apoptosis. Although other factors, such as the neuronal subtype, the intensity of AMPK activation, the type of insult, the AMPK subunits expressed as well as the localisation of AMPK within the cell may contribute to the outcome of AMPK activation.

Since Concannon *et al.* demonstrated AMPK activation after a drop in ATP levels following decreased mitochondrial membrane potential, and our group has found Mcu-mediated mitochondrial Ca^{2+} uptake to lead to excitotoxic cell death, I hypothesised that AMPK may be activated downstream of Mcu, a possibility which is explored in chapter 3 of this thesis.

Both LKB1 and CaMKKβ have been demonstrated to promote AMPK activation in the CNS. The binding of AMP to AMPK increased the phosphorylation of AMPKα at Thr172 by LKB1, whilst AMP binding only had a small effect on α2 and had no effect on α1 phosphorylation by CaMKKβ (Woods et al. 2005). Ca^{2+}/calmodulin on the other hand increased that activation of AMPK by CaMKKβ, raising the possibility that AMPK could be activated directly by Ca^{2+} influx following NMDAR activation independently of rises in AMP. Indeed, AMPK was found to be activated following high K^{+}-induced depolarisation in rat cortical slices, which was abolished by CaMKKβ blocker STO-609; demonstrating that AMPK can be activated by Ca^{2+} without decreased ATP levels (Hawley et al. 2005). CaMKKβ is expressed in rat brain and has been shown to be able to activate AMPK in vitro (Woods et al. 2005). Interestingly, AMPK has been shown to be activated independently of CaMKKβ following glutamate exposure in CGNs (Weisova et al. 2009).

Toxic Aβ oligomers were shown to activate AMPK through CaMKKβ in neurons, demonstrating the possible involvement of AMPK in AD (Mairet-Coello et al. 2013). Interestingly, Mairet-Coello *et al*. showed that AMPK activation in cortical neurons was abolished with CaMKK inhibitor STO-609, suggesting CaMKKβ as the main upstream kinase in cortical neurons. Exposure of hippocampal neurons to kainic acid has also been suggested to induce cell death via the CaMKKβ-AMPK pathway (Lee et al. 2009). Toxic Aβ oligomers were shown to act via the NMDAR and lead to a loss of dendritic spines in neurons *in vitro* and *in vivo* in a mouse model of AD, due to the hyperphosphorylation of Tau by AMPK (Mairet-Coello et al. 2013; Thornton et al. 2011). Intriguingly, memantine was shown to inhibit AMPK activation (Thornton et al. 2011), suggesting that AMPK may be preferentially activated by pathological NMDAR activation. AMPK was found to be activated via CaMKKβ

following an ischaemic insult both in hippocampal slice culture *in vitro* and in mice *in vivo* and to promote neuronal death, which was dependent on the presence of nNOS (McCullough et al. 2005). AMPK activation following metabolic insults or ischaemia has also been suggested to lead to neuroprotective effects in the brain by increasing the activity of metabotropic $GABA_B$ receptors through phosphorylation of its R2 subunit, promoting post-synaptic inwardly rectifying K^+ channels activation and inhibiting pre-synaptic Ca^{2+} channels, suppressing neuronal activity (Kuramoto et al. 2007; Hardie & Frenguelli 2007).

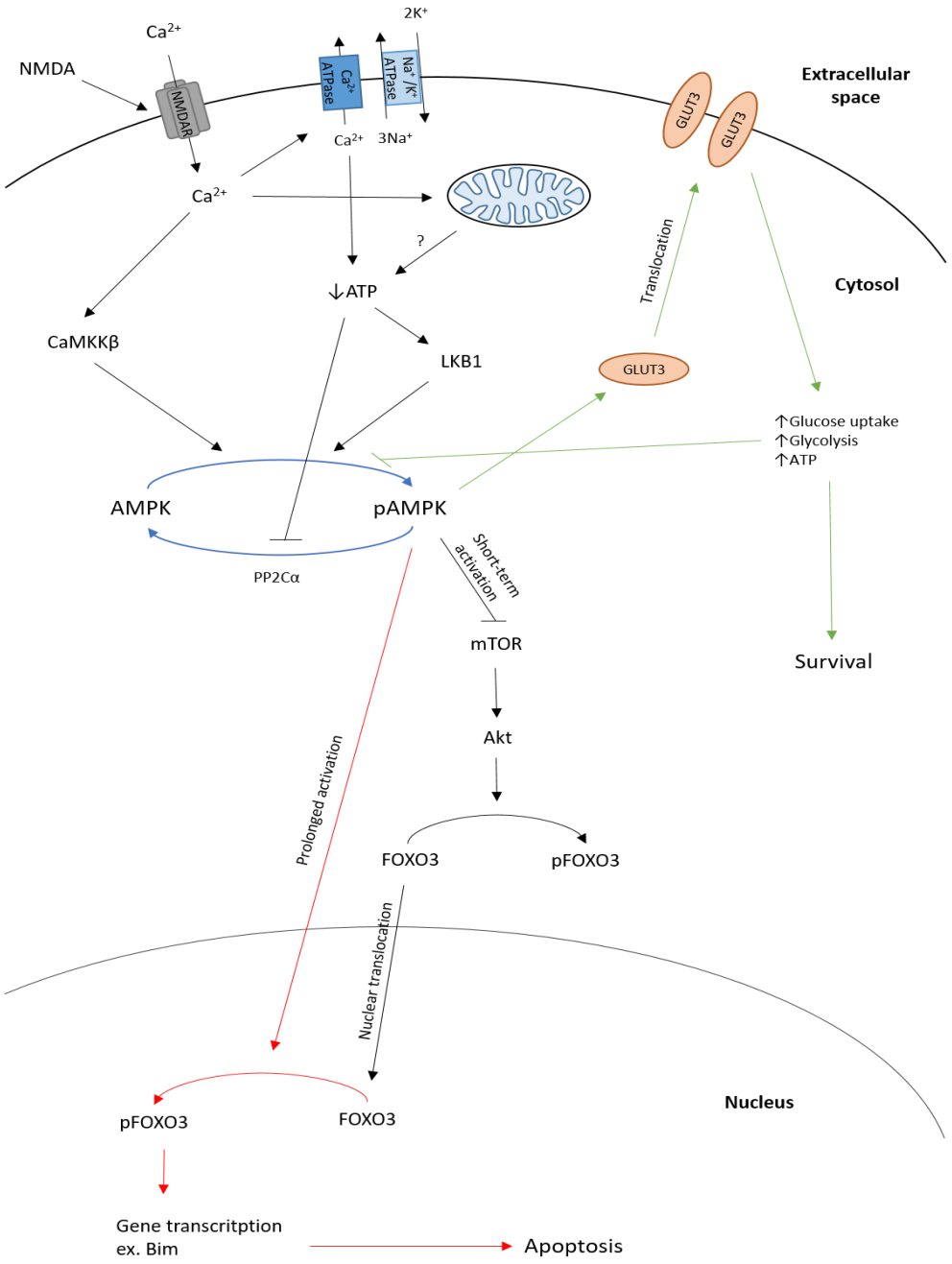

Figure 1.6. The AMPK signalling cascade in neurons. Following the activation of NMDARs, Ca^{2+} enters neurons activating the AMPK kinase CaMKKβ, and the drop in the ATP:AMP ratio (due to the increased activity of ATPases and/or decreased energy production by mitochondria) promotes AMPK phosphorylation by LKB1. AMPK is phosphorylated on T172 by these upstream kinases, and the activity of PP2Cα is inhibited due to the binding of AMP to AMPK. pAMPK can then activate neuroprotective pathways (green arrows), such as the translocation of GLUT3 to the cell membrane, which increases energy production and leads to neuronal survival. However, prolonged AMPK activation can lead to cell death (red arrows), such as following the phosphorylation of FOXO3 in the nucleus, which induces Bim transcription leading to apoptosis. Akt – protein kinase B, AMPK – AMP-activated protein kinase, Bim – Bcl2 like 11, CaMKKβ - Ca^{2+}/calmodulin dependent kinase kinase β, GLUT3 – glucose transporter 3, LKB1 - Liver kinase B1, mTOR – mammalian target of rapamycin, PP2Cα – protein phosphatase 2Cα

1.4. Mitochondrial calcium handling

1.4.1. Importance of mitochondrial calcium handling

The discovery that mitochondria can take up Ca^{2+} from the cytoplasm was made over 50 years ago (Deluca & Engstrom 1961) and since then the importance of mitochondrial Ca^{2+} uptake in regulating respiration (McCormack et al. 1990), buffering cytoplasmic Ca^{2+} (Hajnóczky et al. 1999), and mediating cell death (Bernardi & Rasola 2007) has been firmly established.

First, Ca^{2+} passes through the outer mitochondrial membrane (OMM) via the voltage dependent anion channel (VDAC) (Figure 1.7), which regulates the passage of ions and small molecules, including ATP and NADPH into the mitochondrial intermembrane space (IMS) (Shoshan-Barmatz & Gincel 2003). The inner mitochondrial membrane (IMM) has a battery of uniporters, exchangers and other proteins which regulate the influx and efflux of Ca^{2+} into the mitochondrial matrix.

Ca^{2+} influx into the mitochondrial matrix occurs along the electrochemical gradient created by the respiratory chain across the IMM, mainly through the mitochondrial calcium uniporter (Mcu) (Figure 1.7). Long prior to the genetic identification of Mcu, the uniporter was known to have high selectivity, but low affinity for Ca^{2+} and exhibit sensitivity to ruthenium red (Vasington et al. 1972). Release of Ca^{2+} from intracellular stores, such as the endoplasmic reticulum, in close proximity to mitochondria or from the plasma membrane channels is thought to create high microdomains of Ca^{2+} near mitochondria, allowing for Ca^{2+} influx into mitochondria despite the low affinity of Mcu for Ca^{2+} (Rizzuto et al. 1993).

Mitochondrial Ca^{2+} uptake through Mcu is thought to regulate metabolism in a number of ways, including activation of three mitochondrial dehydrogenases, pyruvate dehydrogenase (PDH), isocitrate dehydrogenase and oxoglutarate dehydrogenase (for a review see Glancy & Balaban 2012). Ca^{2+} activates PDH, by activating phosphatases responsible for its dephosphorylation, and is thought to directly bind the other two dehydrogenases increasing their activity (McCormack et al. 1990). Dehydrogenases increase cellular metabolism through converting NAD^{+} to NADH in the tricarboxylic acid (TCA) cycle, which is essential for the functioning of the ETC which pumps H^{+} into the IMS allowing ATP production by the mitochondrial ATPase (Glancy & Balaban 2012). Therefore, Ca^{2+} influx following synaptic activity could lead to mitochondrial Ca^{2+} uptake, thus upregulating ATP production upon increased demand. This is essential, since oxidative phosphorylation is the main source of ATP for neurons (Fernandez-Fernandez et al. 2012).

Mitochondria can buffer cytoplasmic Ca^{2+} transients when in close proximity to Ca^{2+} entry through plasma membrane channels, including the NMDAR and VGCCs, or release of Ca^{2+} from the ER, thus regulating Ca^{2+} transient duration and localisation (Rizzuto et al. 2012).

Excessive mitochondrial Ca^{2+} uptake leads to a decrease in mitochondrial membrane potential and ATP depletion due to the reversal of the mitochondrial ATPase, causing bioenergetic failure and leading to delayed Ca^{2+} deregulation in culture (Duchen 2012; De Stefani et al. 2016). Mitochondrial Ca^{2+} uptake can also lead to the collapse of the mitochondrial membrane potential and the release of cytochrome c following the opening of the mPTP and rupture of the OMM (Hardingham 2009; Orrenius et al. 2003; Bernardi & Rasola 2007).

Thus, it is essential that mitochondrial Ca^{2+} levels are tightly controlled, to allow for correct functioning of mitochondria, but prevent mitochondrial dysfunction due to Ca^{2+} overload. Thus, it makes sense for a battery of genes to help control the regulation of mitochondrial Ca^{2+}. Although the function and biochemical characteristics of the uniporter have been established, its molecular identity has only recently been found. A number of genes have been identified in the past few years, which are essential for mitochondrial calcium regulation both by modulating Mcu, or being Ca^{2+} channels and exchangers themselves. The discovery and function of these mitochondrial calcium regulatory genes (MCRGs) is described below in more detail.

Recent work by our group has illuminated the importance of Mcu itself as an important mediator of the mitochondrial membrane potential loss and excitotoxic cell death (Qiu et al. 2013). It is important to establish the function and expression of MCRGs in the CNS to better understand their role in mitochondrial Ca^{2+} regulation and excitotoxicity, and to be able to identify potential therapeutic targets for disease. In chapter 4 of this thesis the expression of MCRGs in different neural cell types and neuronal subtypes is investigated, as well as the function of Nclx in neurons and astrocytes.

1.4.2. Mitochondrial calcium regulatory genes

1.4.2.1. The Mcu channel complex

Mcu, previously known as Ccdc109a, was simultaneously discovered by two research groups in 2011 as the likely pore of the Ru360-sensitive mitochondrial Ca^{2+} uniporter (Baughman et al. 2011; De Stefani et al. 2011). De Stefani *et al*. identified the protein by searching the MitoCarta database (a database of mitochondrial proteins) for a protein which had ubiquitous expression, two TMDs and was conserved in organisms known to exhibit ruthenium-red sensitive mitochondrial Ca^{2+} uptake; whilst Baughman *et al*. identified Mcu using three

computational techniques, which investigated evolutionary co-expression with Micu1 (previously identified as a probable uniporter regulator), RNA co-expression with Micu1 in different cell types and protein co-expression with Micu1 in different tissues. The findings of the two groups confirmed that Mcu mediates mitochondrial Ca^{2+} uptake, demonstrating that Mcu KD leads to a decrease in mitochondrial Ca^{2+} uptake *in vitro* and *in vivo*, whilst keeping the mitochondrial membrane potential and respiration intact (Baughman et al. 2011; De Stefani et al. 2011). Mcu was further confirmed to be the pore-forming subunit of the Mcu channel complex by whole-mitoplast voltage-clamping, which showed decreased or increased mitochondrial Ca^{2+} currents following Mcu KD or OE, respectively (Chaudhuri et al. 2013).

Mcu has two TMDs connected by a linker region with a DIME motif, containing negatively charged amino acids critical for Mcu function. The topology of Mcu has been debated, but it is now thought that the N and C termini of Mcu face the mitochondrial matrix (Chaudhuri et al. 2013; Baughman et al. 2011; Lee et al. 2015).

The 40 kDa Mcu protein forms a tetramer in the IMM to create the Ru360-sensitive channel pore, allowing Ca^{2+} influx into the mitochondrial matrix (Lee et al. 2015; Raffaello et al. 2013; Chaudhuri et al. 2013; Kirichok et al. 2004; Vasington et al. 1972). This is supported by the presence of a 170 kDa band when running Mcu on a native gel, which is thought to be part of the large molecular weight Mcu channel complex (around 450 kDa) with other MCRGs (Raffaello et al. 2013; De Stefani et al. 2011; Baughman et al. 2011). The Mcu channel complex is thought to include mitochondrial Ca^{2+} uptake 1 (Micu1) and 2 (Micu2), which are anchored to Mcu by the single-pass membrane protein essential Mcu regulator (Emre) (Figure 1.7; Plovanich et al. 2013; Sancak et al. 2013; Kamer & Mootha 2014).

A negative regulator of Mcu, Mcub, is able to oligomerise with Mcu and can be incorporated into the tetramer formed (Marchi & Pinton 2014). Mcub, previously known as Ccdc109b, was identified by sequence analysis to be a closely related gene to Mcu, sharing 50% of its sequence identity (Raffaello et al. 2013). Mcub has two TMDs and amino acid changes in its pore region which are critical for Ca^{2+} uptake (Raffaello et al. 2013). Co-expression of Mcu and Mcub in lipid bilayers leads to a decreased probability of Ca^{2+} uptake, and Mcub KD has been shown to increase mitochondrial Ca^{2+} influx (Raffaello et al. 2013). This is further supported by Mcub KD being unable to rescue Ca^{2+} uptake during Mcu KD in permeabilised cells, and Mcu showing the same defect when critical amino acids in its pore regions are switched to those of Mcub (Raffaello et al. 2013). It is still unknown however how many Mcub and Mcu subunits make up the tetramer, and whether the presence of Mcub is dominantly negative and abolishes all Ca^{2+} uptake.

Micu1, previously Cbara1, was the first of the Mcu channel complex proteins to be identified in 2010 using the MitoCarta database (Perocchi et al. 2010). Micu1 is found on the IMM and consists of one TMD and two conserved Ca^{2+} sensing EF-hands. Micu2 and Micu3 previously known as Efha1 and Efha2, respectively, were identified as paralogs of Micu1 in vertebrates (Plovanich et al. 2013). Like Micu1, Micu2 and 3 also have EF-hands and an N-terminal mitochondrial targeting sequence, but only Micu2 has been confirmed experimentally to be localised to mitochondria (Plovanich et al. 2013). Micu2 and 3 share 25% sequence identity with Micu1, although their tissue expression patterns differ. Of note, Micu3 is thought to be highly expressed in the CNS, but its function has not been investigated and it was not found to be part of the Mcu channel complex, although this may be due to its low expression in the cells examined (Plovanich et al. 2013; Sancak et al. 2013). Both Micu1 and Micu2 can sense Ca^{2+} levels using their EF-hands (Perocchi et al. 2010; Csordás et al. 2013; Plovanich et al. 2013; Wang et al. 2014; Sancak et al. 2013; Hoffman et al. 2013).

Micu1 has been shown to be a gatekeeper of Mcu at basal cytoplasmic Ca^{2+} concentrations, and to positively cooperate with Mcu to allow greater Ca^{2+} influx following elevations in cytoplasmic Ca^{2+} levels (Csordás et al. 2013; Mallilankaraman et al. 2012b; Perocchi et al. 2010; de la Fuente et al. 2014). Micu1 is thought to block the channel pore at low Ca^{2+} levels by forming hexamers, potentially dimerising with Micu2, thus inhibiting excessive basal Ca^{2+} influx thereby helping to maintain respiration and the mitochondrial membrane potential (Mallilankaraman et al. 2012b; Csordás et al. 2013; Kamer & Mootha 2014; Matesanz-Isabel et al. 2016; Petrungaro et al. 2015). Following higher Ca^{2+} levels, Micu1 is thought to undergo a conformational change due to Ca^{2+} binding to its EF-hands, thus allowing Ca^{2+} influx through the channel (Wang et al. 2014; Waldeck-Weiermair et al. 2015). This could explain Micu1's dual function, controlling the threshold at low Ca^{2+} concentrations with its EF hands blocking Mcu's pore, and allowing Ca^{2+} influx at higher concentrations when its EF hands move after sensing increased Ca^{2+} levels. Although Micu1 and 2 appear to have similar functions, KD studies show that they act independently of each other, and are thought to have distinct roles (Plovanich et al. 2013; Matesanz-Isabel et al. 2016).

Micu1 KD increases the production of reactive oxygen species (ROS) by mitochondria basally in HeLa cells, inhibiting oxidative phosphorylation and triggering cell death (Mallilankaraman et al. 2012b). Micu1 KD also increases H_2O_2 levels and triggers loss of mitochondrial membrane potential, leading to cell death (Csordás et al. 2013). This is expected if Micu1 controls Mcu's threshold, since Micu1 KD will allow an increased Mcu-mediated Ca^{2+} influx, causing mitochondrial Ca^{2+} overload.

Micu1 is essential for mitochondrial Ca^{2+} handling, demonstrated by the death of Micu1 KO mice around birth, possibly due to increased excessive mitochondrial Ca^{2+} uptake leading to the opening of the mPTP (Antony et al. 2016). Interestingly, a mutation in Micu1 leading to the loss of its function has been implicated in a brain disorder (Logan et al. 2014). Loss of Micu1 in patient-derived fibroblasts lead to increased mitochondrial Ca^{2+} uptake following low cytosolic Ca^{2+}, agreeing with the role of Micu1 as the gatekeeper of Mcu (Logan et al. 2014).

Emre, a 10 kDa single TMD protein, was first discovered in 2012 as a member of the Mcu channel complex (Sancak et al. 2013). Emre localises to the IMS where it physically interact with Mcu, activating Mcu-mediated mitochondrial Ca^{2+} uptake, and anchors Micu1 and Micu2 near the Mcu pore allowing the proteins to carry out their gatekeeping function (Sancak et al. 2013; Tsai et al. 2016; Vais et al. 2016; Yamamoto et al. 2016). Although Tsai *et al.* demonstrated that Emre only interacts with Micu1, with Micu2 likely attached to Micu1. Vais *et al.* suggested that the C terminus of Emre is in the mitochondrial matrix and the N terminus is located in the IMS, but both Yamamoto *et al.* and Tsai *et al.* have since shown that the topology is indeed the opposite (Vais et al. 2016; Yamamoto et al. 2016; Tsai et al. 2016). Vais *et al.* recently suggested that the C terminus of Emre senses mitochondrial matrix Ca^{2+} levels and controls Ca^{2+} influx through the uniporter basally. Since the C terminus of Emre faces the IMS and interacts with Micu1 at its C terminus, the observation by Vais *et al.* could be due to the loss of Micu1's gatekeeping function on Mcu following mutation of Emre's C terminus.

1.4.2.2. Other Mcu regulatory genes

Other Mcu regulators exist, which are not thought to be part of the Mcu channel complex. One such protein is Mcu regulator 1 (Mcur1), previously known as Ccdc90a, which was first identified during a screen of mitochondrial membrane proteins for their effect on mitochondrial Ca^{2+} uptake by RNA interference (Mallilankaraman et al. 2012a). The role of Mcur1 as a regulator of Mcu has been disputed by Paupe *et al*., but this has since been disproven by Vais *et al*. (Paupe et al. 2015; Vais et al. 2015). Mcur1 can be found on the IMM and contains two TMDs, with both of its termini facing the IMS, and has a similar tissue expression pattern to that of Mcu (Mallilankaraman et al. 2012a). Mcur1 regulates Mcu-mediated Ca^{2+} uptake both basally and following rises in cytosolic Ca^{2+}, with its KD causing decreases in mitochondrial Ca^{2+} influx (Mallilankaraman et al. 2012a; Vais et al. 2015). Mcur1 physically interacts with Mcu, but was found not to be part of the Mcu-Emre-Micu1-Micu2

complex (Mallilankaraman et al. 2012a; Lee et al. 2015; Vais et al. 2015; Sancak et al. 2013). The role of Mcur1 is yet to be established in neural cells.

Slc25a23, a solute carrier mediating Mg-ATP/Pi transport across the IMM, has been found to accelerate Mcu-mediated Ca^{2+} influx through its interaction with Mcu (Hoffman et al. 2014). Slc25a23 KD decreases cell death caused by oxidative stress in HeLa cells, an effect which was also present following mutation of Slc25a23's EF-hands (Hoffman et al. 2014). Slc25a23 is thought to be activated following high cytoplasmic Ca^{2+} levels in neurons (Rueda et al. 2015; Rueda et al. 2014). Slc25a23 KO in primary cortical neurons leads to an increase in excitotoxic cell death cause by glutamate application, showing the importance of Slc25a23 in preventing the depletion of adenine nucleotides, and thus mPTP opening (Rueda et al. 2015).

1.4.2.3. Alternative routes of mitochondrial Ca^{2+} influx

Although Mcu is thought to be the major pathway of Ca^{2+} influx into the mitochondria, other Mcu-independent routes of Ca^{2+} influx exist (Figure 1.7). Different types of mitochondrial single Ca^{2+} channels have been observed in mitoplasts, and Mcu was found to be responsible for intermediate and extra-large, but not bursting mitochondrial Ca^{2+} channel current (Bondarenko et al. 2013; Bondarenko et al. 2015). Extra-large mitochondrial Ca^{2+} current was shown to compensate for mitochondrial Ca^{2+} uptake following Mcu KD, but xl-MCC occurrence has now been found to be decreased when Emre is knocked down alongside Mcu (Bondarenko et al. 2015).

Uncoupling protein 2 (Ucp2) and 3 (Ucp3) have been shown to play a role in mitochondrial Ca^{2+} influx (Trenker et al. 2007; Waldeck-Weiermair et al. 2010). Initially, Ucp2 was thought to be responsible for Ca^{2+} influx itself, but has since been found to regulate Mcu-mediated uptake of Ca^{2+} released from the ER, but not Ca^{2+} from store-operated Ca^{2+} entry (Waldeck-Weiermair et al. 2010). Ucp2 was demonstrated to increase the occurrence of xl-mitochondrial Ca^{2+} currents dependent on Mcu-mediated Ca^{2+} uptake, but not be important in whole-cell Ca^{2+} currents (Bondarenko et al. 2015). Furthermore, Ucp2 KO was shown to reduce the rescue of cardiomyocytes from ischaemic cell death by Ru360, once again suggesting a regulatory role of Ucp2 on Mcu (Motloch et al. 2015).

Transient receptor potential channel 3 (Trpc3) and ryanodine receptor (Ryr) have been implicated as possible alternative mitochondrial Ca^{2+} uptake routes. Both proteins are localised to different parts of the cell, Ryr to the ER and Trpc3 to the plasma membrane, and have only recently been shown to also be expressed on the IMM (Jakob et al. 2014; Feng et al. 2013; Amaral & Pozzo-Miller 2007). Ryr was demonstrated to allow Ca^{2+} influx into heart mitoplasts, and is expressed on the IMM in rat striatal neurons where it mediates Ca^{2+} influx

following rises in cytosolic Ca^{2+} (Ryu et al. 2011; Jakob et al. 2014). Trpc3 mediates mitochondrial Ca^{2+} influx at high cytoplasmic Ca^{2+} concentrations (>50 μM), thereby modulating the mitochondrial membrane potential, and has been shown to localise to the mitochondria in neurons (Feng et al. 2013). Interestingly, both channels are ruthenium red sensitive (Ryu et al. 2011; Feng et al. 2013). Thus, both Trpc3 and Ryr play a role in mitochondrial Ca^{2+} uptake, helping to regulate respiration and possibly cell death. It is likely that the importance of the co-existing mitochondrial Ca^{2+} uptake channels differs amongst different cells and tissues.

1.4.2.4. Mitochondrial Ca^{2+} efflux pathways

Mitochondrial Ca^{2+} efflux is essential for maintaining mitochondrial Ca^{2+} homeostasis, and is thought to be mediated by a Li^{+}-dependent Na^{+}/Ca^{2+} exchanger in excitable and H^{+}/Ca^{2+} exchanger in non-excitable cells, the identity of which has remained elusive until recently (Figure 1.7; Fiskum & Lehninger 1979; Carafoli et al. 1974; Cai & Lytton 2004b; Cai & Lytton 2004a).

Letm1 was identified as the probable mitochondrial H^{+}/Ca^{2+} exchanger by a genome-wide RNA interference screen in *Drosophila* (Jiang et al. 2009). Letm1 is localised to the IMM where it mediates mitochondrial Ca^{2+} efflux during high mitochondrial Ca^{2+} levels, while at low mitochondrial Ca^{2+} concentrations it is thought to mediate Ca^{2+} influx, thus possibly functioning as both an influx and efflux pathway depending on pH (Jiang et al. 2009; Doonan et al. 2014; Waldeck-Weiermair et al. 2011). Although a recent study which reconstituted Letm1 in liposomes suggested that it may only be responsible for Ca^{2+} efflux under basal conditions (Tsai et al. 2014). Letm1 has also been suggested to assist in the translation of mitochondrial proteins (Bauerschmitt et al. 2010; Lupo et al. 2011). Letm1 KO leads to embryonic death, suggesting that Letm1 plays an essential role in mitochondrial Ca^{2+} handling (Jiang et al. 2013).

Letm1 is deleted in Wolf-Hirschhorn syndrome (WHS), a disorder in humans characterised by delayed growth and development, as well as seizures (Bergemann et al. 2005). Letm1 KD leads to decreased mitochondrial Ca^{2+} influx and efflux (without affecting Mcu-mediated Ca^{2+} uptake), as does mutation of its EF-hands and leads to loss of ATP, increased ROS production and bioenergetic failure (Doonan et al. 2014). Fibroblasts acquired from WHS patients had lower levels of Letm1, and showed decreased Ca^{2+} uptake, ATP levels and increased ROS production (Doonan et al. 2014). In contrast, a study by Waldeck-Weiermair *et al*. found no effect of Letm1 KD on ATP and mitochondrial membrane potential (Waldeck-Weiermair et al. 2011). Heterozygous KO of Letm1 results in the death of only half the animals, with the

other half developing seizures and showing alterations in respiration and ATP production in the brain (Jiang et al. 2013). Interestingly, a recent study found a 50% decrease in Letm1 in cell lines from WHS patients, leading to mitochondrial impairments including increased mitochondrial Ca^{2+}, ROS production, hyperpolarisation of the mitochondrial membrane potential and alterations in mPTP opening (Hart et al. 2014). This implies that loss of Letm1 is important in the aetiology of WHS, and suggests that Letm1 is essential in mitochondrial Ca^{2+} handling in the brain and is expressed in neural cells.

The Na^{+}/Ca^{2+} exchanger responsible for mitochondrial Ca^{2+} efflux in excitable cells is Nclx. Nclx was first identified in 2004 to be responsible for Li^{+}/Ca^{2+} exchange, with a 55kDa and 70 kDa isoforms, of which only the short isoform was detected in the rat brain (Palty et al. 2004). After which Nclx was shown to be the Li^{+}-sensitive Na^{+}/Ca^{2+} exchanger on the IMM, sensitive to CGP-37157, which had previously been shown to block mitochondrial Ca^{2+} efflux (Palty et al. 2010). In line with this, Nclx OE in HeLa cells increases mitochondrial Ca^{2+} efflux (De Marchi et al. 2014).

Although Nclx has been shown to be expressed in the brain, little is known its expression in different neural cells (Cai & Lytton 2004a). Nclx was shown to be expressed in mouse astrocytes, and found to contribute to cytoplasmic Ca^{2+} buffering, thereby influencing store-operated Ca^{2+} entry and glutamate release, and was also found to play a role in proliferation of astrocytes (Parnis et al. 2013).

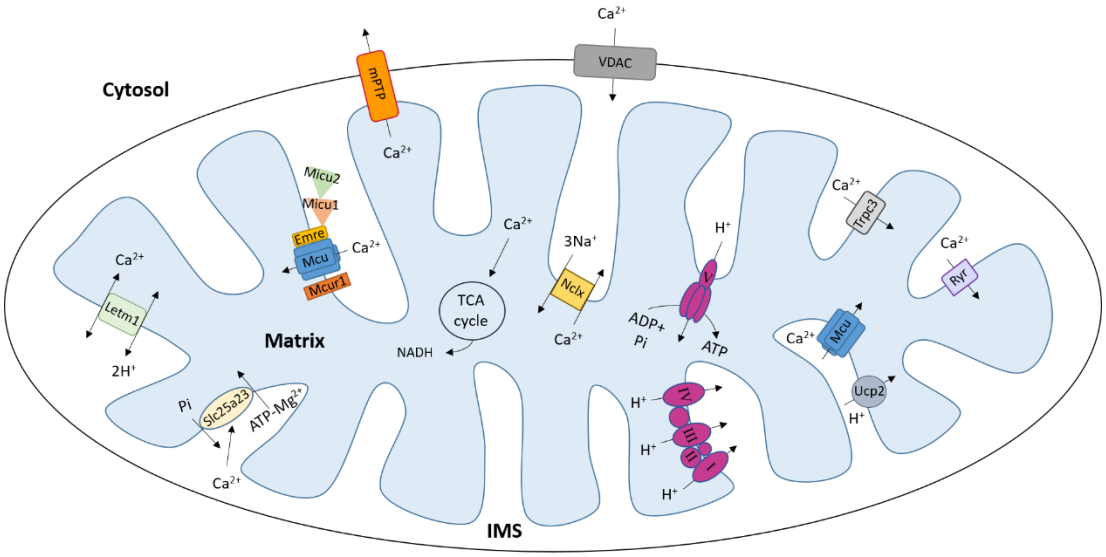

Figure 1.7. Mitochondrial Ca^{2+} levels are regulated by various uniporters, exchangers and other proteins. Ca^{2+} enters from the cytosol into the mitochondrial IMS through VDAC. Mcu forms a tetramer on the inner mitochondrial membrane, which can also include Mcub, to allow Ca^{2+} into the mitochondrial matrix. Mcu exists in a channel complex with Emre, Micu1 and Micu2, which help control Ca^{2+} uptake through Mcu. Other regulatory proteins, namely Mcur1, Slc25a23 and Ucp2 can also modulate Ca^{2+} uptake by Mcu. Alternative routes of Ca^{2+} influx into the matrix include Ryr and Trpc3. The Ca^{2+}/H^{+} exchanger Letm1 is thought to be able to act in reverse and allow not only Ca^{2+} efflux, but also Ca^{2+} influx into the matrix. The $Na^{+}/Ca^{2+}/Li^{+}$ exchanger Nclx is also thought to be responsible for Ca^{2+} efflux from the matrix. Ca^{2+} in the mitochondrial matrix activates several dehydrogenases, increasing respiration and the production of NADH which powers the ETC (I-IV). Excessive Ca^{2+} concentrations in the matrix can lead to cell death, for example due to the opening of the mPTP. Emre – essential Mcu regulator, ETC – electron transport chain, IMS – inner membrane space, Letm1 - Leucine Zipper-EF-Hand Containing Transmembrane Protein 1, Mcu – mitochondrial calcium uniporter, Mcur1 – Mcu regulator 1, Micu1/2/3 – mitochondrial calcium uptake 1/2/3, mPTP – mitochondrial permeability transition pore, NADH – Nicotinamide adenine dinucleotide, Nclx – $Na^{+}/Ca^{2+}/Li^{+}$ exchanger, Ryr – ryanodine receptor, Slc25a23 - SCaMC3, TCA cycle – tricarboxylic acid cycle, Trpc3 – Transient receptor potential channel 3, Ucp2 – uncoupling protein 2, VDAC – voltage-dependent anion channel, I-IV – mitochondrial ETC complexes I-IV, V – ATP synthase

1.5. Aims

Although Ca^{2+} signalling, especially through the NMDAR, is known to be essential in mediating both neuronal survival and death, some of the downstream pathways are still not well understood, and neither is the potential influence of astrocytes in neuroprotection following neuronal activity. The understanding of these mechanisms is essential for developing therapeutic treatments for neurological diseases and brain injury. In this thesis I aim to better understand these Ca^{2+} signalling pathways, and the possible role of astrocytes in providing neuroprotection following neuronal activity.

Our group has found Mcu to be an important mediator of excitotoxic cell death (Qiu et al. 2013), but its downstream effectors remain undetermined. AMPK has been suggested to have a pro-death role in excitotoxicity, and to be activated following mitochondrial dysfunction and a drop in ATP levels in neurons (Concannon et al. 2010). Thus, in Chapter 3 I investigate the role of AMPK as a potential downstream effector of Mcu during excitotoxicity.

Many MCRGs including Mcu have only been discovered in recent years, thus their expression and function in the CNS is not well characterised. MCRGs are essential for mitochondrial Ca^{2+} handling, and therefore play a role in mediating neuronal survival and death. In Chapter 4 I investigate whether MCRGs are differentially expressed in neural cells (neurons vs astrocytes) and neuronal subtypes (CA1 vs CA3 neurons of the hippocampus), and examine the functional importance of Nclx for mitochondrial Ca^{2+} efflux in neurons and astrocytes, following the discovery of its low expression in neurons.

Neuronal activity is known to enhance endogenous antioxidant defences in neurons (Papadia et al. 2008), but recent reports suggest that it may also activate the Nrf2 pathway in astrocytes through the tripartite synapse (Habas et al. 2013). Thus, in Chapter 5 I investigate Nrf2 expression in neurons, and whether Nrf2 target genes are activated in an Nrf2 and astrocyte dependent manner following neuronal activity, or if they are endogenously expressed in neurons themselves.

Chapter 2: Materials and Methods

2.1. Neuronal cultures

2.1.1. Preparation of primary cortical cultures

Cortical cultures were prepared from wild-type E17.5 CD1 or C57BL/6 mouse embryos as previously described (Márkus et al. 2016). Briefly, 24-well plates were coated with laminin (Sigma) and poly-lysine (Sigma) for 2 hours, to allow cells to adhere to the surface of the wells. For calcium imaging experiments, 13 mm diameter coverslips (VWR) were placed into the wells before coating. Mouse embryos were decapitated, their brains removed and the cortices dissected in dissociation medium (DM; 81.8 mM Na_2SO_4, 30 mM K_2SO_4, 5.84 mM $MgCl_2$, 252 µM $CaCl_2$, 1 mM Hepes, 0. 1% Phenol Red, 20 mM Glucose (all Sigma) made up in H_2O), with 1 mM kynurenic acid (Sigma), an NMDAR receptor antagonist, added to prevent excitotoxic cell death. The cortices were then digested with papain (with kynurenic acid present) for 2x20 min, washed with DM and 1% NBA (Neurobasal A solution (Life technologies) supplemented with 1x B27 (Life technologies Ltd.), 1 mM glutamine, 1x antibiotic/antimycotic (Life technologies Ltd.) and 1% rat serum (Harlan laboratories)) then homogenised in 1% NBA. The cell suspension was then diluted to a concentration of 0.28 cortices/2 ml with OptiMEM (+20 mM glucose) and 0.5 ml media was plated down into each well, whilst astrocytes were plated at half that density. The media was aspirated off of the cells after 2.5 hours and replaced with 1 ml fresh 1% NBA or Dulbecco's modified eagle medium (DMEM) supplemented with 10% fetal bovine serum and 1x antibiotic/antimycotic (all Life Technologies Ltd.) for growing pure astrocytes (>96% $GFAP^+$ astrocytes) per well. Cells were fed again on day in vitro (DIV) 4 with 1 ml 1% NBA or DMEM. Arabinofuranoside cytosine (AraC) (4.8 µM, Sigma), which inhibits glial proliferation, was added on DIV0 to pure neuronal cultures (98% $NeuN^+$ neurons and <0.2% $GFAP^+$ astrocytes) and on DIV4 to mixed neuronal cultures (90% $NeuN^+$ neurons and 10% $GFAP^+$ astrocytes) (Deighton et al. 2014). In chapter 5, cultures with No AraC added (15% $GFAP^+$ astrocytes) are used, and the mixed culture used for RNA sequencing had AraC added on DIV7. For calcium imaging experiments, primary astrocytes were grown in flasks, split twice (using 0.05% trypsin-EDTA, Life Technologies) before being plated on coverslips in 24-well plates. The cultures were kept at 37°C with 5% CO_2 in incubators.

For mouse-neuron rat-astrocyte co-cultures, rat cultures were made as the mouse cultures, except rat embryos were used at E20.5 and cell suspensions were diluted to 1/7 cortices per 2 ml. Primary rat astrocytes were plated down at half density and grown in a T75 flask, and split twice before being plated down onto 24-well plates. Mouse neurons were plated on top of the astrocytes and AraC added on DIV0 to obtain a culture with rat astrocytes and mouse neurons.

2.1.2. Neuronal cultures from transgenic mice

Homozygous Nrf2 KO mice were taken from Prof. John D. Hayes at The University of Dundee, where the genotyping of the mice was carried out. Nrf2 KO pups were cultured as described above. In these mice, the bZip region of Nrf2 is replaced with a nuclear localisation signal-β-galactosidase LacZ recombinant gene, rendering Nrf2 non-functional (Itoh et al. 1997). Nrf2 KO mice have been backcrossed onto a C57/BL6 background for several generations (Higgins et al. 2009), thus WT C57/BL6 cultures were used as controls for these mice.

AMPKα1 and α2 floxed mice were obtained from the laboratory of Prof. Mark Evans at The University of Edinburgh, with the lab kindly carrying out the genotyping of the mice. These mice have loxP sites around the catalytic sequence of the α1 and 2 subunits of AMPK, and their removal by Cre administration inhibits AMPK's catalytic activity (Mahmoud et al. 2016; Lantier et al. 2014).

2.2. Stimulations

For all stimulation, the media on cells was changed into a trophically deprived medium, TM_O, consisting of 10% Minimum essential media (MEM, Life technologies) in a salt-glucose-glycine medium (SGG) (containing 114 mM NaCl, 0.219% $NaHCO_3$, 5.292 mM KCl, 1 mM $MgCl_2$, 2 mM $CaCl_2$, 10 mM HEPES, 1 mM Glycine, 30 mM Glucose, 0.5 mM sodium pyruvate, 0.1% Phenol Red; osmolarity 325 mosm/l) with 1x antibiotic/antimycotic for at least 2 hours prior to stimulations, which were carried out on DIV8-10 unless otherwise stated. By this age, neurons develop a synaptic network and express NMDA and AMPA and kainite receptors. For some of the experiments, cells were placed into TM_{ITS}, which is TM_O with insulin-transferrin-sodium selenite (ITS) (Sigma) added, to allow for increased neuronal viability.

When keeping cells to DIV18, 50% of the media on cells was exchanged with NBA without rat serum, but with 10 mM glucose added on DIV9 and DIV12, and 50% of the media was exchanged with TM_{ITS} on DIV14, after which experiments were performed as normal.

2.2.1. Inducing neuronal activity

Synaptic activity was induced by application of $GABA_A$ inhibitor bicuculline with K^+ channel antagonist 4-aminopyridine (Bic/4-AP) in neuronal cultures for 4 or 24h, which induces bursts of action potential firing, the effect of which is thought to be primarily mediated by synaptic NMDAR activation as previously described (Papadia et al. 2008).

Alternatively, neurons were depolarised by addition of 0.41 ml KCl depolarisation solution (final concentration used: 50 mM KCl; made from stock solution: 10mM HEPES, pH 7.2, 170 mM KCl, 1mM MgCl2, 2mM $CaCl_2$) in the presence of NMDAR antagonist MK-801 (5 µM, Abcam) with or without the L-type Ca^{2+} channel agonist FPL64176 (5 µM, Sigma) present to 1 ml TM_O in wells (Hardingham et al. 1999).

2.2.2. Cell death assays

Different concentrations of NMDA (0-100 µM) (Ascent Scientific) were applied to cultures in TM_{ITS} for 10 minutes or 1 hour on DIV9, after which 20 µM MK-801 (Abcam) was applied to block NMDAR activity, as previously described (Qiu et al. 2013; Concannon et al. 2010). Cells were fixed the following day for 20 min in a fixing solution (3% PFA, 4% sucrose in 1x phosphate buffered saline (PBS)), permeabilised with 0.5% NP40 (BDH Chemicals) PBS for 5 minutes and stained with Vectashield mounting medium with DAPI (Vector labs), with a coverslip added to visualise the nuclei of cells. Several images were taken from each well with a DFC350 FX digital camera at 20x on a Leica fluorescence microscope using the Leica AF6000 LX imaging system, with at least 2 wells per condition in each replicate. Neurons showed signs of nuclear pyknosis, characteristic of apoptosis. The number of dead and alive neurons were counted blindly from the images using ImageJ and the percentage of dead neurons in the culture calculated.

For AMPKα1/2flx cultures infected with AVV-GFP or AAV-Cre-GFP, cell death was also calculated by following the fate of single GFP infected cells over 2 consecutive days, after which the average percentage of death from 10 GFP-infected neurons/image was calculated. The first image of neurons was taken before NMDA application for 1h, with the positions of neurons saved, whilst the second image was taken the following day at the same position, before cells were fixed and stained for GFP and DAPI to confirm the death of neurons.

2.2.3. Drugs used

Drugs used: AICAR (Cell Signaling), MG-132 (Sigma), A79662 (Tocris bioscience), STO-609-acetic acid (Sigma), Sulforaphane (Cayman chemical), $CDDO^{TFEA}$ (a gift from Michael Sporn, Dartmouth College)**,** DMF (Sigma), H_2O_2 (Sigma), tBHQ (Sigma)

2.3. Viral infection of cells

Viruses were added to mixed culture on DIV2 in 1% NBA. Various adeno-associated viruses (AAV)-Cre-GFP and AAV-GFP (AAV1, 2, 3 and 6, Vector labs) were added to WT and AMPKα1/2flx mouse cultures in TM_{ITS}. The infection efficiency of the viruses was determined on DIV9, following the fixing of cells, staining them against GFP (anti-GFP antibody

(Invitrogen)) and imaging them. AAV6 added to AMPKα1/2flx cultures was imaged on DIV8-9, prior to cells being fixed.

Mcu-shRNA or scrambled shRNA virus (with an eGFP tag) was added to cultures on DIV2 to knock down Mcu, from which protein was extracted on DIV9. The generation of Mcu and Scr-shRNA viruses has been previously described (Qiu et al. 2013).

2.4. Transfections

Transfections of neurons and astrocytes was carried out using lipofectamine 2000 (Invitrogen). 0.65 µg of DNA plasmid and 2.33 µl lipofectamine were both mixed with 66 µl TM_{ITS} per well and left at room temperature for 20 min. The transfection mix was then diluted in 285 µl TM_{ITS} per well and 333 µl of the mix was added to each well from which media was aspirated. The mix was left on DIV7-8 neurons for 4h and for 1h on DIV3 astrocytes, after which neurons were placed back into conditioned 1% NBA and astrocytes into fresh DMEM.

2.5. RNA isolation, RT-PCR and quantitative PCR

2.5.1. RNA isolation

RNA was isolated from neural cells in culture using the high pure RNA isolation kit (Roche), following the manufacturer's instructions. Briefly, cells were lysed and transferred into the columns provided, the lysate was incubated with DNAse I for 15 minutes, after which the column was washed three times and the RNA eluted in RNAse free H_2O.

Hippocampal region CA1 and 3 tissue was dissected from adult mouse brain slices, and then placed into Roche lysis buffer and homogenized using the QIAGEN QIAshreddar (QIAGEN Ltd.), after which RNA was isolated following the manufacturer's instructions for the Roche High Pure RNA Tissue Kit, including the optional 15 min DNase treatment to avoid DNA contamination.

2.5.2. RT-PCR and quantitative PCR

1-5 µg RNA was converted into cDNA using the Transcriptor First Strand cDNA Synthesis Kit (Roche), following the manufacturer's instructions. Both anchored $oligo(dT)_{18}$ primers and random hexamer primers from the kit were used for cDNA synthesis. The single-cycle Reverse transcription-PCR reaction was run at 25°C for 10 min, 55°C for 30 min and 85°C for 5 min, after which the mix was cooled down to 4°C. At least one No RT (reverse transcriptase) reaction was run with each sample set as a control.

cDNA was diluted to 6ng/µl, of which 1 µl was used for a 15 µl qPCR reaction per gene using FastStart Universal SYBR Green Master Rox (Roche) for real time qPCR in a Stratagene

Mx3000P qPCR System (Agilent Technologies). Next to the cDNA, the qPCR mix contained 0.6 µl of forward and reverse primers, 7.5 µl SYBR green master mix and 5.3 µl RNase free H_2O. Primers were tested before use, and their efficiencies calculated. For each qPCR reaction, at least two replicates and a No RT control were run to avoid false results due to technical errors or DNA contamination. 40 cycles were run to determine the level of each gene of the sample, after which one cycle was run to create a dissociation curve. The cycle temperatures and times were:

95 °C	10 min	
95 °C	30s*	40 cycles
60 °C	40s*	
72 °C	30s	
95 °C	1 min*	
55 °C	30s*	
95 °C	30s*	

*detection of fluorescence

Expression of genes was calculated from the Ct values of each gene using the primer efficiencies previously identified (method previously described in (Livak & Schmittgen 2001)), then normalised to Gapdh or 18s levels in each sample, unless otherwise specified.

2.5.3. Primers used

The qPCR primers used in this thesis can be seen in Table 2.1. Note that some of these primers have been designed by other members of the Hardingham lab.

Gene name	Also known as	Forward primer sequence	Reverse primer sequence
18s		GTGGAGCGATTTGTCTGGTT	CAAGCTTATGACCCGCACTT
Emre	Smdt1	CCTGGGTTGCAGTTCGAC	GTACCTGGCTGAGACCTGAG
Gapdh		GGGTGTGAACCACGAGAAAT	CCTTCCACAATGCCAAAGTT
mGapdh		CACCAGGGCTGCCATTTG	GCCTCACCCCATTTGATGTTA
Gclc		CCAACCATCCGACCCTCTG	TGTTCTGGCAGTGTGAATCC
mH1f0		GTTTGTCTTCCAAGACTTTCTT	CTTTGCCCCTTTAGACAATGGG
Hmox1		AGCACAGGGTGACAGAAGAG	GGAGCGGTGTCTGGGATG
Letm1		TCCTGCGTTTCCAGCTCACCAT	GTCTTCTGTGACACCGAGAGCT
Mcu	Ccdc109a	CGCCAGGAATATGTTTATCCA	CTTGTAATGGGTCTCTCAGTCTCTT
Mcub	Ccdc109b	CACTCCATTATGGGACAGTGG	CGACAACATCGGCTTGACTA
Mcur1	Ccdc90a	AGCCCTCAGAGCAGAAAATG	CCAGCATCTTCTTCTCGTTCA
Micu1	Efha3, Cbara1	GAACTAGCTGTGGGCTCTCG	GGTGGCAAAATATCGGAAAA
Micu2	Efha1	ACATGACACCCCGAGACTTC	CGATCATCTCATTCCCATCC
Micu3	Efha2	AACTCCACCAGTTTGGAAGG	CACCATCTCATTTCCGTCAG
NCLX	Slc8b1,Slc24a6	GAGACCACTGTCCAGATCCTGA	GAGCAGCAACAAGAACTCCACAG
mNCLX		GCTGCAGATCATCAGGAACC	CCTCAGGAGGCTAGCAGAATC
Ndufs2		GGATCCGCTTGCCAAGTC	CTCAATGAGCTTCTCCGTGC
Ryr2		ACCTACTCCGAAGGCTGGTGTT	TTCTTCCGAGGCAGCACCAAAG
Slc25a23		TTGATTGGCAGGAATGGCGAGAC	GTCAGGCATTCACCGATGTCCA
Srxn1		GACGTCCTCTGGATCAAAG	GCAGGAATGGTCTCTCTCTG
Trpc3	Trp3	GCATACTTGTCGCTGTCCAG	CGACTCAGTGACGCTTTGTG
Ucp2	Slc25a8	TAAAGGTCCGCTTCCAGGCTCA	ACGGGCAACATTGGGAGAAGTC
Uqcrc2		TGCTCCTCTGTCAAGAATCG	CAGTGTACGCCATGTTTTCC
xCT		ATACTCCAGAACACGGGCAG	AGTTCCACCCAGACTCGAAC

Table 2.1. qPCR primers. Forward and reverse sequences for primers used for real time qPCR. A small m indicates a mouse specific primer (against rat). Alternative gene names are provided in the second column for MCRGs recently renamed.

2.6. RNA sequencing

RNA-sequencing (RNA-seq) results used in chapter 5, were from RNA-seq carried out on neuronal cultures (DIV0 AraC) and mixed cultures (DIV7 AraC) treated with tBHQ or Bic/4-AP for 4 or 24h. RNA was extracted from three independent cultures and sent off for RNA-seq. RNA-seq data used in chapter 4 were from pure neuronal and astrocyte cultures prepared by Mr. Philip Hasel. RNA was extracted from cultures as described in section 2.5.1. above. RNA-seq as well as the analysis of data was carried out by Edinburgh Genomics, as previously described in (Márkus et al. 2016) as follows:

"Total RNA from mouse cortical neurons was assessed for quality (Agilent Bioanalyzer) and quantity (Invitrogen Qubit) before library preparation. Illumina libraries were prepared from 1 µg of total RNA using TruSeq RNA Sample Prep Kit v2 with a 10 cycle enrichment step as per the manufacturer's recommendations. Final libraries were pooled in equimolar proportions before Illumina sequencing on a HiSeq 2500 platform using 50 base paired-end reads. Raw reads were processed using RTA 1.17.21.3 and Casava 1.8.2 (Illumina)."

Reads were mapped onto to the mouse reference genome (mm10) found in Ensembl release 78, with alignment carried out using Tophat2 (version 2.0.13), using default settings. Htseq (version 0.6.0) was then used to calculate raw gene counts. Following this, differential expression analysis of the raw counts was estimated using DESeq2 (version 1.6.3) (Love et al. 2014) using Ensembl release 78 for metainformation such as gene annotations. The normalisation function of DESeq2 was then used to normalise the read counts. Lastly, estimated gene mRNA expression values were converted to fragments per kilobase of exon per million fragments mapped (FPKM) units.

2.7. Protein extraction and Western blotting

2.7.1. Protein extraction

Protein was collected from neuronal cultures (stimulated or unstimulated as indicated) by adding 40 µl of 1.5x sample buffer heated at 100°C (made up from NuPage sample reducing agent (10x) and NuPage LDS Sample buffer (4x) (Thermo Fisher Scientific)) to each well, with at least 2 wells pooled per sample. Samples were then boiled at 100°C for 10-15 minutes and loaded into wells or frozen at -20°C. 1.5x sample buffer was also directly added to hippocampal tissue dissected from brain slices of adult mice and boiled at 100°C to extract protein.

2.7.2. Western blotting

15-20 µl of protein samples were loaded into premade 4-12% NuPage Bis-Tris gels (Thermo Fisher Scientific) and run at 120 V for around 2 hours in 1xMOPS running buffer (NuPAGE MOPS SDS Running Buffer (20X), Thermo Fisher Scientific) in an XCell Surelock system

gel tank (Invitrogen). SeeBlue Plus2 protein standard (Thermo Fisher) was used as the ladder to indicate the molecular weight of proteins observed.

Proteins were then transferred onto a Polyvinylidene fluoride (PVDF) membrane (Immobilon-P PVDF membrane, 0.45 µm pore size (Millipore)) in 1x Transfer buffer (containing 96 mM glycine, 12 mM Tris (Trizma base) and 20% Methanol (all Sigma)) for 1 hour at 80V in a Criterion blotter tank (Bio-Rad). The PVDF membrane was activated for 1 minute in pure methanol before starting the transfer.

Following the transfer, the blot was blocked in 5% milk (semi-skimmed milk powder, Tesco) TBS (made of 20 mM Tris, 137 mM NaCl (Sigma) and H_2O, pH 7.6) with 0.1% Tween 20 (Sigma) (TBS-T) for 1 hour, after which blots were incubated with the primary antibody in 5% milk TBS-T overnight at 4°C on a roller. For the pAMPKα antibody, 5% BSA TBS-T was used instead of 5% milk TBS-T for all steps. The following day the blots were washed for 2x15 min in TBS-T before the HRP-linked secondary antibody in 5% milk TBS-T was added for 1 hour at room temperature, after which the washing step was repeated. Enhanced chemiluminescence (ECL) solution (containing 100 mM Tris-base (pH 8.5), luminol, p-coumaric acid and H_2O_2 (all Sigma)) was then added to the blot for 1 min, after which chemiluminescence of the membrane was detected on Carestream Kodak BioMax light or XAR film (Sigma), which was developed using Carestream Kodak autoradiography GBX developer/replenisher (Sigma) and fixed in Carestream Kodak autoradiography GBX fixer/replenisher (Sigma). Several exposures were taken for each blot to ensure that the samples were not saturated. The blots were scanned and the best exposures analysed by densitometric analysis using ImageJ, with values being normalised to β-actin levels in each sample as a loading control unless otherwise stated. Blots were stripped using 1x re-blot plus strong solution (Millipore) for 15 minutes after which blots were blocked again for 1 hour in 5% milk TBS-T and then reprobed for another antibody.

2.7.3. Antibodies used

Antibodies used for Western blotting and immunocytochemistry in this thesis:

Primary antibodies: AMPKα rabbit Ab (Cell Signaling, 1:2000), phospho-AMPKα rabbit Ab (Thr172) (Cell Signaling, 1:2000), anti-β-actin Ab (Abcam, 1:10000), anti-Mcu (Sigma, 1:3000), Nrf2 (D1Z9C) rabbit mAb (Cell Signaling, 1:400), anti-Uqcrc2 Ab (Abcam, 1:30000), Neuro-Chrom FluoroPan neuronal marker (Millipore, 1:500), anti-GFP Ab (Invitrogen, 1:500)

Secondary antibodies: Cy3-conjugated AffiniPure Donkey anti-Rabbit IgG (Jackson ImmunoResearch, 1:2000), anti-rabbit IgG, HRP-linked Ab (Cell Signaling, 1:2000), biotinylated anti-rabbit (Vector labs, 1:500) and Cy3-conjugated streptavidin (Stratech, 1:500).

2.8. Immunocytochemistry

Cells were fixed with a fixing solution (containing 3% PFA, 4% sucrose in 1xPBS) for 20 minutes, then permeabilised with PBS + 0.5% NP40 (BDH Chemicals) for 5 minutes, washed in 1xPBS and incubated with the primary antibody in 1xPBS overnight at 4°C on a shaker. Cells were washed 2x15 min with 1xPBS the following day, and the secondary antibody in 1xPBS was added for 1 hour at room temperature on a shaker. The Neuro-Chrom FluoroPan neuronal marker (Merck Millipore) was added after these steps for 2 hours at room temperature. Vectashield+DAPI (Vector labs) and coverslips were then added to the wells and the plates were imaged. In the case of Nrf2 staining, images from all wells were taken at the same fluorescence intensity, to be able to quantify the relative level of the fluorescence intensity of the Nrf2 staining between different conditions. For antibodies used, see section above.

2.9. Calcium imaging

Neurons and astrocytes transfected with cytoplasmic GCamp2 (cytoGCamp2, gift from Karel Svoboda) (Mao et al. 2008) or mitochondrial GCamp2 (mitoGCamp2, gift from Xianhua Wang) (Chen et al. 2011) on DIV7 and were imaged in SGG (equilibrated in a 5% CO_2 incubator) on DIV9-11 using a standard GFP filter set (excitation 480±20; emission 527±15) at 20x on a fluorescent microscope using the Leica AF6000 LX imaging system.

Cells were pre-incubated in the chambers for 10 minutes, with or without CGP-37157 (Sigma), after which the transfected cells were identified on the coverslips and imaged. Cells were imaged for around 2 minutes to allow for the recording of a steady baseline, after which 100 µM ATP was added to astrocytes or KCl depolarisation solution (50 mM K^+) (with MK-801 present) added to neurons to induce an increase in cytosolic and mitochondrial Ca^{2+} levels. Cells were washed with SGG 1 minute after the stimulation and henceforth every 30 seconds for a few minutes, to allow for observation of the rate of Ca^{2+} decay from the cytosol and mitochondria. Ionomycin (Tocris, 50 µM), a plasma and mitochondrial membrane permeable Ca^{2+} ionophore, was added at the end of recordings to establish the maximal Ca^{2+} capacity of each cell F_{max} (Nicholls 2006), following which EGTA was added to chelate Ca^{2+} in cells to give a minimum Ca^{2+} value for each cell F_{min}. Changes in Ca^{2+} levels were then calculated as

$(F-F_{min})/(F_{max}-F)$, which has been shown to have a linear relationship with Ca^{2+} (Qiu et al. 2013), and is based on the equation $[Ca^{2+}] = Kd*(F-F_{min})/(F_{max}-F)$.

2.10. Statistical analysis

Data was analysed using paired or unpaired two-tailed t-tests, depending on whether the data acquired were independent or not. In a few cases ANOVAs were used with post-hoc tests, which is indicated in detail in the figure legends. Statistical analysis was carried out using Graphpad prism (Graphpad Software Inc., La Jolla, CA). All data shown in graphs is represented as mean+SEM (standard error of the mean).

Chapter 3: AMPK is involved in excitotoxicity but is not downstream of the mitochondrial calcium uniporter

3.1. Introduction

Neuronal fate in response to NMDAR activation follows a bell shaped curve, with physiological activation promoting neuronal survival and too little or excessive activation promoting cell death (Hardingham 2009). Excessive activation of NMDARs leads to excitotoxicity, causing large amounts of Ca^{2+} influx into neurons which activates several pro-death pathways, leading to neuronal dysfunction and death (Hardingham 2009). Mitochondrial dysfunction occurs following a severe excitotoxic insult due to excessive mitochondrial Ca^{2+} uptake by the mitochondrial calcium uniporter (Mcu). Mcu has long been thought to be involved in excitotoxic cell death, and the recent discovery of its molecular identity as the Ccdc109a gene (Baughman et al. 2011; De Stefani et al. 2011) allows for its knock-down (KD) instead of using pharmacological inhibitors with off target effects, such as Ru360, to inhibit Mcu. Mcu is located on the inner mitochondrial membrane and is the major route of Ca^{2+} influx into the mitochondrial matrix, thus helping to buffer cytoplasmic Ca^{2+} levels, regulate cellular bioenergetics and activate cell death signalling (McCormack et al. 1990; Hajnóczky et al. 1999; Bernardi & Rasola 2007). Although Mcu has low affinity for Ca^{2+}, it is highly selective for and has high capacity for Ca^{2+}, thus allowing rapid Ca^{2+} entry into the mitochondria during excitotoxicity when cytosolic Ca^{2+} levels are high (Kirichok et al. 2004). Our lab has recently demonstrated that Mcu KD in primary neuronal culture reduces mitochondrial Ca^{2+} influx during excitotoxicity, decreasing mitochondrial depolarization and rescuing cells from excitotoxic cell death (Qiu et al. 2013). Overexpressing Mcu has the opposite effect, increasing mitochondrial depolarization and enhancing cell death. This establishes Mcu as an important mediator of excitotoxic cell death in cortical neurons, although its downstream targets promoting cell death remain elusive.

AMP activated protein kinase (AMPK), a triheteromeric protein with a catalytic α and regulatory β and γ subunits, is an energy sensor that activates ATP-producing pathways and inhibits ATP-consuming pathways following cell stress (Hardie et al. 2012). AMPK is allosterically activated following an increased AMP:ATP ratio due to AMP binding to its γ subunit, preventing dephosphorylation of AMPK (Sanders et al. 2007; Fogarty et al. 2010), which promotes the phosphorylation of T172 on its catalytic α subunit by its upstream kinase LKB1, further activating AMPK (Carling et al. 2008; Hardie 2007; Woods et al. 2003; Hawley et al. 2003). Alternatively, AMPK can be phosphorylated and activated by CaMKKβ following increased cytoplasmic Ca^{2+} levels (Hawley et al. 1996; Carling et al. 2008; Green et al. 2011; Woods et al. 2005; Hawley et al. 2005). The activation of AMPK following a drop in ATP levels makes it an attractive candidate as a downstream target of mitochondrial dysfunction during excitotoxicity. Indeed, prolonged AMPK activation following an excitotoxic insult has

been shown to mediate apoptotic cell death. NMDA stimulation in mouse cortical neurons and glutamate stimulation in cerebellar granule neurons (CGNs) led to decreased ATP levels and mitochondrial membrane potential activating AMPK, which transcriptionally upregulated the BH3-only gene Bim causing neuronal apoptosis (Concannon et al. 2010). The upregulation of Bim was later found to be mediated by AMPK through its activation of FOXO3, in a two-step process (Davila et al. 2012). Firstly AMPK inhibits Akt, promoting FOXO3 nuclear translocation, and secondly AMPK phosphorylates FOXO3 in the nucleus inducing Bim transcription, a step which only occurs following prolonged AMPK activation (Davila et al. 2012). Additionally, LKB1 has been suggested to be the upstream kinase of AMPK in CGNs (Weisová et al. 2012).

Thus I hypothesise that AMPK is activated by LKB-1 due to an increase in AMP:ATP ratio following mitochondrial dysfunction caused by Mcu-mediated Ca^{2+} uptake during excitotoxicity in cortical neurons. Although the role of AMPK has been previously investigated in excitotoxicity following its KD by siRNA or pharmacological inhibition (Concannon et al. 2010; Anilkumar et al. 2013), there have been no studies employing neurons from AMPK KO mice to my knowledge. Here, I investigate the role of AMPK in promoting excitotoxic cell death employing primary cortical cultures from conditional AMPKα1 and 2 double KO mice (Mahmoud et al. 2016; Lantier et al. 2014). Furthermore, I investigate AMPK as a potential downstream effector of Mcu-mediated Ca^{2+} uptake-induced cell death following excitotoxicity by Mcu KD. My results show that although AMPK helps to mediate excitotoxicity in primary cortical neurons, it is not activated by decreases in ATP due to Mcu-mediated mitochondrial Ca^{2+} uptake.

3.2. Results

3.2.1. AMPK gets activated following NMDA treatment

Both Concannon *et al.* and Anilkumar *et al.* have previously shown that AMPK gets activated following an NMDA insult in neurons (Concannon et al. 2010; Anilkumar et al. 2013). I wanted to test whether this was the case in primary mixed neuronal cultures (90% $NeuN^+$ neurons and 10% $GFAP^+$ astrocytes) and if any time points and concentration of NMDA activated AMPK, to determine what concentration to use in subsequent experiments. Primary neuronal cultures were stimulated with a range of NMDA concentrations at different time-points, and AMPK activator AICAR was applied for 1 hour or 30 minutes as a positive control. It was visually obvious that phosphorylated AMPKα (on Thr172) protein levels increase following NMDA stimulation, as seen in an example blot in Fig.3.1A. pAMPKα levels were quantified and normalised to the total AMPKα in each sample (Fig.3.1B). The largest increase in AMPK activation was observed 30 minutes after stimulation with 30 µM NMDA. This was also the only stimulation which was significantly different compared to the control using a one-way ANOVA with Bonferroni *post-hoc* test ($p<0.05$). However, all stimulations showed an upward trend in pAMPK levels, and with many of the stimulations only performed a few times and the general variability of Western blots the lack of significance is not surprising. Since there was a clear visual increase in pAMPK protein levels and a significant increase 30 µM NMDA applied for 30 min, I concluded that AMPK is activated by NMDA, and applied 30 µM NMDA for 30 minutes to activate AMPK in subsequent experiments.

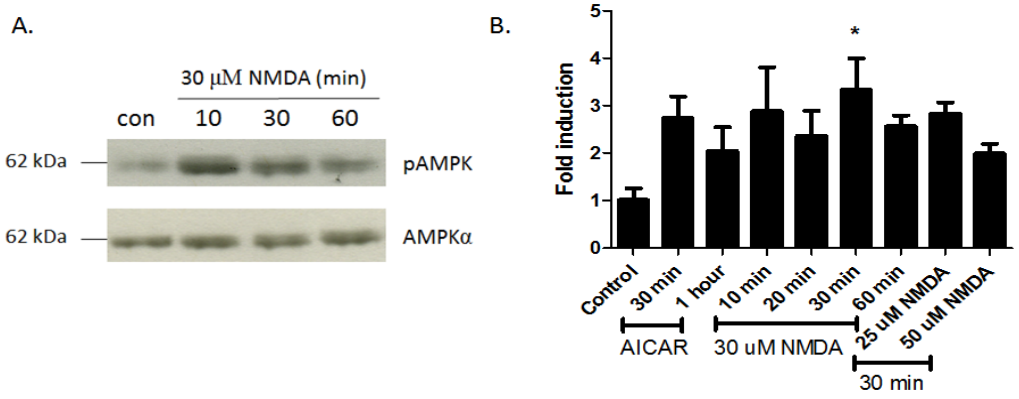

Figure 3.1. pAMPK levels in neuronal culture increase following NMDA treatment. A. Example of a Western blot showing an increase in pAMPKα levels following application of 30 µM NMDA for 10, 30 or 60 minutes, total pan-AMPKα is used as a loading control. **B.** The average values of AMPK activation following AICAR and NMDA treatment at different time points and doses. n=2 for 20 and 60 min 30 µM NMDA treatment and 30 min 25 and 50 µM NMDA treatment, n=4 for the AICAR treatments and for 10 and 30 min 30 µM NMDA treatment, and n=10 for control. Data was normalised to the untreated control and the loading control AMPKα. Error bars=SEM. *$p<0.05$ compared to the control, one-way ANOVA with a Bonferroni *post-hoc* test.

3.2.2. AMPKα gets knocked down by AAV6-Cre-GFP in AMPKα1 and 2 floxed mouse mixed neuronal cultures

To study the role of AMPK in NMDA-mediated excitotoxicity, I used primary cortical cultures made from a conditional AMPKα1 and 2 KO mouse, in which the catalytic sites in AMPKα1 and 2 are floxed (Lantier et al. 2014; Mahmoud et al. 2016). AMPKα1 and 2 are the two catalytic subunits, thus their KO will cease AMPK activity. Since AMPKα1 and 2 are floxed in the mouse, I needed to find a Cre virus which would efficiently knock down AMPKα1/2 in neurons in cortical culture. Thus, I tested the infection efficiency of various different viruses on primary neuronal cultures made from wild-type CD1 mice, which could later be used to infect cultures made from AMPKα1/2 floxed mice. Adeno-associated virus (AAV)1, 2, 5 and 6 with a GFP-tag were added to cultures on day in vitro (DIV) 2 and the percentage of neurons infected was calculated by determining the percentage of GFP-positive neurons in the culture (Fig.3.2). AAV6-GFP had the highest infection rate of neurons out of the four AAVs tested, at 51.4% when adding $2.5x10^4$ genome copies/cell, and even higher efficiencies when tested again. I then examined whether AAV6-GFP had a similar infection rate to that of AAV6-Cre-GFP, and I found both viruses to infect around 55% of neurons on average in primary cortical cultures. This means that results between WT and AMPKα KO conditions will be easily comparable.

I next tested AAV6-Cre-GFP and GFP in AMPKα1/2 floxed mouse primary cortical cultures. Neurons were infected with AAV6-Cre-GFP or AAV6-GFP on DIV2 and protein levels of AMPKα and pAMPK were determined on DIV9. As expected, there was a large reduction in AMPKα as well as pAMPK levels in samples treated with AAV6-Cre-GFP, compared to cells treated with control AAV6-GFP (Fig.3.3A). Control AMPK levels were quite high compared to AMPKα KD samples, so a serial dilution of the samples was carried out to better examine the amount of AMPKα KD (Fig.3.3B). This showed that there was approximately 75% KD of AMPKα levels in cells treated with AAV6-Cre-GFP compared to cells treated with AAV6-GFP, which was consistent across samples. This is slightly higher than the percentage of neuronal infection observed following immunostaining, which may be due to neurons weakly expressing GFP not being picked up above background levels.

Thus AMPKα as well as pAMPKα get knocked down following AAV6-Cre-GFP infection in neuronal culture compared to neuronal cultures infected with AAV6-GFP.

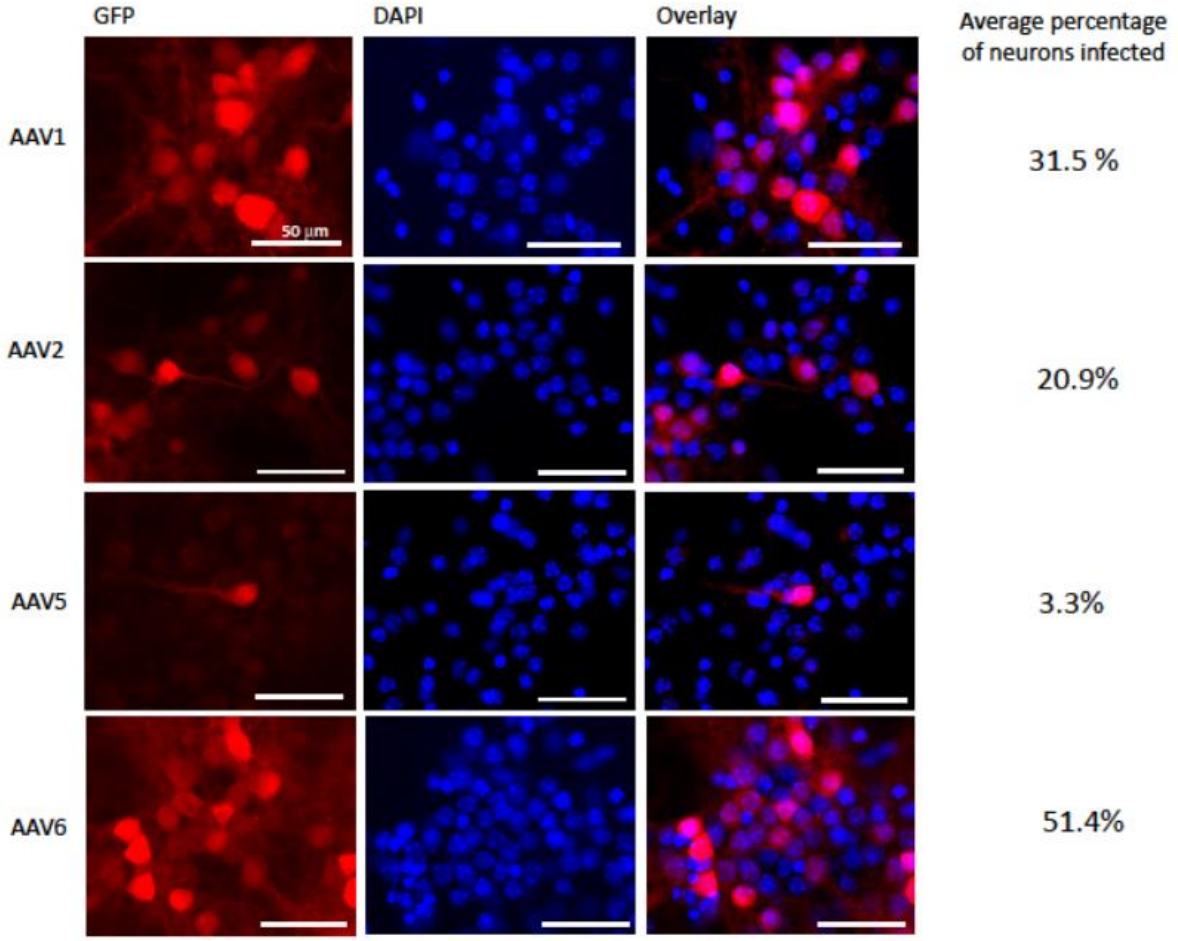

Figure 3.2. The AAV6 virus has the best infection efficiency of neurons in culture out of the different viruses tested (AAV1, 2, 5 and 6). Pictures of neuronal cultures immunostained with GFP, DAPI and their overlay are shown for the four viruses (AAV1, 2, 5 and 6). The percentage of neurons infected with the virus was calculated from the images and the average percentage of neurons infected (from 2 images) for each virus is shown on the right. 10^{10} genome copies (GC) were added/well for all 4 AAV types. This is equal to around $2.5x10^4$ GC/cell.

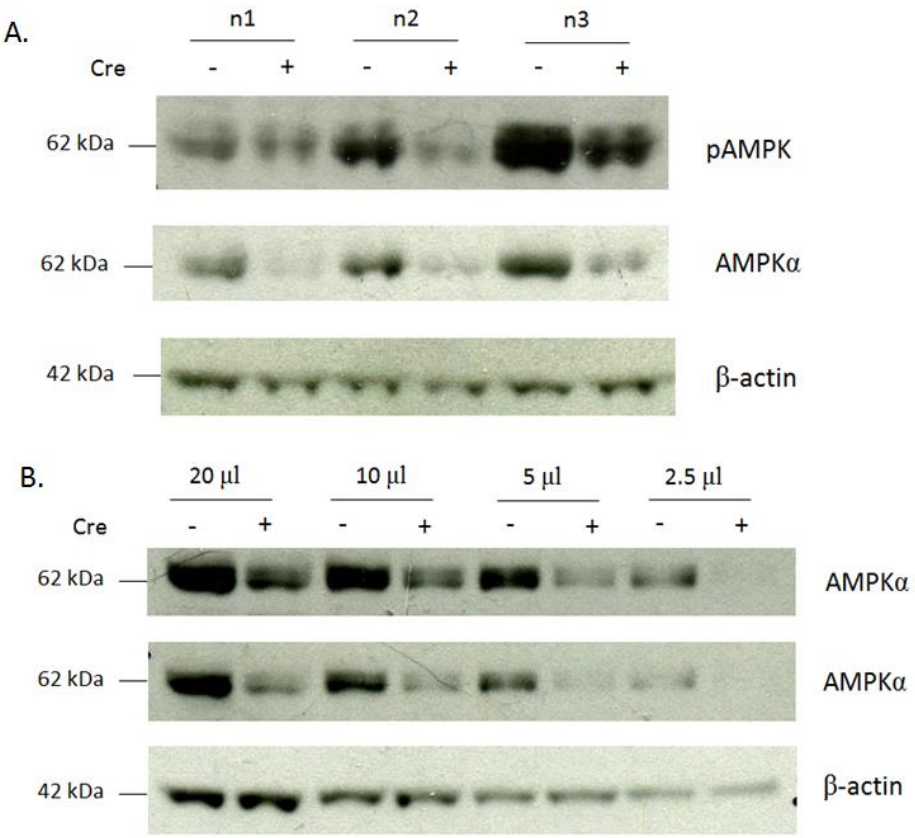

Figure 3.3. AMPKα expression is decreased in AMPKα1 and 2 floxed mouse mixed neuronal cultures infected with AAV6-Cre-GFP. A. AMPKα KD by AAV6-Cre-GFP in AMPKα1/2flx mouse cultures causes a decrease in AMPKα expression as well as pAMPK levels compared to the controls infected with AAV6-GFP (n=4). A pan-AMPKα antibody was used. n1, 2 and 3 represent samples from different cultures. **B.** Titration of n1, showing that there is around a 75% AMPK KD in AAV6-Cre-GFP treated samples compared to the control samples. Two different exposures of AMPKα are shown to portray the protein expression levels clearly for both ends of the serial dilution. A similar degree of AMPK KD was observed in the other three samples (not shown).

3.2.3. AMPKα knockdown is neuroprotective against excitotoxic cell death

Next, I examined the effect of AMPK KD on NMDA-mediated excitotoxic cell death. AMPK has been shown to be a mediator of excitotoxic cell death through inducing transcription of the pro-apoptotic BH3-only gene Bim (Davila et al. 2012; Concannon et al. 2010). Our lab generally uses a cell death assay in which a range of NMDA concentrations (0-50 µM) are added for an hour to cultures followed by addition of NMDAR blocker MK-801, with cultures fixed the following day (Qiu et al. 2013). I also tested a different assay used by Concannon *et al*. to induce excitotoxic cell death, where different NMDA concentrations (0-100 µM) were added for 10 minutes followed by two washes instead of MK-801 application (Concannon et al. 2010). This protocol was suggested to kill neurons through apoptosis, unlike our protocol which induces neuronal death through several different pathways. I found the protocol used by Concannon *et al*. quite variable, thus I adapted a block with MK-801 following the 10 minute NMDA insult instead of the washes, and found the results to be more consistent. Unfortunately, this cell death assay produced cell death levels which were too low to observe a rescue from, even at a 100 µM NMDA (Supplementary figure 1), thus I decided to use our 1 hour NMDA cell death assay protocol. The EC_{50} concentration for the 1h NMDA stimulation was around 30 µM NMDA.

The cell death assay was performed on primary cortical cultures from AMPKα1/2flx mice treated with either AAV6-Cre-GFP or AAV6-GFP (for AMPKα KD and control respectively). The percentage of neuronal death following NMDA application to cultures was calculated from images of DAPI staining (Fig 3.4B). There was a small but significant reduction in cell death following 30, 40 and 50 µM NMDA stimulation in AAV6-Cre-GFP treated samples compared to those treated with AAV6-GFP (Fig 3.4A). Thus, AMPKα KD in cortical cultures is neuroprotective against excitotoxic cell death.

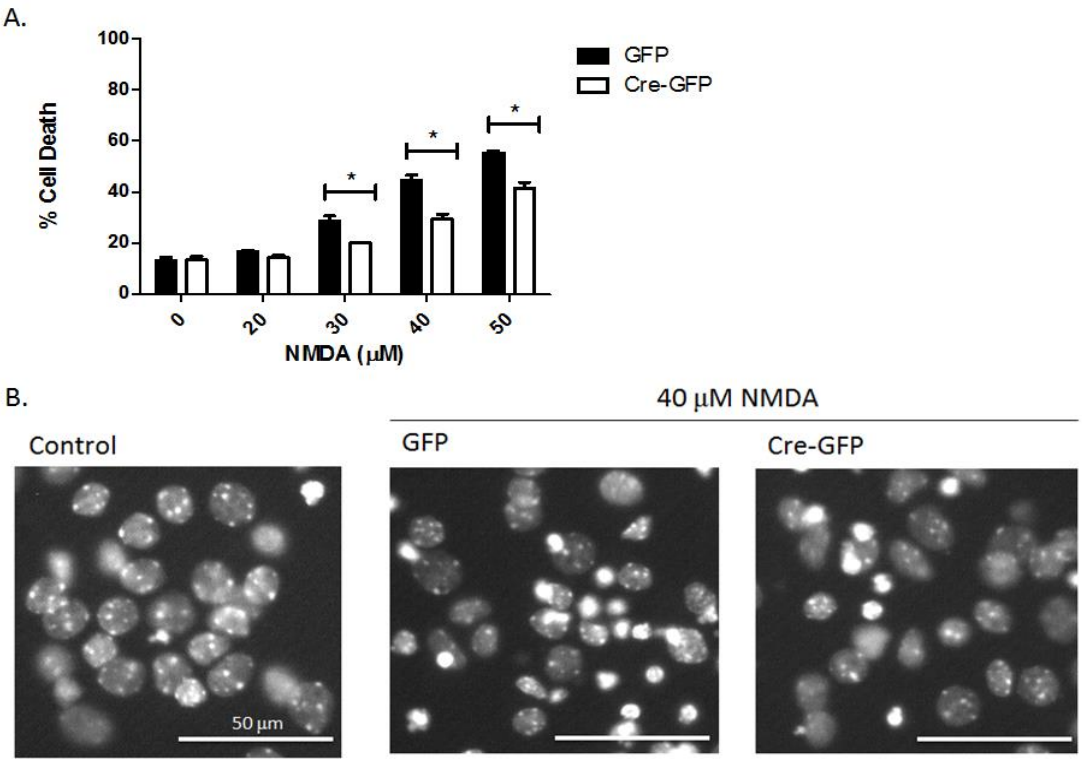

Figure 3.4. AMPKα KD in primary cortical cultures made from AMPKα1/2flx mice decreases cell death caused by excitotoxicity. A. Cell death was induced by different concentrations of NMDA (0-50 μM) applied for 1 h. Cell death is shown as the overall percentage of dead neurons in the culture, calculated from 4 images/n, with each image containing around 3-400 neurons. n=4. Error bars=SEM. *p<0.05 between the control and AMPK KD samples at different concentrations of NMDA, analysed using a 2-way ANOVA with Bonferroni *post-hoc* test. **B.** Example pictures of the neurons with DAPI staining from the control and after applying 40 μM NMDA to GFP or Cre-GFP treated neurons.

3.2.4. AAV6-Cre-GFP infected neurons in AMPKα1/2 floxed cultures are partially rescued from excitotoxic cell death

Although a significant reduction in cell death following AMPKα KD in the whole culture was established, I wanted to examine whether this was due to the neurons in which AMPKα was knocked down themselves, since I only found 50-60% of cells to be infected with AAV6-Cre-GFP and around a 75% KD of AMPKα protein in cultures (Section 3.2.2). Thus, the fate of individual GFP-infected neurons was followed over 2 consecutive days in the cultures described in section 3.2.3, to confirm that the cell death was caused by AMPK KD itself. Pictures were taken of GFP-infected neurons prior to the NMDA insult and before the cells were fixed, from which the fate of individual neurons was followed and the percentage of dead neurons was calculated. An example of following the fate of an individual neuron can be seen in Fig.3.5B. There was a reduction in cell death in neurons treated with AAV6-Cre-GFP following 30, 40 and 50 μM NMDA treatment compared to control neurons treated with AAV6-GFP, although the decrease in cell death was only significant following 30 or 40 μM NMDA application (Fig.3.5A). This may be due to following the fate of only a small number of neurons in these experiments. The basal cell death was much lower when following GFP-infected neurons than in the whole culture. This was not due to GFP-infected neurons being healthier, but because only neurons which were alive before NMDA treatment were examined, whilst the whole culture will have had basal cell death prior to NMDA treatment and these cells were also counted. Although in both analyses, neuronal death was found to be similar in WT and AMPKα treated cultures at baseline and following mild NMDA treatment (20 μM NMDA). Cell death was much higher when following individual neurons, which was likely due to AAV6-infected neurons being much more vulnerable to cell death than other uninfected neurons in the culture. Thus, the neuroprotection observed following AMPKα KD against excitotoxic cell death, is due to the AAV6-Cre-GFP infected neurons in the culture.

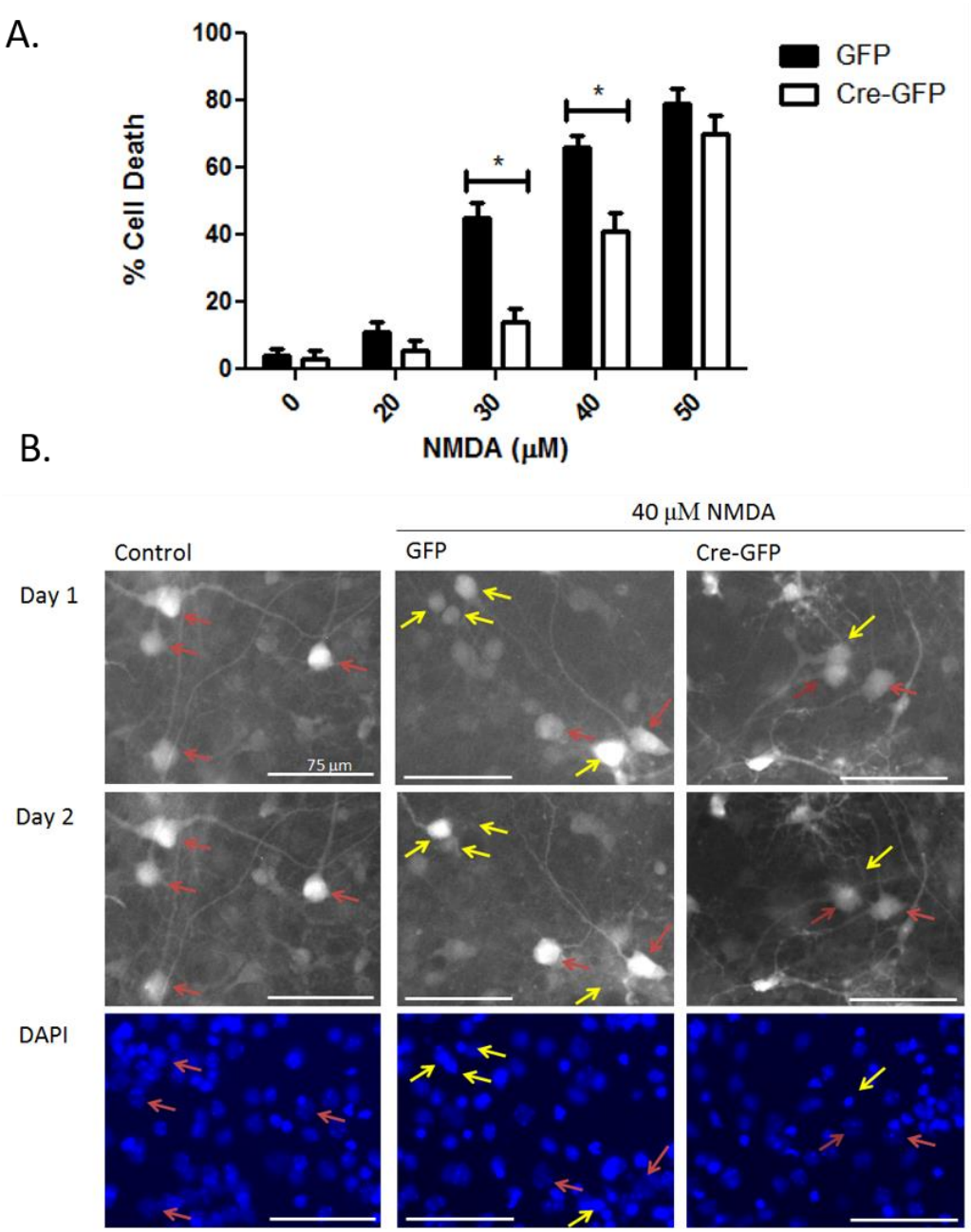

Figure 3.5. AAV6-Cre-GFP infected neurons in AMPKα1/2flx culture show decreased cell death following an excitotoxic insult. Cell death was induced by different concentrations of NMDA (0-50 µM) applied for 1 h. Cell death was calculated from individual GFP infected neurons (n=10/image), by observing the viability of cells over the course of 2 consecutive days, and the mean cell death of 10 neurons/image was calculated. **A.** Percentage cell death caused by different concentrations of NMDA in neurons with or without AMPKα. **B.** An example of how the number of dead cells was calculated. Images of the live GFP or Cre-GFP infected neurons untreated or treated with 40 µM NMDA on days 1 and 2 are shown, as well as the corresponding DAPI pictures taken after fixing the cells to confirm cell death. Red arrows show cells which were still alive on Day 2, and yellow arrows show cells which died between Day 1 and Day 2. n=4. Error bars=SEM. *p<0.05 between GFP and Cre-GFP virus treated samples at different concentrations of NMDA, analysed by a 2-way ANOVA with Bonferroni *post-hoc* test.

3.2.5. Mcu KD has no significant effect on pAMPK levels in neurons at baseline or following NMDA stimulation

Mitochondrial dysfunction has long been known to help mediate excitotoxic cell death, and Mcu which has recently been identified as Ccdc109a was hypothesised to mediate this effect (Baughman et al. 2011; De Stefani et al. 2011). Our group recently confirmed the role of Mcu as an important mediator of excitotoxicity (Qiu et al., 2013). Mcu KD led to decreased mitochondrial Ca^{2+} influx, and rescued neurons from cell death and mitochondrial depolarisation. Although the role of Mcu in excitotoxic cell death is now established, which downstream pathways it targets to achieve this is still unclear.

AMPK undergoes allosteric activation after AMP binds to its γ subunit, and can then be phosphorylated by its upstream kinase LKB-1 on Thr172 on its α subunit (Woods et al. 2003; Hawley et al. 2003). Decrease in ATP levels following mitochondrial dysfunction due to an excitotoxic insult has been shown to activate AMPK previously in CGNs (Concannon et al. 2010; Davila et al. 2012). Following observations made in sections 3.2.3 and 3.2.4 that AMPK plays a destructive role in NMDA-mediated excitotoxicity, I hypothesised that AMPK may be a downstream effector of Mcu.

To test whether AMPK is downstream of Mcu, Mcu was knocked down in WT mouse cortical cultures by Mcu-shRNA virus or Scrambled-shRNA virus was added to controls on DIV2, and their effect on pAMPKα and total pan-AMPKα protein levels was investigated. AMPKα levels were examined at baseline, as well as following 30 µM NMDA insult for 30 minutes with or without Mcu KD. For examples of blots see Fig.3.6A. Samples treated with Mcu-shRNA showed a marked significant decrease in Mcu levels compared to samples treated with Scr-shRNA (Fig.3.6C). pAMPK levels were quite variable in the Mcu-shRNA control compared to the Scr-shRNA control, but overall there was no significant effect on pAMPK levels between the Scr and Mcu KD in either the control or following 30 µM NMDA treatment for 30 minutes (Fig.3.6B). Thus, these results show that activation of AMPK is not downstream of Mcu, or the resulting mitochondrial dysfunction, following an excitotoxic insult.

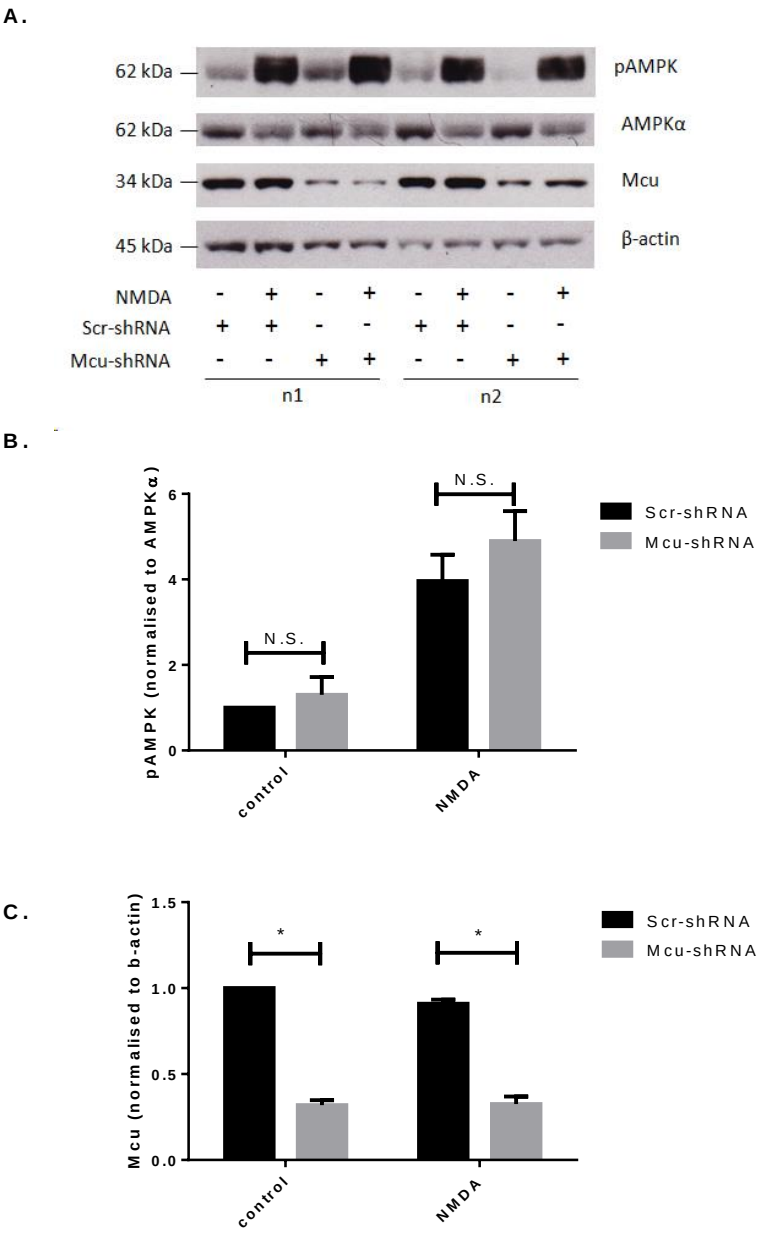

Figure 3.6. Mcu KD by Mcu-shRNA has no significant effect on pAMPK levels in neurons. A. Example blot for two different experiments where Mcu protein levels were knocked down by Mcu-shRNA virus. pAMPKα, pan-AMPKα, Mcu and β-actin are shown with no treatment and after treatment with 30 µM NMDA for 30 minutes. **B.** Analysis of Western blots for pAMPK protein levels when normalised to AMPKα **C.** Analysis of Western blots for Mcu protein levels when normalised to β-actin loading control. n=5 for both (b) and (c). Error bars=SEM. *p<0.05 compared to Scr-shRNA, analysed with a two-way ANOVA with Bonferroni *post-hoc* test. N.S.=not significant.

3.3. Discussion

3.3.1. Conclusion

I hypothesised that AMPK would be a downstream effector of Mcu in excitotoxicity. The experiments presented in this chapter clearly demonstrate that AMPK plays a small, but significant role in mediating NMDA-induced excitotoxic cell death; but AMPK activation is not a result of Ca^{2+} influx through Mcu and the subsequent decrease in mitochondrial membrane potential leading to ATP depletion, as pAMPK protein levels are not significantly altered following Mcu KD. Thus even though AMPK plays a role in NMDA-induced excitotoxicity, its mode of activation as well as the downstream targets of Mcu-mediated cell death during excitotoxicity remain unknown. At basal and more physiological NMDA concentrations (20 µM), AMPKα1/2 KD did not induce cell death, possibly indicating that AMPK only promotes cell death following application of pathological NMDA concentrations.

3.3.2. AMPK plays a small but significant role in NMDA-induced excitotoxicity in cortical neurons

AMPK has previously been implicated to have a dual role in excitotoxic cell death. Transient AMPK activation has been shown to be neuroprotective during excitotoxicity (Anilkumar et al. 2013; Culmsee et al. 2001; Weisova et al. 2009; Weisová et al. 2012). Indeed, levels of cell death were not significantly different basally and following 20 µM NMDA application in AAV6-GFP and AAV6-Cre-GFP treated AMPKα1/2flx cortical culture Fig.3.5A and 3.6A. This indicates that AMPK does not mediate cell death at baseline or at low levels of NMDA treatment, which is in line with previous observations that AMPK does not induce cell death following transient increases in pAMPK (Davila et al. 2012). Although transient activation of AMPK is thought to have neuroprotective effects, I did not observe this following the addition of 20 µM NMDA, since there was no increase in cell death following AMPKα1/2 KD. AMPKα1/2 KD at higher NMDA concentrations (30, 40 and 50 µM NMDA) had a protective effect against excitotoxic cell death, both on the whole culture level and when following the fate of GFP-infected neurons. A higher overall cell death was detected in GFP-infected neurons, likely due to the viral infection making neurons more vulnerable to the excitotoxic insult. The protection provided by AAV6-Cre-GFP over AAV6-GFP to neurons against excitotoxic cell death following 30 and 40 µM NMDA was larger when looking at individual neurons than in the overall culture, showing that the protection in these culture was indeed due to AMPKα1/2 KD. These results agree with previous studies showing that prolonged AMPK activation mediates glutamate and NMDA-induced cell death in neurons (Concannon et al. 2010; Davila et al. 2012).

AMPK promotes ATP-producing pathways, whilst downregulating ATP consuming pathways in cells (Hardie et al. 2012). This can be protective short term, but cannot help neurons recover from a severe excitotoxic insult. A two-step computational model proposed by Davila *et al*. attempts to explain the dual role of AMPK on neuronal fate following glutamate exposure (Davila et al. 2012). Firstly, AMPK downregulates the Akt pathway promoting the translocation of dephosphorylated FOXO3 to the nucleus, and secondly FOXO3 is phosphorylated by AMPK in the nucleus to promote increased expression of Bim. Since the first step of the process takes some time, the second step only occurs following prolonged AMPK activation. Although the pro-death role of prolonged AMPK activation in excitotoxicity has been demonstrated, it was done using AMPK KD by siRNA or pharmacological inhibition by Compound C, rather than using neurons from an AMPK KO mouse. For the first time, I show that AMPK plays a destructive role in NMDA-induced excitotoxicity in cortical neurons using an AMPKα1/2 conditional KO mouse. Further experiments will need to be carried out to establish the role of AMPK in excitotoxicity *in vivo*.

It is important to note, that my excitotoxic cell death assay differed from that used by Concannon *et al*., and that my approach leads to a number of cell death pathways, and not only delayed apoptotic cell death (Concannon et al. 2010). Thus, it is possible that using this assay AMPK mediates cell death not only through Bim-mediated apoptosis as seen by Concannon *et al*., but also through other pathways. Therefore, the downstream mediators of AMPK during excitotoxicity in cortical cultures should be further investigated.

Although I found AMPK activation to have pro-death effects during excitotoxicity, its potential pro-survival effects under different experimental conditions cannot be ruled out. Preconditioning with FCCP to activate AMPK has been shown to be neuroprotective against subsequent excitotoxic insult, whilst preconditioning with low levels of AICAR to activate AMPK is neuroprotective against oxidative, excitotoxic and metabolic insults in neurons (Weisová et al. 2012; Culmsee et al. 2001; Anilkumar et al. 2013), similarly to neuroprotection provided by NMDAR activation following ischaemic preconditioning or preconditioning by neuronal activity. Thus, it is tempting to speculate that preconditioning with synaptic activity may transiently activate AMPK, providing the neuron with protective effects against later insults. AMPK activation may follow the dual role of NMDAR activation whereby it exerts neuroprotective effects following transient activation by synaptic activity and neurodestructive effects following excessive NMDAR activation.

3.3.3. AMPK activation is not dependent on Mcu during excitotoxicity

Mitochondrial dysfunction plays a large role in excitotoxic cell death, and has long been thought to be mediated by Mcu allowing Ca^{2+} influx into the mitochondria following an excitotoxic insult (Hardingham 2009). Due to the recent molecular identification of Mcu (De Stefani et al. 2011; Baughman et al. 2011), our group was able to KD Mcu and demonstrate that it mediates mitochondrial dysfunction and subsequent cell death following NMDA-induced excitotoxicity (Qiu et al. 2013). Thus, I investigated whether AMPK was a downstream effector of Mcu during excitotoxicity. Various groups have shown a decrease in ATP levels and mitochondrial dysfunction following NMDA or glutamate exposure leading to an increase in AMPK levels (Weisova et al. 2009; Concannon et al. 2010). I demonstrate in this chapter that AMPK is activated by different NMDA concentrations, and our group recently showed a decrease in ATP levels following exposure of neurons to 100 µM NMDA as well as after milder synaptic activity (Hasel et al. 2015). This could explain transient AMPK activation being neuroprotective and prolonged AMPK activation leading to excitotoxic cell death, as both milder and more severe stimuli decrease ATP levels and most likely increase pAMPK levels. Decreased ATP levels following NMDA stimulation leads to increased ADP and AMP levels, which bind to AMPK allosterically activating it and triggering AMPKα phosphorylation at Thr172 by LKB-1 (Carling et al. 2008). Surprisingly, my results showed that Mcu KD does not affect pAMPK levels basally or following NMDA stimulation, suggesting that AMPK is not downstream of Mcu-mediated decrease in ATP levels during excitotoxicity.

Previous research has implicated Mcu upstream of AMPK activation. Blocking Mcu with Ru360 was shown to increase pAMPK levels, whilst Mcur1 KD, a protein thought to regulate Mcu, has been shown to result in an increased AMP:ATP ratio leading to AMPK activation (Cárdenas et al. 2010; Mallilankaraman et al. 2012a). Both of these results suggest that AMPK is activated following decreased mitochondrial Ca^{2+} influx. This is likely due to the dual role of mitochondrial Ca^{2+} in regulating cell fate, since physiological mitochondrial Ca^{2+} levels promote cell survival, whilst both too little and too much mitochondrial Ca^{2+} influx promote cell death. Overactivation of Mcu leads to mitochondrial depolarisation and decreases in ATP, whilst Mcu block may decrease respiration resulting in decreased ATP production, thus both could lead to AMPK activation. Additionally, Ru360 and Mcur1 KD could have off target effects causing AMPK activation. The results shown in this thesis using a direct Mcu KD, rather than pharmacological inhibition is more likely to be accurate.

It is a possibility that Mcu KD was not sufficient enough to effect pAMPK levels, and perhaps using an Mcu KO mouse may give more conclusive results. KD of Mcu in AMPKα1/2 mouse cultures could help to determine whether these two pathways are distinct and whether they mediate additive neurodestructive effects during excitotoxicity. It is quite likely that AMPK is activated through a different pathway, possibilities of which are outlined below.

The lack of change in AMPK activation upon Mcu KD means that the search for the downstream effector(s) of Mcu continues. There are several possible pathways through which Mcu could mediate its effect. One possibility is the activation of PARP-1, which is activated following DNA damage caused by peroxynitrite (Duchen 2012). Peroxynitrite is formed by NO, produced by nNOS, and superoxide, which is released primarily from mitochondria following an excitotoxic insult leading to mitochondrial depolarisation due to Mcu-mediated Ca^{2+} uptake, but can also be produced by NADPH oxidase (Duan et al. 2007; Duchen et al. 2008; Duchen 2012). Thus, peroxynitrite activates PARP-1, which forms poly-ADP ribose (PAR) polymers, which promote the release of the apoptosis-inducing factor (AIF) from mitochondria leading to PARP-1 dependent (caspase-independent) cell death (Duan et al. 2007; Yu et al. 2002). Furthermore, PARP-1 activation depletes NAD^+ which may help induce mitochondrial depolarisation (Duchen 2012). c-Jun N-terminal protein kinase (JNK) has also been shown to be activated by ROS production by mitochondria, making it another potential downstream effector of Mcu-mediated Ca^{2+} uptake-induced cell death (Soriano et al. 2008b). Ca^{2+} uptake through Mcu following an excitotoxic insults causes Ca^{2+} accumulation in the mitochondria, and may lead to the opening of the mitochondrial permeability transition pore (mPTP) resulting in the release of cytochrome C from mitochondria initiating apoptosis (Brustovetsky et al. 2002; White & Reynolds 1996; Ichas & Mazat 1998; Orrenius et al. 2003; Bernardi & Rasola 2007; Abramov & Duchen 2008).

3.3.4. Possible alternative pathways of AMPK activation in cortical neurons

Since I found that AMPK helps to mediate excitotoxicity, but is not downstream of Mcu, alternative pathways playing a possible role in its activation need to be further explored.

3.3.4.1. Which upstream kinase is responsible for AMPK activation?

Results by Concannon *et al*. and Davila *et al*. point to AMPK activation following mitochondrial dysfunction and an increased AMP:ATP ratio, likely mediated by LKB-1 which phosphorylates AMPK following AMP binding (Davila et al. 2012; Concannon et al. 2010). Indeed, Weisova *et al*. demonstrated that CaMKKβ blocker KN-93 did not inhibit GLUT3 translocation mediated by AMPK activation, implicating LKB1 as the upstream kinase of AMPK in CGNs (Weisova et al. 2009). Although there is a definite drop in ATP levels

following NMDA stimulation that would lead to an increase in ADP and AMP levels, whether this decrease in ATP levels is downstream of Mcu and mitochondrial dysfunction is unclear. Our group recently demonstrated using the genetically encoded probe AT1.03 that ATP levels in neurons drop within minutes, prior to mitochondrial dysfunction occurring (Hasel et al. 2015). This suggests that the initial drop in ATP levels is not downstream of Mcu-mediated Ca^{2+} uptake leading to mitochondrial depolarisation and the reversal of the mitochondrial ATPase, but stems from a different source. Indeed, overactivation of the Na^{+}/K^{+} ATPase on the plasma membrane following an excitotoxic insult can cause increases in the AMP:ATP ratio (Greenwood & Connolly 2007), which could lead to activation of AMPK by LKB-1, independently of Mcu and mitochondrial dysfunction.

Although Weisova *et al.* did not find CaMKKβ to be important in activating AMPK in CGNs (Weisova et al. 2009), it does not mean that it cannot phosphorylate AMPK in other neuronal subtypes, at different developmental time points or using different excitotoxic cell death assays. CaMKKβ is an attractive candidate for AMPK phosphorylation following excitotoxicity, due to its activation following rises in intracellular Ca^{2+} (Woods et al. 2005). CamKKβ has been shown to have high expression levels in the brain (Woods et al. 2005), and I found both LKB1 and CaMKKβ mRNA to be expressed in our primary cortical cultures (Márkus and Hardingham unpublished RNA-seq data). AMPK activation by CaMKKβ has been demonstrated by a number of groups in different neuronal subtypes. CamKKβ was shown to be involved in activating AMPK in the hypothalamus (K. Anderson et al. 2008), while Mairet-Coello *et al*. showed that AMPK phosphorylation following NMDA activation is eliminated by CaMKK inhibitor STO-609 in mature mouse primary cortical and hippocampal neurons (DIV21) (Mairet-Coello et al. 2013). STO-609 also inhibited the AMPK phosphorylation in rat cortical slices following high K^{+} induced depolarisation leading to Ca^{2+} influx, which was independent of ATP loss (Hawley et al. 2005); confirming previous findings that the presence of AMP is not required for AMPK activation by CaMKKβ (Woods et al. 2005). Thus, it is entirely possible that AMPK is activated by CaMKKβ in our cortical cultures, independently of ATP loss and this should be further investigated.

AMPK has been suggested to translocate to the nucleus following insults in HeLa cells (Kodiha et al. 2007). Interestingly, AMPKα2 was shown to preferentially localise to the nucleus in neurons and other cells, suggesting a possible subunit specific effect of AMPKα2 activation on mediating changes in gene transcription (Turnley et al. 1999; Salt et al. 1998). If AMPKα2 is localised to the nucleus basally, it may need nuclear Ca^{2+} to be activated by CaMKKβ, which would mean that excessive activation of NMDARs would be required for

the second step of FOXO3 activation suggested by Davila *et al*. and may be subunit specific. The subunit specificity of AMPK would be intriguing to investigate, since the two different α subunits may effect different downstream cascades. The spatio-temporal profile of AMPK activation could be tested to allow for a better understanding of the cellular location of AMPK. I tried imaging AMPK in real-time using an AMPK FRET probe (Tsou et al. 2011), but found it to have narrow dynamic range; nevertheless similar probes could be used to test AMPK activity following NMDA application in real-time.

It is possible that AMPK is activated by both LKB1 and CaMKKβ in cortical neurons, and that the mode of activation depends on the duration and intensity of NMDAR activation, as well as the NMDAR subunit composition or possibly the site of Ca^{2+} entry. These factors could determine the duration of AMPK activation and thus whether this activation provides neuroprotection or contributes to neuronal death. It is also possible that activation of AMPK by CaMKKβ only occurs following excessive NMDAR activation and large influxes of Ca^{2+}, mediating its pro-death effect. Inhibition of CamKKβ with STO-609 or other CaMKK inhibitors during NMDA application should show whether the CamKKβ pathway is involved in activating AMPK during excitotoxicity in our cortical cultures. It is also likely that expression of LKB1 and CaMKKβ differs in neuronal subtypes, such as CGNs and cortical neurons, which may result in activation of AMPK through different pathways in these neurons.

3.3.4.2. AMPK activation in neurological disorders involving excitotoxicity

AMPK has been implicated in a number of different neurodegenerative conditions, such as Alzheimer's disease (AD). Thornton *et al*. and Mairet-Coello *et al*. demonstrated that toxic amyloid β (Aβ) activates AMPK via CaMKKβ promoting phosphorylation of Tau in mature neurons, the hyperphosphorylation of which plays an important role in AD (Mairet-Coello et al. 2013; Thornton et al. 2011). Mairet-Coello *et al.* demonstrated that activation of the CaMKKβ-AMPK pathway by toxic Aβ mediates the loss of dendritic spines through phosphorylation of Tau both in hippocampal neurons *in vitro* and in a mouse model of AD *in vivo* (Mairet-Coello et al. 2013). Both groups found that toxic Aβ exerted its effect through NMDAR activation. Intriguingly, Thornton *et al*. showed that pre-treatment of neurons with memantine, a mild NMDAR antagonist licensed for AD treatment, inhibited NMDA-induced activation of AMPK by CaMKKβ (Thornton et al. 2011). This is of interest, since memantine is thought to allow synaptic NMDAR activity, whilst preferentially blocking pathological NMDAR activation, suggesting that AMPK may be preferentially activated following excessive NMDAR activation.

Intriguingly, AMPK was found to be phosphorylated following middle cerebral artery occlusion (MCAO), which was abolished in an nNOS KO mouse, suggesting that AMPK activation may be activated downstream of nNOS (McCullough et al. 2005). McCullough *et al*. found that KO of PARP-1 did not abolish AMPK phosphorylation by MCAO, suggesting that AMPK is downstream of nNOS, but not PARP-1. Of note, AMPK has been suggested to be activated by peroxynitrite itself, independently of AMP, in endothelial cells (Zou et al. 2003), providing a potential explanation for the above results. Although, superoxide used in the formation of peroxynitrite is thought to be primarily mitochondrial in origin, possibly implicating Mcu in this pathway (Duan et al. 2007). It is possible that AMPK is activated due to NO production itself, since AMPK has been shown to be phosphorylated by CaMKKβ following rises in ROS following hypoxia, independently of changes in ATP levels (Mungai et al. 2011). This further suggests that prolonged AMPK activation may be coupled to pathological NMDAR activation, since nNOS is known to associate with the C terminal of the NMDA GluN2B subunit via PSD-95, which is preferentially coupled to excitotoxic cell death (Martel et al. 2012). The possibility of AMPK being preferentially activated downstream of Glun2B containing NMDARs could be tested using a knock-in mouse previously employed by our group, in which the C terminal tail of the GluN2B subunit is switched with that of GluN2A (Martel et al. 2012).

Thus, how AMPK is activated during excitotoxicity is yet to be established. It is entirely possible that the AMPK phosphorylation in neurons is controlled by multiple pathways, the activation of which may depend on the duration and intensity of NMDAR activation as well as the neuronal subtype and developmental stage, and may decide the duration of AMPK activation and whether it has pro-survival or pro-death consequences. Various groups have demonstrated a role for AMPK in stroke, as well as in Alzheimer's and Huntington's disease (Mairet-Coello et al. 2013; Ju et al. 2012; Thornton et al. 2011; Manwani & McCullough 2013; Cai et al. 2012; McCullough et al. 2005). Although AMPK is shown to be protective in some diseases, it is not in others. Nevertheless, I find AMPK to have a destructive role in NMDA excitotoxicity *in vitro* in primary cortical cultures, making it a potential therapeutic target alongside Mcu, as well as their downstream effectors, in treating diseases involving NMDAR-mediated excitotoxic cell death, such as stroke and chronic neurodegenerative diseases. It would be interesting to examine AMPK downstream of pathological NMDA receptor activation *in vivo* in the conditional AMPKα1/2 KO mouse, to determine whether these results translate *in vivo*.

Chapter 4: Mitochondrial Ca^{2+} regulatory genes are differentially expressed in neurons and astrocytes and in different neuronal subtypes

4.1. Introduction

Mitochondrial Ca^{2+} uptake plays a role in regulating energy production, buffering cytosolic Ca^{2+} as well as mediating cell death (McCormack et al. 1990; Hajnóczky et al. 1999; Bernardi & Rasola 2007). Thus, the handling of mitochondrial Ca^{2+} basally and following cytoplasmic Ca^{2+} influx from the plasma membrane or intracellular stores is key to cell survival, especially in neurons which have a high metabolic demand and rely heavily on oxidative phosphorylation as their source of ATP (Fernandez-Fernandez et al. 2012; Harris et al. 2012; Kann & Kovács 2007). The molecular identity of several mitochondrial Ca^{2+} regulatory genes (MCRGs) has come to light in recent years, which influence mitochondrial Ca^{2+} influx and efflux thereby playing a role in maintaining mitochondrial health and neuronal survival.

Mcu was identified as the channel pore of the mitochondrial Ca^{2+} uniporter on the IMM (De Stefani et al. 2011; Baughman et al. 2011). Mcu is predicted to oligomerise into tetramers to create the channel pore, allowing Ca^{2+} uptake into the mitochondrial matrix (Lee et al. 2015; Raffaello et al. 2013; Chaudhuri et al. 2013). Several genes have been identified which are present in the Mcu complex (Emre, Micu1 and Micu2), thought to be around 450 kDa, or that regulate Mcu in some other way (Baughman et al. 2011). Mcub is the dominant negative isoform of Mcu, which can oligomerise with Mcu preventing Ca^{2+} influx through the channel pore (Raffaello et al. 2013). Emre anchors Micu1 and Micu2 to Mcu and is essential for Mcu function (Sancak et al. 2013; Tsai et al. 2016; Vais et al. 2016; Yamamoto et al. 2016). Micu1 and 2 are gatekeepers of Ca^{2+} influx at low cytosolic Ca^{2+} concentrations, blocking Mcu's pore using their Ca^{2+}-sensing EF-hands, and Micu1 positively cooperates with Mcu at higher cytosolic Ca^{2+} concentrations, allowing increased Ca^{2+} influx, following Ca^{2+} binding to its EF-hands inducing a conformational change (Perocchi et al. 2010; Csordás et al. 2013; Plovanich et al. 2013; Wang et al. 2014; Sancak et al. 2013; Kamer & Mootha 2014; Mallilankaraman et al. 2012b; Matesanz-Isabel et al. 2016; de la Fuente et al. 2014; Waldeck-Weiermair et al. 2015). Micu3, a paralogue of Micu1 and 2, has been described as a probable Mcu regulator in the CNS, but its function has not been further investigated (Plovanich et al. 2013). Mcur1 is another possible regulator of Mcu, although it does not appear to be part of the Mcu-Emre-Micu1/2 uniporter complex (Mallilankaraman et al. 2012a; Paupe et al. 2015; Sancak et al. 2013; Lee et al. 2015). Slc25a23 is a solute carrier which mediates Mg-ATP/Pi exchange across the IMM, and has recently been shown to accelerate Mcu-mediated Ca^{2+} influx during high cytoplasmic Ca^{2+} levels in neurons (Hoffman et al. 2014; Llorente-Folch et al. 2015; Rueda et al. 2014). Uncoupling protein 2 (Ucp2) and 3 (Ucp3) have also been suggested to regulate Mcu-dependent mitochondrial Ca^{2+} uptake following large cytoplasmic Ca^{2+} influxes (Trenker et al. 2007; Waldeck-Weiermair et al. 2010; Waldeck-Weiermair et al.

2011; Bondarenko et al. 2015). Several possible routes of Ca^{2+} entry into the mitochondrial matrix independent of Mcu have been described, including Ryr and Trpc3 (Jakob et al. 2014; Feng et al. 2013). Mitochondrial Ca^{2+} efflux is thought to occur through a Li^{+}-sensitive Na^{+}/Ca^{2+} exchanger in excitable and H^{+}/Ca^{2+} exchanger in non-excitable cells (Palty & Sekler 2012). Letm1, thought to be the Ca^{2+}/H^{+} exchanger, has been found to mediate not only Ca^{2+} efflux, but also Ca^{2+} influx at low mitochondrial Ca^{2+} concentrations (Jiang et al. 2009; Tsai et al. 2014). Nclx was identified as the Na^{+}/Ca^{2+} exchanger in 2010, and shown to mediate mitochondrial Ca^{2+} efflux through the IMM (Palty et al. 2010).

Although many MCRGs have been shown to be expressed in the brain (Raffaello et al. 2013; Plovanich et al. 2013; Mallilankaraman et al. 2012a; De Stefani et al. 2011; De Stefani et al. 2016), their mRNA expression pattern and function in different neural cells and neuronal subtypes has not been investigated and may vary, potentially influencing mitochondrial Ca^{2+} handling in these cell types. Since multiple different mitochondrial Ca^{2+} influx and efflux pathways, as well as different regulators of Mcu seem to co-exist, it would be important to determine which MCRGs are highly expressed in neurons, and whether a different expression profile of MCRGs may make certain subtypes of neurons more vulnerable to insults.

In chapter 3, I examined the possible role of AMPK downstream of Mcu following an excitotoxic insult, and although I found AMPK to help mediate excitotoxic cell death, Mcu KD had no effect on AMPK phosphorylation. Nevertheless, Mcu's importance in excitotoxicity has been previously demonstrated by our group (Qiu et al. 2013). It is likely that other MCRGs also play a role in NMDA-mediated excitotoxic cell death in neurons. Interestingly, neurons of the CA1 region of the hippocampus show higher sensitivity to superoxide and NMDA-mediated excitotoxic insult, than CA3 neurons (Strasser & Fischer 1995; Ikegaya & Matsuki 2002; Cronberg et al. 2005; Gee et al. 2006; Yang et al. 2000; Wilde et al. 1997), to which neuronal subtype-specific MCRG expression may contribute.

In this chapter I investigate the expression pattern of MCRG mRNA in different neural cells (mouse primary cortical neurons vs astrocytes) as well as in different neuronal subtypes (CA1 vs CA3 neurons of the adult mouse hippocampus). I found differential MCRG mRNA expression patterns in different neural cells and neuronal subtypes. Of note, I found Nclx mRNA to be expressed at very low levels in neurons compared to astrocytes, questioning whether Nclx is indeed the major mitochondrial Ca^{2+} efflux pathway in neurons; and thus investigated its function in neurons vs astrocytes further using Nclx inhibitor CGP-37157, and surprisingly found that it inhibited Ca^{2+} efflux in both neurons and astrocytes.

Some of the results in this chapter have been published in:

Márkus, N.M. et al., 2016. Expression of mRNA Encoding Mcu and Other Mitochondrial Calcium Regulatory Genes Depends on Cell Type, Neuronal Subtype, and Ca^{2+} Signaling. *PLOS ONE*, 11(2), p.e0148164.

4.2. Results

4.2.1. mRNA expression of MCRGs differs between cortical neurons and astrocytes

I examined the mRNA expression of MCRGs by real-time (RT)-qPCR in a mouse primary cortical astrocyte-free neuronal culture (<0.2% $GFAP^+$ astrocytes) compared to a primary cortical astrocytic culture (>96% $GFAP^+$ astrocytes). All genes were normalised to 18s and then to mRNA levels in a mixed neuronal culture (90% $NeuN^+$ neurons, 10% $GFAP^+$ astrocytes). The results were then expressed as a ratio of astrocyte to neuronal mRNA expression for each MCRG (Fig.4.1A). The mRNA expression of some of the essential components of the Mcu complex, Mcu, Mcub, Emre, as well as Letm1 and Slc25a23 did not significantly differ between neurons and astrocytes. The mRNA expression of potential Mcu regulator Micu3, and alternative mitochondrial Ca^{2+} uptake channels Ryr2 and Trpc3, was significantly higher in neurons than astrocytes. The mRNA expression of Mcu regulators Micu1, Micu2 and Mcur1, as well as Ucp2 and Nclx was significantly higher in astrocytes than in neurons. Notably, the expression of Ucp2 and Nclx (Slc8b1) was much higher in astrocytes than neurons.

I next examined the mRNA expression of these genes using an RNA sequencing dataset made from primary mouse neuronal and astrocytic cultures by Mr. Philip Hasel (Fig.4.1B). The RNA-seq reads for each gene were normalised to the total number of reads, and an astrocyte:neuron expression ratio for each MCRG was calculated. Qualitatively, the expression profile of MCRGs looked very similar by both methods. Several genes, Mcu, Mcub and Slc25a23, which showed no significant change in expression in the RT-qPCR samples were expressed significantly higher in neurons in the RNA-seq data, although these changes were modest.

Since the data was normalised to 18s rather than a mitochondrial protein encoding genes, the question remained whether these changes observed could have been due to chance or changes in the mitochondrial number. Thus I examined genes from the nuclear-encoded mitochondrial electron transport chain (ETC) complexes II-V in the RNA-seq data set between primary neurons and astrocytes (Fig.4.1C). The results clearly show that there were only small changes between the genes of ETC complexes II-V between neurons and astrocytes, suggesting that the difference in MCRG mRNA expression will lead to differential mitochondrial Ca^{2+} handling in the two neural cell types.

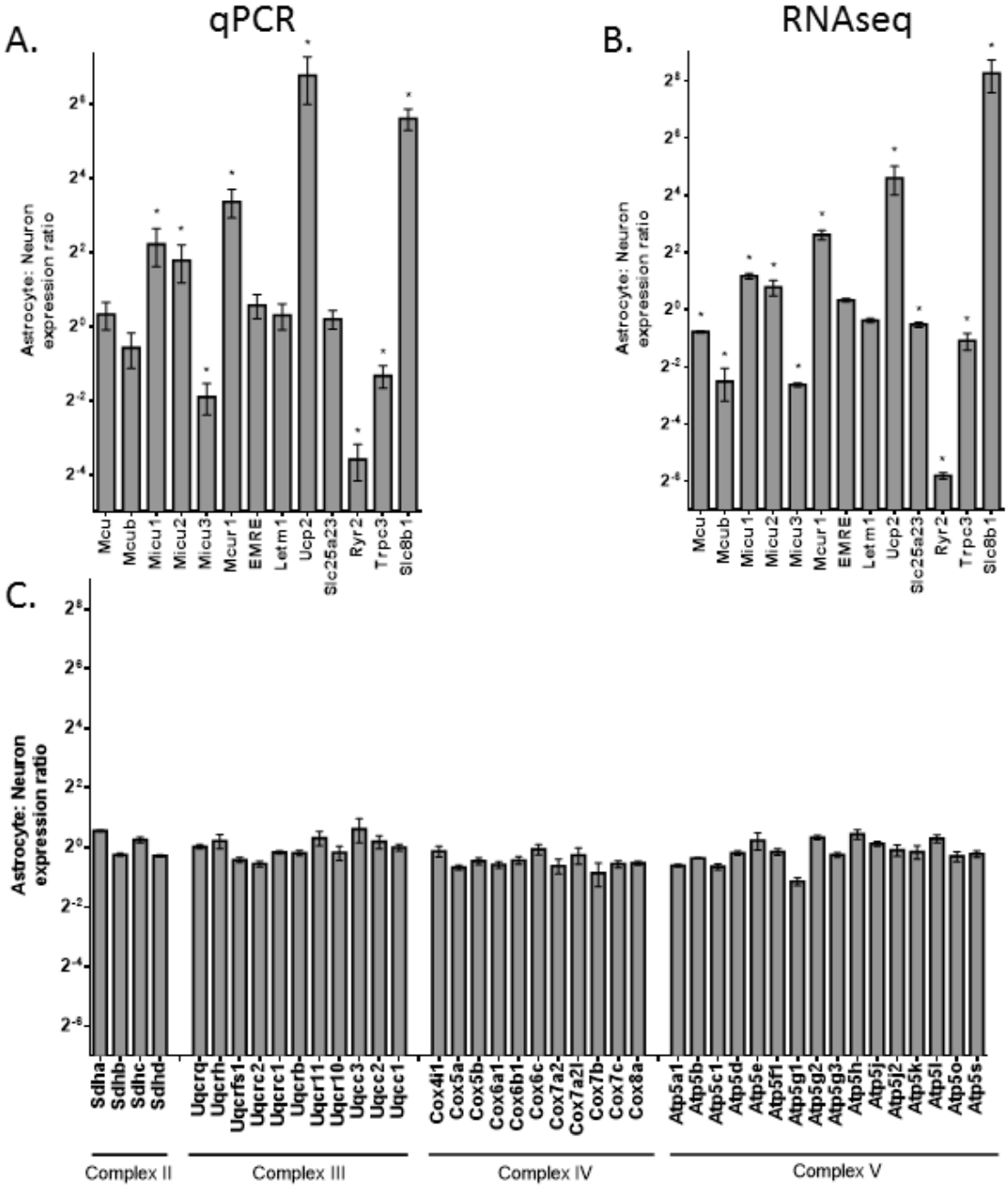

Figure 4.1. The mRNA expression levels of MCRGs differ between primary mouse cortical neurons and astrocytes. A. RT-qPCR expression of the mRNA levels of MCRGs in cortical astrocytes vs neurons. mRNA levels of the MCRGs in neuronal and astrocytic samples was normalised to 18s, and an astrocyte:neuron ratio of gene expression in relation to a mixed neuronal culture was calculated. Two-tailed paired t-test. *p≤0.05. p-values, respectively: 0.019, 0.030, 0.004, 0.002, 0.034, 1E-07, 0.007, 0.0002 (n=6 for Slc8b1 and Trpc3 and n=7 for the rest). **B**. Read densities for MCRGs shown in (A) analysed from an RNA-seq data set of pure neurons and astrocytes, with a ratio of astrocytes to neurons calculated. *p≤0.05. p-values, respectively: 0.001, 0.014, 2E-4, 0.023, 4E-4, 0.002, 0.043, 0.004, 0.005, 0.005, 5E-4. n=3. **C**. RNA-seq data set showing astrocyte:neuron ratio of MCRGs in ETC complexes II-V. n=3. Error bars=SEM. Note that all graphs are on a logarithmic scale. Note that Nclx is shown as Slc8b1.

4.2.2. mRNA expression of MCRGs and Mcu protein expression differs between the CA1 and CA3 regions of the hippocampus

I also wanted to investigate whether MCRGs are differentially expressed in different neuronal subtypes, and used neurons in the CA1 vs CA3 region of the hippocampus as a model. The CA1 and CA3 regions of the hippocampus have previously been shown to have differential basal gene expression in mice (Newrzella et al. 2007).

I extracted the CA1 and CA3 regions from adult mouse hippocampal slices and examined their MCRG mRNA expression by RT-qPCR. I found that MCRG expression differed between the two regions. Mcu, Micu3, Mcur1 and Ryr2 mRNA were all expressed at significantly higher levels in the CA3 region, whilst Micu2, Ucp2, Trpc3 and Nclx (Slc8b1) showed significantly higher expression in the CA1 region of the hippocampus (Fig.4.2.A). Although significant, most of these changes were small, but Mcu expression was around two-fold higher in the CA3 region, whilst Trpc3 was around two-fold higher in the CA1 region of the hippocampus.

Bcl-2 related ovarian killer (Bok) was included as a positive control, since it is known to be expressed at much higher levels in CA3 than in CA1 neurons, which I also observed, validating the extraction method (Newrzella et al. 2007) (Fig.4.2.A). The mRNA levels of MCRGs were normalised to Gapdh, but I also examined the mRNA levels of the ETC genes Uqcrc2 (mitochondrial complex III) and Ndufs2 (mitochondrial complex I), as well as 18s to control for possible changes of mitochondrial expression between these regions, but found no significant differences between their expression in CA1 and CA3 (Fig.4.2.A).

Since I found Mcu mRNA levels to be two-fold higher in CA3 neurons, I investigated whether this difference could be observed at the protein level. Indeed, I found Mcu protein levels to be significantly higher in samples taken from the CA3 region of the hippocampus, than from the CA1 region (Fig.4.2B,C). The results were normalised to mitochondrial complex III protein Uqcrc2, but I also found the same results when normalising to β-actin levels (data not shown).

Thus, the data shows that MCRG mRNA expression levels differ between the CA1 and CA3 region of the hippocampus, and at least in the case of Mcu this translates to the protein level.

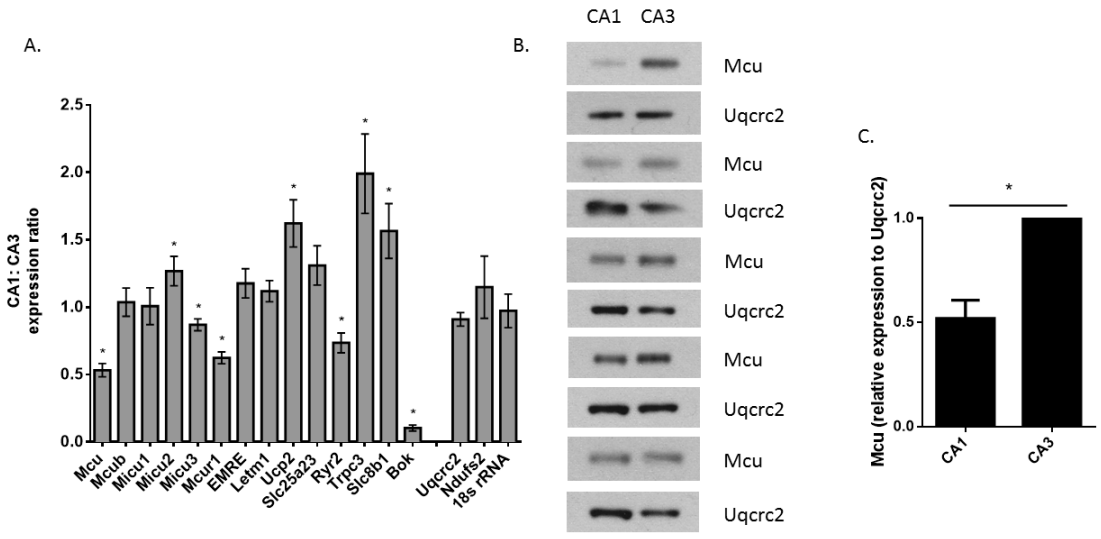

Figure 4.2. The mRNA expression levels of MCRGs, as well as Mcu protein levels, differ between the CA1 and CA3 regions of the adult mouse hippocampus. Paired mRNA and protein samples from the CA1 and CA3 region of the hippocampus were obtained from adult mouse brain slices. **A**. MCRGs mRNA expression in the CA1 and CA3 region of the adult mouse hippocampus. mRNA levels were normalised to Gapdh and the CA1:CA3 expression ratio was calculated for each gene. Bok, which is known to be highly enriched in CA3 neurons, was included as a positive control. Mitochondrial ETC genes Uqcrc2 and Ndufs2, as well as 18s expression levels are shown to exclude the possibility of Gapdh mRNA expression differing largely between the two regions. Two-tailed paired t-test. *p≤0.05. p-values, respectively: 3E-06, 0.033, 0.024, 0.0001, 0.005, 0.005, 0.015, 0.021, 2E-08. Micu3, Mcur1, Trpc3, Bok, Uqcrc2, Ndufs2, 18s (n=7), Mcub (n=9), Slc8b1 (n=10), n=11 for the rest. **B**. Western blots showing Mcu protein levels in CA1 and CA3 taken from the hippocampus of one mouse for each sample pair with mitochondrial ETC protein Uqcrc2 used as a loading control. n=5. **C**. Analysis of (B) showing Mcu levels in CA1 normalised to CA3. Two-tailed paired t-test. *p=0.006. n=5. Error bars=SEM. Note that Nclx is shown as Slc8b1.

4.2.3. The relative expression of MCRGs compared to each other differs in cortical neurons

Although I examined changes in MCRG mRNA expression in cortical neurons vs astrocytes and between CA1 and CA3 regions of the hippocampus, I did not examine the relative expression of these genes to each other in culture. Unlike RT-qPCR, RNA-seq allows for direct comparison between the relative levels of the different genes in samples. Thus, using an RNA-seq data set, I looked at the relative expression of MCRGs to each other in astrocyte-free cortical neurons, by plotting the FPKM values for each MCRG. FPKM is calculated as the number of fragments per kilobase of exon per million fragments mapped.

This revealed large differences in MCRG mRNA expression levels, and that Mcur1, Ucp2 and Slc8b1 (Nclx) are expressed at very low levels in primary neuronal culture (Fig.4.3). These

genes showed a much higher expression in astrocytes than neurons, suggesting that these genes are very weakly expressed in neurons, thus it is tempting to speculate that they probably have low protein expression in neurons and may only be functional in astrocytes.

This finding is very interesting considering that the Na^+/Ca^{2+} exchanger Nclx is thought to mediate Ca^{2+} efflux from mitochondria in excitable cells, thus neurons (Nita et al. 2015). I therefore investigated the role of Nclx in neurons and astrocytes further.

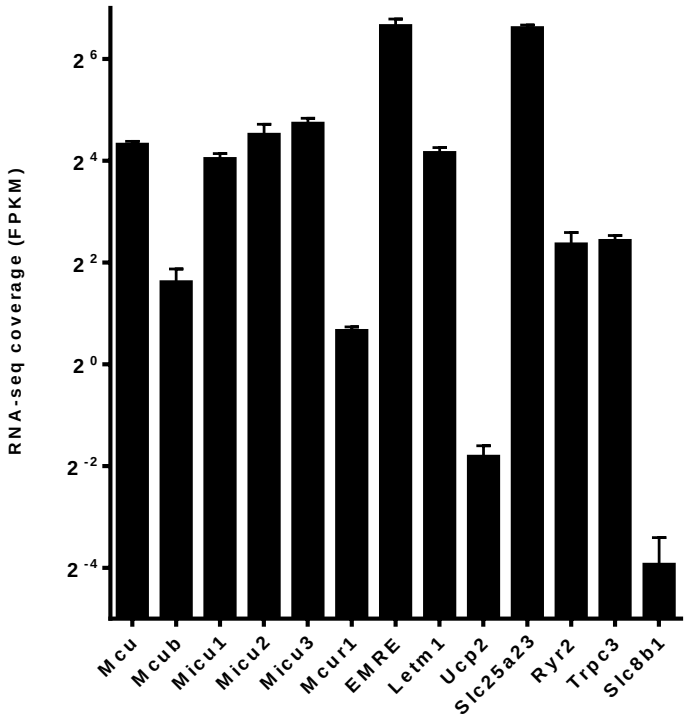

Figure 4.3. Relative mRNA expression of MCRGs differs in neurons in a cortical neuronal culture. FPKM values of MCRGs in neurons show the relative levels of these genes to each other. Note the very low expression of Slc8b1 (Nclx). n=3. Error bars=SEM.

4.2.4. Neuronal Nclx mRNA expression is low in the presence or absence of astrocytes

Since I found Nclx mRNA levels to be low in neurons compared to astrocytes, as well as compared to other MCRGs, I investigated whether Nclx expression in neurons was perhaps dependent on the presence of astrocytes. I found levels of Nclx mRNA in mixed culture to be higher than in an astrocyte-free neuronal culture by qPCR, but whether this rise in Nclx levels was indeed due to neurons, or due to the small percentage of astrocytes (10%) present in the mixed cortical culture was unclear. Thus, I used a co-culturing technique developed by our group, where primary mouse neurons are overlaid on top of confluent rat astrocytes, enabling me to distinguish neurons from astrocytes using mouse species-specific primers. Levels of

Nclx mRNA in mouse neurons in mixed co-culture were similar to levels in astrocyte-free neuronal culture, with Nclx expression in mixed culture being 14-fold and in astrocytes 400-fold higher on average than in astrocyte-free neuronal culture (Fig.4.4). Results were normalised to mouse-specific histone protein H1f0 primers, but similar results were seen when normalising to mouse-specific Gapdh (data not shown). This suggests that Nclx is not upregulated in neurons in the presence of astrocytes, which may indicate low protein expression of Nclx, and the presence of alternative Ca^{2+} efflux routes in neurons.

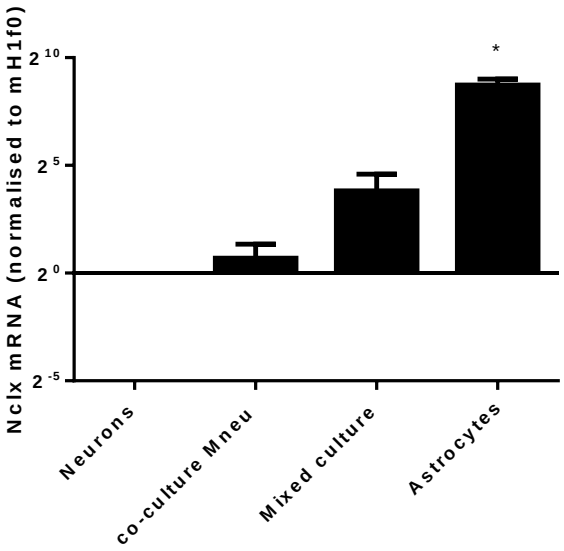

Figure 4.4. Neurons in the presence of astrocytes express similar levels of Nclx mRNA as neurons in an astrocyte-free culture, but much less than astrocytes. Samples were normalised to mouse-specific H1f0, a histone protein. n=3. *p=0.0435. Paired two-tailed t-test. Note the logarithmic scale. Mneu= mouse neurons.

4.2.5. The Nclx inhibitor CGP-37157 partially inhibits mitochondrial Ca^{2+} efflux in astrocytes

I next tested whether Nclx was functionally present in the astrocytes, using the genetically encoded mitochondrial GCamp2 (mitoGCamp2) to visualise mitochondrial Ca^{2+} levels, and cytoplasmic GCamp2 (cytoGCamp2) to monitor cytoplasmic Ca^{2+} levels in astrocytes in real time (Mao et al. 2008; Chen et al. 2011). ATP has been shown to increase cytoplasmic Ca^{2+} levels in astrocytes through its activation of metabotropic receptors prompting Ca^{2+} release from the ER and subsequently activation of store-operated Ca^{2+} channels on the plasma membrane, leading to further rises in intracellular Ca^{2+} (Kresse et al. 2005; Parnis et al. 2013). Thus, I used ATP to increase cytoplasmic and mitochondrial Ca^{2+} levels in astrocytes and monitored the Ca^{2+} decay which followed. I used CGP-37157 which is an inhibitor of Nclx, although it has some off target effects on other Ca^{2+} channels in cells, such as voltage gated Ca^{2+} channels (including L-type Ca^{2+} channels), store-operated Ca^{2+} channels and the ER Ca^{2+} ATPase (Ruiz et al. 2014; Parnis et al. 2013).

The percentage of (F-Fmin)/(Fmax-F) was calculated, where Fmax was determined by the addition of ionomycin (Nicholls 2006), and Fmin was calculated as the minimal amount of Ca^{2+} following Ca^{2+} chelation by EGTA. The results are presented as the percentage of Ca^{2+} out of the maximum mitochondrial or cytosolic Ca^{2+} level reached after ATP application, every minute for four minutes.

I found that pre-treatment of astrocytes with CGP-37157 for 10 minutes significantly delayed the recovery of Ca^{2+} levels in mitochondria following ATP-mediated mitochondrial Ca^{2+} influx, compared to control astrocytes (Fig.4.5A). Slower decay of Ca^{2+} was observed even four minutes after ATP application to astrocytes pre-treated with CGP-37157 compared to control. I also examined the cytoplasmic Ca^{2+} decay kinetics following ATP-mediated rises in cytoplasmic Ca^{2+}, and found a small, but significantly faster Ca^{2+} decay in CGP-37157 treated astrocytes compared to untreated astrocytes (Fig.4.5B). This may have been the result of less Ca^{2+} efflux from mitochondria, thus less Ca^{2+} in the cytoplasm. For example raw traces from calcium imaging, see Supplementary figure 2.

I found mitochondrial Ca^{2+} levels to be significantly lower in CGP-37157 treated astrocytes both at baseline and after ATP-mediated Ca^{2+} influx (Fig.4.5.C,D). The total amount of mitochondrial Ca^{2+} influx, calculated from the peak mitochondrial Ca^{2+} levels minus the average baseline Ca^{2+}, was also significantly larger in control astrocytes (Fig.4.5E). This suggests that CGP-37157 may have a slight inhibitory effect on mitochondrial Ca^{2+} uptake, and raises the question of whether lower amount of mitochondrial Ca^{2+} influx delays Ca^{2+} decay kinetics. Thus, I examined the top and bottom 50% of CGP-37157 pre-treated astrocytes stimulated with ATP according to their total amount of mitochondrial Ca^{2+} influx, and found the top 50% to have a similar average total Ca^{2+} influx to control astrocytes (Supplementary figure 3A). The higher level of Ca^{2+} influx in these top 50% of CGP-37157 treated astrocytes led to quicker mitochondrial Ca^{2+} decay than the average of all CGP-37157 treated astrocytes, but Ca^{2+} decay kinetics were still significantly delayed compared to control astrocytes (Supplementary figure 3B). Thus, although the amount of mitochondrial Ca^{2+} influx influences Ca^{2+} decay, this does not explain the inhibition of mitochondrial Ca^{2+} efflux seen by CGP-37157. Cytoplasmic Ca^{2+} levels at baseline and after Ca^{2+} influx were unchanged (Fig.4.5F-H).

Thus, the data shows that CGP-37157 does indeed inhibit mitochondrial Ca^{2+} efflux in astrocytes, as previously shown (Parnis et al. 2013).

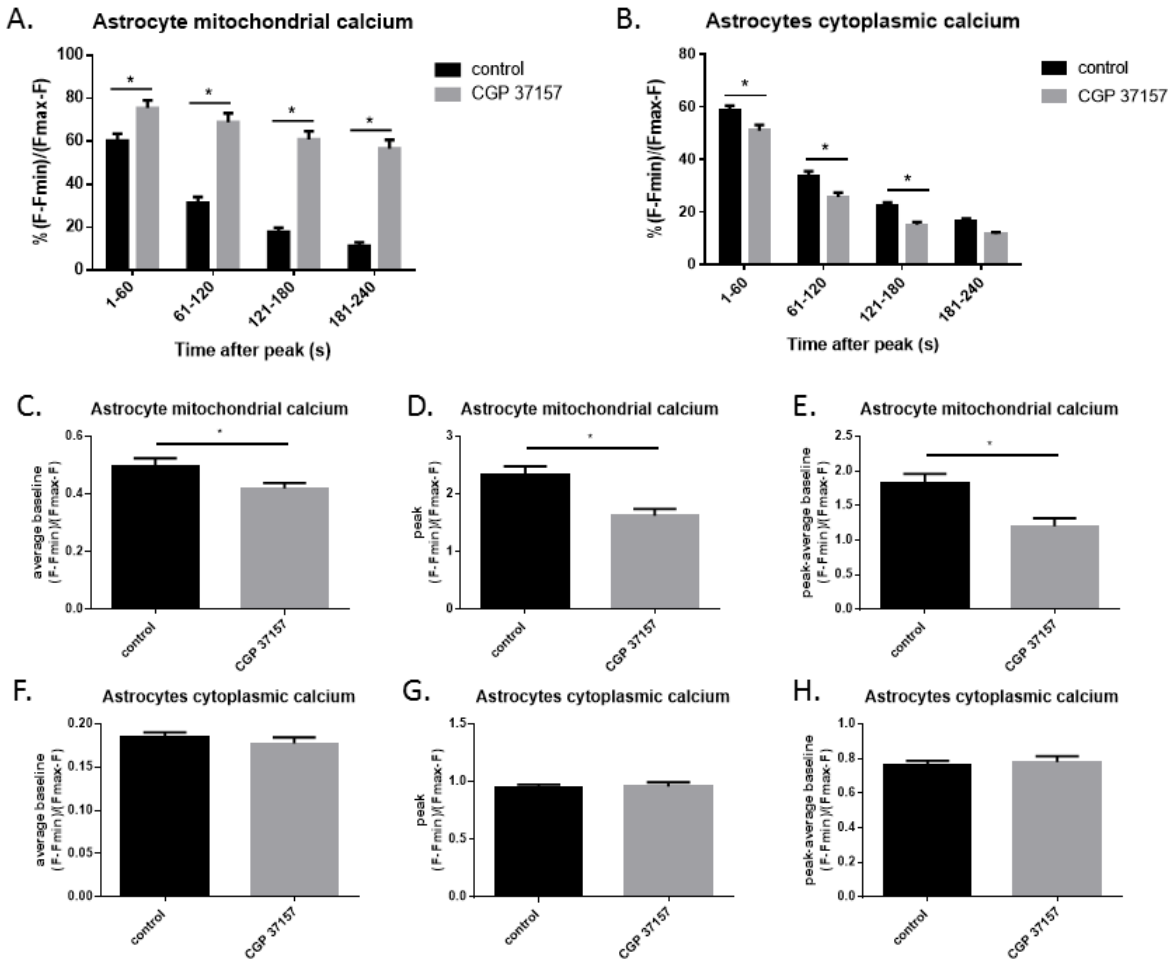

Figure 4.5. Mitochondrial Ca^{2+} efflux is diminished by Nclx inhibitor CGP-37157 following ATP-induced rises in Ca^{2+} levels in astrocytes. A. Mitochondrial Ca^{2+} decay 1-4 minutes after the peak of ATP-induced mitochondrial Ca^{2+} influx in pure cortical astrocytes, ± pre-treatment with CGP-37157 (10 µM). ATP was applied for 1 minute to the astrocytes before it was washed out. Mitochondrial Ca^{2+} was measured using mitoGCamp2, which was transfected into astrocytes. All Ca^{2+} imaging values were calculated as (F-Fmin)/(Fmax-F), where Fmax was determined as the total Ca^{2+} capacity of the astrocyte and Fmin was determined by EGTA application to chelate all the Ca^{2+}. Ca^{2+} decay in each astrocyte was normalised to the peak of the mitochondrial Ca^{2+} influx as 100%, with the minimal calcium at baseline set as 0%. Two-way ANOVA with Bonferroni post-hoc correction. *p≤0.05. p=0.0005 for the first time point, p<0.0001 for the others. n=71 for control and n=58 for CGP-37517 treated astrocytes (9 coverslips from 3 separate cultures). **B**. Cytoplasmic Ca^{2+} decay in astrocytes following ATP treatment. Analysis was done as described in (A). Cytoplasmic Ca^{2+} levels were measured using cytoGCamp2. ANOVA with Bonferroni post-hoc correction. *p≤0.05. p-values, respectively: 0.0015, 0.0009, 0.0029. n=166 for control and n=176 for CGP treated astrocytes (14 coverslips from 4 separate cultures). **C-E**. Mitochondrial Ca^{2+} levels ±CGP treatment. Average baseline Ca^{2+} levels (C) *p=0.0261, maximal Ca^{2+} level (D) *p=0.0008 and the total rise in Ca^{2+} levels in each astrocyte calculated by the peak-average baseline Ca^{2+} (E) *p=0.0018. Unpaired two-tailed t-test. **F-H**. As in (C-E), respectively, except cytoplasmic Ca^{2+} levels shown. Unpaired two-tailed t-tests (C-H). Mean+SEM.

4.2.6. The Nclx inhibitor CGP-37157 partially inhibits mitochondrial Ca^{2+} efflux in neurons

I next examined whether CGP-37157 could also inhibit mitochondrial Ca^{2+} efflux in neurons in a mixed neuronal culture. I used mitoGCamp2 and cytoGCamp2 to image neurons as described in section 4.2.5. Instead of ATP, I applied a KCl depolarisation solution (50 mM K^+) to depolarise neurons and induce Ca^{2+} influx through L-type Ca^{2+} channels, with MK-801 present to prevent excessive NMDAR activation. One minute following application of high K^+, cells were washed to increase the rate of Ca^{2+} decay. I found that as in astrocytes, there was a large significant delay in mitochondrial Ca^{2+} decay following pre-treatment of neurons with CGP-37157 compared to untreated neurons (Fig.4.6A). This large difference could be observed and was significant even four minutes following KCl application. Similarly to astrocytes, there was a significantly quicker decay in cytoplasmic Ca^{2+} levels in CGP-37157 treated neurons compared to control (Fig.4.6B). For example traces of Ca^{2+} decay in neurons in a mixed culture, see Supplementary figure 4. Interestingly, unlike in astrocytes, in neurons there was no difference in mitochondrial Ca^{2+} levels at baseline or following depolarization-mediated rises in Ca^{2+} levels (Fig.4.6C-E). However, there was a decreased rise in cytoplasmic Ca^{2+} levels following depolarization in CGP-37157 treated neurons (Fig.4.6F-H). This is likely due to the off-target effect of CGP-37157 on VGCCs, including L-type Ca^{2+} channels, previously demonstrated in neurons (Ruiz et al. 2014; Baron & Thayer 1997).

Since I observed partial inhibition of mitochondrial Ca^{2+} efflux by CGP-37157 in neurons in a mixed culture, I investigated whether this was also the case in neurons in an astrocyte-free neuronal culture (<0.2% astrocytes). Neurons in pure neuronal cultures were treated the same way as neurons in mixed culture. Interestingly, I saw the same results in neurons in a pure neuronal culture as with neurons in mixed culture; mitochondrial Ca^{2+} decay kinetics were largely and significantly reduced following pre-treatment of neurons with CGP-37157 (Fig.4.7A). Similarly to astrocytes and neurons in mixed culture, there was a quicker recovery in cytoplasmic Ca^{2+} levels in neurons in astrocyte-free neuronal culture pre-treated with CGP-37157 (Fig.4.7B). Note that in neurons, cytoplasmic Ca^{2+} levels dropped below baseline Ca^{2+} levels after stimulation (Fig.4.6B and 4.7B). For example traces of Ca^{2+} decay in neurons in an astrocyte-free culture, see Supplementary figure 5. Interestingly, mitochondrial baseline Ca^{2+} levels in CGP-37157 treated neurons in pure neuronal culture and mitochondrial Ca^{2+} influx following KCl application was decreased compared to control (Fig.4.7C-E). Since the total mitochondrial Ca^{2+} influx was lower in CGP-37157 treated neurons than in control neurons following KCl stimulation, I examined the top and bottom 50% of CGP-37157 treated neurons according to their total mitochondrial Ca^{2+} uptake, and found that the top 50% showed

similar levels of total mitochondrial Ca^{2+} influx to untreated neurons (Supplementary figure 3C). As in astrocytes, the top 50% of CGP-37157 treated neurons showed increased Ca^{2+} decay kinetics compared to all CGP-37157 treated neurons, but Ca^{2+} decay was still significantly delayed compared to untreated neurons (Supplementary figure 3D), showing that although the amount of mitochondrial Ca^{2+} influx influences mitochondrial Ca^{2+} decay, it is not responsible for the delay seen due to CGP-37157 pre-treatment of neurons. As in neurons in mixed culture, the rise in cytoplasmic Ca^{2+} levels was decreased following KCl-treatment in CGP-37157 treated neurons compared to control (Fig.4.7F-H).

Thus, CGP-37157 pre-treatment partially inhibits mitochondrial Ca^{2+} efflux in neurons, following KCl-induced rises in intracellular Ca^{2+}, independently of the presence of astrocytes.

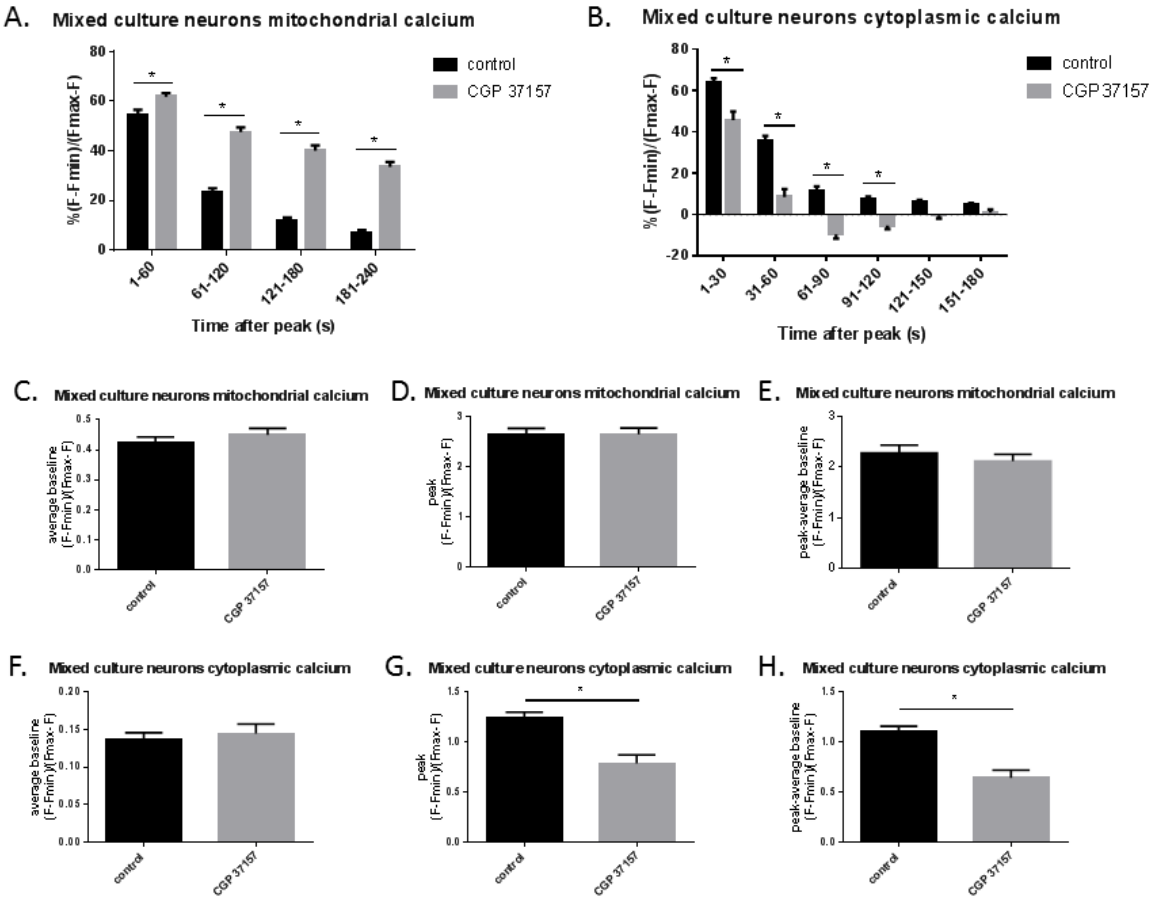

Figure 4.6. Mitochondrial Ca^{2+} efflux is diminished by Nclx inhibitor CGP-37157 following a KCl-induced depolarisation of neurons in a mixed culture. A. Mitochondrial Ca^{2+} efflux at the times indicated following exposure of neurons to high K^+ (50 mM) ± 10-minute pre-treatment with CGP-37157. Mitochondrial Ca^{2+} was measured using mitoGCamp2. All Ca^{2+} imaging values were calculated as (F-Fmin)/(Fmax-F), where Fmax was determined as the total amount of Ca^{2+} entering neurons following addition of ionomycin, whilst Fmin was determined by addition of EGTA to chelate all the Ca^{2+} in neurons. Ca^{2+} efflux was normalised to the peak of mitochondrial Ca^{2+} levels as 100% in each neuron with the minimal Ca^{2+} level at baseline set as 0%. Two-way ANOVA with Bonferroni post-hoc correction. *p≤0.05. p=0.0441 for the first time point, p<0.0001 for the others. n=80 for control and n=88 for CGP-37157 treated neurons (16 coverslips from 6 distinct cultures). **B**. Cytoplasmic Ca^{2+} efflux in neurons following KCl treatment. Analysis was done as described in (A). Cytoplasmic Ca^{2+} levels were measured using cytoGCamp2. Two-way ANOVA with Bonferroni post-hoc correction. *p≤0.05. p<0.0001 for the first three timepoints, thereafter p=0.0003. n=81 for control and n=73 for CGP treated neurons (11 coverslips from 4 separate cultures). **C -E**. Mitochondrial Ca^{2+} levels ±CGP treatment in neurons. Average baseline Ca^{2+} levels (C), maximal Ca^{2+} level (D), and the total Ca^{2+} influx in each astrocyte calculated by the peak-average baseline Ca^{2+} (E). **F-H**. As in (C-E), respectively, but cytoplasmic Ca^{2+} levels. *p<0.0001. Unpaired two-tailed t-tests (C-H). Mean+SEM.

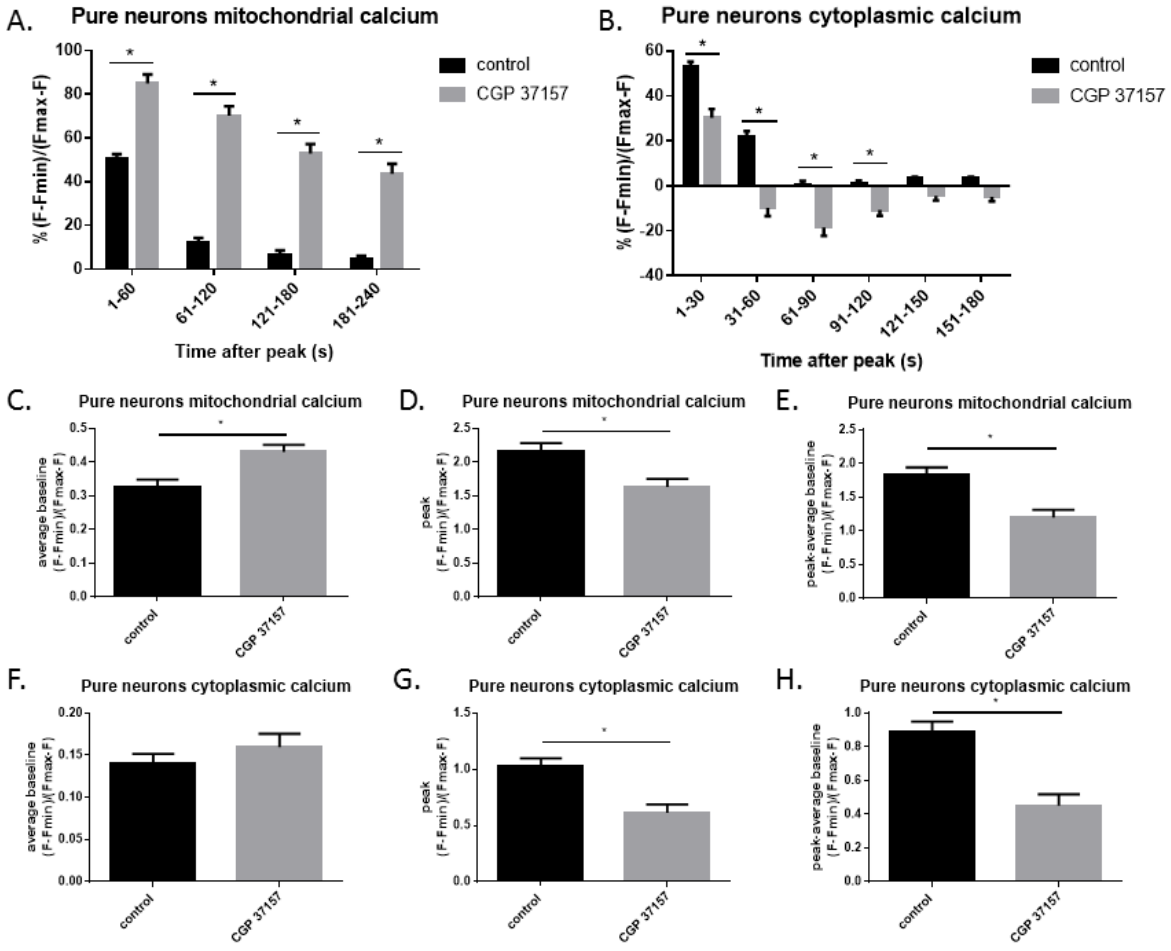

Figure 4.7. Mitochondrial Ca^{2+} efflux is diminished by Nclx inhibitor CGP-37157 following KCl-induced depolarisation of neurons in an astrocyte-free neuronal culture. A. The Ca^{2+} efflux from mitochondria after the times indicated ± 10-minute CGP-37157 pre-treatment, following KCl-induced rises in Ca^{2+} levels. Mitochondrial Ca^{2+} was measured using mitoGCamp2. All Ca^{2+} imaging values were calculated as (F-Fmin)/(Fmax-F), where Fmax was determined as the total amount of Ca^{2+} in neurons following ionomycin application, whilst Fmin was determined by adding EGTA to chelate all the Ca^{2+}. Ca^{2+} efflux was normalised to the peak of mitochondrial Ca^{2+} levels following KCl addition as 100% in each neuron with the minimum Ca^{2+} at baseline set as 0%. Two-way ANOVA with Bonferroni post-hoc correction. *p<0.0001. n=64 for control and n=65 for CGP-37517 treated (12 coverslips from 5 separate cultures). **B**. Cytoplasmic Ca^{2+} efflux in neurons following KCl treatment. Analysis was done as described in (A). Cytoplasmic Ca^{2+} levels were measured using cytoGCamp2. Two-way ANOVA with Bonferroni post-hoc correction. *p≤0.05. p<0.0001 for the first 3 timepoints, then p=0.0019. respectively. n=60 for control and n=42 for CGP treated (7 and 8 coverslips, respectively from 3 separate cultures). **C-E**. Mitochondrial Ca^{2+} levels ±CGP treatment in neurons. Average baseline Ca^{2+} levels (C) *p=0.0009, maximal Ca^{2+} level (D) *p=0.0033, and the total Ca^{2+} influx in each astrocyte calculated by the peak-average baseline Ca^{2+} (E) *p=0.0001. **F-H**. As in (C-E), respectively, but cytoplasmic Ca^{2+} levels. *p<0.0001. Unpaired two-tailed t-tests (C-H). Mean+SEM.

4.3. Discussion

4.3.1. Conclusion

I show in this chapter that mRNA expression of MCRGs differs between different neural cells (neurons and astrocytes), as well as between different neuronal subtypes (CA1 and CA3 neurons of the hippocampus), probably influencing the mitochondrial Ca^{2+} handling in these cells. I found that expression of the Na^{+}/Ca^{2+} exchanger Nclx was very low in cortical neurons compared to astrocytes and relative to the expression levels of other MCRGs in neurons. Thus I investigated whether mitochondrial Ca^{2+} efflux occurred in our cortical neurons, and whether it was mediated by Nclx. I found mitochondrial Ca^{2+} efflux to be attenuated in the presence of Nclx inhibitor CGP-37157 after the stimulation of astrocytes or neurons, both in a pure neuronal and a mixed neuronal culture. Although whether mitochondrial Ca^{2+} efflux in neurons was mediated by Nclx or another Ca^{2+} exchanger is still unclear.

4.3.2. MCRG mRNA expression differs between neurons and astrocytes

Several MCRGs have been shown to be expressed in the brain, but their expression and function in different neural cells is still unknown (Raffaello et al. 2013; Plovanich et al. 2013; Mallilankaraman et al. 2012a; De Stefani et al. 2011; De Stefani et al. 2016). I compared the mRNA expression of MCRGs in two different neural cells, cortical neurons and astrocytes, and found that several of the genes were differentially expressed. This differential expression was not due to chance or the abundance of mitochondria, since mRNA levels of mitochondrial ETC complexes II-V did not exhibit large changes between neurons and astrocytes. Micu3 has previously been shown to have high mRNA expression in the nervous system and skeletal muscle (Plovanich et al. 2013). I found Micu3 mRNA expression to be significantly higher in cortical neurons than in astrocytes, suggesting that the high expression of Micu3 observed in the nervous system is dependent on neurons. Both Trpc3 and Ryr2 had significantly higher mRNA expression in neurons than astrocytes, however this result should be treated with caution, since although both of these proteins have been found to be expressed on the IMM in neural cells, they are also expressed in other parts of the cell, Ryr2 in the ER and Trpc3 on the plasma membrane (Jakob et al. 2014; Feng et al. 2013). Therefore, expression of these genes in mitochondria needs to be further investigated, either by mRNA extraction from mitochondrial fractions or quantification of these genes in mitochondria by immunocytochemistry, to determine whether these genes are indeed differentially expressed in mitochondria in different neural cells.

Interestingly, some of the core components of the Mcu complex, Mcu, Mcub and Emre, which are thought to be essential for Mcu function are expressed at similar levels in neurons and

astrocytes. Although I observed a small but significant increase in Mcu and Mcub expression in neurons with RNA-seq, I found Mcub levels to be lower than Mcu levels in neurons, bringing into question the functional importance of Mcub in neurons and astrocytes. Mcub is known to be the dominant-negative isoform of Mcu, and is thought to oligomerise with Mcu and inhibit Ca^{2+} uptake through the channel pore (Raffaello et al. 2013). Indeed, the Mcu:Mcub ratio seems to differ between different tissues in adult mice, which may point to Mcub only playing an important role in some cell types (Raffaello et al. 2013). Furthermore, results by our group show that Mcub KO in neurons does not influence Ca^{2+} levels basally or following NMDA-mediated Ca^{2+} influx (Márkus et al. 2016). Since Raffaello *et al.* showed lower expression of Mcub than Mcu in the adult mouse brain, it is unlikely that this expression pattern changes throughout development, suggesting that Mcub may not play an important role in neurons. Although it is possible that Mcub expression is dynamically induced under certain conditions, such as KCl-mediated neuronal depolarisation which our group has demonstrated (Márkus et al. 2016).

Expression of Slc25a23, a solute carrier mediating Mg-ATP/Pi exchanger which helps to enhance Mcu-mediated Ca^{2+} uptake in neurons (Hoffman et al. 2014), also showed similar expression in the two cell types. Letm1, which is thought to be the H^+/Ca^{2+} exchanger and has been shown to mediate both mitochondrial Ca^{2+} influx and efflux (Jiang et al. 2009; Doonan et al. 2014; Waldeck-Weiermair et al. 2011), also showed similar mRNA expression in neurons and astrocytes.

The mRNA expression of mitochondrial regulators Micu1, Micu2 and Mcur1 was higher in astrocytes. Micu1 and 2 are responsible for gatekeeping of Mcu, and Micu1 is also thought to positively cooperate with Mcu at higher cytoplasmic Ca^{2+} levels, to allow increased mitochondrial Ca^{2+} influx (Perocchi et al. 2010; Csordás et al. 2013; Plovanich et al. 2013). Thus, it is possible that Mcu is repressed more at baseline Ca^{2+} levels, and shows increased Ca^{2+} uptake at higher cytoplasmic Ca^{2+} concentrations, but this should be functionally investigated. It is important to know that Micu1, 2 and 3 are expressed at similarly high levels in neurons. This suggests that Micu1 and 2 levels in astrocytes may be higher to compensate for the low expression of Micu3, the function of which has not been investigated.

Both Ucp2 and Nclx had much higher mRNA expression in astrocytes than neurons, and interestingly both of these genes were expressed at very low levels in neurons when comparing FPKM values of MCRGs. This implies that these genes are present in astrocytes, but may have low protein expression and lower functional importance in neurons. Ucp2 helps to regulate Mcu-mediated Ca^{2+} influx (Waldeck-Weiermair et al. 2010), whilst Nclx is responsible for

mitochondrial Ca^{2+} efflux (Palty et al. 2010). The low expression of Nclx in neurons is highly unexpected, since mitochondrial Ca^{2+} efflux in excitable cells has been suggested to be mediated by a Na^{+}/Ca^{2+} exchanger (Palty & Sekler 2012). This poses the question of whether Nclx is expressed at all in neurons, and if it is not which other exchanger mediates neuronal mitochondrial Ca^{2+} efflux.

It is important to note that mRNA levels do not always reflect protein levels in cells, thus these findings may not necessarily translate to the protein level. Further experiments are needed to determine protein level changes between different neural cell types. Unfortunately, there are no antibodies available for many of these genes, and I found commercially available antibodies I tested to be unspecific. If these results translate to the protein level, the functional consequences of the differential gene expression in neurons vs astrocytes could be examined.

It is quite possible that MCRG expression profile is also different in other neural cells, such as microglia and oligodendrocytes.

Our group has shown that MCRG mRNA expression is also influenced by neuronal activity, KCl/FPL-induced Ca^{2+} influx repressed both Letm1 and Mcu mRNA levels in neurons, and Bic/4-AP-induced Ca^{2+} influx also led to decreased Mcu mRNA expression (Márkus et al. 2016; Qiu et al. 2013). This shows that the expression profile of MCRGs is dynamically regulated by neuronal activity. This suggests that mitochondria are slightly decoupled from cytoplasmic Ca^{2+} influxes following synaptic activity, taking up less Ca^{2+} due to decreased Mcu expression, which is likely to play a neuroprotective role. It would be interesting to investigate the expression profile of MCRGs following pathological NMDAR activation, which is known to lead to neuronal death and may influence MCRGs to increase the coupling of cytoplasmic Ca^{2+} influx to mitochondrial Ca^{2+} uptake.

4.3.3 MCRG mRNA expression differs between neuronal subtypes

To examine whether MCRG mRNA expression differs between different neuronal subtypes, I compared neurons of the CA1 and CA3 region of the adult mouse hippocampus. I found these two neuronal subtypes to have differential MCRG mRNA expression profiles. Micu2, Ucp2, Trpc3 and Nclx were expressed significantly higher in CA1 neurons of the hippocampus, whilst Mcu, Micu3, Mcur1 and Ryr2 mRNA were expressed at significantly higher levels in CA3 neurons.

The functional significance of Micu2 is still debated, although it has been suggested to function as a gatekeeper of Mcu at low cytoplasmic Ca^{2+} levels (Plovanich et al. 2013; Matesanz-Isabel et al. 2016). This, coupled with lower expression of Mcu itself may point to

lower mitochondrial Ca^{2+} influx in CA1 neurons at baseline. Although both Ucp2 and Nclx mRNA seem to be expressed at a higher level in CA1 neurons, they are both expressed at very low levels in neurons (according to our RNA-seq data), thus this change may not bear functional significance. As mentioned above, the change in Ryr2 levels needs to be confirmed to be in mitochondrial Ryr2 expression and not changes in its expression on the ER. The function of Micu3 is still unknown, thus its functional significance cannot be determined, although Micu3 was only expressed at slightly higher levels in CA3 neurons. Mcur1 has been suggested to increase mitochondrial Ca^{2+} influx through its regulation of Mcu (Mallilankaraman et al. 2012a; Vais et al. 2015), however expression levels of both Mcur1 and Mcu are higher in CA3 neurons than CA1, thus these changes are likely not to lead to alterations in Mcu regulation.

The higher mRNA expression levels of Mcu in CA3 neurons agrees with results from the Allen Mouse Brain Atlas (experiment ID: 69608519, see mouse.brain-map.org) (Lein et al. 2007), as well as the Allen Human Brain Atlas (probe ID: A_23_P346405, see www.brain-map.org) (Hawrylycz et al. 2012), suggesting that the result translates to humans. I also found Mcu protein levels to be higher in the CA3 compared to the CA1 neurons. This shows that at least some mRNA levels reflect the protein levels of these genes. It is possible that the differential expression of Mcu in these two neuronal subtypes will lead to different amounts of mitochondrial Ca^{2+} uptake. Physiologically this could mean increased cytoplasmic Ca^{2+} buffering and increased neuronal metabolism in CA3 neurons, whilst it may be detrimental during excessive cytoplasmic Ca^{2+} uptake.

CA1 neurons are known to have higher vulnerability to transient ischaemic insults, NMDA excitotoxicity and ROS induced death than CA3 neurons (Strasser & Fischer 1995; Ikegaya & Matsuki 2002; Cronberg et al. 2005; Gee et al. 2006; Yang et al. 2000; Wilde et al. 1997). Although some explanations for this have been suggested (Cronberg et al. 2005; Coultrap et al. 2005; Gee et al. 2006), it is tempting to speculate that differential MCRGs may contribute to this effect. Our group has previously shown that Mcu KD leads to decreased NMDA-mediated excitotoxic death in cortical neurons (Qiu et al. 2013). I found Mcu to be expressed at lower levels in CA1 than in CA3 neurons, which is the opposite of what I would expect to cause increased susceptibility to NMDA-induced excitotoxicity, unless the downregulation of Mcu is an adaptive response in these neurons.

A number of other mitochondrial Ca^{2+} uptake routes have been described, and results by our group also suggest that Mcu is not the only Ca^{2+} uptake pathway in mitochondria (Qiu et al. 2013). Interestingly, Trpc3 is expressed two-fold higher in CA1 than the CA3 neurons, whilst

Mcu is expressed two-fold lower. Trpc3 has recently been shown to be localised to the IMM in neurons and not just to the plasma membrane, and has been suggested to be an alternative mitochondrial Ca^{2+} influx route independent of Mcu-mediated Ca^{2+} uptake. Since Trpc3 was shown to mediate mitochondrial Ca^{2+} influx mostly following high cytoplasmic Ca^{2+} levels (Feng et al. 2013), it is possible that Trpc3 allows for greater mitochondrial Ca^{2+} influx than Mcu. Since CA1 neurons express less Mcu and more Trpc3 than CA3 neurons, it is possible that Trpc3 may be a more prominent route of mitochondrial Ca^{2+} influx in CA1 neurons, whilst Mcu-mediated Ca^{2+} uptake may be more important in CA3 neurons. It is tempting to speculate that this increased Trpc3 expression in CA1 neurons may cause increased mitochondrial Ca^{2+} overload following application of NMDA, leading to the selective vulnerability of these neurons. Although this hypothesis should be taken with caution, considering that Trpc3 mRNA expression may reflect changes of Trpc3 expression on the plasma membrane rather than the IMM. Nevertheless, the role of increased Trpc3 expression in CA1 neurons is an intriguing topic for further investigation.

It is likely that other subtypes of neurons also show differential expression patterns of MCRGs, which may influence mitochondrial Ca^{2+} handling in these cells, potentially influencing their vulnerability to certain insults. Many ND diseases which involve excitotoxicity are known to impact specific neuronal subtypes in the brain (Hardingham & Bading 2010; Zhang et al. 2016), thus the possible role of neuronal subtype-specific MCRG expression in these neurons would be interesting to investigate.

4.3.4. Is Nclx responsible for mitochondrial Ca^{2+} efflux in neurons?

I show that pre-treatment with Nclx inhibitor CGP-37157 decreases mitochondrial Ca^{2+} efflux in astrocytes and neurons following stimulation with ATP or KCl, respectively. CGP-37157 has previously been shown to block mitochondrial Ca^{2+} efflux in astrocytes, along with siRNA KD of Nclx (Parnis et al. 2013), suggesting that Nclx is indeed responsible for mitochondrial Ca^{2+} efflux in astrocytes. This agrees with my findings that Nclx is expressed in astrocytes at the mRNA level, and that mitochondrial Ca^{2+} efflux is decreased following pre-treatment with CGP-37157.

Surprisingly, I found CGP-37157 to also partially inhibits mitochondrial Ca^{2+} efflux in neurons, both in a mixed culture (10% astrocytes) and in astrocyte-free neuronal culture (<0.2% astrocytes). This is unexpected given my finding that Nclx mRNA expression is very low in neurons, not only in comparison to astrocytes, but also in relation to the expression of other MCRGs. Additionally, Nclx mRNA expression was not increased in neurons in the presence of astrocytes. I found cytoplasmic Ca^{2+} influx to be lower in neurons treated with

CGP-37157 following KCl application, which may be due its off target effects on VGCCs previously described in cortical and dorsal root ganglion neurons (Ruiz et al. 2014; Baron & Thayer 1997). Use of CGP-37157 has also been credited with reducing excitotoxic cell death, due to its blockage of VGCCs reducing Ca^{2+} influx following NMDA application (Ruiz et al. 2014). The increased cytoplasmic Ca^{2+} decay observed in both neurons and astrocytes may be due to increased mitochondrial Ca^{2+} retention.

CGP-37157 has previously been shown to partially inhibit mitochondrial Ca^{2+} efflux in cortical and dorsal root ganglion neurons (Ruiz et al. 2014; Baron & Thayer 1997). I also only see a partial block of mitochondrial Ca^{2+} efflux in neurons and astrocytes, suggesting that other Ca^{2+} efflux pathways are present, or that CGP-37157 does not fully block Nclx-mediated Ca^{2+} efflux.

Although Ruiz *et al.* showed Nclx expression by immunoblotting in cortical neurons, the results do not look convincing, and they did not validate their Nclx antibody (Ruiz et al. 2014). The low Nclx mRNA expression in neurons suggests that at least one alternative mitochondrial Ca^{2+} efflux pathway must exist. It is also possible that the decrease I observe in mitochondrial Ca^{2+} efflux following high K^+ in CGP-37157 pre-treated neurons is due to off-target effects of CGP-37157 on known or unknown mitochondrial Ca^{2+} efflux pathways other than Nclx. Indeed, the probable mitochondrial Ca^{2+}/H^+ exchanger Letm1 has been suggested to be partially inhibited by CGP-37157 (Jiang et al. 2009). Additionally, Letm1 has been implicated in the aetiology of Wolf-Hirschhorn syndrome (WHS), a disorder characterised by delayed growth and development, as well as seizures (Bergemann et al. 2005; Doonan et al. 2014). Heterozygous KO of Letm1 in mice has been shown to cause seizures (Jiang et al. 2013), and cell lines from WHS patients have shown decreases in Letm1 and mitochondrial impairments (Hart et al. 2014), making it tempting to speculate that Letm1 plays an important role in mitochondrial Ca^{2+} handling in the brain and is expressed in neural cells. Three other Na^+/Ca^{2+} exchanger family members, Ncx1, 2 and 3, have been shown to have mitochondrial localisation in neurons and astrocytes, with Ncx3 shown to be localised to the OMM in cortical neurons (Gobbi et al. 2007; Scorziello et al. 2013; Wood-Kaczmar et al. 2013). Additionally Ncx2 and 3 have recently been demonstrated to mediate mitochondrial Ca^{2+} efflux in cortical and dopaminergic neurons (Scorziello et al. 2013; Wood-Kaczmar et al. 2013), and would be interesting genes to investigate. Since Ncx1, 2 and 3 belong to the same family of exchangers as Nclx (Khananshvili 2013), it is tempting to speculate that they may also be inhibited by CGP-37157.

This could be further investigated using an Nclx KO mouse. Indeed, our group has acquired an Nclx KO mouse, in which a 13 base-pair deletion causes a frameshift mutation, rendering Nclx non-functional. Mitochondrial Ca^{2+} decay could be monitored following ATP or KCl stimulation of Nclx KO astrocytes or neurons, respectively. Additionally, the effect of CGP-37157 could be tested on Nclx KO cultures. If Nclx KO has no effect on mitochondrial Ca^{2+} efflux in neurons, but CGP-37157 inhibits Ca^{2+} efflux, I could be certain that mitochondrial Ca^{2+} efflux is mediated by another exchanger in neurons which is also inhibited by CGP-37157. Identification of this pathway would be important in neurons, given the importance of mitochondrial Ca^{2+} handling in these cells. Our group has shown that Mcu KD results in decreased excitotoxic cell death following NMDA application to cortical neurons (Qiu et al. 2013). Thus, it is tempting to speculate that blockade of mitochondrial Ca^{2+} efflux during excitotoxicity would exacerbate neuronal death due to excessive mitochondrial Ca^{2+} overload. In astrocytes, Nclx was shown to be important for buffering cytoplasmic Ca^{2+} levels, release of neurotransmitters as well as for astrocyte proliferation (Parnis et al. 2013).

A recent paper suggested that Nclx is expressed in dopaminergic neurons and is inhibited in Parkinson's disease leading to mitochondrial dysfunction due to loss of Pink1, which mediates Nclx's phosphorylation by PKA (Kostic et al. 2015). Kostic *et al.* show that Pink1 KO decreases mitochondrial Ca^{2+} efflux in dopaminergic neurons leading to cell death, and that this is rescued by Nclx expression, however they do not demonstrate the endogenous presence of Nclx in dopaminergic neurons. Thus, it is possible that Pink1 KO also influences other mitochondrial Ca^{2+} efflux pathways other than Nclx in neurons, but can still be rescued by exogenous Nclx expression. It is also possible that although I observe very low Nclx levels in cortical neurons, Nclx may be expressed at higher levels in other brain regions. Interestingly, Wood-Kaczmar *et al.* has previously implicated Ncx2 and 3 to be the mitochondrial Ca^{2+} efflux proteins downstream of Pink1 signalling in human dopaminergic neurons (Wood-Kaczmar et al. 2013). Thus, Ncx2 and 3 could be examined as potential alternative routes of mitochondrial Ca^{2+} efflux in neurons.

Chapter 5: Nrf2 target genes can be controlled by neuronal activity without the presence of Nrf2 or astrocytes

5.1. Introduction

Nrf2 is the master regulator of antioxidant defences (Lee et al. 2005; Loboda et al. 2016). Nrf2 is basally bound to Keap1 in the cytoplasm and targeted for degradation, but upon oxidative stress or small molecule activators of Nrf2, it dissociates from Keap1 and translocates to the nucleus (Vargas & Johnson 2009; Kensler et al. 2007; Loboda et al. 2016), where it binds to the antioxidant responsive element (ARE) in the promoter region of antioxidant and phase II detoxifying genes, many of which are components of the Trx-Prx and the glutathione (GSH) antioxidant systems, initiating their transcription (Loboda et al. 2016; Itoh et al. 1997; Jain et al. 2005).

The Nrf2 pathway is known to be active in astrocytes (Vargas & Johnson 2009), whilst Nrf2 mRNA levels and Nrf2 target gene induction following pharmacological activation of Nrf2 have been shown to be low in neurons (Bell, Al-Mubarak, et al. 2011; Shih et al. 2003; Kraft et al. 2004; Jimenez-Blasco et al. 2015), although this has been debated by some groups (Satoh et al. 2006; Yin et al. 2010; Zhang et al. 2009a). Yin *et al*. for instance observed upregulation of Nrf2 target genes and Nrf2 itself in neuronal hippocampal culture, which they attributed to Nrf2 activation in neurons (Yin et al. 2010). Our group has demonstrated that H_2O_2 activates Nrf2 target genes in a mixed cortical culture (10% astrocytes), but not in neuronal cortical cultures (<0.2% astrocytes), showing that activation of the pathway is astrocyte dependent (Bell, Al-Mubarak, et al. 2011). In this chapter I show using Western blotting and immunocytochemistry that the Nrf2 pathway is active in astrocytes in cortical cultures, but not in neurons.

Reactive oxygen species (ROS) are a by-product of cellular metabolism, produced following oxidative phosphorylation in mitochondria and by NADPH oxidase in the cytoplasm in neurons (Brennan et al. 2009; Hongpaisan et al. 2004). Small amounts of ROS are important for various cellular functions, such as cell signalling, but excessive ROS formation can lead to oxidative stress and cell death (Popa-Wagner et al. 2013). Despite their high metabolic demand, neurons have lower antioxidant capacity than astrocytes (Findlay et al. 2005; Dringen et al. 1999). The knock-out (KO) of Nrf2 has been shown to result in increased neuronal death following oxidative insults (Kensler et al. 2007). Thus, astrocytes provide neurons with non-cell autonomous neuroprotection against oxidative insults through the activation of the Nrf2 pathway, such as the supply of GSH precursors to neurons, to boost their antioxidant defences (Shih et al. 2003; Escartin et al. 2011).

A recent paper by Habas *et al*. suggested that neuronal activity modulates the Nrf2 pathway in astrocytes through the tripartite synapse, upregulating Nrf2 target genes and providing

neuroprotection to hippocampal neurons in culture (Habas et al. 2013). They showed upregulation of Nrf2 target genes and increased Nrf2 protein levels following neuronal activity. Since ROS production is increased in neurons following neuronal activity, due to increased metabolism, neuronal signalling to astrocytes could couple antioxidant support from astrocytes to neuronal activity.

However, neuronal activity through the activation of synaptic NMDA receptors (NMDARs) can induce neuroprotective effects in neurons themselves. Synaptic NMDAR activity inhibits pro-death gene expression, such as activation of the PI3K/Akt pathway promoting the nuclear export of FOXO, and promotes pro-survival gene expression, such as the activation of the ERK1/2 pathway and CaMKIV to induce CREB-dependent gene expression (Hardingham & Bading 2010; Papadia & Hardingham 2007). Neuronal activity through synaptic NMDAR-mediated Ca^{2+} influx also upregulates antioxidant defences in neurons themselves, such as genes involved in the Trx-Prx and GSH antioxidant systems, some of which are known Nrf2 target genes (Papadia et al. 2008; Baxter et al. 2015). As Nrf2 is present at low levels in neurons, which I confirm in this chapter, upregulation of Nrf2 target genes in neurons will need to be mediated by transcription factors other than Nrf2. Indeed our group showed that Nrf2 target gene sulfiredoxin 1 (Srxn1) is activated by neuronal activity in neurons by acting on promoter elements that have consensus sequences for AP-1, as well as Nrf2 (Papadia et al. 2008; Soriano et al. 2009). Therefore, I wanted to examine whether induction of Nrf2 target genes shown by Habas *et al*. following neuronal activity, is indeed dependent on Nrf2 and astrocytes, or whether these Nrf2 target genes can be activated in neurons themselves.

Thus, I hypothesise that Nrf2 target genes can be activated cell-autonomously in neurons following neuronal activity, independently of both astrocytes and Nrf2. The results presented in this chapter show that some Nrf2 target genes, but not all can be activated in neurons themselves by neuronal activity, the activation of which is independent of the presence of Nrf2 or astrocytes; and that Nrf2 protein levels do not significantly increase upon neuronal activity.

Some of the results in this chapter have been published in:

Deighton, R.F.*; Márkus, N.M.*; Al-Mubarak, B; Bell, K.F.S.; Papadia, S; Meakin, P.J.; Chowdhry, S; Hayes, J.D.; Hardingham, G.E. 2014. Nrf2 target genes can be controlled by neuronal activity in the absence of Nrf2 and astrocytes. *Proceedings of the National Academy of Sciences of the United States of America*, 111(18), pp.1818–1820

and

Bell, K.F.S.; Al-Mubarak, B*; Martel. M*.; McKay*, S; Wheelan, N*; Hasel, P*; Márkus, N.M.*; Baxter, P.; Deighton, R.F.; Serio, A; Bilican, B.; Chowdhry, S; Meakin, P.J.; Ashford, M.L.J.; Wyllie, D.J.A.; Scannevin, R.H.; Chandran, S.; Hayes, J.D.; Hardingham, G.E. 2015. Neuronal development is promoted by weakened intrinsic antioxidant defences due to epigenetic repression of Nrf2. *Nature communications*, 6(May), p.7066

*contributed equally to the work

5.2. Results

5.2.1. Nrf2 is weakly expressed in neurons

The presence of Nrf2 in astrocytes is well established (Vargas & Johnson 2009). However, whether the Nrf2 pathway is active in neurons has been a source of controversy. Some groups such as Yin *et al*. have shown Nrf2 induction in neurons, but many of these experiments were carried out using primary mixed neuronal culture (around 10% astrocytes) (Yin et al. 2010), which our group has found to contain enough astrocytes to activate Nrf2 target genes (Bell, Al-Mubarak, et al. 2011). Here, I examined Nrf2 protein levels in a mouse primary cortical astrocytes, a mixed (10% astrocytes, 90% neurons) and an astrocyte-free pure neuronal culture (<0.2% astrocytes) (Fig.5.1A). Nrf2 levels were elevated in astrocytes compared to mixed and neuronal culture, but were almost undetectable in neurons, even after treatment with Nrf2 activator tert-Butylhydroquinone (tBHQ) or the proteasome inhibitor MG-132 (Fig.5.1A). Since MG-132 inhibits degradation of proteins in the cell (Cui et al. 2013), Nrf2 levels just above the point of detection after its addition demonstrates the weak expression of Nrf2 in neurons. Although Nrf2 levels in neuronal culture are very low, Nrf2 is still present in mixed culture. To examine whether expression of Nrf2 in mixed culture is due to the presence of astrocytes or if Nrf2 is upregulated in the neurons themselves, I examined Nrf2 levels in neurons and astrocytes in a mixed culture by immunocytochemistry (Fig.5.1B). The results show that Nrf2 levels are elevated in astrocytes by tBHQ or MG-132 in mixed culture, but not in neurons (pointed out by white arrows). This shows that the Nrf2 pathway is active in astrocytes in a mixed cortical culture, but not in neurons due to their low expression of Nrf2.

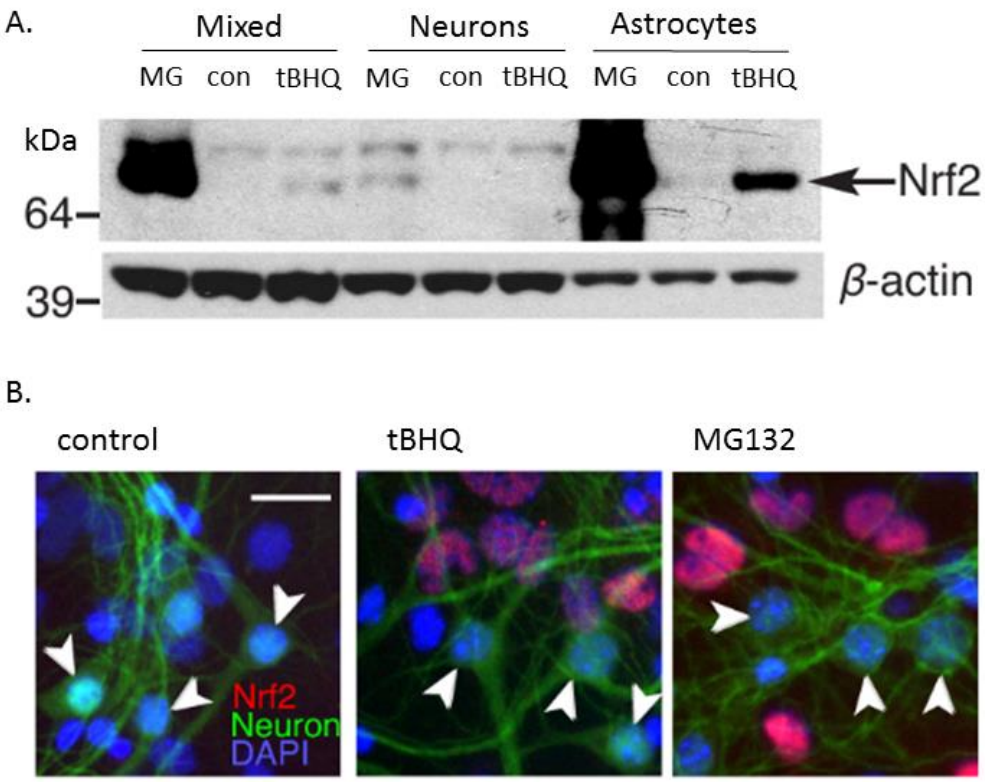

Figure 5.1. Nrf2 is present in astrocytes, but is only weakly expressed in neurons in mouse primary cortical culture. A. Western blot of Nrf2 protein levels in astrocytes compared to mixed and neuronal culture at baseline and following addition of Nrf2 activator tBHQ (10 µM, 8h) and proteasomal inhibitor MG-132 (5 µM, 16h). Note that long exposure times were needed to detect the bands. Representative blot of n=3. **B.** Nrf2 is activated by tBHQ and MG-132 in astrocytes, but not in neurons in a mixed culture. Cultures stained for anti-Nrf2 (red), neuronal marker (green) and DAPI (blue). Arrows point to neurons in mixed culture. Representative images of n=5. Scale bar=25 µm.

5.2.2. Srxn1, xCT, Hmox1, Gclc and Nqo1 are Nrf2 target genes

I decided to examine the effect of synaptic activity on a number of well-known Nrf2 target genes, Srxn1 (which reactivates hyperoxidised peroxiredoxins), system xc^- (xCT) (a glutamate-cystine transporter), glutamate-cysteine ligase catalytic subunit (Gclc) (which catalyses the rate-limiting step in GSH synthesis), haem-oxygenase 1 (Hmox1) (which breaks down the haem group) and NAD(P)H quinone dehydrogenase 1 (Nqo1) (responsible for the reduction of quinones) (Soriano et al. 2008a; Soriano et al. 2009; Bell, Al-Mubarak, et al. 2011; Sasaki et al. 2002; Lacher et al. 2015; Vargas & Johnson 2009; Kensler et al. 2007; Loboda et al. 2016), two of which Habas *et al.* had studied (Habas et al. 2013). To confirm that these genes were indeed targets of the Nrf2 pathway in astrocytes, but not in neurons, I examined their mRNA expression in mouse cortical mixed WT and Nrf2 knock-out (KO) cultures made from an Nrf2 KO mouse (Itoh et al. 1997) with or without addition of Nrf2 activator tBHQ, and found all five genes to be induced by tBHQ in an Nrf2-dependent manner (Fig.5.2). Since I found activation of the Nrf2 pathway to be weak in neurons (Section 5.2.1.), I wanted to confirm that these genes were activated by tBHQ in an astrocyte-dependent manner. Thus, I applied tBHQ to neuronal and astrocyte enriched cultures (AE; ~15% astrocytes), to which no AraC was added to stop glial proliferation, to recreate culture conditions used by Habas *et al*. (Habas et al. 2013). I found all five genes to be largely significantly increased following tBHQ treatment of astrocytes (Fig.5.3). Although there was a significant increase in Srxn1 and Hmox1 mRNA levels in neuronal culture following tBHQ treatment (Fig.5.3.A,C), these changes were very small in comparison to induction in AE culture, thus were likely due to the small number of astrocytes present in pure neuronal culture. Therefore, Srxn1, xCT, Hmox1, Gclc and Nqo1 are Nrf2 target genes which are activated in response to tBHQ in an Nrf2 and astrocyte-dependent manner.

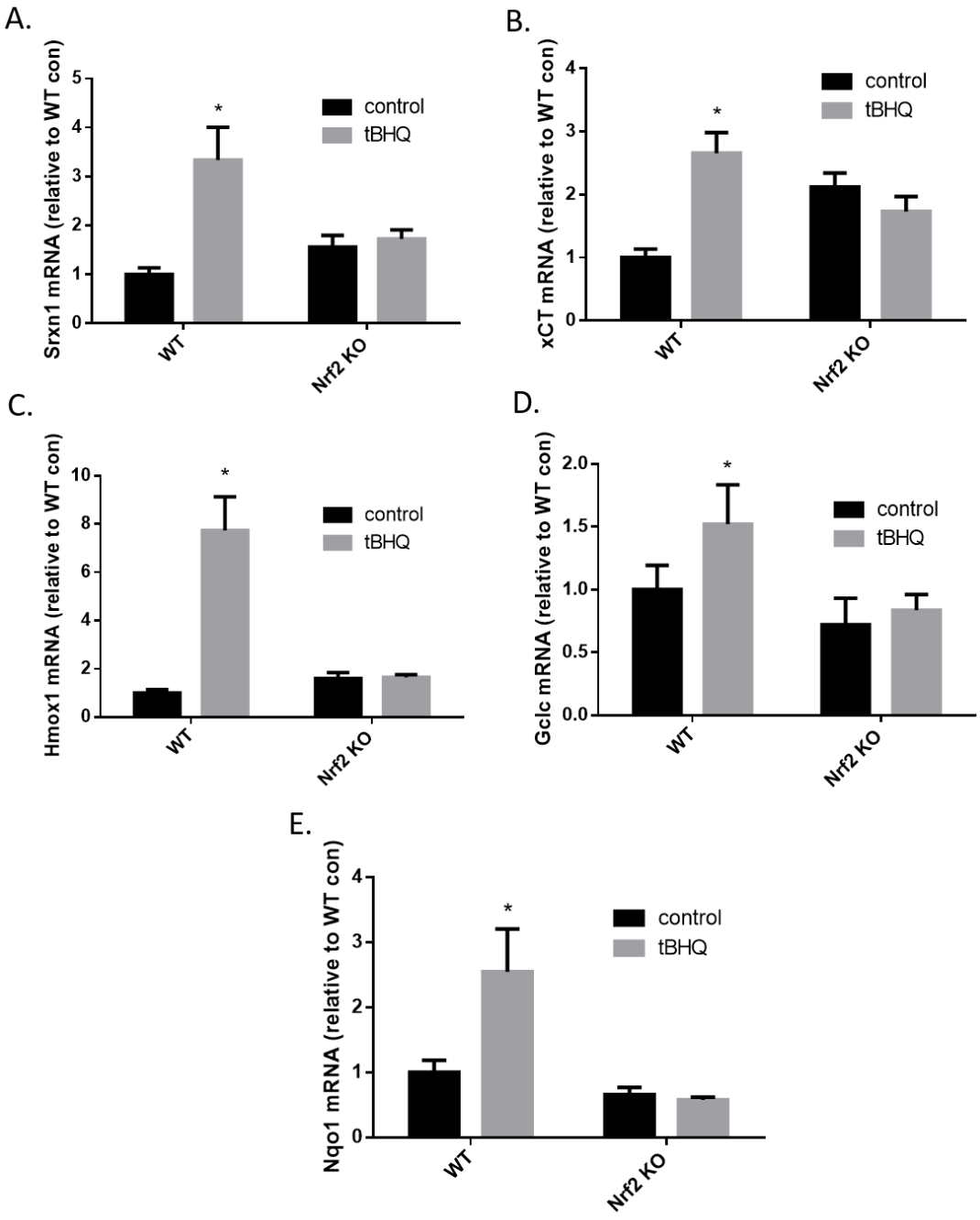

Figure 5.2. Srxn1, xCT, Hmox1, Gclc and Nqo1 are induced by Nrf2 activator tBHQ in an Nrf2 dependent manner. mRNA levels of Srxn1, xCT, Hmox1, Gclc and Nqo1 were detected using real-time (RT)-qPCR in WT or Nrf2 KO mixed culture (**A-E**, respectively). Values were normalised to Gapdh and then to the WT control. n=6 for WT, n=7 for Nrf2 KO (Srxn1 and xCT) and n=4 Nrf2 KO (Hmox1, Gclc, Nqo1), paired two-tailed t-test. *p≤0.05 compared to their own control. p-values, respectively: 0.0079, 0.0012, 0.0032, 0.0134, 0.0232. Error bars=SEM.

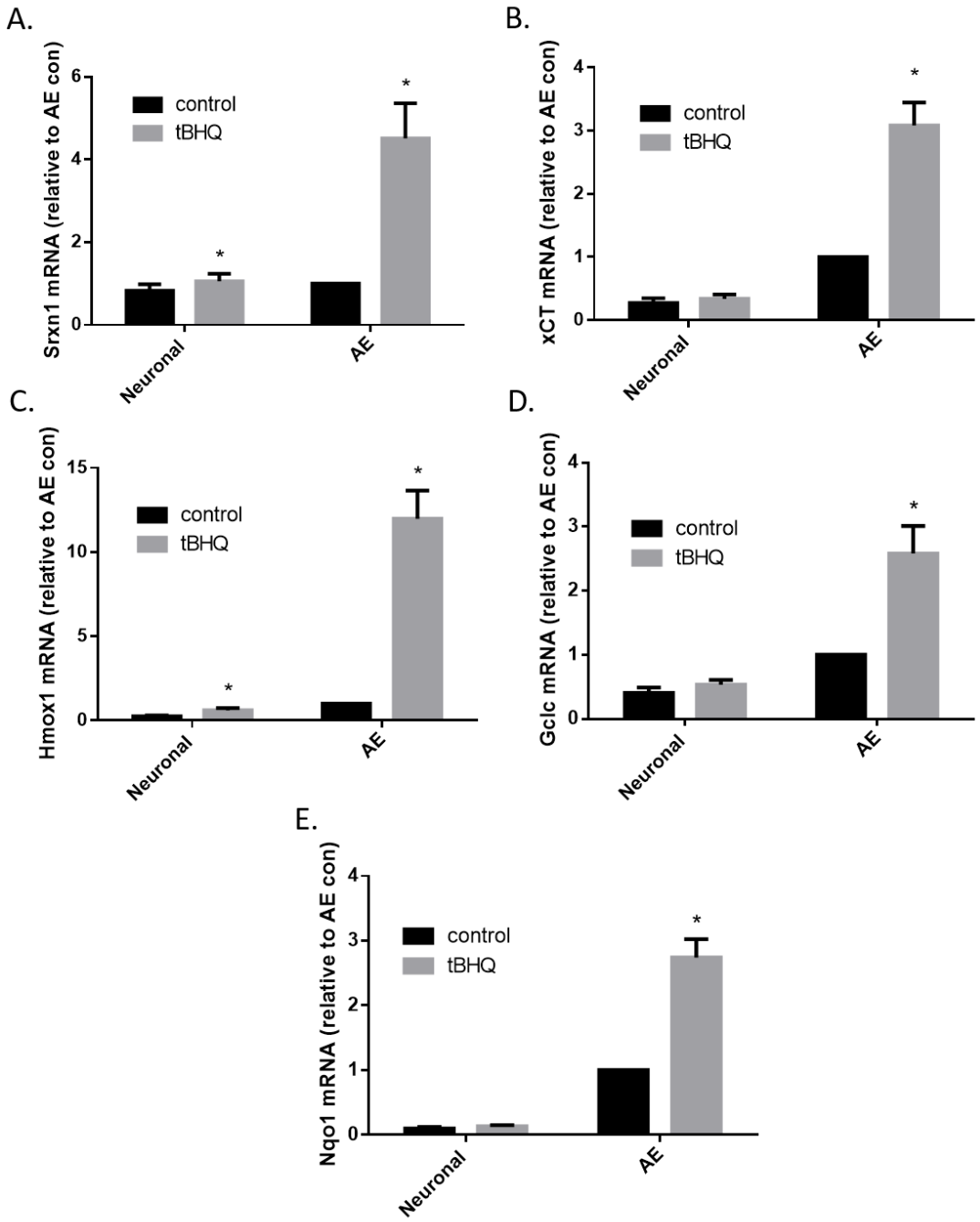

Figure 5.3. Srxn1, xCT, Hmox1, Gclc and Nqo1 are induced by Nrf2 activator tBHQ in an astrocyte dependent manner. mRNA levels of Srxn1, xCT, Hmox1, Gclc and Nqo1 (**A-E**, respectively) measured by RT-qPCR in a neuronal or AE culture. Values were normalised to 18s and then to the AE control. n=6. Paired two-tailed t-test. *p≤0.05 compared to their own control. p-values, respectively: 0.0216, 0.0090, 0.0023, 0.0217, 0.0012, 0.0146, 0.0017. Error bars=SEM.

5.2.3. Srxn1, xCT, Hmox1 and Gclc are induced by neuronal activity independently of astrocytes

Neurons are known to possess some of their own antioxidant defences, many of which are activated downstream of synaptic NMDARs (Papadia et al. 2008). Some of the antioxidant genes upregulated in neurons following neuronal activity are known Nrf2 target genes, such as Srxn1 (Papadia et al. 2008). Habas *et al*. recently suggested that Nrf2 target genes Gclc and Nqo1 are upregulated following neuronal activity by neurons signalling to astrocytes and activating the Nrf2 pathway (Habas et al. 2013). I wanted to examine whether induction of Nrf2 target genes seen by Habas *et al.* could be due to the activation of these genes in neurons themselves in response to increased synaptic activity. I applied $GABA_A$ receptor antagonist bicuculline and K^+ channel antagonist 4-aminopyridine (Bic/4-AP) to cultures, which increases neuronal AP firing, by blocking inhibitory inputs to neurons and elevates burst frequency, leading to synaptic NMDAR-mediated Ca^{2+} influx into neurons (Papadia et al. 2008). I compared mRNA levels of Nrf2 target genes Srxn1, xCT, Hmox1, Gclc and Nqo1 following Bic/4-AP treatment in a neuronal (<0.2% astrocytes) and AE (15% astrocytes) culture (Fig.5.4). Srxn1 levels were significantly higher following 4 and 24h Bic/4-AP treatment in both neuronal and AE culture (Fig.5.4A). xCT levels were significantly upregulated after 24h in both cultures and after 4h in neuronal culture (Fig.5.4B.). Levels of Hmox1 were significantly induced after 24h Bic/4-AP treatment in neuronal culture and there was a strong, but non-significant increase ($p=0.0538$) in Hmox1 levels following 24h Bic/4-AP activity in AE culture (Fig.5.4C). Note that 24h Bic/4-AP activity does significantly increase Hmox1 levels in a mixed culture (Fig.5.5C). Gclc mRNA levels were significantly induced following 24h Bic/4-AP stimulation and there was an upward trend following 4h stimulation (Fig.5.4D). Levels of Nqo1 remained unchanged following Bic/4-AP stimulation both in neuronal and AE culture (Fig.5.4E). Thus, some Nrf2 target genes, but not all, can be activated by neuronal activity, the activation of which is independent of the presence of astrocytes in cortical culture.

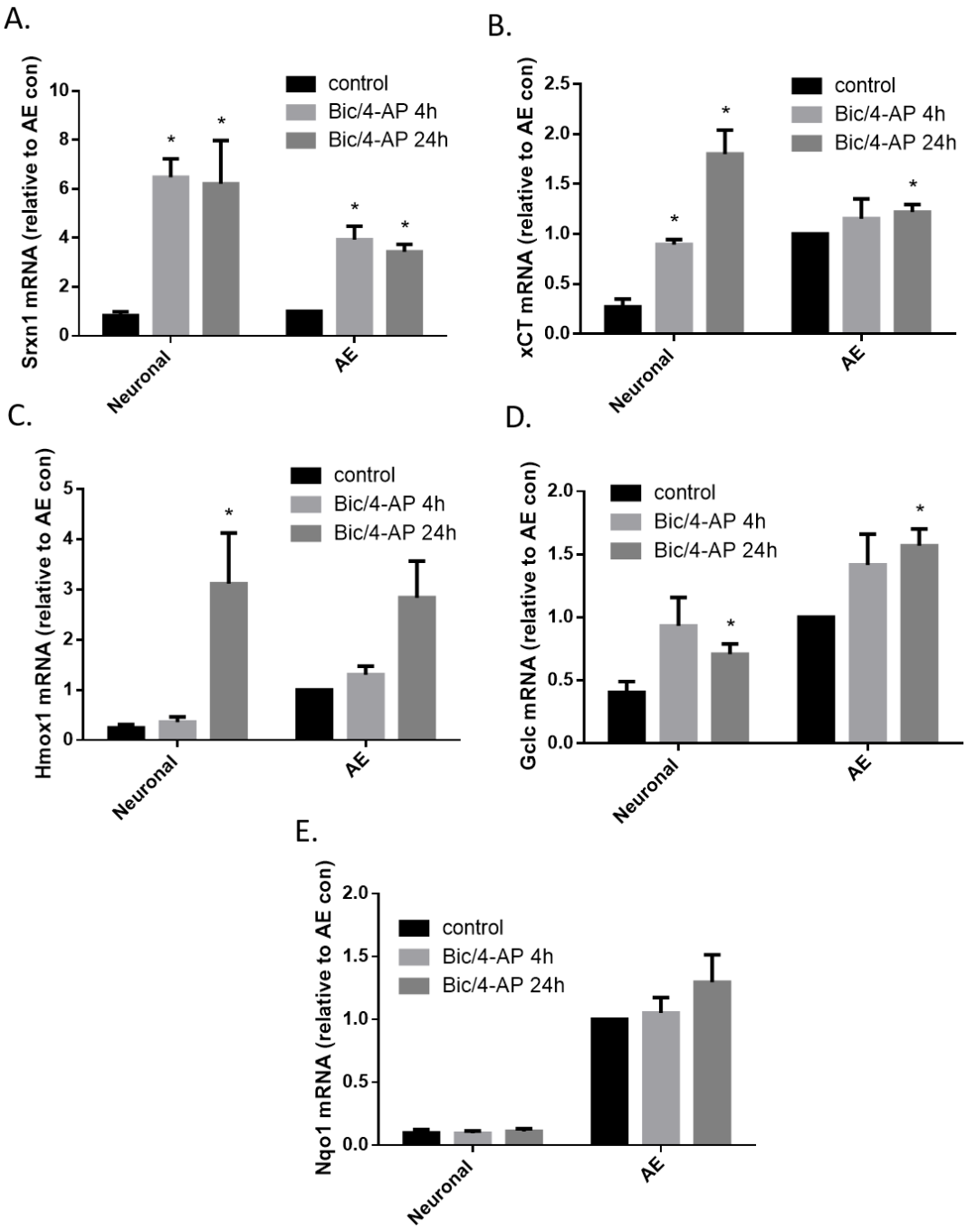

Figure 5.4. Srxn1, xCT, Hmox1 and Gclc, but not Nqo1, are induced by Bic/4-AP in neuronal and AE culture. mRNA levels of Srxn1, xCT, Hmox1, Gclc and Nqo1 (**A-E**, respectively) detected using RT-qPCR in neuronal or AE culture following Bic/4-AP treatment for 4h or 24h. Values were normalised to 18s and then to the AE control. n=6. Paired two-tailed t-test. *p≤0.05 compared to their own control. p-values, respectively: 0.0003, 0.0238, 0.0031, 0.0005, <0.0001, 0.0018, 0.0334, 0.0290, 0.0224, 0.0081. Error bars=SEM.

5.2.4. Srxn1, xCT, Hmox1 and Gclc are induced by neuronal activity independently of Nrf2

Since Nrf2 is mainly expressed in astrocytes (section 5.2.1.), and Nrf2 target genes can be activated by neuronal activity independently of astrocytes (section 5.2.3.), I hypothesised that these Nrf2 target genes can be activated independently of Nrf2 itself. I tested this by applying Bic/4-AP to mixed WT or Nrf2 KO cultures and measured mRNA levels of Nrf2 target genes by RT-qPCR (Fig.5.5). Srxn1 and xCT levels were significantly increased following 4h and 24h Bic/4-AP treatment in both WT and Nrf2 KO cultures (Fig.5.5A,B). Hmox1 levels were significantly increased following 24h Bic/4-AP treatment (Fig.5.5C), while Gclc was significantly induced following 4h Bic/4-AP treatment in both cultures (Fig.5.5D). In contrast, Nqo1 levels were not increased in either culture following neuronal activity (Fig.5.5E). Note that these results reflect the induction pattern seen in neuronal and AE culture (Fig.5.4), with the exception of Gclc which was increased after 24h Bic/4-AP in neuronal and AE culture, although in all cultures, it showed an upward trend at both time points. This demonstrates that these Nrf2 target genes, except for Nqo1, are upregulated independently of Nrf2 following neuronal activity in a mixed culture.

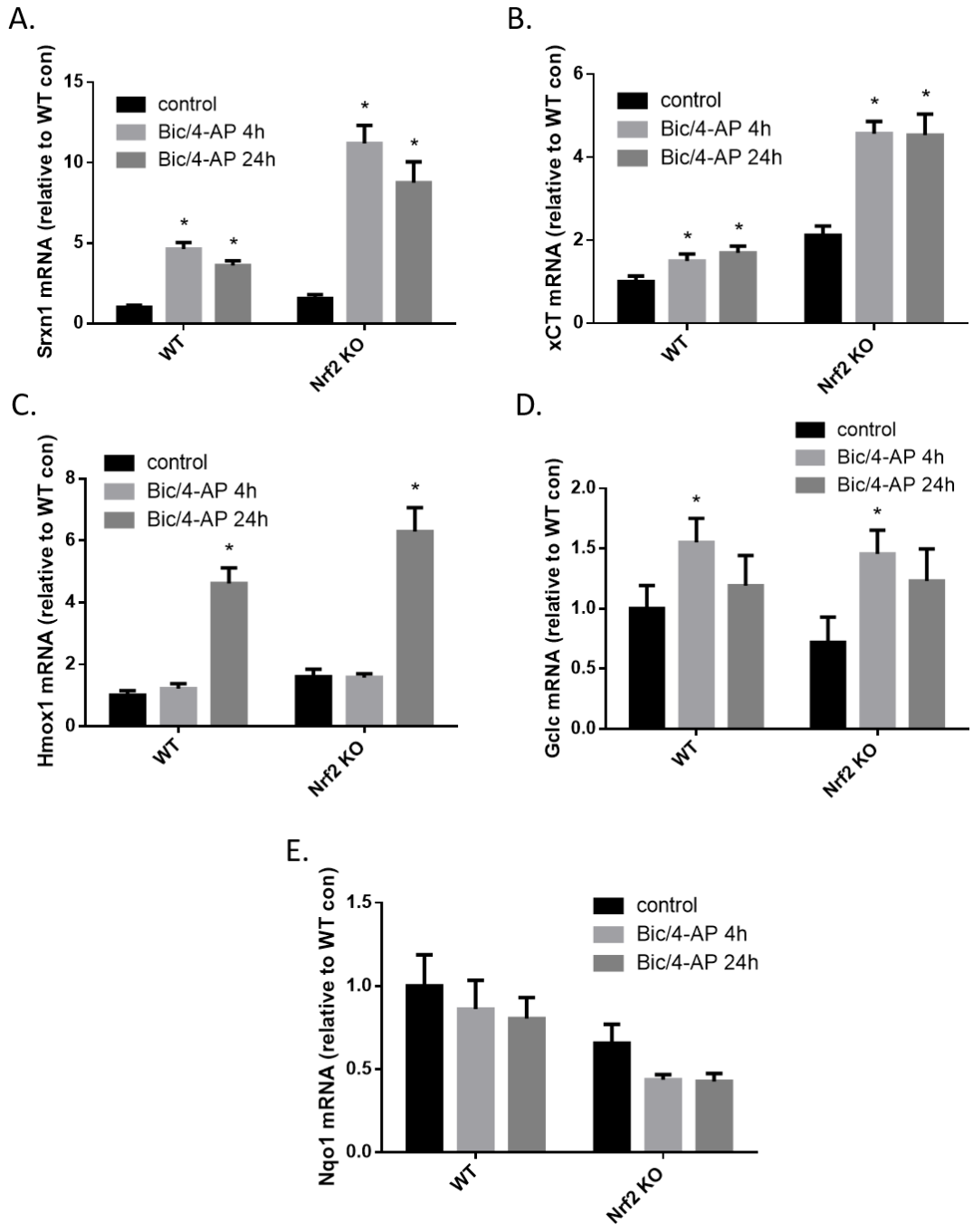

Figure 5.5. Nrf2 target genes Srxn1, xCT, Hmox1 and Gclc are induced by Bic/4-AP in WT and Nrf2 KO culture. mRNA levels of Srxn1, xCT, Hmox1, Gclc and Nqo1 (**A-E**, respectively) were tested following 4 and 24h Bic/4-AP treatment in WT and Nrf2 KO mixed cultures by RT-qPCR. Values were normalised to Gapdh and then to the WT control. n=6 for WT, n=7 for Nrf2 KO (Srxn1 and xCT) and n=4 for Nrf2 KO (Hmox1, Gclc, Nqo1). Paired two-tailed t-test. *p≤0.05 compared to their own control. p-values, respectively: 0.0002, 0.0003, 0.0014, <0.0001, 0.0182, 0.0135, <0.0001, 0.0007, 0.0010, 0.0104, 0.0043, 0.0184. Error bars=SEM.

5.2.5. Nrf2 protein levels are not increased by neuronal activity

Habas *et al*. found increased nuclear Nrf2 protein levels in AE culture following neuronal activity, and suggested this to be the result of neuronal signalling to astrocytes via the tripartite synapse (Habas et al. 2013). Since I found Nrf2 target gene induction following neuronal activity to be independent of astrocytes and Nrf2 (Sections 5.2.3 and 4), I hypothesised that Nrf2 protein levels would likely be unaffected. The Nrf2 antibody used by Habas *et al*. produced many non-specific bands in my hands (data not shown), thus I used a different Nrf2 antibody (D1Z9C, Cell Signaling). I validated the antibody using WT and Nrf2 KO primary mouse astrocyte cultures, and indeed found the band present at the expected molecular weight of ~66kDa for Nrf2 to be absent from the Nrf2 KO samples (Fig.5.6A). Note that the faint band at a slightly higher molecular weight than Nrf2 seen in many of the blots is unspecific. Nrf2 protein levels on day in vitro (DIV) 10 were not significantly increased by either Bic/4-AP treatment or depolarization with high K^+ (with NMDAR antagonist MK-801 present) in the presence or absence of L-type Ca^{2+} channel agonist FPL-64176 (KCl or KCl/FPL treatment) in an AE culture (Fig.5.6B-C). High K^+ treatment is known to depolarise neurons and lead to L-type Ca^{2+} channel mediated Ca^{2+} influx (Hardingham et al. 1999). In contrast, Nrf2 protein levels were significantly increased following addition of Nrf2 activators sulforaphane (SLF) and tBHQ, as well MG-132 (Fig.5.6B-C).

Since Habas *et al*. only saw an increase in Nrf2 levels following 24h neuronal activity at a more mature developmental stage (DIV14), I also examined Nrf2 levels at a later developmental time point (DIV18). I observed no significant increase in Nrf2 protein levels following Bic/4-AP or KCl(/FPL) treatment of DIV18 AE cultures (Fig.5.7), whilst Nrf2 protein levels were significantly increased after tBHQ and MG-132 treatment and there was a strong trend for Nrf2 activation by SLF ($p=0.0532$).

Thus, Nrf2 protein levels are not significantly increased by neuronal activity in AE culture, further suggesting that the induction of Nrf2 target genes by neuronal activity is Nrf2 independent.

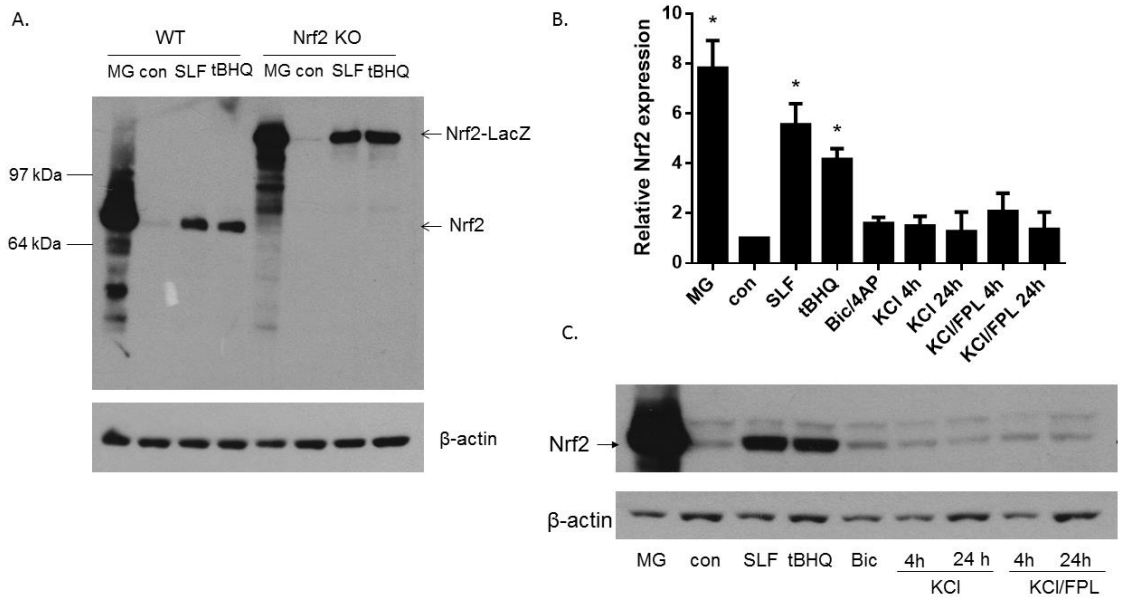

Figure 5.6. Nrf2 protein levels are not significantly induced following Bic/4-AP treatment of DIV10 AE culture. A. The Nrf2 antibody is specific for Nrf2. An example blot is shown of WT and Nrf2 KO astrocyte samples untreated or treated with Nrf2 activators tBHQ (10 µM), SLF (5 µM) or MG-132 (10 µM) for 16h. The bands seen at a higher molecular weight in the Nrf2 KO samples is due to the KO process, part of the Nrf2 gene is replaced with 5.8 kb LacZ cDNA resulting in the production of the first 301 residues of Nrf2 bound to LacZ (Itoh et al. 1997). Since the Nrf2 antibody targets human Nrf2 around Ala275, Nrf2 bound to LacZ is detected. **B.** Densitometric analysis of Nrf2 levels following Bic/4-AP (24h) or KCl(/FPL) treatment of DIV10 AE culture from Western blots, as well as treatment with Nrf2 activators, an example trace of which can be seen in **C.** Note that the MG-132 treated lane is oversaturated. Results were normalised to β-actin and the control. Note that the faint band seen slightly above Nrf2 is non-specific. n=5 for con, MG, SLF, Bic-4AP, KCl and KCl/FPL 4h, n=4 for KCl and KCl/FPL 24h, and n=3 for tBHQ. Paired two-tailed t-tests. *p≤0.05 compared to control. p-values, respectively: 0.0035, 0.0058, 0.0183. Error bars=SEM.

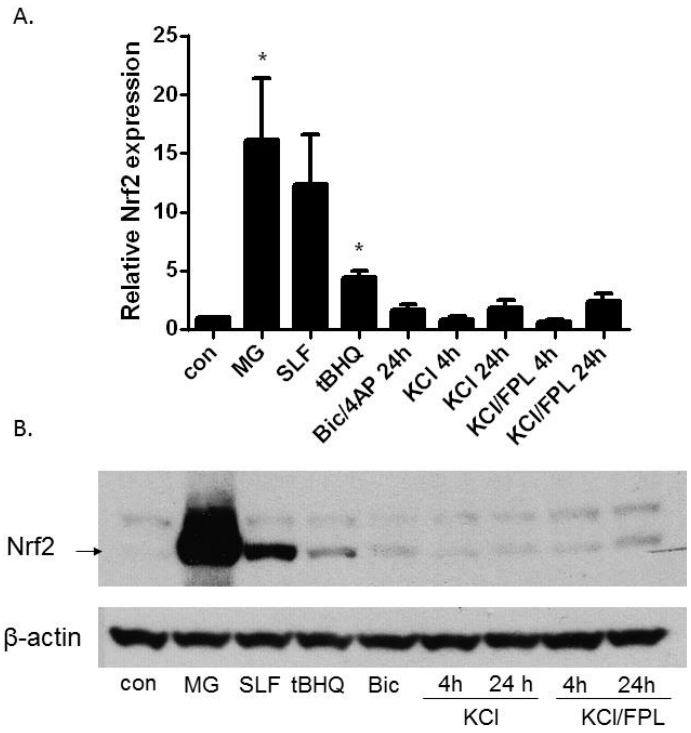

Figure 5.7. Nrf2 protein levels are not significantly induced following Bic/4-AP treatment of DIV18 AE culture. A. Densitometric analysis of Nrf2 protein levels following Bic/4-AP or KCl(/FPL) treatment, or treatment with Nrf2 activators of DIV18 AE culture from Western blots, an example exposure of which can be seen in **B.** Note that the MG-132 lane is over saturated. Results were normalised to β-actin and the control. n=5. Paired two-tailed t-tests. *p≤0.05 compared to control. p-values, respectively: 0.0454, 0.0045. Error bars=SEM.

5.2.6. Nrf2 protein levels are not significantly induced by neuronal activity in astrocytes in a mixed culture

Nrf2 target genes can be activated independently of Nrf2 and astrocytes (section 5.2.5.), but this does not mean that Nrf2 target genes are not activated by Nrf2 in astrocytes to some extent in a mixed culture. Thus, I examined Nrf2 protein levels in neurons and astrocytes in a WT mixed culture using immunocytochemistry (example images can be seen in Fig.5.1.). The relative intensity of the staining was compared between different conditions in neurons and astrocytes. Nrf2 activators, SLF, tBHQ, MG-132 and $CDDO^{TFEA}$ significantly increased Nrf2 levels in astrocytes, but not in neurons, further supporting results shown in section 5.2.1 (Fig.5.8A-C,F). Interestingly, application of hydrogen peroxide (H_2O_2) also significantly increased Nrf2 protein levels in astrocytes (Fig.5.8E). H_2O_2 is known to produce oxidative stress which activates Nrf2, and our group has previously shown that H_2O_2 induces Nrf2 target gene expression in an astrocyte dependent manner (Bell, Al-Mubarak, et al. 2011), but this is the first time this is shown on the protein level. Nrf2 levels were not significantly increased in neurons or astrocytes following Bic/4-AP application, although there was a slight increase in Nrf2 levels in astrocytes (Fig.5.8D). This further confirms findings from section 5.2.5., that Nrf2 protein levels are not significantly increased following Bic/4-AP treatment, and supports the idea that the Nrf2 target genes are activated by neuronal activity independently of Nrf2 and astrocytes. Furthermore, this further proves that the Nrf2 pathway is activated in astrocytes, but only weakly expressed in neurons.

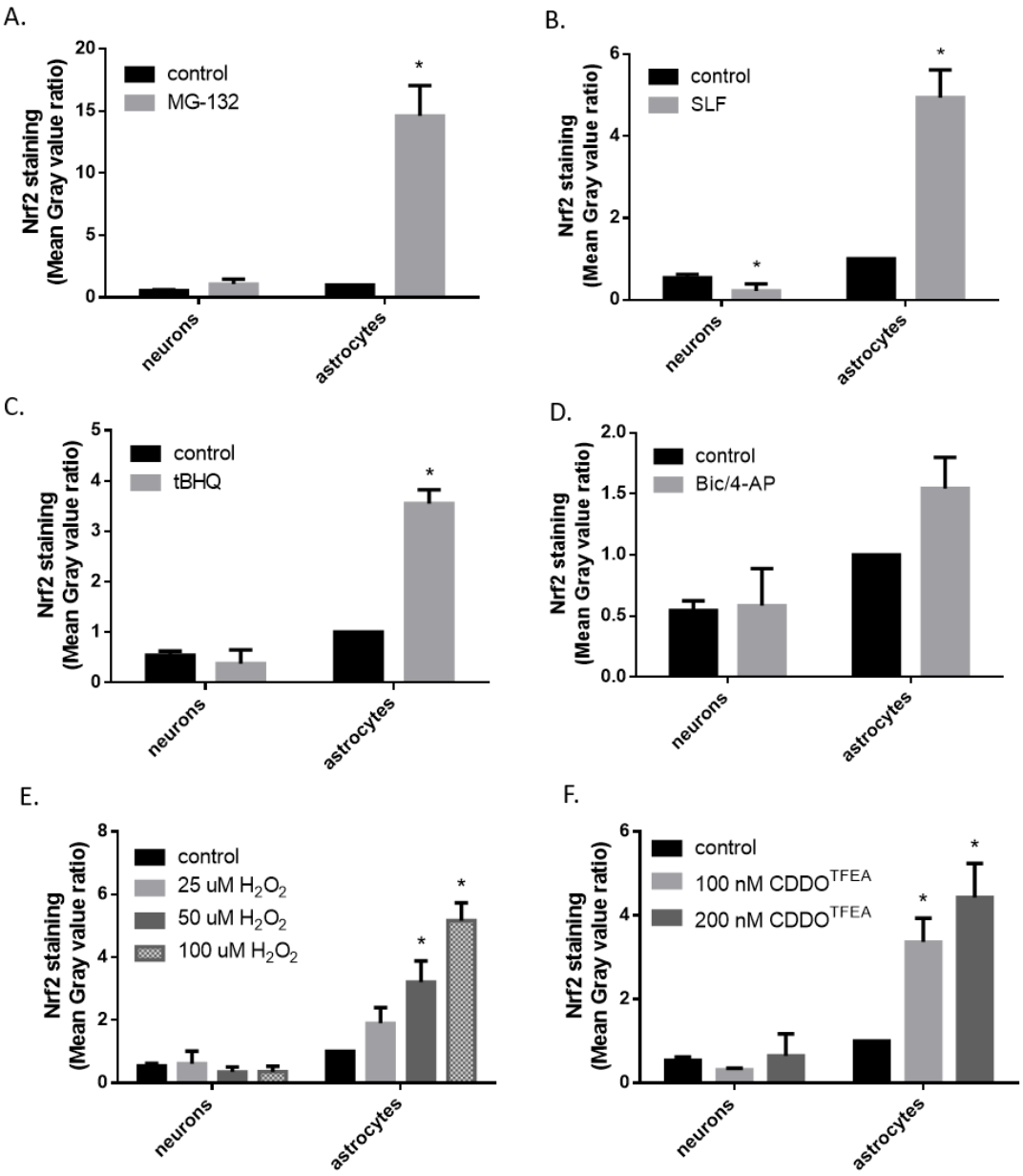

Figure 5.8. Nrf2 levels are increased by Nrf2 activators and H_2O_2 in astrocytes in a mixed culture, but not increased following Bic/4-AP treatment in either neurons or astrocytes. A-F. The relative Nrf2 level intensity was quantified in neurons and astrocytes in Nrf2 immunostained mixed culture from mean grey values (at least 25 neurons and astrocytes/image, 3 images/n) and normalised to control astrocyte Nrf2 values. Secondary antibody-only controls were subtracted from the results to avoid bleed-through from the GFP channel. Nrf2 levels were significantly increased in astrocytes by Nrf2 activators MG-132 (5 µM, 16h), SLF (10 µM, 8h), tBHQ (10 µM, 8h) and $CDDO^{TFEA}$ (8h) (A,B,C,F respectively), as well as 50 and 100 µM H_2O_2 (E), but not by Bic/4-AP treatment (24h) (D). n=4 for control, tBHQ, SLF, 100 µM H_2O_2, and n=3 for 25 and 50 µM H_2O_2, DMF, F3, Bic/4-AP. Two-tailed paired t-tests, except for H_2O_2 and $CDDO^{TFEA}$ where a one-way ANOVA with Dunnett's *post-hoc* test was used. *p≤0.05 compared to their own control. p-values, respectively: 0.0114, 0.0424, 0.0101, 0.0025, 0.0004, 0.0045. For example images of Nrf2 immunostaining in a mixed culture see figure 5.1.

5.2.7. Some, but not all, Nrf2 target genes are upregulated by neuronal activity

Although I examined five Nrf2 target genes, the question remained whether other Nrf2 target genes are also upregulated by neuronal activity, and if their activation is Nrf2 and astrocyte dependent.

Thus, I used an RNA-seq data set of neuronal and mixed cultures treated with tBHQ or Bic/4-AP for 4 or 24h, to look at a wider range of Nrf2 target genes.

I identified a group of 154 genes which were induced by Nrf2 activator tBHQ in mixed, but not in neuronal culture. Note that only one gene, Jun, was significantly upregulated by tBHQ in neuronal culture, and was therefore excluded from the list of tBHQ-induced genes. Of the 154 genes, 55 known genes were significantly induced ≥1.5-fold by tBHQ in mixed culture, but not in pure neuronal culture (Fig.5.9A-B) (For the list of genes, see supplementary table 1). Of note, I found these 55 tBHQ-induced Nrf2 target genes to have a higher basal expression in mixed, then in neuronal culture, indicating that they are likely expressed at higher levels basally in astrocytes (Fig.5.9C).

From the 55 tBHQ-induced Nrf2 target genes I identified, I found 16 to be significantly induced by 4h Bic/4-AP treatment (Fig.5.10A), and 17 genes to be induced by 24h Bic/4-AP treatment in pure neuronal culture (Fig.5.10B) (For the list of genes, see supplementary table 2 and 3). Of interest, the genes I examined in sections 5.2.3 and 5.2.4 were also upregulated by neuronal activity in the RNA-seq data set, Srxn1 and xCT were induced following 4 and 24h Bic/4-AP, whilst Gclc was induced after 4h and Hmox1 after 24h Bic/4-AP treatment in neuronal culture. As I observed in sections 5.2.3 and 5.2.4, Nqo1 was not significantly upregulated following neuronal activity in either neuronal or mixed culture. Thus, neuronal activity induces a significant percentage of Nrf2 target genes in pure neuronal culture, despite neurons having a non-functional Nrf2 pathway.

Although some of the 55 tBHQ-induced Nrf2 target genes were upregulated following neuronal activity in pure neuronal culture, 35 were not (For the list of genes, see supplementary table 4). If Nrf2 is activated in astrocytes following neuronal activity as suggested by Habas *et al.*, these 35 tBHQ-induced Nrf2 target genes should show increased expression following Bic/4-AP treatment in mixed culture. Thus, I studied the expression of this group of genes in mixed culture following 4 and 24h Bic/4-AP treatment, and found them not to be significantly induced, with the average $\log_2$ fold change of the genes around 0 (Fig.5.10A-C). In contrast, these 35 genes showed robust significant upregulation following tBHQ treatment, with a $\log_2$ fold change around 1 (Fig.5.10C).

This indicates that neuronal activity does not induce Nrf2 in astrocytes, since activation of Nrf2 would lead to a significant upregulation of these genes, as is observed with tBHQ stimulation.

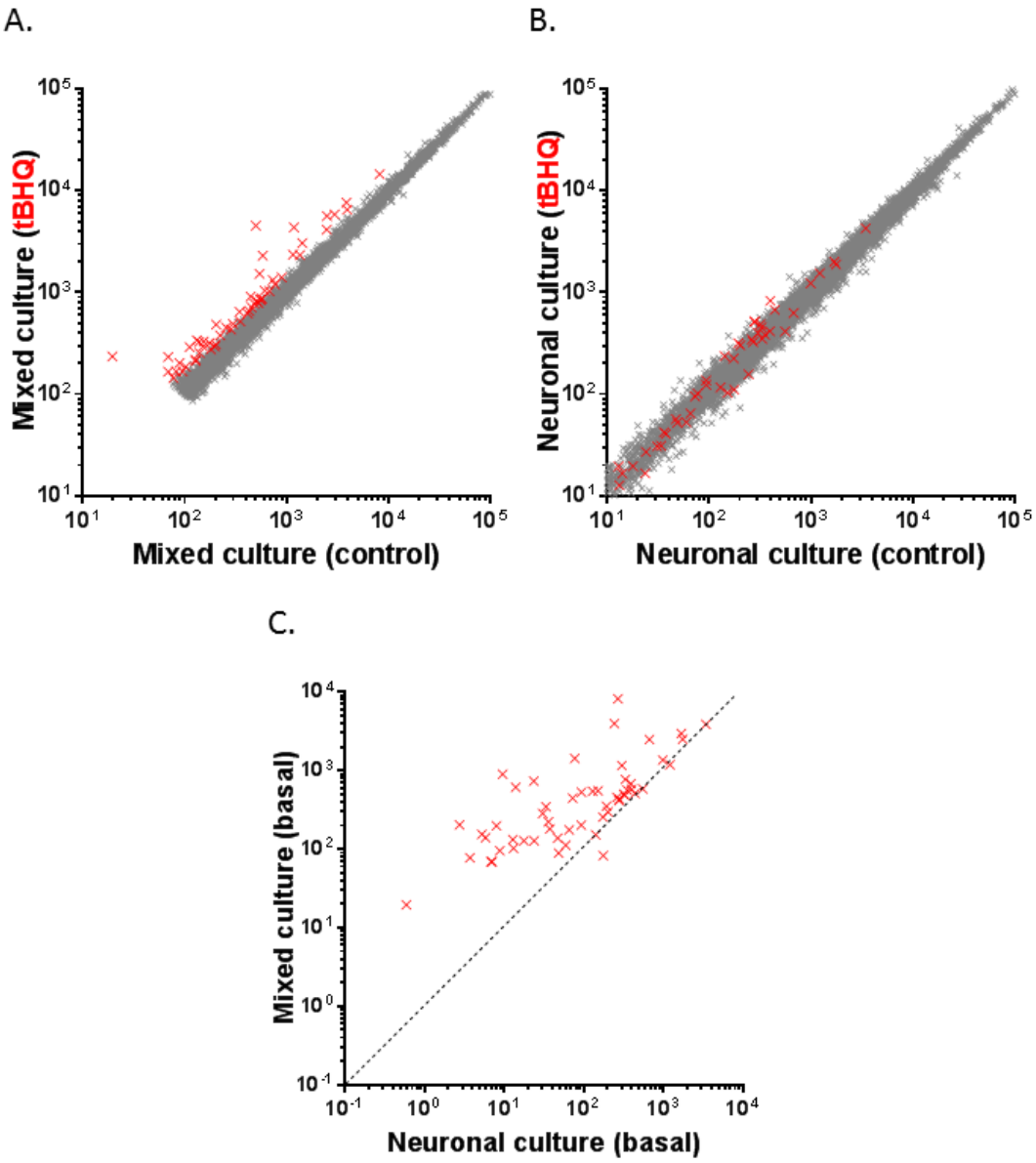

Figure 5.9. There are 55 Nrf2 target genes which are significantly induced ≥1.5-fold by tBHQ in mixed, but not in neuronal culture. A. Raw reads for the 55 genes significantly induced ≥1.5-fold by tBHQ (8h, 10 µM) in mixed culture, indicated in red, and genes not significantly induced by tBHQ in mixed culture, indicated in grey, compared to the untreated mixed culture. Note that only genes with over a 100 raw reads on average between the two conditions have been included. **B.** The raw reads for the genes from (A) in pure neuronal culture treated with tBHQ. Note that the 55 Nrf2 target genes (red) are not significantly upregulated. **C.** The 55 tBHQ-induced Nrf2 target genes are expressed at higher levels basally in mixed than in neuronal culture. n=3.

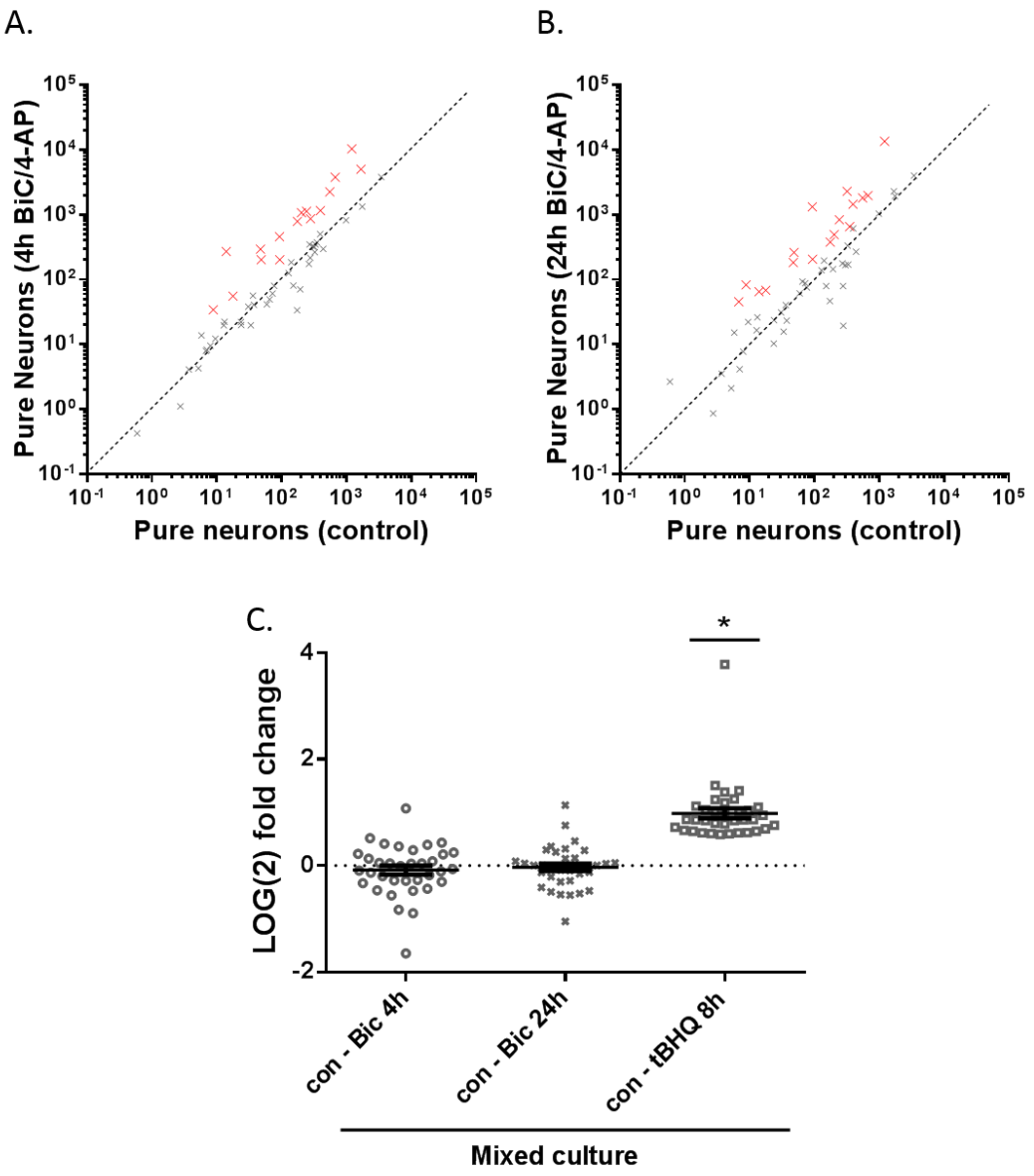

Figure 5.10. Some tBHQ-induced Nrf2 target genes are induced by Bic/4-AP treatment in neuronal culture, whilst the other Nrf2 target genes are not significantly upregulated in mixed culture. A. Raw reads of the 16 significantly upregulated genes following 4h Bic/4-AP treatment in neuronal culture shown in red, with the rest of the 55 tBHQ-induced Nrf2 target genes shown in grey. **B.** 17 of the 55 tBHQ-induced Nrf2 target genes are significantly upregulated in neuronal culture following 24h Bic/4-AP treatment. Shown as in (A) **C.** The group of 35 tBHQ-induced Nrf2 target genes not upregulated in pure neuronal culture following Bic/4-AP are not significantly upregulated in mixed culture following 4 or 24h Bic/4-AP. In contrast, this group of genes are significantly upregulated following tBHQ (10 µM, 8h) treatment in mixed culture. Data shown as the $\log_2$ fold-change of genes following Bic/4-AP or tBHQ treatment compared to the control mixed culture. Paired two-tailed t-test. *p=0.0010. Error bars=SEM.

5.3. Discussion

5.3.1. Conclusion

I found that the Nrf2 pathway is active in astrocytes, but not in neurons due to their weak expression of Nrf2; and that Srxn1, xCT, Hmox1 and Gclc are indeed Nrf2 target genes in astrocytes. I did not observe a significant increase in Nrf2 protein levels following neuronal activity during development or in more mature cultures; and found that some, but not all Nrf2 target genes can be induced by neuronal activity independently of astrocytes and Nrf2. Furthermore, I did not find a significant increase in the expression of a group of tBHQ-induced Nrf2 target genes (which were not upregulated in neurons following neuronal activity) following neuronal activity in a mixed culture, providing further evidence against Nrf2 activation in astrocytes following neuronal activity.

5.3.2. The Nrf2 pathway is active in astrocytes, but not in neurons

The role of the Nrf2 pathway in astrocytes has been well established (Vargas & Johnson 2009), and many studies show that Nrf2 is expressed at much lower levels in neurons than astrocytes (Bell, Al-Mubarak, et al. 2011; Shih et al. 2003; Kraft et al. 2004; Jimenez-Blasco et al. 2015). However, some groups such as Yin *et al*., have suggested that the Nrf2 pathway is active in neurons (Satoh et al. 2006; Yin et al. 2010; Zhang et al. 2009a). The observation by Yin *et al.* is likely due to their use of "neuronal" cultures which can contain up to 10% astrocytes, which is equivalent to the astrocyte content of my mixed culture. I show in this chapter by Western blotting that Nrf2 is present at very low levels in neurons, and that Nrf2 activation by tBHQ has minimal effect in neuronal culture and only produces a small increase in mixed culture compared to astrocytes. I show by immunocytochemistry that the increase in Nrf2 levels in mixed culture following the addition of Nrf2 activators is due to astrocytes. Thus, the source of controversy in the field likely stems from the ability of a small percentage of astrocytes being able to induce Nrf2 target gene expression in culture, even though the Nrf2 pathway is not active in neurons. Our group has recently shown that Nrf2 is epigenetically silenced early in development in neurons to allow for correct neuronal development (Bell et al. 2015), which explains my observations. It would be interesting to examine Nrf2 levels *in vivo* in aged animals, to see if perhaps the epigenetic repression of Nrf2 is reversed.

5.3.3. Neuronal activity does not significantly increase Nrf2 protein levels, but can activate some Nrf2 target genes, independently of Nrf2 and astrocytes

Neurons have low antioxidant defences, expressing low levels of catalase and GSH, and are known to receive non-cell autonomous support from astrocytes whose antioxidant defences are much stronger (Kraft et al. 2004; Vargas & Johnson 2009; Shih et al. 2003), often through

activation of the Nrf2 pathway which I show is mostly restricted to astrocytes. However, neurons do have their own antioxidant defences. Physiological neuronal activity via synaptic NMDARs leads to Ca^{2+} influx, as well as Ca^{2+} release from intracellular stores (Hardingham et al. 2001b), promoting pro-survival CREB-dependent gene expression in neurons, upregulating antioxidant systems, and shutting down pro-death pathways (Papadia et al. 2008; Hardingham & Bading 2010; Baxter et al. 2015). Neurons have a high metabolic demand, especially during neuronal activity, thus it makes sense for neuronal activity to be coupled to mitochondrial metabolism, since more active neurons require more ATP, for example for restoring ionic gradients following Ca^{2+} influx (Harris et al. 2012; Kann & Kovács 2007). Mitochondria are known to be anchored upon increased Ca^{2+} influx, helping to meet neurons' elevated ATP demand (Harris et al. 2012). Increased production of ATP by oxidative phosphorylation results in elevated ROS production in mitochondria themselves and by NADPH oxidase in the cytoplasm following NMDAR activation (Hongpaisan et al. 2004; Brennan et al. 2009). Small amounts of ROS are important for signalling and other vital cellular functions, but excessive ROS production leads to oxidative damage, mitochondrial dysfunction and cell death (Popa-Wagner et al. 2013). Thus, it is understandable for neuronal activity to be coupled to increased antioxidant defences to help eliminate excess ROS formed.

Habas *et al*. recently found that Nrf2 target genes Gclc and Nqo1 were increased following neuronal activity, which they attributed to neuronal signalling to astrocytes through the tripartite synapse, Nrf2 being activated and inducing the transcription of its target genes in astrocytes, providing non-cell autonomous neuroprotection (Habas et al. 2013). Contrary to this, my results show that neuronal activity can induce several Nrf2 target genes, including as Srxn1, xCT, Hmox1 and Gclc, not only independently of Nrf2, but also of astrocytes. Furthermore, unlike Habas *et al*., I found Nrf2 protein levels not to be significantly induced following neuronal activity in mixed culture. Moreover, I studied a group of 35 tBHQ-induced Nrf2 target genes, which were not induced following neuronal activity in pure neuronal culture, and found them not to be significantly upregulated following neuronal activity in mixed culture (Fig.5.11). Although some of these genes showed an increase in response to activity, others showed a decrease, and overall the profile of fold inductions was normally distributed around log_2FC=zero, strongly suggesting no induction of the Nrf2 pathway in astrocytes.

Thus, some antioxidant genes which are targets of Nrf2 in astrocytes are upregulated in neurons following NMDAR-mediated Ca^{2+} influx, showing that neurons have cell-autonomous antioxidant defences similar to Nrf2-mediated antioxidant defences in astrocytes,

helping to maintain redox balance and eliminate ROS formed following increased metabolic demand. Neurons possessing activity-dependent antioxidant defences is understandable, since it would be energetically costly to keep antioxidant pathways continuously activated, and excessive antioxidant support may inhibit important redox signalling from occurring. This way antioxidant genes are only transcribed when required, and non-cell autonomous protection via the Nrf2 pathway in astrocytes provides basal protection for neurons, for instance through the supply of GSH precursors (Shih et al. 2003).

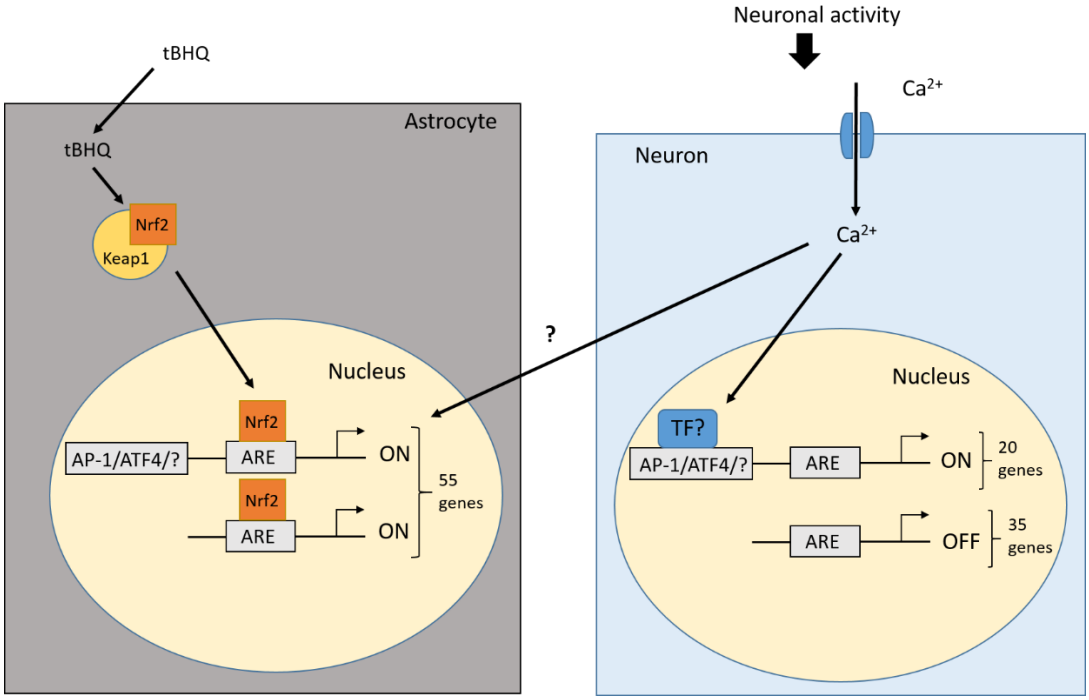

Figure 5.11. Neuronal activity induces the expression of some, but not all tBHQ-induced Nrf2 target genes. tBHQ induced a group of 55 Nrf2 target genes in astrocytes, 20 of which were induced following neuronal activity in pure neuronal culture. Most likely tBHQ-induced Nrf2 target genes containing consensus sequences for the binding of transcription factors (TFs) other than Nrf2, such as AP-1 and ATF4, are activated by neuronal activity, whilst ARE-only containing Nrf2 target genes are not. It is possible that some Nrf2 target genes are activated in astrocytes following neuronal activity, but this is likely independent of Nrf2 activation.

5.3.3.1 The antioxidant pathways affected by the upregulation of Nrf2 target genes following neuronal activity

The Nrf2 target genes I examined are involved in several different antioxidant pathways, including the Trx-Prx system and GSH synthesis. Srxn1 is responsible for catalysing the reduction of hyperoxidised Prxs in an ATP dependent manner, which is essential for neurons to keep Prxs active. Our group has previously shown that Srxn1 can be activated by neuronal activity through promoter elements containing AP-1 sites (Papadia et al. 2008). The results in

this chapter are in agreement with this, showing that Srxn1 is upregulated following 4 and 24h Bic/4-AP treatment, independently of astrocytes and Nrf2.

Our lab has recently published work confirming that synthesis and recycling of GSH is controlled by synaptic NMDAR-mediated Ca^{2+} influx in neurons (Baxter et al. 2015). Transcription of xCT, a cystine/glutamate exchanger which helps supply cysteine for glutathione synthesis, has been shown to be induced in primary cortical neuronal cultures independently of Nrf2, by activating transcription factor 4 (ATF4), whose translation is upregulated following PI3K activation by synaptic NMDAR activity (Lewerenz et al. 2014). Here I show that both xCT and Gclc, responsible for catalysing the rate-limiting step in GSH synthesis, are upregulated following neuronal activity in an Nrf2 and astrocyte independent manner, further confirming the role of NMDAR-mediated Ca^{2+} influx in modulating glutathione use and synthesis, helping to eliminate ROS cell autonomously to achieve redox balance. The PI3K pathway has also been shown to activate Nrf2 itself (Lee et al. 2001), but Lewerenz *et al*. found xCT activation in cortical neurons to be independent of Nrf2 (Lewerenz et al. 2014). I found Nrf2 expression levels to be low in neurons themselves, which explains why activation of the PI3K pathway downstream of synaptic NMDAR activation will not lead to Nrf2 activation. Astrocytes provide the precursors needed by neurons to synthesise their own GSH (Shih et al. 2003). Thus, when the demand for antioxidant is higher, neurons upregulate genes important for GSH synthesis, such as Gclc and xCT, to boost their intrinsic antioxidant defences.

Hmox1 is involved in the breakdown of the haem group into iron, carbon monoxide and biliverdin, which can be further broken down into bilirubin by biliverdin reductase, with both biliverdin and bilirubin having antioxidant properties (Schipper et al. 2009; Vargas & Johnson 2009; Loboda et al. 2016). I show that Hmox1 is activated in neurons themselves independently of astrocytes or Nrf2. Interestingly, it has been suggested that Hmox1 is an ATF4 target gene, and the ARE of Hmox1 was shown to have AP-1-like binding sites (Harding et al. 2003; Soriano et al. 2008a; Inamdar et al. 1996). Thus, Hmox1 could be activated by the same pathway as Srxn1 or xCT. Interestingly, Yin *et al*. observed an increase in Hmox1 and neuroprotection against oxidative stress following addition of geniposide, and found that cell death was increased with a PI3K inhibitor, suggesting that Hmox1 may be downstream of PI3K and ATF4 in hippocampal neurons (Yin et al. 2010). Furthermore, I found biliverdin reductase (Blvrb) to be increased following 4 and 24h Bic/4-AP treatment of neuronal cultures using RNA-seq (Supplementary tables 2 and 3).

Nqo1, which is responsible for reduction of quinones, is thought to be an Nrf2 specific target gene (Dinkova-Kostova & Talalay 2010). Indeed, Nqo1 mRNA levels were upregulated following treatment with tBHQ, however there was no increase of Nqo1 in WT or Nrf2 KO cultures following neuronal activity, suggesting that Nqo1 is indeed Nrf2 specific and cannot be induced by neuronal activity. Unlike me, Habas *et al*. saw an increase in Nqo1 levels following neuronal activity. Additionally, I found 35 of the 55 tBHQ-induced Nrf2 target genes, identified by RNA-seq, to not be significantly induced following neuronal activity in pure neuronal cultures, indicating that not all Nrf2 target genes can be activated by neuronal activity.

5.3.3.2. Why do the findings in this thesis differ from those of Habas *et al.*?

There were several differences between the techniques used in this thesis and those used by Habas *et al*. (Habas et al. 2013), some of which are outlined below and may help to explain the discrepancies between our results.

Habas *et al*. examined the Nrf2 dependence of Nrf2 target gene induction by siRNA-mediated knock-down, which can result in incomplete Nrf2 KD and unwanted off-target effects. Since I employed an Nrf2 KO mouse in which Nrf2 is completely genetically eliminated (Itoh et al. 1997), my results are more likely to truly reflect the Nrf2 requirement of gene induction following neuronal activity.

Habas *et al*. saw increased Nrf2 target gene mRNA expression in their neuronal culture, which they attributed to the presence of astrocytes. Their neuronal culture contained 4% astrocytes, whilst my neuronal cultures contain <0.2% astrocytes, making contamination from astrocytes unlikely. I observed Nrf2 target gene induction in neuronal culture at similar levels to that in mixed and AE cultures (10 and 15% astrocytes, respectively), suggesting that gene induction is independent of astrocytes themselves, which was further proven by Nrf2 target gene induction following neuronal activity in Nrf2 KO cultures. Furthermore, I show using an RNA-seq data set that the group of tBHQ-induced Nrf2 target genes which were not significantly upregulated in pure neuronal culture following neuronal activity, were not significantly induced in mixed culture following neuronal activity, suggesting that Nrf2 is not the transcription factor responsible for inducing Nrf2 target gene expression following neuronal activity. Moreover, Habas *et al*. did not detect increased Nrf2 protein levels in their neuronal culture, thus it is unclear how they came to the conclusion that the gene induction they observed in neuronal culture was due to Nrf2 activation in astrocytes.

However, Habas *et al*. did show increased nuclear Nrf2 levels in astrocytes following neuronal activity in AE cultures. In contrast, I found Nrf2 protein levels not to be significantly increased

following neuronal activity, either by Bic/4-AP or KCL(/FPL) treatment, in AE culture. Habas *et al*. used an Nrf2 antibody (H300, Santa Cruz Biotechnology) which produced multiple unspecific bands, making the identification of Nrf2 in some blots difficult. The H300 antibody failed to work in my hands, thus I used a more specific Nrf2 antibody (D1Z9C, Cell Signaling), which I validated using Nrf2 KO cultures (Itoh et al. 1997). A recent paper comparing different Nrf2 antibodies confirms that the D1Z9C antibody is highly specific for Nrf2, more so than the H300 Nrf2 antibody which produces numerous non-specific bands (Kemmerer et al. 2015).

Habas *et al*. examined nuclear Nrf2 levels separately, and suggested in their reply to our paper that this may be the cause of the differences in our results (Habas et al. 2014). Although they examined cytoplasmic levels separately, Nrf2 levels seemed undetectable in their cytoplasmic fractions, thus looking at total Nrf2 levels should only show nuclear Nrf2 levels; which in my hands indicated no significant increase in Nrf2 levels following neuronal activity. Additionally, unlike Habas *et al*., I also examined Nrf2 levels by immunocytochemistry (DIV9), and found no significant increase in Nrf2 levels in astrocytes or neurons following Bic/4-AP treatment of a mixed culture, although there was a trend for increased Nrf2 levels in astrocytes. Thus, these experiments should be repeated to determine whether this effect persists, and if it does whether it is due to neuronal activity or perhaps an indirect effect of 4-AP on astrocytes. Possible indirect effects of 4-AP on astrocytes could be tested by addition of tetrodotoxin alongside Bic/4-AP treatment to silence neuronal activity.

Habas *et al*. used their cultures at a later developmental stage (DIV14) than I did (DIV10), arguing that GABAergic neurons are not yet mature at early developmental stages, thus $GABA_A$ receptor antagonist bicuculline could not fully exert its effect. But, even in DIV18 AE culture, I did not observe a significant increase in Nrf2 protein levels following Bic/4-AP treatment. Furthermore, I saw no significant effect of 4 or 24h KCl(/FPL) treatment on Nrf2 protein levels at either developmental stage. Habas *et al*. also examined the transcription of Nrf2 target genes at this later developmental stage (DIV14), whilst I examined them at DIV9. Despite this, I found several Nrf2 target genes, including Gclc which Habas *et al*. examined, to be induced following neuronal activity in DIV9 culture, independently of Nrf2 or astrocytes. Interestingly, Habas *et al*. reported seeing an effect on Nrf2 protein levels with high K^+ in immature neurons. However, my results showed that KCl/FPL treatment induced Nrf2 target gene expression in an Nrf2 and astrocyte independent manner (data not shown), which together with no significant increase seen in Nrf2 protein levels following neuronal activity in immature (DIV10) or more mature neurons (DIV18), suggests that the differences in the developmental stage of neurons used is unlikely to be the cause of the discrepancies in our results. Although

it is possible that some of the Nrf2 target genes may not be induced in more mature neurons. xCT for instance has been shown to be expressed on immature neurons, contributing to their survival, but not on mature neurons which are thought to be unable to take up cystine, and will only transport cysteine for GSH synthesis through EAAC1 transporters (Bridges et al. 2012; Robert et al. 2014). xCT has been shown to be expressed in mature neurons in culture, but this seems to be an effect of culturing itself (Aoyama et al. 2008; Bridges et al. 2012). Thus, whether the upregulation of Nrf2 target gene expression persist at a more mature developmental stage should be further investigated, as well as the effects of neuronal activity on astrocytes and the Nrf2 pathway *in vivo*, since neuronal cultures cannot reproduce the *in vivo* environment, and communication between astrocytes and neurons may differ *in vivo*.

It is possible that Nrf2 is upregulated following neuronal activity in certain neuronal subtypes, brain regions or in different species, since Habas *et al*. worked on primary rat hippocampal whilst I used primary mouse cortical cultures. Additionally, different cellular environments may also influence gene expression, of note Habas *et al*. used aCSF to carry out their experiments whilst I used TMo. Thus comparison of Nrf2 levels following neuronal activity in different brain regions would be of interest. It is important to note that even with a small significant effect of neuronal activity on Nrf2 in astrocytes, Nrf2 levels will be much lower than with Nrf2 activators tBHQ and SLF, and most likely cannot be picked up by Western blotting.

5.3.4. Possible cooperation of neuronal activity and the Nrf2 pathway in neuroprotection, and their potential clinical implications

Neurons have a high metabolic demand, but low antioxidant defences, and are therefore susceptible to oxidative damage (Harris et al. 2012). As I show in this chapter, neuronal activity can induce the transcription of some Nrf2 target genes, some of which are involved in the Trx-Prx and the GSH antioxidant systems. Thus, both neuronal activity and Nrf2 activation are potential therapeutic targets for treatments of conditions involving oxidative stress. ROS-mediated oxidative damage and excitotoxicity have been implicated in ND disorders, stroke and TBI (Popa-Wagner et al. 2013; Bell & Hardingham 2011a; Bell & Hardingham 2011b). Additionally, ROS have been hypothesised by the "free-radical theory of ageing" to accumulate oxidative damage gradually over time, making neurons more vulnerable to insults as they age (Schipper 2004). Therefore, it is likely that the Nrf2 pathway and synaptic activity both play a neuroprotective role in ageing.

5.3.4.1. Potential clinical implications of neuronal activity in neurodegenerative diseases

Neuronal activity has been shown to have protective effects both *in vitro* and *in vivo*. Preconditioning neuronal cultures with Bic/4-AP is neuroprotective against H_2O_2-mediated cell death and excitotoxicity, independently of the presence of astrocytes (Baxter et al. 2015; Qiu et al. 2013). Srxn1, a target gene I examined in this chapter, has been shown to be responsible for some of the neuroprotective effects of synaptic NMDAR activity against H_2O_2-induced cell death (Papadia et al. 2008). Preconditioning with Bic/4-AP also provides protection against OGD, a technique used to recreate stroke *in vitro*, up to 3 days after Bic/4-AP application (Tauskela et al. 2008). It will be interesting to see whether other Nrf2 target genes induced by neuronal activity contribute to the neuroprotection provided by synaptic NMDAR activity against H_2O_2-induced and excitotoxic cell death.

Environmental enrichment (EE) in rats, such as enriching the cages of animals with novel objects, has been shown to induce Bdnf and phosphorylate CREB, providing neuroprotection against spontaneous apoptotic cell death and excitotoxicity (Young et al. 1999). Furthermore, EE along with exercise was shown to decrease age-related spatial learning decline, partly via reversing decreased Bdnf expression (O'Callaghan et al. 2009). CREB phosphorylation and Bdnf activation are known downstream protective effects of synaptic NMDAR activity, and Nichols *et al*. found EE in rats to increase glutamatergic synaptic signalling (Nichols et al. 2007). Thus, one may propose that EE increases neuronal activity, which partly through synaptic NMDAR activity activates anti-apoptotic pathways and upregulates antioxidant defences, such as antioxidant Nrf2 target genes induced in neurons via neuronal activity shown in this chapter. Indeed, Young *et al*. has shown EE to increase learning and memory, known to involve NMDARs. Thus, it is plausible that EE could help to reduce ROS build up during ageing and neurodegeneration, through antioxidant gene expression mediated by synaptic NMDAR activity. Indeed, EE has been found to delay the onset of symptoms and disease progression in different mouse models of HD, and to help combat oxidative stress by increasing antioxidant defences in a mouse model of AD, whilst cognitively stimulating activities in humans are thought to reduce the likelihood of developing AD (Spires & Hannan 2005; Herring et al. 2010). Neurons experiencing increased neuronal activity throughout their lifetime due to EE may accumulate less ROS, in line with the "free-radical theory of ageing", and thus may be less susceptible to neurodegeneration and cognitive decline. Thus, synaptic NMDAR activity could be targeted to enhance antioxidant defences in different disease models in neurons themselves rather than in astrocytes. The neuroprotective effects of synaptic NMDAR activity helps to explain the clinical failure of most NMDAR antagonists, which inhibit the activation of all NMDARs (Hardingham & Bading 2010). In contrast to traditional

NMDAR antagonist, memantine, which has been licensed for the treatment of AD, is an uncompetitive NMDAR antagonist which blocks extrasynaptic NMDAR activity following bath application of glutamate, whilst allowing physiological synaptic NMDAR activity (Xia et al. 2010; Lipton 2006). Thus, memantine does not inhibit synaptic NMDAR-mediated antioxidant defences, such as the upregulation of Srxn1, demonstrated by our group *in vitro* and *in vivo* (Papadia et al. 2008). Therefore, the protective effect of memantine lies in its ability to only inhibit toxic NMDAR activation, whilst sparing neuroprotective synaptic NMDAR-mediated pathways important for cell survival. Furthermore, enhancing neuronal activity, for instance by increasing cognitive stimulation, may also increase neurons' antioxidant defences and have a neuroprotective effect against diseases involving oxidative stress.

5.3.4.2. The neuroprotective effect of Nrf2 upregulation in neurodegenerative diseases

Nrf2 is activated in astrocytes by oxidative stress as well as by Nrf2 activators such as tBHQ and $CDDO^{TFEA}$ *in vitro* and *in vivo,* mediating the induction of several antioxidant and detoxifying genes in astrocytes, providing non-cell autonomous neuroprotection against oxidative stress (Kraft et al. 2004). Nrf2 target genes, Hmox1 and Srxn1, have been shown to be induced by mild oxidative stress by exogenous H_2O_2 application *in vitro* in primary mouse mixed cultures and human embryonic-stem cell (hESC) derived astrocytes; activation of which was found to be astrocyte and Nrf2 dependent in mouse mixed cultures (Bell, Al-Mubarak, et al. 2011). Additionally, Shih *et al*. showed that neuroprotection against oxidative stress by Nrf2 OE or tBHQ administration is conferred by astrocytes (Shih et al. 2003). Indeed, I confirmed by immunostaining that Nrf2 is directly activated by H_2O_2 in astrocytes, but not in neurons in mixed culture. Furthermore, Nrf2 activation by $CDDO^{TFEA}$ is neuroprotective against H_2O_2-induced cell death, dependent on astrocytes through the induction of the GSH system both in mouse primary neuronal cultures and hESC-derived neurons (Gupta et al. 2012). This is thought to be due to the supply of GSH precursors by astrocytes to neurons (Shih et al. 2003).

The Nrf2 pathway has been shown to provide neuroprotection during stroke, by activation of its target genes such as Srxn1 and Gclc (Jiang et al. 2016; Xue et al. 2016; Zhou et al. 2015b; Bell, Fowler, et al. 2011). Nrf2 target genes are upregulated following OGD contributing to ischemic preconditioning *in vitro,* and following middle cerebral artery occlusion (MCAO) *in vivo* (Bell, Al-Mubarak, et al. 2011). Furthermore, injection of SLF or tBHQ into rodents showed neuroprotective effects against MCAO in various experiments (Jiang et al. 2016). Moreover, Nrf2 target gene expression by Nrf2 has also been shown to be protective in TBI (Hong et al. 2010; Shu et al. 2016).

Pharmacological activation of the Nrf2 pathway and Nrf2 overexpression (OE) have been shown to provide neuroprotection against oxidative stress and inflammation in several ND diseases, such as AD, HD and PD (Buendia et al. 2016; Gan & Johnson 2014; Johnson et al. 2008; Esteras et al. 2016). For instance, Nrf2-GFAP mice which overexpress Nrf2 in astrocytes, have been shown to have neuroprotective effects when crossed with mouse models of neurodegenerative diseases, such as ALS (Vargas et al. 2008) and PD (Gan et al. 2012; Chen et al. 2009). Of interest, an Nrf2 activator, DMF, has been approved for the treatment of multiple sclerosis (Brennan et al. 2015; Linker et al. 2011).

5.3.4.3. Does the activation of both pathways provide added neuroprotection?

As both the Nrf2 pathway and neuronal activity through activation of synaptic NMDARs can induce Nrf2 target genes providing neuroprotective effects against several insults involved in diseases (discussed above), the question arises whether the two pathways are distinct or have additive neuroprotective effect against various insults.

Our group recently showed that not only is the GSH system regulated by neuronal activity in neurons themselves, but preconditioning with neuronal activity and $CDDO^{TFEA}$ combined has an additive neuroprotective effect against H_2O_2-induced cell death (Baxter et al. 2015). Thus, the two pathways do cooperate to protect neurons against oxidative stress. The Nrf2 target genes found to be upregulated by neuronal activity in this chapter, some of which are involved in the Trx-Prx and GSH antioxidant systems, may help mediate this effect. It is possible that Nrf2 target genes are upregulated following neuronal activity cell autonomously to allow neurons to eliminate ROS formed due to increased metabolism, whilst the astrocytic Nrf2 pathway provides general support to neurons following oxidative stress and other insults, such as by supplying precursors for GSH synthesis (Shih et al. 2003). It will be important to investigate the interaction of these two pathways in disease, and determine the biological purpose for the dual control of some of these Nrf2 target genes.

5.3.4.4. The potential additive neuroprotective effect of targeting the two pathways simultaneously in neurological diseases

Since the two pathways are distinct and provide additive neuroprotection against oxidative stress *in vitro* (Baxter et al. 2015), it would be intriguing to see whether enhancing the two pathways simultaneously has an additive protective effect against stroke, cognitive decline or in ND diseases. It is possible that Nrf2 activators, such as $CDDO^{TFEA}$ or DMF in conjunction with EE could produce additive protective effect in these conditions. Furthermore, memantine, which would allow for synaptic NMDAR-mediated antioxidant gene expression whilst blocking excitotoxicity, could also be used in conjunction with Nrf2 activators in various

diseases to provide increased neuroprotection. Whether the Nrf2 pathway in astrocytes can provide additional protection to neurons during excitotoxicity should also be examined, since excitotoxicity is known to be involved in several ND diseases as well as stroke (Hardingham & Bading 2010; Hardingham et al. 2002). Bic/4-AP preconditioning has been shown to be neuroprotective against NMDA-induced excitotoxicity (Qiu et al. 2013), and it would be interesting to see whether this protection is Nrf2 and astrocytes independent, and if Nrf2 target genes contribute to neuroprotection. To test this, preconditioning with Bic/4-AP in conjunction with $CDDO^{TFEA}$ could be applied to WT and Nrf2 KO cultures *in vitro*. The dependence of these protective effects on different Nrf2 target genes could also be investigated, by knocking down the genes. If these approaches have an additive neuroprotective effect, whether they persist in aged mice and *in vivo* should also be investigated.

Thus, the Nrf2 pathway and neuronal activity can be activated to provide additive neuroprotection, and their simultaneous targeting clinically may help combat various ND diseases.

Chapter 6: Concluding remarks

The research presented in this thesis aims to provide better insight into neuroprotective and neurodestructive Ca^{2+} signalling pathways, largely mediated by NMDARs in neurons, as well as the possible effect of neuronal activity on inducing antioxidant gene transcription in astrocytes. The key conclusions are:

- AMPK is involved in mediating excitotoxicity, but is not activated downstream of Mcu.
- MCRGs are differentially expressed in different neural cells (neurons vs astrocytes) and neuronal subtypes (CA1 vs CA3 neurons of the hippocampus). Of note the Na^{+}/Ca^{2+} exchanger Nclx is expressed at very low levels in neurons.
- Nrf2 is weakly expressed in neurons, nevertheless some Nrf2 target genes can be activated cell autonomously in neurons following neuronal activity, independently of Nrf2 or astrocytes.

Excitotoxicity and oxidative stress are implicated in various acute and chronic neurodegenerative diseases, as well as in brain injury (Parsons & Raymond 2014; Gan & Johnson 2014; Hardingham & Bading 2010). Unfortunately, NMDAR antagonists have failed in clinical trials for stroke and TBI, likely due to their inhibition of physiological NMDAR activity which is essential for cell survival (Ikonomidou & Turski 2002; Paoletti et al. 2013). Furthermore, small molecule antioxidants have also largely failed in human clinical trials for CNS diseases (Kamat et al. 2008), likely due to their inability to mimic the complex antioxidant and detoxification systems in neural cells. Thus, it is imperative to better understand the pro-survival and pro-death signalling cascades downstream of NMDAR activation, as well as the pathways controlling the brain's endogenous antioxidant defences, to find new targets for developing alternative therapies to combat excitotoxicity and oxidative stress in these diseases. Inhibition of pro-death signals in concert with enhanced endogenous antioxidant responses both in neurons and astrocytes, could be used as a combined approach in alleviating neuronal death. Specific inhibition of extrasynaptic NMDARs or GluN2B containing NMDARs, which are known to preferentially couple to pro-death pathways, is another viable option. For instance, decoupling the C terminal domain of GluN2B containing NMDARs using small peptides has shown some promise (Aarts & Tymianski 2003).

Mitochondrial dysfunction plays a large role in excitotoxicity and our group has found Mcu to be a key mediator of excitotoxic cell death (Qiu et al. 2013). Due to the importance of mitochondrial Ca^{2+} signalling in both physiological and pathological circumstances, the inhibition of Mcu is likely to lead to similar issues to those experienced with NMDAR antagonists. Thus, in Chapter 3 I investigated AMPK as a potential downstream effector of

Mcu during excitotoxicity, but found AMPK not to be activated downstream of Mcu-mediated Ca^{2+} uptake. Nevertheless, AMPK activation does promote excitotoxic death, although its route of activation and downstream effector(s) still need to be better established, especially due to the possible pro-survival effects mediated by AMPK (Anilkumar et al. 2013; Culmsee et al. 2001; Weisova et al. 2009). It is likely that AMPK is phosphorylated by CaMKKβ following Ca^{2+} influx independently of increases in AMP (Hawley et al. 2005; Mairet-Coello et al. 2013; Woods et al. 2005; Anderson et al. 2008). The search for Mcu's downstream effector(s) following excitotoxicity also continues, with JNK, PARP-1 and mPTP opening being likely candidates (Brustovetsky et al. 2002; White & Reynolds 1996; Ichas & Mazat 1998; Orrenius et al. 2003; Bernardi & Rasola 2007; Abramov & Duchen 2008; Duan et al. 2007; Yu et al. 2002; Soriano et al. 2008b). Whether Mcu and AMPK mediate neuronal death through distinct pathways should be further examined, with the downstream effectors of Mcu and AMPK being potential therapeutic targets, which would likely cause less adverse effects compared to targeting molecules further up in the signalling cascades.

The molecular identity of Mcu and other MCRGs has only come to light in recent years, with the function of many of the genes still debated. Since the cell specific expression of MCRGs in the brain was unknown, in Chapter 4 I investigated the expression of MCRGs and found them to be differentially expressed in neurons and astrocytes as well as neuronal subtypes, providing a clearer picture of which MCRGs may be more important in each cell type. Interestingly, certain neuronal subtypes are more susceptible to excitotoxicity and other insults (such as CA1 and CA3 neurons of the hippocampus (Strasser & Fischer 1995; Ikegaya & Matsuki 2002; Cronberg et al. 2005; Gee et al. 2006; Yang et al. 2000; Wilde et al. 1997)), and since mitochondria play such a key role in mediating excitotoxic cell death, it is tempting to speculate that the differential expression of these genes could be a coping mechanism, or perhaps the cause of their increased susceptibility to cell death. Thus, it is essential to investigate whether the results seen in Chapter 4 translate to the protein level and to study the function of these genes further, to help determine the functional outcome of the differences in MCRG expression for neuronal health. Understanding the function of these genes may aid in finding therapeutic targets, for instance although Mcu cannot be blocked due to its likely adverse effect on metabolism, inhibiting one of its regulators may reduce Mcu-mediated Ca^{2+} influx following a pathological insult. Since Mcu plays an important role in mediating excitotoxicity (Qiu et al. 2013), the correct functioning of mitochondrial Ca^{2+} efflux pathway(s) is likely to also be essential for neuronal survival during excitotoxicity. Surprisingly, I found Nclx expression levels to be very low in neurons, suggesting that Nclx may not be the predominant mitochondrial Ca^{2+} efflux pathway in neurons, even though it is

thought to be the main exchanger in excitable cells (Palty & Sekler 2012). The importance of Nclx for mitochondrial Ca^{2+} efflux in neurons shall be further addressed using cultures from an Nclx KO mouse, with further studies focusing on potential alternative mitochondrial Ca^{2+} efflux pathways in neurons, such as Letm1, Ncx1, Ncx2 and Ncx3 (Gobbi et al. 2007; Scorziello et al. 2013; Wood-Kaczmar et al. 2013; Jiang et al. 2009). Once the identity of the exchanger in neurons is established, its importance for neuronal health can be studied.

Interestingly, a mild NMDAR antagonist, memantine, which is thought to preferentially inhibit excessive NMDAR activation whilst sparing physiological synaptic NMDAR activation, has been licensed for the treatment of moderate to severe AD (Xia et al. 2010; Léveillé et al. 2008; Zhou et al. 2015a). Memantine is also in clinical trials for HD (Kumar et al. 2015) and vascular dementia (Lipton 2006) with promising results. Moreover, memantine has shown some benefits in patients with PD (Varanese et al. 2010). Furthermore, rodent experiments suggest that memantine may be neuroprotective in mild TBI (Effgen & Morrison 2016) as well as following stroke (Chen et al. 1992; Chen et al. 1998).

Interestingly, AMPK activation by CaMKKβ following NMDA treatment of neurons was abolished by memantine pre-treatment, as was AMPK activation after Aβ treatment which leads to tau phosphorylation and toxicity (Thornton et al. 2011; Mairet-Coello et al. 2013). This suggests that AMPK plays a pro-death role in AD and is not activated following physiological synaptic NMDAR activity, although this should be further examined. Moreover, this provides evidence that memantine blocks pro-death pathways, and its inhibition of other signalling cascades such as Mcu-mediated excitotoxic death is likely. In addition, memantine allows physiological neuronal activity to take place, including the upregulation of neuronal antioxidant defences such as Nrf2 target genes including genes involved in the GSH system, which is known to be dysregulated in several ND diseases (Johnson et al. 2012). Thus, memantine or similar drugs preferentially blocking extrasynaptic NMDARs are likely to have therapeutic benefit in a number of ND diseases.

Another possibility in tackling these diseases is increasing endogenous antioxidant defences to reduce oxidative stress. The data presented in Chapter 5 demonstrates that whilst the Nrf2 pathway is expressed at very low levels in neurons, some Nrf2 target genes are activated in neurons following neuronal activity independently of Nrf2 and astrocytes, contrary to previous reports (Habas et al. 2013). Thus, astrocytes can provide antioxidant support, such as supplying GSH to neurons during oxidative stress via Nrf2 (Shih et al. 2003), whilst neurons enhance their endogenous antioxidant capacity following physiological activity via transcription factors other than Nrf2, such as ATF4 and AP-1 (Papadia et al. 2008; Soriano et

al. 2009; Lewerenz et al. 2014), compensating for the epigenetic silencing of Nrf2 in neurons during early development (Bell et al. 2015) and increasing GSH production. Treating neurons with medium from human embryonic stem-cell (hESC) derived astrocytes treated with Nrf2 activator $CDDO^{TFEA}$ provides GSH-dependent neuroprotection against H_2O_2-mediated cell death (Gupta et al. 2012). Furthermore, our group demonstrated that preconditioning mixed mouse cultures with $CDDO^{TFEA}$ and Bic/4-AP has additive neuroprotective effects against H_2O_2-mediated cell death (Baxter et al. 2015). Since the two pathways are distinct and help to maintain redox homeostasis in neural cells, it is tempting to speculate that Nrf2 pathway activation in astrocytes in concert with increasing neuronal activity may have additive neuroprotective effects in diseases involving oxidative stress.

Indeed, $CDDO^{TFEA}$ and $CDDO^{EA}$ have been shown to be neuroprotective in rodent models of ALS and HD (Stack et al. 2010; Neymotin et al. 2011). Additionally, Nrf2 activators SLF and tBHQ are neuroprotective in mouse models of stroke (Jiang et al. 2016; Shih et al. 2005). Furthermore, Nrf2-GFAP mice, which selectively overexpress Nrf2 in astrocytes, are neuroprotective in various ND diseases, such as ALS and PD (Vargas et al. 2008; Gan et al. 2012; Chen et al. 2009). Interestingly, an Nrf2 activator, DMF (also known as BG-12), has been approved for treating relapsing remitting MS (Linker et al. 2011; Cada et al. 2013; Bomprezzi 2015). Thus, it is tempting to speculate that DMF or other Nrf2 activators could be used as a therapeutic approach in other ND diseases. Indeed, DMF has been tested in mouse models of HD and PD showing some promising results (Ellrichmann et al. 2011; Ahuja et al. 2016). Since correct redox balance is crucial in neural cells, prolonged activation of the Nrf2 pathway may lead to reductive stress. Thus, use of an Nrf2 pro-drug, which would only be converted to its active form upon oxidative stress, could exert its effect only when and where enhanced antioxidant defences were required, providing a more sophisticated treatment (Satoh et al. 2013).

Environmental enrichment in rodents, activating glutamatergic signalling *in vivo*, is neuroprotective and has been shown to have beneficial effects in models of AD and HD (Young et al. 1999; Nichols et al. 2007; Spires & Hannan 2005; Herring et al. 2010). Additionally, a cognitively active lifestyle was reported to reduce the likelihood of developing AD in humans (Spires & Hannan 2005). Thus, promoting a more cognitively active lifestyle may have some benefits in ND diseases, likely at least partially due to enhanced neuronal antioxidant defences following increased neuronal activity. Alternatively, neuronal activity could be pharmacologically enhanced, although this may be problematic due to too much system disinhibition leading to seizures.

Therefore, the use of memantine or drugs targeting specific NMDAR-mediated pro-death pathways in conjunction with drugs increasing antioxidant defences in neurons and/or astrocytes, such as DMF, may provide additional neuroprotection for some ND diseases and the possible additive therapeutic benefits of these approaches should be investigated.

The results presented in this thesis have been acquired using primary neuronal cultures, which although a great model system for deciphering molecular mechanisms in neural cells, do have their limitations. Thus, it is imperative that the findings in this thesis are studied and confirmed *in vivo*. Additionally, the experiments were performed in developing neurons, thus whether the results found persist in older cells/animals should also be examined, especially in light of the possible therapeutic manipulation of these pathways in ND diseases, which often present at a later age. Although rodents are a good model organism, results acquired do not always translate well to human clinical trials, likely due to species specific differences; thus the replication of the results in this thesis in human cells is desirable. For instance, neural cells generated from human embryonic stem cells (hESCs) or human pluripotent stem cells (hPSCs) from patients, which have been previously employed to study ND diseases as well as the neuroprotective capacity of astrocytes (Gupta et al. 2013b; Gupta et al. 2013a), could be used to investigate the findings presented in this thesis in humans *in vitro*.

It can be hoped that the data presented in this thesis will enhance the understanding of pro-survival and pro-death Ca^{2+}-mediated signalling cascades and lead to the establishment of new therapeutic targets for ND diseases and brain injury.

Bibliography

Aarts, M.M. & Tymianski, M., 2003. Novel treatment of excitotoxicity: Targeted disruption of intracellular signalling from glutamate receptors. *Biochemical Pharmacology*, 66(6), pp.877–886.

Abramov, A.Y. & Duchen, M.R., 2008. Mechanisms underlying the loss of mitochondrial membrane potential in glutamate excitotoxicity. *Biochimica et Biophysica Acta - Bioenergetics*, 1777(7-8), pp.953–964.

Ahuja, M. et al., 2016. Distinct Nrf2 Signaling Mechanisms of Fumaric Acid Esters and Their Role in Neuroprotection against 1-Methyl-4-Phenyl-1,2,3,6-Tetrahydropyridine-Induced Experimental Parkinson's-Like Disease. *The Journal of neuroscience : the official journal of the Society for Neuroscience*, 36(23), pp.6332–51.

Almeida, A., Bolaños, J.P. & Medina, J.M., 1999. Nitric oxide mediates glutamate-induced mitochondrial depolarization in rat cortical neurons. *Brain Research*, 816(2), pp.580–586.

Al-Mubarak, B., Soriano, F.X. & Hardingham, G.E., 2009. Synaptic NMDAR activity suppresses FOXO1 expression via a cis-acting FOXO binding site: FOXO1 is a FOXO target gene. *Channels (Austin, Tex.)*, 3(4), pp.233–8.

Amaral, M.D. & Pozzo-Miller, L., 2007. TRPC3 channels are necessary for brain-derived neurotrophic factor to activate a nonselective cationic current and to induce dendritic spine formation. *The Journal of neuroscience : the official journal of the Society for Neuroscience*, 27(19), pp.5179–5189.

Anderson, K.A. et al., 2008. Hypothalamic CaMKK2 contributes to the regulation of energy balance. *Cell metabolism*, 7(5), pp.377–88.

Anilkumar, U. et al., 2013. AMP-activated protein kinase (AMPK)-induced preconditioning in primary cortical neurons involves activation of MCL-1. *Journal of Neurochemistry*, 124(5), pp.721–734.

Antony, A.N. et al., 2016. MICU1 regulation of mitochondrial Ca(2+) uptake dictates survival and tissue regeneration. *Nature communications*, 7, p.10955.

Aoyama, K. et al., 2000. Nitration of manganese superoxide dismutase in cerebrospinal fluids is a marker for peroxynitrite-mediated oxidative stress in neurodegenerative diseases. *Annals of neurology*, 47(4), pp.524–7.

Aoyama, K. & Nakaki, T., 2015. Glutathione in Cellular Redox Homeostasis: Association with the Excitatory Amino Acid Carrier 1 (EAAC1). *Molecules*, 20(5), pp.8742–8758.

Aoyama, K., Watabe, M. & Nakaki, T., 2008. Regulation of neuronal glutathione synthesis. *Journal of pharmacological sciences*, 108(3), pp.227–238.

Archer, S.L., 2016. Acquired Mitochondrial Abnormalities, Including Epigenetic Inhibition of Superoxide Dismutase 2, in Pulmonary Hypertension and Cancer: Therapeutic Implications. *Advances in experimental medicine and biology*, 903, pp.29–53.

Ballaz, S. et al., 2013. Ascorbate prevents cell death from prolonged exposure to glutamate in an in vitro model of human dopaminergic neurons. *Journal of Neuroscience Research*, 91(12), pp.1609–1617.

Bano, D. et al., 2005. Cleavage of the plasma membrane Na+/Ca2+ exchanger in excitotoxicity. *Cell*, 120(2), pp.275–285.

Baron, K.T. & Thayer, S.A., 1997. CGP37157 modulates mitochondrial Ca2+ homeostasis in cultured rat dorsal root ganglion neurons. *European journal of pharmacology*, 340(2-3), pp.295–300.

Barone, M.C., Sykiotis, G.P. & Bohmann, D., 2011. Genetic activation of Nrf2 signaling is sufficient to ameliorate neurodegenerative phenotypes in a Drosophila model of Parkinson's disease. *Disease models & mechanisms*, 4(5), pp.701–707.

Bauerschmitt, H. et al., 2010. Ribosome-binding proteins Mdm38 and Mba1 display overlapping functions for regulation of mitochondrial translation. *Molecular biology of the cell*, 21(12), pp.1937–44.

Baughman, J.M. et al., 2011. Integrative genomics identifies MCU as an essential component of the mitochondrial calcium uniporter. *Nature*, 476(7360), pp.341–345.

Baxter, P.S. et al., 2015. Synaptic NMDA receptor activity is coupled to the transcriptional control of the glutathione system. *Nature communications*, 6, p.6761.

Bell, K.F.S., Fowler, J.H., et al., 2011. Activation of Nrf2-regulated glutathione pathway genes by ischemic preconditioning. *Oxidative medicine and cellular longevity*, 2011, p.689524.

Bell, K.F.S., Al-Mubarak, B., et al., 2011. Mild oxidative stress activates Nrf2 in astrocytes, which contributes to neuroprotective ischemic preconditioning. *Proceedings of the National Academy of Sciences of the United States of America*, 108(1), pp.E1–2; author

reply E3–4.

Bell, K.F.S. et al., 2015. Neuronal development is promoted by weakened intrinsic antioxidant defences due to epigenetic repression of Nrf2. *Nature communications*, 6(May), p.7066.

Bell, K.F.S. & Hardingham, G.E., 2011a. CNS peroxiredoxins and their regulation in health and disease. *Antioxidants & Redox Signaling*, 14(8), pp.1467–1477.

Bell, K.F.S. & Hardingham, G.E., 2011b. The influence of synaptic activity on neuronal health. *Current opinion in neurobiology*, 21(2), pp.299–305.

Bergemann, A.D., Cole, F. & Hirschhorn, K., 2005. The etiology of Wolf-Hirschhorn syndrome. *Trends in genetics*, 21(3), pp.188–95.

Bernardi, P. & Rasola, A., 2007. Calcium and cell death: the mitochondrial connection. *Sub-cellular biochemistry*, 45, pp.481–506.

Boillée, S., Vande Velde, C. & Cleveland, D.W., 2006. ALS: a disease of motor neurons and their nonneuronal neighbors. *Neuron*, 52(1), pp.39–59.

Bomprezzi, R., 2015. Dimethyl fumarate in the treatment of relapsing-remitting multiple sclerosis: an overview. *Therapeutic advances in neurological disorders*, 8(1), pp.20–30.

Bondarenko, A.I. et al., 2013. Mitochondrial Ca(2+) uniporter (MCU)-dependent and MCU-independent Ca(2+) channels coexist in the inner mitochondrial membrane. *Pflugers Archiv : European journal of physiology*, pp.0–9.

Bondarenko, A.I. et al., 2015. UCP2 modulates single-channel properties of a MCU-dependent Ca2+ inward current in mitochondria. *Pflugers Archiv European Journal of Physiology*, 467(12), pp.2509–2518.

Bonventre, J. V, 1997. Roles of phospholipases A2 in brain cell and tissue injury associated with ischemia and excitotoxicity. *Journal of lipid mediators and cell signalling*, 17(1), pp.71–9.

Brennan, A.M. et al., 2009. NADPH oxidase is the primary source of superoxide induced by NMDA receptor activation. *Nature Neuroscience*, 12(7), pp.857–863.

Brennan, M.S. et al., 2015. Dimethyl fumarate and monoethyl fumarate exhibit differential effects on KEAP1, NRF2 activation, and glutathione depletion in vitro. *PloS one*,

10(3), p.e0120254.

Bridges, R. et al., 2012. Thinking outside the cleft to understand synaptic activity: contribution of the cystine-glutamate antiporter (System xc-) to normal and pathological glutamatergic signaling. *Pharmacological reviews*, 64(3), pp.780–802.

Brown, G.C. & Borutaite, V., 2008. Regulation of apoptosis by the redox state of cytochrome c. *Biochimica et biophysica acta*, 1777(7-8), pp.877–81.

Brustovetsky, N. et al., 2002. Calcium-induced Cytochrome c release from CNS mitochondria is associated with the permeability transition and rupture of the outer membrane. *Journal of Neurochemistry*, 80(2), pp.207–218.

Buendia, I. et al., 2016. Nrf2-ARE pathway: An emerging target against oxidative stress and neuroinflammation in neurodegenerative diseases. *Pharmacology and Therapeutics*, 157, pp.84–104.

Bunton-Stasyshyn, R.K.A. et al., 2014. SOD1 Function and Its Implications for Amyotrophic Lateral Sclerosis Pathology: New and Renascent Themes. *The Neuroscientist : a review journal bringing neurobiology, neurology and psychiatry*, 21(5), pp.1–11.

Burnashev, N. & Szepetowski, P., 2015. NMDA receptor subunit mutations in neurodevelopmental disorders. *Current Opinion in Pharmacology*, 20, pp.73–82.

Cada, D.J., Levien, T.L. & Baker, D.E., 2013. Dimethyl fumarate. *Hospital pharmacy*, 48(8), pp.668–79.

Cai, X. & Lytton, J., 2004a. Molecular cloning of a sixth member of the K+-dependent Na+/Ca2+ exchanger gene family, NCKX6. *The Journal of biological chemistry*, 279(7), pp.5867–76.

Cai, X. & Lytton, J., 2004b. The cation/Ca(2+) exchanger superfamily: phylogenetic analysis and structural implications. *Molecular biology and evolution*, 21(9), pp.1692–703.

Cai, Z. et al., 2012. Roles of AMP-activated protein kinase in Alzheimer's disease. *Neuromolecular medicine*, 14(1), pp.1–14.

Calkins, M.J. et al., 2005. Protection from mitochondrial complex II inhibition in vitro and in vivo by Nrf2-mediated transcription. *Proceedings of the National Academy of Sciences of the United States of America*, 102(1), pp.244–9.

Cao, J. et al., 2005. The PSD95-nNOS interface: A target for inhibition of excitotoxic p38 stress-activated protein kinase activation and cell death. *Journal of Cell Biology*, 168(1), pp.117–126.

Carafoli, E. et al., 1974. The release of calcium from heart mitochondria by sodium. *Journal of molecular and cellular cardiology*, 6(4), pp.361–71.

Cárdenas, C. et al., 2010. Essential regulation of cell bioenergetics by constitutive InsP3 receptor Ca2+ transfer to mitochondria. *Cell*, 142(2), pp.270–83.

Carling, D., 2004. The AMP-activated protein kinase cascade - A unifying system for energy control. *Trends in Biochemical Sciences*, 29(1), pp.18–24.

Carling, D., Sanders, M.J. & Woods, A., 2008. The regulation of AMP-activated protein kinase by upstream kinases. *International journal of obesity (2005)*, 32 Suppl 4, pp.S55–9.

Chaudhuri, D. et al., 2013. MCU encodes the pore conducting mitochondrial calcium currents. *eLife*, 2(i), p.e00704.

Chen, H.S. et al., 1992. Open-channel block of N-methyl-D-aspartate (NMDA) responses by memantine: therapeutic advantage against NMDA receptor-mediated neurotoxicity. *The Journal of neuroscience : the official journal of the Society for Neuroscience*, 12(11), pp.4427–36.

Chen, H.S. V et al., 1998. Neuroprotective concentrations of the N-methyl-D-aspartate open-channel blocker memantine are effective without cytoplasmic vacuolation following post-ischemic administration and do not block maze learning or long-term potentiation. *Neuroscience*, 86(4), pp.1121–1132.

Chen, M. et al., 2011. Differential mitochondrial calcium responses in different cell types detected with a mitochondrial calcium fluorescent indicator, mito-GCaMP2. *Acta biochimica et biophysica Sinica*, 43(10), pp.822–30.

Chen, P. et al., 2009. Nrf2-mediated neuroprotection in the MPTP mouse model of Parkinson's disease: Critical role for the astrocyte. *Proceedings of the National Academy of Sciences of the United States of America*, 106(8), pp.2933–8.

Choi, D.W., 1988. Calcium-mediated neurotoxicity: relationship to specific channel types and role in ischemic damage. *Trends in neurosciences*, 11(10), pp.465–9.

Cohen, S.M. et al., 2015. The impact of NMDA receptor hypofunction on GABAergic

neurons in the pathophysiology of schizophrenia. *Schizophrenia Research*, 167(1-3), pp.98–107.

Concannon, C.G. et al., 2010. AMP kinase-mediated activation of the BH3-only protein Bim couples energy depletion to stress-induced apoptosis. *The Journal of Cell Biology*, 189(1), pp.83–94.

Coultrap, S.J. et al., 2005. Differential expression of NMDA receptor subunits and splice variants among the CA1, CA3 and dentate gyrus of the adult rat. *Brain research. Molecular brain research*, 135(1-2), pp.104–11.

Cronberg, T. et al., 2005. Selective sparing of hippocampal CA3 cells following in vitro ischemia is due to selective inhibition by acidosis. *The European journal of neuroscience*, 22(2), pp.310–6.

Csordás, G. et al., 2013. MICU1 controls both the threshold and cooperative activation of the mitochondrial Ca^{2+} uniporter. *Cell metabolism*, 17(6), pp.976–87.

Cui, H. et al., 2007. PDZ protein interactions underlying NMDA receptor-mediated excitotoxicity and neuroprotection by PSD-95 inhibitors. *The Journal of neuroscience*, 27(37), pp.9901–15.

Cui, W. et al., 2013. Preventive and therapeutic effects of mg132 by activating nrf2-are signaling pathway on oxidative stress-induced cardiovascular and renal injury. *Oxidative Medicine and Cellular Longevity*, 2013.

Culmsee, C. et al., 2001. AMP-activated protein kinase is highly expressed in neurons in the developing rat brain and promotes neuronal survival following glucose deprivation. *J Mol Neurosci*, 17(1), pp.45–58.

Dasgupta, B. & Milbrandt, J., 2007. Resveratrol stimulates AMP kinase activity in neurons. *Proceedings of the National Academy of Sciences of the United States of America*, 104(17), pp.7217–22.

Davila, D. et al., 2012. Two-step activation of FOXO3 by AMPK generates a coherent feed-forward loop determining excitotoxic cell fate. *Cell Death and Differentiation*, 19(10), pp.1677–1688.

Deighton, R.F. et al., 2014. Nrf2 target genes can be controlled by neuronal activity in the absence of Nrf2 and astrocytes. *Proceedings of the National Academy of Sciences of the United States of America*, 111(18), pp.1818–1820.

Deluca, H.F. & Engstrom, G.W., 1961. Calcium uptake by rat kidney mitochondria. *Proceedings of the National Academy of Sciences of the United States of America*, 47, pp.1744–50.

Dinkova-Kostova, A.T. & Talalay, P., 2010. NAD(P)H:quinone acceptor oxidoreductase 1 (NQO1), a multifunctional antioxidant enzyme and exceptionally versatile cytoprotector. *Archives of Biochemistry and Biophysics*, 501(1), pp.116–123.

Doonan, P.J. et al., 2014. LETM1-dependent mitochondrial Ca2+ flux modulates cellular bioenergetics and proliferation. *FASEB Journal*, 28(11), pp.4936–4949.

Dringen, R. et al., 2015. Glutathione-Dependent Detoxification Processes in Astrocytes. *Neurochemical Research*, 40(12), pp.2570–2582.

Dringen, R., Pfeiffer, B. & Hamprecht, B., 1999. Synthesis of the Antioxidant Glutathione in Neurons: Supply by Astrocytes of CysGly as Precursor for Neuronal Glutathione. *The Journal of Neuroscience*, 19(2), pp.562–569.

Duan, Y., Gross, R.A. & Sheu, S.-S., 2007. Ca2+-dependent generation of mitochondrial reactive oxygen species serves as a signal for poly(ADP-ribose) polymerase-1 activation during glutamate excitotoxicity. *The Journal of physiology*, 585(Pt 3), pp.741–58.

Duchen, M.R., 2012. Mitochondria, calcium-dependent neuronal death and neurodegenerative disease. *Pflügers Archiv : European journal of physiology*, 464(1), pp.111–21.

Duchen, M.R., Verkhratsky, A. & Muallem, S., 2008. Mitochondria and calcium in health and disease. *Cell calcium*, 44(1), pp.1–5.

Dumont, M. et al., 2009. Triterpenoid CDDO-methylamide improves memory and decreases amyloid plaques in a transgenic mouse model of Alzheimer's disease. *Journal of Neurochemistry*, 109(2), pp.502–512.

Edrey, Y.H. & Salmon, A.B., 2014. Revisiting an age-old question regarding oxidative stress. *Free radical biology & medicine*, 71(164), pp.368–78.

Effgen, G.B. & Morrison, B., 2016. Memantine Reduced Cell Death, Astrogliosis, and Functional Deficits in an in vitro Model of Repetitive Mild Traumatic Brain Injury. *Journal of neurotrauma*.

Ellrichmann, G. et al., 2011. Efficacy of fumaric acid esters in the R6/2 and YAC128 models

of Huntington's disease. *PloS one*, 6(1), p.e16172.

Escartin, C. et al., 2011. Nuclear factor erythroid 2-related factor 2 facilitates neuronal glutathione synthesis by upregulating neuronal excitatory amino acid transporter 3 expression. *The Journal of neuroscience : the official journal of the Society for Neuroscience*, 31(20), pp.7392–401.

Esteras, N., Dinkova-Kostova, A.T. & Abramov, A.Y., 2016. Nrf2 activation in the treatment of neurodegenerative diseases: a focus on its role in mitochondrial bioenergetics and function. *Biological chemistry*, 397(5), pp.383–400.

Feng, S. et al., 2013. Canonical transient receptor potential 3 channels regulate mitochondrial calcium uptake. *Proceedings of the National Academy of Sciences of the United States of America*, 110(27), pp.11011–6.

Fernandez-Fernandez, S., Almeida, A. & Bolaños, J.P., 2012. Antioxidant and bioenergetic coupling between neurons and astrocytes. *Biochemical Journal*, 443, pp.3–11.

Figueroa-Méndez, R. & Rivas-Arancibia, S., 2015. Vitamin C in Health and Disease: Its Role in the Metabolism of Cells and Redox State in the Brain. *Frontiers in physiology*, 6(DEC), p.397.

Findlay, V.J., Tapiero, H. & Townsend, D.M., 2005. Sulfiredoxin: a potential therapeutic agent? *Biomedicine&Pharmacotherapy*, 59(7), pp.374–379.

Fiskum, G. & Lehninger, A.L., 1979. Regulated release of Ca2+ from respiring mitochondria by Ca2+/2H+ antiport. *Journal of Biological Chemistry*, 254(14), pp.6236–6239.

Fogarty, S. et al., 2010. Calmodulin-dependent protein kinase kinase-beta activates AMPK without forming a stable complex: synergistic effects of Ca2+ and AMP. *The Biochemical journal*, 426(1), pp.109–18.

Foster, T.C., Kyritsopoulos, C. & Kumar, A., 2016. Central role for NMDA receptors in redox mediated impairment of synaptic function during aging and Alzheimer's disease. *Behavioural brain research*.

Fricker, M. et al., 2010. Implication of TAp73 in the p53-independent pathway of Puma induction and Puma-dependent apoptosis in primary cortical neurons. *Journal of neurochemistry*, 114(3), pp.772–83.

Fryer, L.G.D., Parbu-Patel, A. & Carling, D., 2002. The Anti-diabetic drugs rosiglitazone and metformin stimulate AMP-activated protein kinase through distinct signaling

pathways. *The Journal of biological chemistry*, 277(28), pp.25226–32.

Fujita, K. et al., 2011. Nrf2-mediated induction of p62 controls Toll-like receptor-4-driven aggresome-like induced structure formation and autophagic degradation. *Proceedings of the National Academy of Sciences of the United States of America*, 108(4), pp.1427–32.

Gan, L. et al., 2012. Astrocyte-specific overexpression of Nrf2 delays motor pathology and synuclein aggregation throughout the CNS in the alpha-synuclein mutant (A53T) mouse model. *The Journal of neuroscience : the official journal of the Society for Neuroscience*, 32(49), pp.17775–87.

Gan, L. & Johnson, J. a, 2014. Oxidative damage and the Nrf2-ARE pathway in neurodegenerative diseases. *Biochimica et biophysica acta*, 1842(8), pp.1208–18.

Ge, W. et al., 2006. Neuronal tissue-specific ribonucleoprotein complex formation on SOD1 mRNA: alterations by ALS SOD1 mutations. *Neurobiology of disease*, 23(2), pp.342–50.

Gee, C.E. et al., 2006. NMDA receptors and the differential ischemic vulnerability of hippocampal neurons. *The European journal of neuroscience*, 23(10), pp.2595–603.

Gegg, M.E., Clark, J.B. & Heales, S.J.R., 2005. Co-culture of neurones with glutathione deficient astrocytes leads to increased neuronal susceptibility to nitric oxide and increased glutamate-cysteine ligase activity. *Brain Research*, 1036(1-2), pp.1–6.

Glancy, B. & Balaban, R.S., 2012. Role of mitochondrial Ca2+ in the regulation of cellular energetics. *Biochemistry*, 51(14), pp.2959–73.

Gobbi, P. et al., 2007. Mitochondrial localization of Na+/Ca2+ exchangers NCX1-3 in neurons and astrocytes of adult rat brain in situ. *Pharmacological research*, 56(6), pp.556–65.

Gongol, B. et al., 2013. AMPK 2 exerts its anti-inflammatory effects through PARP-1 and Bcl-6. *Proceedings of the National Academy of Sciences*, 110(8), pp.3161–3166.

Graffmo, K.S. et al., 2013. Expression of wild-type human superoxide dismutase-1 in mice causes amyotrophic lateral sclerosis. *Human Molecular Genetics*, 22(1), pp.51–60.

Gray, J.A., Zito, K. & Hell, J.W., 2016. Non-ionotropic signaling by the NMDA receptor: controversy and opportunity. *F1000Research*, 5(May), pp.1–8.

Green, M.F., Anderson, K.A. & Means, A.R., 2011. Characterization of the CaMKKβ-AMPK signaling complex. *Cellular signalling*, 23(12), pp.2005–12.

Greenwood, S.M. & Connolly, C.N., 2007. Dendritic and mitochondrial changes during glutamate excitotoxicity. *Neuropharmacology*, 53(8), pp.891–8.

Greer, E.L. et al., 2007. The energy sensor AMP-activated protein kinase directly regulates the mammalian FOXO3 transcription factor. *Journal of Biological Chemistry*, 282(41), pp.30107–30119.

Gupta, K. et al., 2012. Human embryonic stem cell derived astrocytes mediate non-cell-autonomous neuroprotection through endogenous and drug-induced mechanisms. *Cell death and differentiation*, 19(5), pp.779–87.

Gupta, K., Chandran, S. & Hardingham, G.E., 2013a. Human stem cell-derived astrocytes and their application to studying Nrf2-mediated neuroprotective pathways and therapeutics in neurodegeneration. *British journal of clinical pharmacology*, 75(4), pp.907–18.

Gupta, K., Hardingham, G.E. & Chandran, S., 2013b. NMDA receptor-dependent glutamate excitotoxicity in human embryonic stem cell-derived neurons. *Neuroscience letters*, 543, pp.95–100.

Habas, A. et al., 2013. Neuronal activity regulates astrocytic Nrf2 signaling. *Proceedings of the National Academy of Sciences of the United States of America*, 110(45), pp.18291–6.

Habas, A. et al., 2014. Reply to Deighton et al.: Neuronal activity regulates distinct antioxidant pathways in neurons and astrocytes. *Proceedings of the National Academy of Sciences*, 111(18), pp.1821–1822.

Hajnóczky, G., Hager, R. & Thomas, A.P., 1999. Mitochondria suppress local feedback activation of inositol 1,4, 5-trisphosphate receptors by Ca2+. *The Journal of biological chemistry*, 274(20), pp.14157–62.

Halliwell, B., 2006. Oxidative stress and neurodegeneration: Where are we now? *Journal of Neurochemistry*, 97(6), pp.1634–1658.

Hardie, D.G., 2007. AMP-activated/SNF1 protein kinases: conserved guardians of cellular energy. *Nature reviews. Molecular cell biology*, 8(10), pp.774–785.

Hardie, D.G. & Frenguelli, B.G., 2007. A neural protection racket: AMPK and the

GABA(B) receptor. *Neuron*, 53(2), pp.159–62.

Hardie, D.G., Ross, F.A. & Hawley, S.A., 2012. AMPK: a nutrient and energy sensor that maintains energy homeostasis. *Nature Reviews Molecular Cell Biology*, 13(4), pp.251–262.

Harding, H.P. et al., 2003. An integrated stress response regulates amino acid metabolism and resistance to oxidative stress. *Molecular cell*, 11(3), pp.619–33.

Hardingham, G.E., 2006a. 2B synaptic or extrasynaptic determines signalling from the NMDA receptor. *The Journal of physiology*, 572(Pt 3), pp.614–5.

Hardingham, G.E. et al., 1999. Control of recruitment and transcription-activating function of CBP determines gene regulation by NMDA receptors and L-type calcium channels. *Neuron*, 22(4), pp.789–98.

Hardingham, G.E., 2009. Coupling of the NMDA receptor to neuroprotective and neurodestructive events. *Biochemical Society Transactions*, 37(6), p.1147.

Hardingham, G.E., 2006b. Pro-survival signalling from the NMDA receptor. *Biochemical Society transactions*, 34(Pt 5), pp.936–8.

Hardingham, G.E., Arnold, F.J. & Bading, H., 2001a. A calcium microdomain near NMDA receptors: on switch for ERK-dependent synapse-to-nucleus communication. *Nature neuroscience*, 4, pp.565–566.

Hardingham, G.E., Arnold, F.J. & Bading, H., 2001b. Nuclear calcium signaling controls CREB-mediated gene expression triggered by synaptic activity. *Nature neuroscience*, 4, pp.261–267.

Hardingham, G.E. & Bading, H., 2010. Synaptic versus extrasynaptic NMDA receptor signalling: implications for neurodegenerative disorders. *Nature reviews. Neuroscience*, 11(10), pp.682–96.

Hardingham, G.E. & Bading, H., 2003. The Yin and Yang of NMDA receptor signalling. *Trends in Neurosciences*, 26(2), pp.81–89.

Hardingham, G.E., Fukunaga, Y. & Bading, H., 2002. Extrasynaptic NMDARs oppose synaptic NMDARs by triggering CREB shut-off and cell death pathways. *Nature neuroscience*, 5(5), pp.405–14.

Harris, J.J., Jolivet, R. & Attwell, D., 2012. Synaptic Energy Use and Supply. *Neuron*, 75(5),

pp.762–777.

Hart, L. et al., 2014. LETM1 haploinsufficiency causes mitochondrial defects in cells from humans with Wolf-Hirschhorn syndrome: implications for dissecting the underlying pathomechanisms in this condition. *Disease models & mechanisms*, 7(5), pp.535–45.

Hasel, P. et al., 2015. Selective dendritic susceptibility to bioenergetic, excitotoxic and redox perturbations in cortical neurons. *Biochimica et biophysica acta*, 1853(9), pp.2066–76.

Haskew-Layton, R.E. et al., 2010. Controlled enzymatic production of astrocytic hydrogen peroxide protects neurons from oxidative stress via an Nrf2-independent pathway. *Proceedings of the National Academy of Sciences of the United States of America*, 107(40), pp.17385–90.

Hawley, S. a et al., 2003. Complexes between the LKB1 tumor suppressor, STRAD alpha/beta and MO25 alpha/beta are upstream kinases in the AMP-activated protein kinase cascade. *Journal of biology*, 2(4), p.28.

Hawley, S.A. et al., 2005. Calmodulin-dependent protein kinase kinase-beta is an alternative upstream kinase for AMP-activated protein kinase. *Cell metabolism*, 2(1), pp.9–19.

Hawley, S.A. et al., 1996. Characterization of the AMP-activated protein kinase kinase from rat liver and identification of threonine 172 as the major site at which it phosphorylates AMP-activated protein kinase. *The Journal of biological chemistry*, 271(44), pp.27879–87.

Hawrylycz, M.J. et al., 2012. An anatomically comprehensive atlas of the adult human brain transcriptome. *Nature*, 489(7416), pp.391–9.

Herring, A. et al., 2010. Reduction of cerebral oxidative stress following environmental enrichment in mice with alzheimer-like pathology. *Brain Pathology*, 20(1), pp.166–175.

Higgins, L.G. et al., 2009. Transcription factor Nrf2 mediates an adaptive response to sulforaphane that protects fibroblasts in vitro against the cytotoxic effects of electrophiles, peroxides and redox-cycling agents. *Toxicology and Applied Pharmacology*, 237(3), pp.267–280.

Hoffman, N.E. et al., 2013. MICU1 Motifs Define Mitochondrial Calcium Uniporter Binding and Activity. *Cell reports*, 5(6), pp.1576–88.

Hoffman, N.E. et al., 2014. SLC25A23 augments mitochondrial Ca^{2+} uptake, interacts with

MCU, and induces oxidative stress-mediated cell death. *Molecular biology of the cell*, 25(6), pp.936–47.

Hogan-Cann, A.D. & Anderson, C.M., 2016. Physiological Roles of Non-Neuronal NMDA Receptors. *Trends in pharmacological sciences*, 37(9), pp.750–67.

Hong, Y. et al., 2010. The role of Nrf2 signaling in the regulation of antioxidants and detoxifying enzymes after traumatic brain injury in rats and mice. *Acta pharmacologica Sinica*, 31(11), pp.1421–30.

Hongpaisan, J., Winters, C.A. & Andrews, S.B., 2004. Strong calcium entry activates mitochondrial superoxide generation, upregulating kinase signaling in hippocampal neurons. *The Journal of neuroscience : the official journal of the Society for Neuroscience*, 24(48), pp.10878–87.

Ichas, F. & Mazat, J.P., 1998. From calcium signaling to cell death: two conformations for the mitochondrial permeability transition pore. Switching from low- to high-conductance state. *Biochimica et biophysica acta*, 1366(1-2), pp.33–50.

Ikegaya, Y. & Matsuki, N., 2002. Regionally selective neurotoxicity of NMDA and colchicine is independent of hippocampal neural circuitry. *Neuroscience*, 113(2), pp.253–6.

Ikonomidou, C., 1999. Blockade of NMDA Receptors and Apoptotic Neurodegeneration in the Developing Brain. *Science*, 283(5398), pp.70–74.

Ikonomidou, C., Stefovska, V. & Turski, L., 2000. Neuronal death enhanced by N-methyl-D-aspartate antagonists. *Proceedings of the National Academy of Sciences of the United States of America*, 97(23), pp.12885–90.

Ikonomidou, C. & Turski, L., 2002. Why did NMDA receptor antagonists fail clinical trials for stroke and traumatic brain injury? *The Lancet. Neurology*, 1(6), pp.383–6.

Inamdar, N.M., Ahn, Y.I. & Alam, J., 1996. The heme-responsive element of the mouse heme oxygenase-1 gene is an extended AP-1 binding site that resembles the recognition sequences for MAF and NF-E2 transcription factors. *Biochemical and biophysical research communications*, 221(3), pp.570–576.

Itoh, K. et al., 1997. An Nrf2/small Maf heterodimer mediates the induction of phase II detoxifying enzyme genes through antioxidant response elements. *Biochemical and biophysical research communications*, 236(2), pp.313–22.

Jain, A.K., Bloom, D. a & Jaiswal, A.K., 2005. Nuclear import and export signals in control of Nrf2. *The Journal of biological chemistry*, 280(32), pp.29158–68.

Jakob, R. et al., 2014. Molecular and functional identification of a mitochondrial ryanodine receptor in neurons. *Neuroscience Letters*, 575, pp.7–12.

Janáky, R. et al., 1999. Glutathione and signal transduction in the mammalian CNS. *Journal of Neurochemistry*, 73(3), pp.889–902.

Jiang, D. et al., 2013. Letm1, the mitochondrial Ca2+/H+ antiporter, is essential for normal glucose metabolism and alters brain function in Wolf-Hirschhorn syndrome. *Proceedings of the National Academy of Sciences of the United States of America*, 110(24), pp.E2249–54.

Jiang, D., Zhao, L. & Clapham, D.E., 2009. Genome-Wide RNAi Screen Identifies Letm1 as a Mitochondrial Ca2+/H+ Antiporter. *Science*, 326(5949), pp.144–147.

Jiang, S. et al., 2016. Nrf2 Weaves an Elaborate Network of Neuroprotection Against Stroke. *Molecular neurobiology*.

Jiang, X. et al., 2005. The excitoprotective effect of N-methyl-D-aspartate receptors is mediated by a brain-derived neurotrophic factor autocrine loop in cultured hippocampal neurons. *Journal of Neurochemistry*, 94(3), pp.713–722.

Jimenez-Blasco, D. et al., 2015. Astrocyte NMDA receptors' activity sustains neuronal survival through a Cdk5-Nrf2 pathway. *Cell death and differentiation*, 22(11), pp.1877–89.

Johnson, J.A. et al., 2008. The Nrf2-ARE pathway: an indicator and modulator of oxidative stress in neurodegeneration. *Annals of the New York Academy of Sciences*, 1147, pp.61–9.

Johnson, W.M., Wilson-Delfosse, A.L. & Mieyal, J.J., 2012. Dysregulation of glutathione homeostasis in neurodegenerative diseases. *Nutrients*, 4(10), pp.1399–1440.

Joshi, G. et al., 2015. Increased Alzheimer's disease-like pathology in the APP/ PS1ΔE9 mouse model lacking Nrf2 through modulation of autophagy. *Neurobiology of aging*, 36(2), pp.664–79.

Ju, T.-C., Lin, Y.-S. & Chern, Y., 2012. Energy dysfunction in Huntington's disease: insights from PGC-1α, AMPK, and CKB. *Cellular and molecular life sciences : CMLS*, 69(24), pp.4107–20.

Kamat, C.D. et al., 2008. Antioxidants in central nervous system diseases: preclinical promise and translational challenges. *Journal of Alzheimer's disease : JAD*, 15(3), pp.473–93.

Kamer, K.J. & Mootha, V.K., 2014. MICU1 and MICU2 play nonredundant roles in the regulation of the mitochondrial calcium uniporter. *EMBO Reports*, 15(3), pp.299–307.

Kann, O. & Kovács, R., 2007. Mitochondria and neuronal activity. *American journal of physiology. Cell physiology*, 292(2), pp.C641–57.

Kanninen, K. et al., 2009. Intrahippocampal injection of a lentiviral vector expressing Nrf2 improves spatial learning in a mouse model of Alzheimer's disease. *Proceedings of the National Academy of Sciences of the United States of America*, 106(38), pp.16505–10.

Kaur, S.J., McKeown, S.R. & Rashid, S., 2016. Mutant SOD1 mediated pathogenesis of Amyotrophic Lateral Sclerosis. *Gene*, 577(2), pp.109–118.

Keelan, J., Vergun, O. & Duchen, M.R., 1999. Excitotoxic mitochondrial depolarisation requires both calcium and nitric oxide in rat hippocampal neurons. *Journal of Physiology*, 520(3), pp.797–813.

Kemmerer, Z.A. et al., 2015. Comparison of human Nrf2 antibodies: A tale of two proteins. *Toxicology Letters*, 238(2), pp.83–89.

Kensler, T.W. et al., 2013. Keap1-nrf2 signaling: a target for cancer prevention by sulforaphane. *Topics in current chemistry*, 329(1), pp.163–77.

Kensler, T.W., Wakabayashi, N. & Biswal, S., 2007. Cell survival responses to environmental stresses via the Keap1-Nrf2-ARE pathway. *Annual review of pharmacology and toxicology*, 47, pp.89–116.

Khananshvili, D., 2013. The SLC8 gene family of sodium-calcium exchangers (NCX) - structure, function, and regulation in health and disease. *Molecular aspects of medicine*, 34(2-3), pp.220–35.

Kilbride, S.M. et al., 2010. AMP-activated Protein Kinase Mediates Apoptosis in Response to Bioenergetic Stress through Activation of the Pro-apoptotic Bcl-2 Homology Domain-3-only Protein BMF. *Journal of Biological Chemistry*, 285(46), pp.36199–36206.

Kim, E. & Sheng, M., 2004. PDZ domain proteins of synapses. *Nature reviews. Neuroscience*, 5(10), pp.771–81.

Kirichok, Y., Krapivinsky, G. & Clapham, D.E., 2004. The mitochondrial calcium uniporter is a highly selective ion channel. *Nature*, 427(6972), pp.360–4.

Kodiha, M. et al., 2007. Localization of AMP kinase is regulated by stress, cell density, and signaling through the MEK-->ERK1/2 pathway. *American journal of physiology. Cell physiology*, 293(5), pp.C1427–36.

Konwinski, R.R. et al., 2004. Oltipraz, 3H-1,2-dithiole-3-thione, and sulforaphane induce overlapping and protective antioxidant responses in murine microglial cells. *Toxicology Letters*, 153(3), pp.343–355.

Kostic, M. et al., 2015. PKA Phosphorylation of NCLX Reverses Mitochondrial Calcium Overload and Depolarization, Promoting Survival of PINK1-Deficient Dopaminergic Neurons. *Cell Reports*, 13(2), pp.376–386.

Kraft, A.D., Johnson, D. a & Johnson, J. a, 2004. Nuclear factor E2-related factor 2-dependent antioxidant response element activation by tert-butylhydroquinone and sulforaphane occurring preferentially in astrocytes conditions neurons against oxidative insult. *The Journal of neuroscience : the official journal of the Society for Neuroscience*, 24(5), pp.1101–12.

Kresse, W. et al., 2005. Zinc ions are endogenous modulators of neurotransmitter-stimulated capacitative Ca2+ entry in both cultured and in situ mouse astrocytes. *European Journal of Neuroscience*, 21(6), pp.1626–1634.

Kumar, A. et al., 2015. Huntington's disease: An update of therapeutic strategies. *Gene*, 556(2), pp.91–97.

Kuramoto, N. et al., 2007. Phospho-Dependent Functional Modulation of GABAB Receptors by the Metabolic Sensor AMP-Dependent Protein Kinase. *Neuron*, 53(2), pp.233–247.

de la Fuente, S. et al., 2014. Dynamics of mitochondrial Ca2+ uptake in MICU1-knockdown cells. *The Biochemical journal*, 458(1), pp.33–40.

Lacher, S.E. et al., 2015. Beyond antioxidant genes in the ancient NRF2 regulatory network. *Free Radical Biology and Medicine*, 88, pp.452–465.

Lantier, L. et al., 2014. AMPK controls exercise endurance, mitochondrial oxidative capacity, and skeletal muscle integrity. *FASEB Journal*, 28(7), pp.3211–3224.

LaPash Daniels, C.M. et al., 2012. Beneficial effects of Nrf2 overexpression in a mouse model of Alexander disease. *The Journal of neuroscience : the official journal of the*

Society for Neuroscience, 32(31), pp.10507–15.

Lau, D. & Bading, H., 2009. Synaptic activity-mediated suppression of p53 and induction of nuclear calcium-regulated neuroprotective genes promote survival through inhibition of mitochondrial permeability transition. *The Journal of neuroscience : the official journal of the Society for Neuroscience*, 29(14), pp.4420–9.

Lee, J.M. et al., 2001. Phosphatidylinositol 3-Kinase, Not Extracellular Signal-regulated Kinase, Regulates Activation of the Antioxidant-Responsive Element in IMR-32 Human Neuroblastoma Cells. *Journal of Biological Chemistry*, 276(23), pp.20011–20016.

Lee, J.-M. et al., 2003. NF-E2-related factor-2 mediates neuroprotection against mitochondrial complex I inhibitors and increased concentrations of intracellular calcium in primary cortical neurons. *The Journal of biological chemistry*, 278(39), pp.37948–56.

Lee, J.-M. et al., 2005. Nrf2, a multi-organ protector? *FASEB journal : official publication of the Federation of American Societies for Experimental Biology*, 19(9), pp.1061–6.

Lee, J.Y. et al., 2009. Temporal expression of AMP-activated protein kinase activation during the kainic acid-induced hippocampal cell death. *Journal of neural transmission*, 116(1), pp.33–40.

Lee, Y. et al., 2015. Structure and function of the N-terminal domain of the human mitochondrial calcium uniporter. *EMBO reports*, 16(10), pp.1318–33.

Lein, E.S. et al., 2007. Genome-wide atlas of gene expression in the adult mouse brain. *Nature*, 445(7124), pp.168–76.

Léveillé, F. et al., 2009. Excitotoxic insults lead to peroxiredoxin hyperoxidation. *Oxidative medicine and cellular longevity*, 2(2), pp.110–3.

Léveillé, F. et al., 2008. Neuronal viability is controlled by a functional relation between synaptic and extrasynaptic NMDA receptors. *FASEB journal : official publication of the Federation of American Societies for Experimental Biology*, 22(12), pp.4258–71.

Léveillé, F. et al., 2010. Suppression of the intrinsic apoptosis pathway by synaptic activity. *The Journal of neuroscience : the official journal of the Society for Neuroscience*, 30(7), pp.2623–35.

Lewerenz, J. et al., 2014. Phosphoinositide 3-kinases upregulate system xc(-) via eukaryotic

initiation factor 2α and activating transcription factor 4 - A pathway active in glioblastomas and epilepsy. *Antioxidants & redox signaling*, 20(18), pp.2907–22.

Lewis, K.N. et al., 2015. Regulation of Nrf2 signaling and longevity in naturally long-lived rodents. *Proceedings of the National Academy of Sciences*, 112(12), p.201417566.

Li, J. et al., 2005. Stabilization of Nrf2 by tBHQ confers protection against oxidative stress-induced cell death in human neural stem cells. *Toxicological sciences : an official journal of the Society of Toxicology*, 83(2), pp.313–28.

Li, Y. et al., 1995. Dilated cardiomyopathy and neonatal lethality in mutant mice lacking manganese superoxide dismutase. *Nature genetics*, 11(4), pp.376–81.

Linker, R.A. et al., 2011. Fumaric acid esters exert neuroprotective effects in neuroinflammation via activation of the Nrf2 antioxidant pathway. *Brain : a journal of neurology*, 134(Pt 3), pp.678–92.

Lipton, S. a, 2006. Paradigm shift in neuroprotection by NMDA receptor blockade: memantine and beyond. *Nature reviews. Drug discovery*, 5(2), pp.160–170.

Livak, K.J. & Schmittgen, T.D., 2001. Analysis of Relative Gene Expression Data Using Real-Time Quantitative PCR and the 2−ΔΔCT Method. *Methods*, 25(4), pp.402–408.

Llorente-Folch, I. et al., 2015. The regulation of neuronal mitochondrial metabolism by calcium. *The Journal of physiology*, 593(16), pp.3447–62.

Loboda, A. et al., 2016. Role of Nrf2/HO-1 system in development, oxidative stress response and diseases: an evolutionarily conserved mechanism. *Cellular and molecular life sciences : CMLS*, 73(17), pp.3221–47.

Logan, C. V et al., 2014. Loss-of-function mutations in MICU1 cause a brain and muscle disorder linked to primary alterations in mitochondrial calcium signaling. *Nature genetics*, 46(2), pp.188–93.

Love, M.I., Huber, W. & Anders, S., 2014. Moderated estimation of fold change and dispersion for RNA-seq data with DESeq2. *Genome biology*, 15(12), p.550.

Luo, Z., Zang, M. & Guo, W., 2010. AMPK as a metabolic tumor suppressor: control of metabolism and cell growth. *Future oncology*, 6(3), pp.457–70.

Lupo, D. et al., 2011. Mdm38 is a 14-3-3-like receptor and associates with the protein synthesis machinery at the inner mitochondrial membrane. *Traffic*, 12(10), pp.1457–

1466.

Mahmoud, A.D. et al., 2016. AMP-activated Protein Kinase Deficiency Blocks the Hypoxic Ventilatory Response and Thus Precipitates Hypoventilation and Apnea. *American Journal of Respiratory and Critical Care Medicine*, 193(9), pp.1032–43.

Mairet-Coello, G. et al., 2013. The CAMKK2-AMPK kinase pathway mediates the synaptotoxic effects of Aβ oligomers through Tau phosphorylation. *Neuron*, 78(1), pp.94–108.

Majewska, M.D., Bell, J. a & London, E.D., 1990. Regulation of the NMDA receptor by redox phenomena: inhibitory role of ascorbate. *Brain research*, 537(1-2), pp.328–32.

Mallilankaraman, K., Cárdenas, C., et al., 2012a. MCUR1 is an essential component of mitochondrial Ca2+ uptake that regulates cellular metabolism. *Nature cell biology*, 14(12), pp.1336–43.

Mallilankaraman, K., Doonan, P., et al., 2012b. MICU1 is an essential gatekeeper for MCU-mediated mitochondrial Ca(2+) uptake that regulates cell survival. *Cell*, 151(3), pp.630–44.

Mandir, A.S. et al., 2000. NMDA But Not Non-NMDA Excitotoxicity is Mediated by Poly(ADPRibose) Polymerase. *The Journal of Neuroscience*, 20(21), pp.8005–8011.

Manwani, B. & McCullough, L.D., 2013. Function of the master energy regulator adenosine monophosphate-activated protein kinase in stroke. *Journal of neuroscience research*, 91(8), pp.1018–29.

Mao, T. et al., 2008. Characterization and subcellular targeting of GCaMP-type genetically-encoded calcium indicators. *PLoS ONE*, 3(3), pp.1–10.

Marchi, S. & Pinton, P., 2014. The mitochondrial calcium uniporter complex: molecular components, structure and physiopathological implications. *The Journal of physiology*, 592(5), pp.829–39.

De Marchi, U. et al., 2014. NCLX protein, but not LETM1, mediates mitochondrial Ca2+ extrusion, thereby limiting Ca2+-induced NAD(P)H production and modulating matrix redox state. *The Journal of biological chemistry*, 289(29), pp.20377–85.

Márkus, N.M. et al., 2016. Expression of mRNA Encoding Mcu and Other Mitochondrial Calcium Regulatory Genes Depends on Cell Type, Neuronal Subtype, and Ca2+ Signaling. *PloS one*, 11(2), p.e0148164.

Martel, M.-A. et al., 2009. Inhibiting pro-death NMDA receptor signaling dependent on the NR2 PDZ ligand may not affect synaptic function or synaptic NMDA receptor signaling to gene expression. *Channels*, 3(1), pp.12–5.

Martel, M.-A. et al., 2012. The Subtype of GluN2 C-terminal Domain Determines the Response to Excitotoxic Insults. *Neuron*, 74(3), pp.543–556.

Massie, A. et al., 2015. Main path and byways: non-vesicular glutamate release by system xc(-) as an important modifier of glutamatergic neurotransmission. *Journal of neurochemistry*, 135(6), pp.1062–79.

Matesanz-Isabel, J. et al., 2016. Functional roles of MICU1 and MICU2 in mitochondrial Ca2+ uptake. *Biochimica et Biophysica Acta (BBA) - Biomembranes*, 1858(6), pp.1110–1117.

McCormack, J.G., Halestrap, a P. & Denton, R.M., 1990. Role of calcium ions in regulation of mammalian intramitochondrial metabolism. *Physiological reviews*, 70(2), pp.391–425.

McCullough, L.D. et al., 2005. Pharmacological inhibition of AMP-activated protein kinase provides neuroprotection in stroke. *Journal of Biological Chemistry*, 280(21), pp.20493–20502.

McKay, S. et al., 2013. Recovery of NMDA receptor currents from MK-801 blockade is accelerated by Mg2+ and memantine under conditions of agonist exposure. *Neuropharmacology*, 74, pp.119–25.

McMahon, M. et al., 2003. Keap1-dependent proteasomal degradation of transcription factor Nrf2 contributes to the negative regulation of antioxidant response element-driven gene expression. *The Journal of biological chemistry*, 278(24), pp.21592–600.

Mennerick, S. & Zorumski, C.F., 2001. Neural activity and survival in the developing nervous system. *Molecular neurobiology*, 22(1-3), pp.41–54.

Minokoshi, Y. et al., 2004. AMP-kinase regulates food intake by responding to hormonal and nutrient signals in the hypothalamus. *Nature*, 428(6982), pp.569–74.

Momcilovic, M., Hong, S.P. & Carlson, M., 2006. Mammalian TAK1 activates Snf1 protein kinase in yeast and phosphorylates AMP-activated protein kinase in vitro. *Journal of Biological Chemistry*, 281(35), pp.25336–25343.

Moroni, F. et al., 2001. Poly(ADP-ribose) polymerase inhibitors attenuate necrotic but not

apoptotic neuronal death in experimental models of cerebral ischemia. *Cell death and differentiation*, 8(9), pp.921–32.

Motloch, L.J. et al., 2015. UCP2 modulates cardioprotective effects of Ru360 in isolated cardiomyocytes during ischemia. *Pharmaceuticals*, 8(3), pp.474–482.

Mungai, P.T. et al., 2011. Hypoxia Triggers AMPK Activation through Reactive Oxygen Species-Mediated Activation of Calcium Release-Activated Calcium Channels. *Molecular and Cellular Biology*, 31(17), pp.3531–3545.

Newrzella, D. et al., 2007. The functional genome of CA1 and CA3 neurons under native conditions and in response to ischemia. *BMC genomics*, 8, p.370.

Neymotin, A. et al., 2011. Neuroprotective effect of Nrf2/ARE activators, CDDO ethylamide and CDDO trifluoroethylamide, in a mouse model of amyotrophic lateral sclerosis. *Free radical biology & medicine*, 51(1), pp.88–96.

Nguyen, T., Yang, C.S. & Pickett, C.B., 2004. The pathways and molecular mechanisms regulating Nrf2 activation in response to chemical stress. *Free radical biology & medicine*, 37(4), pp.433–41.

Nicholls, D.G., 2006. Simultaneous monitoring of ionophore- and inhibitor-mediated plasma and mitochondrial membrane potential changes in cultured neurons. *Journal of Biological Chemistry*, 281(21), pp.14864–14874.

Nichols, J.A. et al., 2007. Environmental enrichment selectively increases glutamatergic responses in layer II/III of the auditory cortex of the rat. *Neuroscience*, 145(3), pp.832–840.

Nita, L.I., Hershfinkel, M. & Sekler, I., 2015. Life after the birth of the mitochondrial Na+/Ca2+ exchanger, NCLX. *Science China Life Sciences*, 58(1), pp.59–65.

Noh, Y.H. et al., 2009. Sulfiredoxin translocation into mitochondria plays a crucial role in reducing hyperoxidized peroxiredoxin III. *Journal of Biological Chemistry*, 284(13), pp.8470–8477.

O'Callaghan, R.M., Griffin, É. W. & Kelly, Á. M., 2009. Long-term treadmill exposure protects against age-related neurodegenerative change in the rat hippocampus. *Hippocampus*, 19(10), pp.1019–1029.

Olney, J.W., 1969. Brain lesions, obesity, and other disturbances in mice treated with monosodium glutamate. *Science*, 164(880), pp.719–721.

Olney, J.W. et al., 2002. Drug-induced apoptotic neurodegeneration in the developing brain. *Brain pathology (Zurich, Switzerland)*, 12(4), pp.488–98.

Olney, J.W. et al., 2000. Ethanol-induced apoptotic neurodegeneration in the developing brain. *Apoptosis*, 5(6), pp.515–521.

Olney, J.W. & Ho, O.L., 1970. Brain damage in infant mice following oral intake of glutamate, aspartate or cysteine. *Nature*, 227(5258), pp.609–11.

Orrenius, S., Zhivotovsky, B. & Nicotera, P., 2003. Regulation of cell death: the calcium-apoptosis link. *Nature reviews. Molecular cell biology*, 4(7), pp.552–65.

Pachernegg, S., Strutz-Seebohm, N. & Hollmann, M., 2012. GluN3 subunit-containing NMDA receptors: Not just one-trick ponies. *Trends in Neurosciences*, 35(4), pp.240–249.

Palty, R. et al., 2004. Lithium-calcium exchange is mediated by a distinct potassium-independent sodium-calcium exchanger. *The Journal of biological chemistry*, 279(24), pp.25234–40.

Palty, R. et al., 2010. NCLX is an essential component of mitochondrial Na+/Ca2+ exchange. *Proceedings of the National Academy of Sciences of the United States of America*, 107(1), pp.436–41.

Palty, R. & Sekler, I., 2012. The mitochondrial Na+/Ca2+ exchanger. *Cell Calcium*, 52(1), pp.9–15.

Paoletti, P., Bellone, C. & Zhou, Q., 2013. NMDA receptor subunit diversity: impact on receptor properties, synaptic plasticity and disease. *Nature reviews. Neuroscience*, 14(6), pp.383–400.

Papadia, S. et al., 2005. Nuclear Ca2+ and the cAMP response element-binding protein family mediate a late phase of activity-dependent neuroprotection. *The Journal of neuroscience : the official journal of the Society for Neuroscience*, 25(17), pp.4279–87.

Papadia, S. et al., 2008. Synaptic NMDA receptor activity boosts intrinsic antioxidant defenses. *Nature Neuroscience*, 11(4), pp.476–487.

Papadia, S. & Hardingham, G.E., 2007. The Dichotomy of NMDA Receptor Signaling. *The Neuroscientist*, 13(6), pp.572–579.

Parnis, J. et al., 2013. Mitochondrial exchanger NCLX plays a major role in the intracellular

Ca2+ signaling, gliotransmission, and proliferation of astrocytes. *The Journal of neuroscience : the official journal of the Society for Neuroscience*, 33(17), pp.7206–19.

Parsons, M.P. & Raymond, L.A., 2014. Extrasynaptic NMDA receptor involvement in central nervous system disorders. *Neuron*, 82(2), pp.279–93.

Patenaude, A., Murthy, M.R. V & Mirault, M.E., 2005. Emerging roles of thioredoxin cycle enzymes in the central nervous system. *Cellular and Molecular Life Sciences*, 62(10), pp.1063–1080.

Paupe, V. et al., 2015. CCDC90A (MCUR1) is a cytochrome c oxidase assembly factor and not a regulator of the mitochondrial calcium uniporter. *Cell Metabolism*, 21(1), pp.109–116.

Perocchi, F. et al., 2010. MICU1 encodes a mitochondrial EF hand protein required for Ca(2+) uptake. *Nature*, 467(7313), pp.291–6.

Petrungaro, C. et al., 2015. The Ca2+-dependent release of the Mia40-induced MICU1-MICU2 dimer from MCU regulates mitochondrial Ca2+ uptake. *Cell Metabolism*, 22(4), pp.721–733.

Plovanich, M. et al., 2013. MICU2, a paralog of MICU1, resides within the mitochondrial uniporter complex to regulate calcium handling. *PloS one*, 8(2), p.e55785.

Popa-Wagner, A. et al., 2013. ROS and Brain Diseases: The Good, the Bad, and the Ugly. *Oxidative Medicine and Cellular Longevity*, 2013, pp.1–14.

Potter, W.B. et al., 2010. Metabolic regulation of neuronal plasticity by the energy sensor AMPK. *PloS one*, 5(2), p.e8996.

Prentice, H., Modi, J.P. & Wu, J.-Y., 2015. Mechanisms of Neuronal Protection against Excitotoxicity, Endoplasmic Reticulum Stress, and Mitochondrial Dysfunction in Stroke and Neurodegenerative Diseases. *Oxidative medicine and cellular longevity*, 2015, p.964518.

Qiu, J. et al., 2013. Mitochondrial calcium uniporter Mcu controls excitotoxicity and is transcriptionally repressed by neuroprotective nuclear calcium signals. *Nature communications*, 4, p.2034.

Qiu, S. et al., 2007. Ascorbate transport by primary cultured neurons and its role in neuronal function and protection against excitotoxicity. *Journal of neuroscience research*, 85(5), pp.1046–56.

Rada, P. et al., 2011. SCF/{beta}-TrCP promotes glycogen synthase kinase 3-dependent degradation of the Nrf2 transcription factor in a Keap1-independent manner. *Molecular and cellular biology*, 31(6), pp.1121–33.

Raffaello, A. et al., 2013. The mitochondrial calcium uniporter is a multimer that can include a dominant-negative pore-forming subunit. *The EMBO journal*, 32(17), pp.2362–76.

Reaume, A.G. et al., 1996. Motor neurons in Cu/Zn superoxide dismutase-deficient mice develop normally but exhibit enhanced cell death after axonal injury. *Nature genetics*, 13(1), pp.43–7.

Regan, M.C., Romero-Hernandez, A. & Furukawa, H., 2015. A structural biology perspective on NMDA receptor pharmacology and function. *Current Opinion in Structural Biology*, 33, pp.68–75.

Rice, M.E., 2000. Ascorbate regulation and its neuroprotective role in the brain. *Trends in neurosciences*, 23(5), pp.209–16.

Rizzuto, R. et al., 1993. Microdomains with high Ca2+ close to IP3-sensitive channels that are sensed by neighboring mitochondria. *Science*, 262(5134), pp.744–747.

Rizzuto, R. et al., 2012. Mitochondria as sensors and regulators of calcium signalling. *Nature reviews. Molecular cell biology*, 13(9), pp.566–78.

Robert, S.M. et al., 2014. Role of glutamate transporters in redox homeostasis of the brain. *Neurochemistry international*, 73(1), pp.181–91.

Rosen, D.R. et al., 1993. Mutations in Cu/Zn superoxide dismutase gene are associated with familial amyotrophic lateral sclerosis. *Nature*, 362(6415), pp.59–62.

Rueda, C.B. et al., 2014. Ca2 + regulation of mitochondrial function in neurons. *Biochimica et Biophysica Acta - Bioenergetics*, 1837(10), pp.1617–1624.

Rueda, C.B. et al., 2015. Mitochondrial ATP-Mg/Pi carrier SCaMC-3/Slc25a23 counteracts PARP-1-dependent fall in mitochondrial ATP caused by excitotoxic insults in neurons. *The Journal of neuroscience : the official journal of the Society for Neuroscience*, 35(8), pp.3566–81.

Ruiz, A., Alberdi, E. & Matute, C., 2014. CGP37157, an inhibitor of the mitochondrial Na+/Ca2+ exchanger, protects neurons from excitotoxicity by blocking voltage-gated Ca2+ channels. *Cell death & disease*, 5, p.e1156.

Rushmore, T.H., Morton, M.R. & Pickett, C.B., 1991. The antioxidant responsive element: Activation by oxidative stress and identification of the DNA consensus sequence required for functional activity. *Journal of Biological Chemistry*, 266(18), pp.11632–11639.

Ryu, S.-Y. et al., 2011. Single channel characterization of the mitochondrial ryanodine receptor in heart mitoplasts. *The Journal of biological chemistry*, 286(24), pp.21324–21329.

Salt, I. et al., 1998. AMP-activated protein kinase: greater AMP dependence, and preferential nuclear localization, of complexes containing the alpha2 isoform. *The Biochemical journal*, 334 (Pt 1), pp.177–87.

Sancak, Y. et al., 2013. EMRE is an essential component of the mitochondrial calcium uniporter complex. *Science (New York, N.Y.)*, 342(6164), pp.1379–82.

Sanders, M.J. et al., 2007. Investigating the mechanism for AMP activation of the AMP-activated protein kinase cascade. *The Biochemical journal*, 403(1), pp.139–48.

Sasaki, H. et al., 2002. Electrophile response element-mediated induction of the cystine/glutamate exchange transporter gene expression. *Journal of Biological Chemistry*, 277(47), pp.44765–44771.

Satoh, T. et al., 2006. Activation of the Keap1/Nrf2 pathway for neuroprotection by electrophilic phase II inducers. *Proceedings of the National Academy of Sciences of the United States of America*, 103(3), pp.768–73.

Satoh, T., McKercher, S.R. & Lipton, S.A., 2013. Nrf2/ARE-mediated antioxidant actions of pro-electrophilic drugs. *Free radical biology & medicine*, 65, pp.645–57.

Schipper, H.M., 2004. Brain iron deposition and the free radical-mitochondrial theory of ageing. *Ageing Research Reviews*, 3(3), pp.265–301.

Schipper, H.M. et al., 2009. Heme oxygenase-1 and neurodegeneration: Expanding frontiers of engagement. *Journal of Neurochemistry*, 110(2), pp.469–485.

Scorziello, A. et al., 2013. NCX3 regulates mitochondrial Ca(2+) handling through the AKAP121-anchored signaling complex and prevents hypoxia-induced neuronal death. *Journal of cell science*, 126(Pt 24), pp.5566–77.

Sheng, Y. et al., 2014. Superoxide dismutases and superoxide reductases. *Chemical Reviews*, 114(7), pp.3854–3918.

Shih, A.Y. et al., 2003. Coordinate regulation of glutathione biosynthesis and release by Nrf2-expressing glia potently protects neurons from oxidative stress. *The Journal of neuroscience : the official journal of the Society for Neuroscience*, 23(8), pp.3394–3406.

Shih, A.Y., Li, P. & Murphy, T.H., 2005. A small-molecule-inducible Nrf2-mediated antioxidant response provides effective prophylaxis against cerebral ischemia in vivo. *The Journal of neuroscience : the official journal of the Society for Neuroscience*, 25(44), pp.10321–35.

Shoshan-Barmatz, V. & Gincel, D., 2003. The voltage-dependent anion channel: characterization, modulation, and role in mitochondrial function in cell life and death. *Cell biochemistry and biophysics*, 39(3), pp.279–92.

Shu, L. et al., 2016. The neuroprotection of hypoxic preconditioning on rat brain against traumatic brain injury by up-regulated transcription factor Nrf2 and HO-1 expression. *Neuroscience Letters*, 611, pp.74–80.

Singh, A. et al., 2009. Nrf2-dependent sulfiredoxin-1 expression protects against cigarette smoke-induced oxidative stress in lungs. *Free Radical Biology and Medicine*, 46(3), pp.376–386.

Son, T.G. et al., 2010. Plumbagin, a novel Nrf2/ARE activator, protects against cerebral ischemia. *Journal of neurochemistry*, 112(5), pp.1316–26.

Soriano, F.X., Léveillé, F., et al., 2008a. Induction of sulfiredoxin expression and reduction of peroxiredoxin hyperoxidation by the neuroprotective Nrf2 activator 3H-1,2-dithiole-3-thione. *Journal of neurochemistry*, 107(2), pp.533–43.

Soriano, F.X. et al., 2006. Preconditioning doses of NMDA promote neuroprotection by enhancing neuronal excitability. *The Journal of neuroscience : the official journal of the Society for Neuroscience*, 26(17), pp.4509–18.

Soriano, F.X., Martel, M.-A., et al., 2008b. Specific targeting of pro-death NMDA receptor signals with differing reliance on the NR2B PDZ ligand. *The Journal of neuroscience : the official journal of the Society for Neuroscience*, 28(42), pp.10696–710.

Soriano, F.X. et al., 2009. Transcriptional regulation of the AP-1 and Nrf2 target gene sulfiredoxin. *Molecules and cells*, 27(3), pp.279–82.

Spires, T.L. & Hannan, A.J., 2005. Nature, nurture and neurology: Gene-environment

interactions in neurodegenerative disease. FEBS Anniversary Prize Lecture delivered on 27 June 2004 at the 29th FEBS Congress in Warsaw. *FEBS Journal*, 272(10), pp.2347–2361.

Stack, C. et al., 2010. Triterpenoids CDDO-ethyl amide and CDDO-trifluoroethyl amide improve the behavioral phenotype and brain pathology in a transgenic mouse model of Huntington's disease. *Free Radical Biology and Medicine*, 49(2), pp.147–158.

De Stefani, D. et al., 2011. A forty-kilodalton protein of the inner membrane is the mitochondrial calcium uniporter. *Nature*, 476(7360), pp.336–340.

De Stefani, D., Rizzuto, R. & Pozzan, T., 2016. Enjoy the Trip: Calcium in Mitochondria Back and Forth. *Annual review of biochemistry*, 85(1), pp.161–92.

Strasser, U. & Fischer, G., 1995. Quantitative measurement of neuronal degeneration in organotypic hippocampal cultures after combined oxygen/glucose deprivation. *Journal of neuroscience methods*, 57(2), pp.177–86.

Tashiro, A. et al., 2006. NMDA-receptor-mediated, cell-specific integration of new neurons in adult dentate gyrus. *Nature*, 442(August), pp.929–933.

Tauskela, J.S. et al., 2008. Elevated synaptic activity preconditions neurons against an in vitro model of ischemia. *Journal of Biological Chemistry*, 283(50), pp.34667–34676.

Thorn, T.L. et al., 2015. A Cytotoxic, Co-operative Interaction Between Energy Deprivation and Glutamate Release From System xc- Mediates Aglycemic Neuronal Cell Death. *ASN neuro*, 7(6).

Thornton, C. et al., 2011. AMP-activated protein kinase (AMPK) is a tau kinase, activated in response to amyloid β-peptide exposure. *The Biochemical journal*, 434(3), pp.503–12.

Trenker, M. et al., 2007. Uncoupling proteins 2 and 3 are fundamental for mitochondrial Ca2+ uniport. *Nature cell biology*, 9(4), pp.445–52.

Tsai, M.-F. et al., 2016. Dual functions of a small regulatory subunit in the mitochondrial calcium uniporter complex. *eLife*, 5.

Tsai, M.-F. et al., 2014. Functional reconstitution of the mitochondrial Ca2+/H+ antiporter Letm1. *The Journal of general physiology*, 143(1), pp.67–73.

Tsou, P. et al., 2011. A fluorescent reporter of AMPK activity and cellular energy stress. *Cell metabolism*, 13(4), pp.476–86.

Tsvetkov, A.S. et al., 2013. Proteostasis of polyglutamine varies among neurons and predicts neurodegeneration. *Nature chemical biology*, 9(9), pp.586–92.

Tu, J. et al., 2015. Cell-Permeable Peptide Targeting the Nrf2-Keap1 Interaction: A Potential Novel Therapy for Global Cerebral Ischemia. *Journal of Neuroscience*, 35(44), pp.14727–14739.

Turnley, A.M. et al., 1999. Cellular Distribution and Developmental Expression of AMP-Activated Protein Kinase Isoforms in Mouse Central Nervous System. *Journal of Neurochemistry*, 72(4), pp.1707–1716.

Vais, H. et al., 2016. EMRE Is a Matrix Ca(2+) Sensor that Governs Gatekeeping of the Mitochondrial Ca(2+) Uniporter. *Cell reports*, 14(3), pp.403–10.

Vais, H. et al., 2015. MCUR1, CCDC90A, Is a Regulator of the Mitochondrial Calcium Uniporter. *Cell metabolism*, 22(4), pp.533–5.

Varanese, S., Howard, J. & Di Rocco, A., 2010. NMDA antagonist memantine improves levodopa-induced dyskinesias and "on-off" phenomena in Parkinson's disease. *Movement disorders : official journal of the Movement Disorder Society*, 25(4), pp.508–10.

Vargas, M.R. et al., 2008. Nrf2 Activation in Astrocytes Protects against Neurodegeneration in Mouse Models of Familial Amyotrophic Lateral Sclerosis. *Journal of Neuroscience*, 28(50), pp.13574–13581.

Vargas, M.R. & Johnson, J. a, 2009. The Nrf2-ARE cytoprotective pathway in astrocytes. *Expert reviews in molecular medicine*, 11(June), p.e17.

Vashishta, A. et al., 2009. Nuclear factor of activated T-cells isoform c4 (NFATc4/NFAT3) as a mediator of antiapoptotic transcription in NMDA receptor-stimulated cortical neurons. *The Journal of neuroscience*, 29(48), pp.15331–15340.

Vasington, F.D. et al., 1972. The effect of ruthenium red on Ca 2+ transport and respiration in rat liver mitochondria. *Biochimica et biophysica acta*, 256(1), pp.43–54.

De vos, K.J. et al., 2007. Familial amyotrophic lateral sclerosis-linked SOD1 mutants perturb fast axonal transport to reduce axonal mitochondria content. *Human Molecular Genetics*, 16(22), pp.2720–2728.

Wakabayashi, N. et al., 2003. Keap1-null mutation leads to postnatal lethality due to constitutive Nrf2 activation. *Nature genetics*, 35(3), pp.238–45.

Waldeck-Weiermair, M. et al., 2011. Leucine zipper EF hand-containing transmembrane protein 1 (Letm1) and uncoupling proteins 2 and 3 (UCP2/3) contribute to two distinct mitochondrial Ca 2+ uptake pathways. *Journal of Biological Chemistry*, 286(32), pp.28444–28455.

Waldeck-Weiermair, M. et al., 2015. Rearrangement of MICU1 multimers for activation of MCU is solely controlled by cytosolic Ca(2.). *Scientific reports*, 5, p.15602.

Waldeck-Weiermair, M. et al., 2010. The contribution of UCP2 and UCP3 to mitochondrial Ca2+ uptake is differentially determined by the source of supplied Ca2+. *Cell Calcium*, 47(5), pp.433–440.

Wang, L. et al., 2014. Structural and mechanistic insights into MICU1 regulation of mitochondrial calcium uptake. *The EMBO journal*, pp.1–12.

Wang, Y. et al., 2011. Poly(ADP-ribose) (PAR) binding to apoptosis-inducing factor is critical for PAR polymerase-1-dependent cell death (parthanatos). *Science signaling*, 4(167), p.ra20.

Wang, Y., Dawson, V.L. & Dawson, T.M., 2009. Poly(ADP-ribose) signals to mitochondrial AIF: A key event in parthanatos. *Experimental Neurology*, 218(2), pp.193–202.

Weisova, P. et al., 2009. Regulation of Glucose Transporter 3 Surface Expression by the AMP-Activated Protein Kinase Mediates Tolerance to Glutamate Excitation in Neurons. *Journal of Neuroscience*, 29(9), pp.2997–3008.

Weisová, P. et al., 2012. "Mild mitochondrial uncoupling" induced protection against neuronal excitotoxicity requires AMPK activity. *Biochimica et Biophysica Acta (BBA) - Bioenergetics*, 1817(5), pp.744–753.

White, R.J. & Reynolds, I.J., 1996. Mitochondrial depolarization in glutamate-stimulated neurons: an early signal specific to excitotoxin exposure. *The Journal of neuroscience : the official journal of the Society for Neuroscience*, 16(18), pp.5688–97.

Wilde, G.J. et al., 1997. Differential vulnerability of the CA1 and CA3 subfields of the hippocampus to superoxide and hydroxyl radicals in vitro. *Journal of neurochemistry*, 69(2), pp.883–6.

Wirkner, K. et al., 1999. Ethanol-induced inhibition of NMDA receptor channels. *Neurochemistry international*, 35(2), pp.153–62.

Wood-Kaczmar, A. et al., 2013. The role of the mitochondrial NCX in the mechanism of

neurodegeneration in Parkinson's disease. *Advances in experimental medicine and biology*, 961, pp.241–9.

Woods, A. et al., 2005. Ca2+/calmodulin-dependent protein kinase kinase-beta acts upstream of AMP-activated protein kinase in mammalian cells. *Cell metabolism*, 2(1), pp.21–33.

Woods, A. et al., 2003. LKB1 Is the Upstream Kinase in the AMP-Activated Protein Kinase Cascade. *Current Biology*, 13(22), pp.2004–2008.

Wyllie, D.J. a, Livesey, M.R. & Hardingham, G.E., 2013. Influence of GluN2 subunit identity on NMDA receptor function. *Neuropharmacology*, 74, pp.4–17.

Xia, P. et al., 2010. Memantine preferentially blocks extrasynaptic over synaptic NMDA receptor currents in hippocampal autapses. *The Journal of neuroscience : the official journal of the Society for Neuroscience*, 30(33), pp.11246–50.

Xu, J. et al., 2009. Extrasynaptic NMDA receptors couple preferentially to excitotoxicity via calpain-mediated cleavage of STEP. *The Journal of neuroscience : the official journal of the Society for Neuroscience*, 29(29), pp.9330–43.

Xu, W. et al., 2007. Calpain-mediated mGluR1alpha truncation: a key step in excitotoxicity. *Neuron*, 53(3), pp.399–412.

Xue, F. et al., 2016. Nrf2/antioxidant defense pathway is involved in the neuroprotective effects of Sirt1 against focal cerebral ischemia in rats after hyperbaric oxygen preconditioning. *Behavioural brain research*, 309, pp.1–8.

Yamakura, F. et al., 1998. Inactivation of human manganese-superoxide dismutase by peroxynitrite is caused by exclusive nitration of tyrosine 34 to 3-nitrotyrosine. *Journal of Biological Chemistry*, 273(23), pp.14085–14089.

Yamamoto, T. et al., 2016. Analysis of the structure and function of EMRE in a yeast expression system. *Biochimica et biophysica acta*, 1857(6), pp.831–9.

Yang, G. et al., 2000. Regional difference of neuronal vulnerability in the murine hippocampus after transient forebrain ischemia. *Brain Research*, 870(1-2), pp.195–198.

Yang, L. et al., 2009. Neuroprotective effects of the triterpenoid, CDDO methyl amide, a potent inducer of Nrf2-mediated transcription. *PLoS ONE*, 4(6).

Yin, F. et al., 2010. Geniposide induces the expression of heme oxygenase-1 via PI3K/Nrf2-signaling to enhance the antioxidant capacity in primary hippocampal neurons.

Biological & pharmaceutical bulletin, 33(11), pp.1841–6.

Young, D. et al., 1999. Environmental enrichment inhibits spontaneous apoptosis, prevents seizures and is neuroprotective. *Nature medicine*, 5(4), pp.448–53.

Yu, S. et al., 2002. Mediation of poly(ADP-ribose) polymerase-1-dependent cell death by apoptosis-inducing factor. *Science (New York, N.Y.)*, 297(5579), pp.259–63.

Zhang, J. et al., 2009a. PKCdelta mediates Nrf2-dependent protection of neuronal cells from NO-induced apoptosis. *Biochemical and biophysical research communications*, 386(4), pp.750–6.

Zhang, S.-J. et al., 2007. Decoding NMDA receptor signaling: identification of genomic programs specifying neuronal survival and death. *Neuron*, 53(4), pp.549–62.

Zhang, S.-J. et al., 2009b. Nuclear calcium signaling controls expression of a large gene pool: identification of a gene program for acquired neuroprotection induced by synaptic activity. *PLoS genetics*, 5(8), p.e1000604.

Zhang, Y. et al., 2016. Dysfunction of NMDA receptors in Alzheimer's disease. *Neurological sciences : official journal of the Italian Neurological Society and of the Italian Society of Clinical Neurophysiology*, 37(7), pp.1039–47.

Zheng, S. et al., 2010. NMDA-induced neuronal survival is mediated through nuclear factor I-A in mice. *Journal of Clinical Investigation*, 120(7), pp.2446–2456.

Zhou, X. et al., 2015a. Extrasynaptic NMDA Receptor in Excitotoxicity: Function Revisited. *The Neuroscientist*, 21(4), pp.337–344.

Zhou, Y. et al., 2015b. Sulfiredoxin-1 attenuates oxidative stress via Nrf2/ARE pathway and 2-Cys Prdxs after oxygen-glucose deprivation in astrocytes. *Journal of molecular neuroscience : MN*, 55(4), pp.941–50.

Zou, M.-H. et al., 2003. Activation of 5'-AMP-activated kinase is mediated through c-Src and phosphoinositide 3-kinase activity during hypoxia-reoxygenation of bovine aortic endothelial cells. Role of peroxynitrite. *The Journal of biological chemistry*, 278(36), pp.34003–10.

Appendix

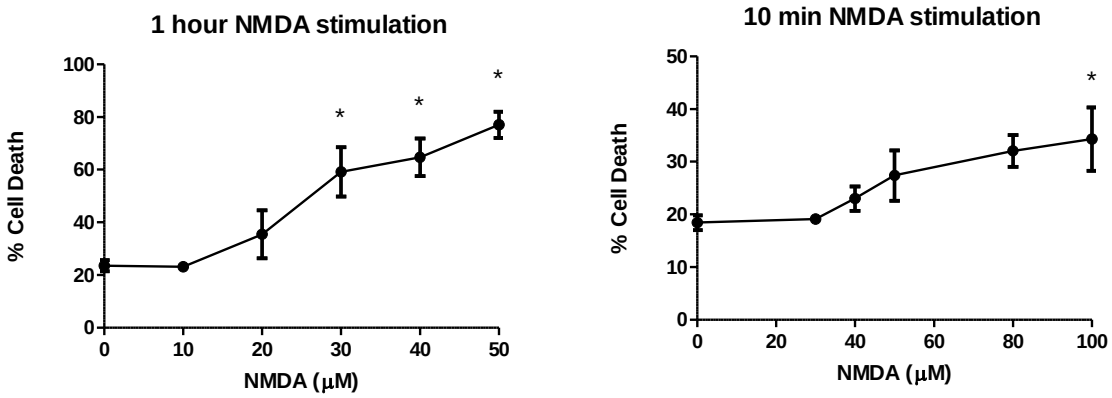

Supplemental figure 1. NMDA toxicity curves for (A) 1 hour or (B) 10 min stimulation of primary cortical neuronal cultures with different NMDA concentrations. Points represent the mean from multiple experiments (n=4 for (A) and n=3 for (B)). Error bars=SEM. *p<0.05 compared to the control, analysed with a one-way ANOVA with Dunnett's *post-hoc* test. Note the difference in the scale of the y axis in (A) and (B).

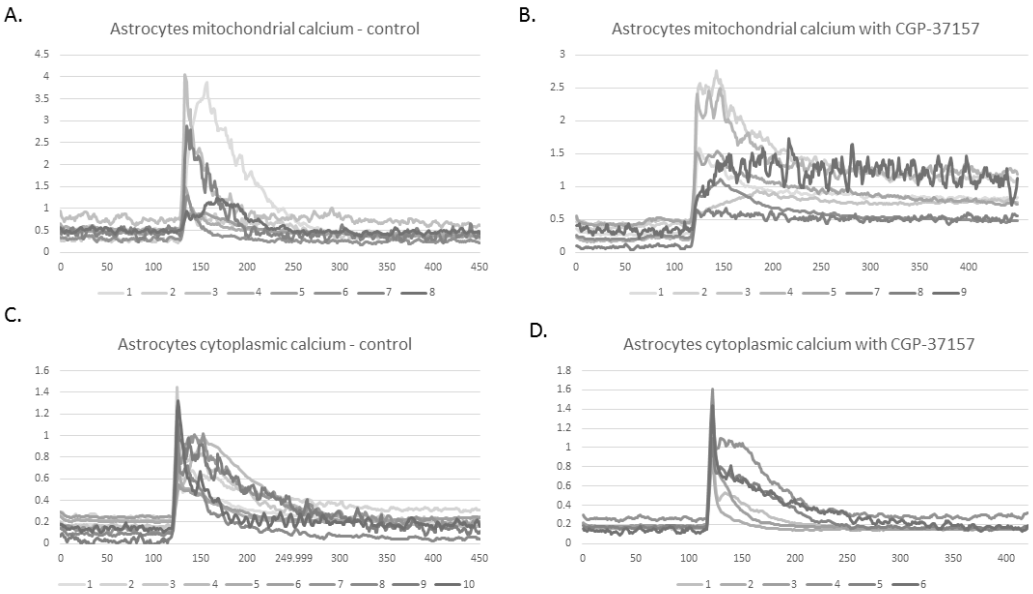

Supplementary figure 2. Example raw traces of Ca^{2+} decay following ATP application to astrocytes. A-B. Example traces of mitochondrial Ca^{2+} decay in astrocytes stimulated with ATP with (B) or without (A) CGP-37157 pre-stimulation (10 min). **C-D.** Example traces of cytoplasmic Ca^{2+} decay in control astrocytes (C) or astrocytes pre-treated with CGP-37157 (D). The traces in each graph represent single astrocytes on the same coverslip. The x-axis shows time (s). Recordings were taken every second, and a rolled average calculated every 5 seconds.

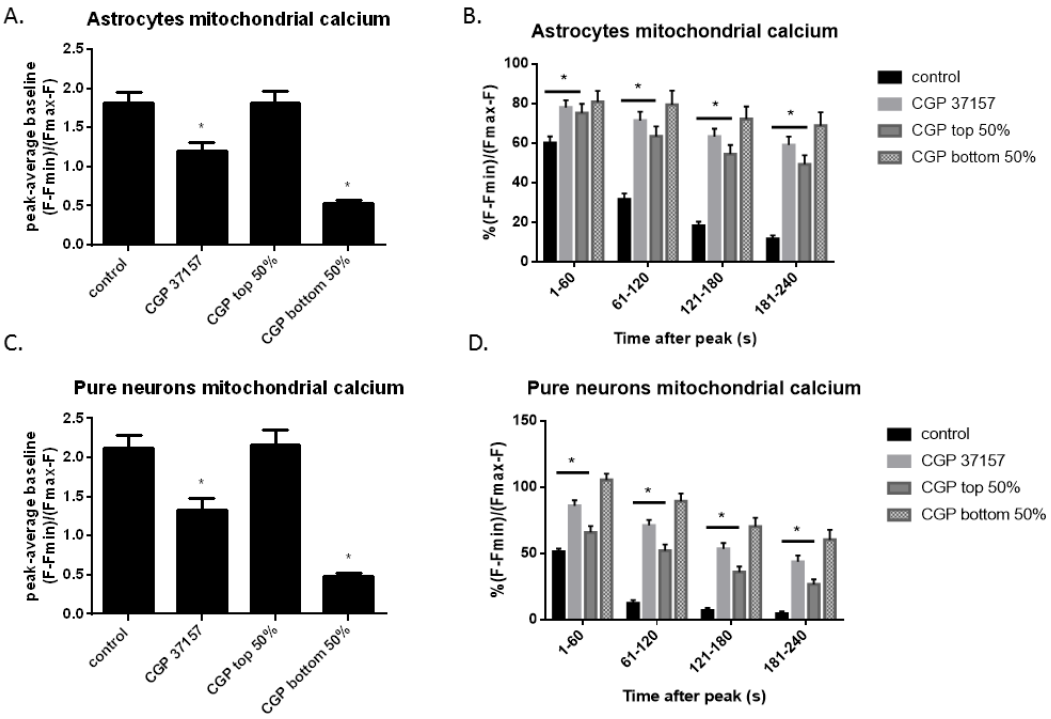

Supplementary figure 3. The amount of mitochondrial Ca^{2+} influx following stimulation of neural cells influences mitochondrial Ca^{2+} decay kinetics. A. Whilst there is lower amount mitochondrial Ca^{2+} influx following ATP stimulation of CGP-37157 treated astrocytes than in control astrocytes, the top 50% of CGP-37157 treated astrocytes according to their total mitochondrial Ca^{2+} influx have similar levels of total mitochondrial Ca^{2+} influx to control astrocytes. Unpaired two-tailed t-tests. *p≤0.05. p=0.0018 and p<0.0001, respectively. **B.** Although the top 50% of CGP-37157 pre-treated astrocytes displays faster mitochondrial Ca^{2+} decay kinetics following ATP stimulation than the total average of CGP-37157 pre-treated astrocytes, there is still a significant delay in mitochondrial Ca^{2+} decay compared to control astrocytes. Two-way ANOVA with Bonferroni *post-hoc* test. *p≤0.05. p=0.0106, then p<0.0001 for the rest. **C.** Same as (A), except neurons in astrocyte-free neuronal culture treated with high K^+. *p≤0.05. p=0.0005 and p<0.0001, respectively. **D.** Same as B, except neurons in astrocyte-free neuronal culture treated with high K^+. *p≤0.05. p=0.0044, then p<0.0001 for the rest.

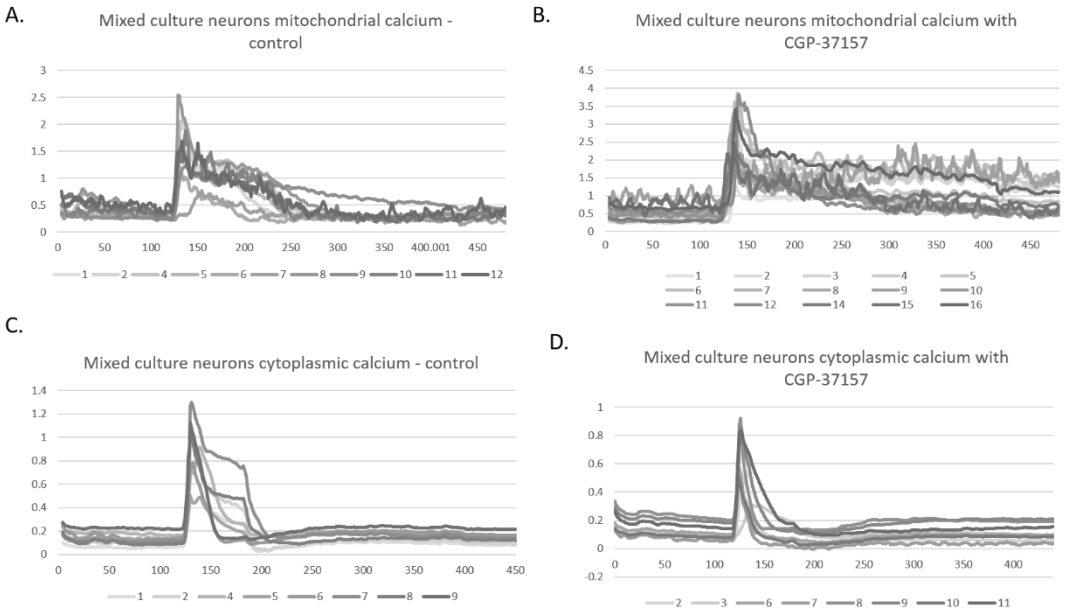

Supplementary figure 4. Example raw traces of Ca^{2+} decay following KCl application to neurons in a mixed culture. A-B. Example traces of mitochondrial Ca^{2+} decay in neurons stimulated with KCl with (B) or without (A) CGP-37157 present. **C-D.** Example traces of cytoplasmic Ca^{2+} decay following KCl-induced depolarisation of control neurons (C) or neurons pre-treated with CGP-37157 (D). The traces in each graph represent single neurons on the same coverslip. The x-axis shows time (s). Recordings were taken every second, and a rolled average was calculated every 5 seconds.

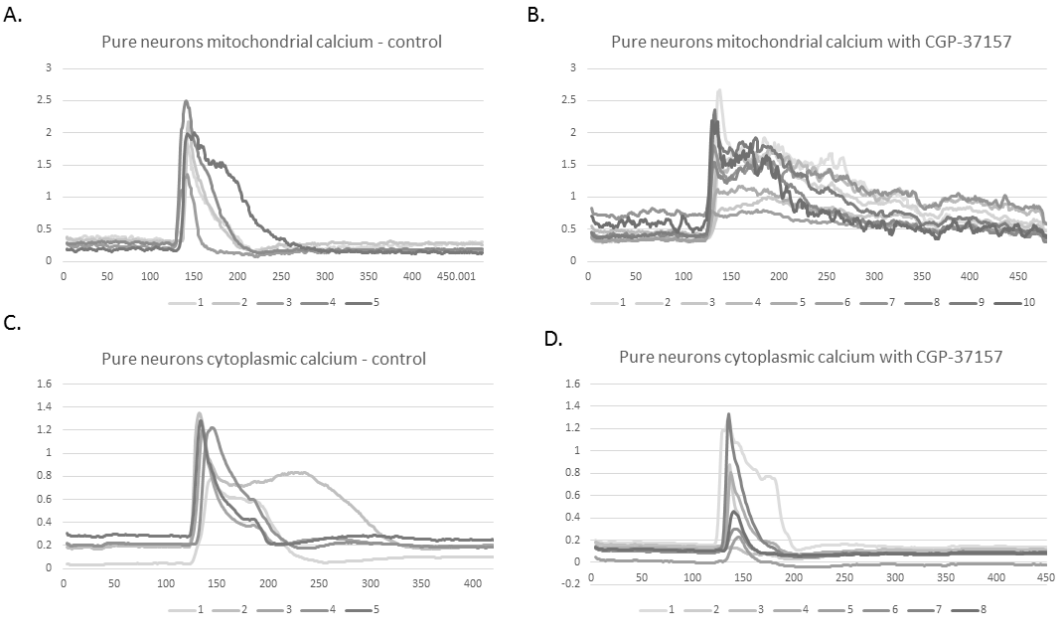

Supplementary figure 5. Example raw traces of Ca^{2+} decay following KCl application to neurons in an astrocyte-free neuronal culture. A-B. Example traces of mitochondrial Ca^{2+} decay in neurons stimulated with KCl with (B) or without (A) CGP-37157 present. **C-D.** Example traces of cytoplasmic Ca^{2+} decay following KCl-induced depolarisation in control neurons (C) or neurons pre-treated with CGP-37157 (D). The traces represent single neurons in astrocyte-free neuronal culture on the same coverslip. The x-axis shows time (s). Recordings were taken every second, and a rolled average was calculated every 5 seconds.

Ensemble gene ID	Gene name	Fold-induction by tBHQ (Mix)	p_{adj}-values
ENSMUSG00000020620	Abca8b	1.647771992	0.0000421
ENSMUSG00000032849	Abcc4	2.052724696	6.08E-16
ENSMUSG00000076435	Acsf2	1.58236664	9.74E-08
ENSMUSG00000039116	Adgrg6	1.535699232	0.008179017
ENSMUSG00000045875	Adra1a	1.560437013	0.025671195
ENSMUSG00000033715	Akr1c14	2.364852566	4.95E-13
ENSMUSG00000015134	Aldh1a3	1.541880181	0.000130289
ENSMUSG00000063558	Aox1	2.844437816	0.00000674
ENSMUSG00000037683	Armc3	1.515747116	0.04826957
ENSMUSG00000074892	B3galt5	1.811962751	0.0000127
ENSMUSG00000027381	Bcl2l11	1.675577971	0.0000494
ENSMUSG00000040466	Blvrb	2.49056564	1.09E-08
ENSMUSG00000022947	Cbr3	2.171760717	0.000000103
ENSMUSG00000070348	Ccnd1	1.529765761	0.000289206
ENSMUSG00000073802	Cdkn2b	1.930454405	0.009158467
ENSMUSG00000056501	Cebpb	2.181531906	0.005772088
ENSMUSG00000046818	Ddit4l	1.800405691	0.00000635
ENSMUSG00000038776	Ephx1	2.140991041	2.67E-37
ENSMUSG00000078161	Erich3	1.568707623	0.000381001
ENSMUSG00000022707	Gbe1	1.543835483	0.0000203
ENSMUSG00000032350	Gclc	1.98550662	2.03E-26
ENSMUSG00000028124	Gclm	2.272822126	6.44E-52
ENSMUSG00000049092	Gpr137c	1.535332048	0.0000281
ENSMUSG00000031584	Gsr	1.740832641	1.31E-17
ENSMUSG00000032348	Gsta4	2.063372676	3.62E-32
ENSMUSG00000058135	Gstm1	1.798422723	5.96E-36
ENSMUSG00000004038	Gstm3	1.97128279	0.029885617
ENSMUSG00000005413	Hmox1	9.367309395	7.45E-216
ENSMUSG00000022323	Hrsp12	1.568839801	5.09E-08
ENSMUSG00000041548	Hspb8	1.725879597	3.61E-10
ENSMUSG00000027070	Lrp2	1.688167405	0.001205087
ENSMUSG00000022324	Matn2	1.534955439	0.001462768
ENSMUSG00000054619	Mettl7a1	1.500366287	0.002425834

ENSMUSG00000008540	Mgst1	1.823180458	7.48E-15
ENSMUSG00000092274	Neat1	1.642970561	0.01840806
ENSMUSG00000003849	Nqo1	2.652431297	5.11E-10
ENSMUSG00000074063	Osgin1	13.78345543	5.51E-23
ENSMUSG00000049112	Oxtr	1.993355818	0.000172173
ENSMUSG00000031379	Pir	2.380511433	0.0000843
ENSMUSG00000021822	Plau	1.660325943	0.0280684
ENSMUSG00000028378	Ptgr1	1.727154326	0.009873294
ENSMUSG00000005716	Pvalb	1.537239228	0.039673796
ENSMUSG00000015846	Rxra	1.617530387	0.00000168
ENSMUSG00000050195	Scd4	1.81112659	0.000332861
ENSMUSG00000037762	Slc16a9	1.829158715	0.026845756
ENSMUSG00000028645	Slc2a1	1.682345448	9.95E-21
ENSMUSG00000025993	Slc40a1	2.432396268	0.000161414
ENSMUSG00000027737	Slc7a11 (xCT)	3.971487223	3.28E-77
ENSMUSG00000027227	Sord	1.536066166	0.00000319
ENSMUSG00000026532	Spta1	3.315431621	5.91E-11
ENSMUSG00000005803	Sqrdl	1.815976022	0.001275515
ENSMUSG00000032802	Srxn1	3.726150886	4.36E-117
ENSMUSG00000050315	Synpo2	1.513199417	0.00028744
ENSMUSG00000020250	Txnrd1	1.994064131	9.28E-42
ENSMUSG00000011171	Vipr2	2.604952682	7.85E-10

Supplemental table 1. List of the 55 Nrf2 target genes significantly induced ≥1.5-fold by tBHQ (8h) in mixed culture, but not in neuronal culture. The Ensembl ID, gene name, fold induction by tBHQ (10 µM, 8h), and the adjusted p value are shown for each gene. P_{adj} was calculated using DESeq2. n=3.

Ensemble gene ID	Gene name	Fold-induction by 4h Bic/4-AP (Neu)	p_{adj}-values
ENSMUSG00000045875	Adra1a	7.743697176	8.27E-09
ENSMUSG00000015134	Aldh1a3	2.445322021	2.23E-14
ENSMUSG00000027381	Bcl2l11	4.246634069	7.55E-36
ENSMUSG00000040466	Blvrb	5.256086205	2.94E-20
ENSMUSG00000070348	Ccnd1	1.857560079	0.00047168
ENSMUSG00000056501	Cebpb	4.452641531	2.1E-13
ENSMUSG00000032350	Gclc	2.368963465	4.36E-18
ENSMUSG00000049092	Gpr137c	2.702938458	1.17E-08
ENSMUSG00000041548	Hspb8	33.06669871	3.74E-17
ENSMUSG00000092274	Neat1	3.768743593	3.9E-32
ENSMUSG00000021822	Plau	3.184361283	0.0043157
ENSMUSG00000037762	Slc16a9	4.622607931	0.00676989
ENSMUSG00000028645	Slc2a1	4.964378601	4.33E-27
ENSMUSG00000025993	Slc40a1	3.406941281	1.05E-11
ENSMUSG00000027737	Slc7a11 (xCT)	3.251151851	4.07E-32
ENSMUSG00000032802	Srxn1	6.972804746	3.62E-78

Supplementary table 2. Some, but not all of the 55 tBHQ-induced Nrf2 target genes are upregulated following 4h Bic/4-AP treatment of pure neuronal culture. The Ensembl ID, gene name, fold induction by 4h Bic/4-AP in neuronal culture, and the adjusted p value are shown for each gene. P_{adj} was calculated using DESeq2. n=3.

Ensemble gene ID	Gene name	Fold-induction by 24h Bic/4-AP (Neu)	p_{adj}-values
ENSMUSG00000045875	Adra1a	43.628391	0.00217577
ENSMUSG00000027381	Bcl2l11	2.663623322	9.03E-07
ENSMUSG00000040466	Blvrb	4.344412769	4.17E-08
ENSMUSG00000070348	Ccnd1	2.477488506	0.00066831
ENSMUSG00000056501	Cebpb	2.864556509	0.00126478
ENSMUSG00000022707	Gbe1	2.005964912	0.00030995
ENSMUSG00000005413	Hmox1	9.316813788	4.3E-20
ENSMUSG00000041548	Hspb8	9.64344588	0.00051578
ENSMUSG00000092274	Neat1	3.760673316	2.65E-09
ENSMUSG00000021822	Plau	4.997294429	0.00039469
ENSMUSG00000037762	Slc16a9	16.28481285	6.75E-08
ENSMUSG00000028645	Slc2a1	3.361321276	4.77E-10
ENSMUSG00000025993	Slc40a1	5.956486946	9.05E-15
ENSMUSG00000027737	Slc7a11 (xCT)	3.533248065	3.19E-16
ENSMUSG00000027227	Sord	4.320112238	7.49E-12
ENSMUSG00000026532	Spta1	9.496404941	0.0000542
ENSMUSG00000032802	Srxn1	12.1584808	2.08E-79

Supplementary table 3. Some, but not all of the 55 tBHQ-induced Nrf2 target genes are upregulated following 24h Bic/4-AP treatment of pure neuronal culture. The Ensembl ID, gene name, fold induction by 24h Bic/4-AP in neuronal culture, and the adjusted p value are shown for each gene. P_{adj} was calculated using DESeq2. n=3.

Ensemble gene ID	Gene name
ENSMUSG00000020620	Abca8b
ENSMUSG00000032849	Abcc4
ENSMUSG00000076435	Acsf2
ENSMUSG00000039116	Adgrg6
ENSMUSG00000033715	Akr1c14
ENSMUSG00000063558	Aox1
ENSMUSG00000037683	Armc3
ENSMUSG00000074892	B3galt5
ENSMUSG00000022947	Cbr3
ENSMUSG00000073802	Cdkn2b
ENSMUSG00000046818	Ddit4l
ENSMUSG00000038776	Ephx1
ENSMUSG00000078161	Erich3
ENSMUSG00000028124	Gclm
ENSMUSG00000031584	Gsr
ENSMUSG00000032348	Gsta4
ENSMUSG00000058135	Gstm1
ENSMUSG00000004038	Gstm3

Ensemble gene ID	Gene name
ENSMUSG00000022323	Hrsp12
ENSMUSG00000027070	Lrp2
ENSMUSG00000022324	Matn2
ENSMUSG00000054619	Mettl7a1
ENSMUSG00000008540	Mgst1
ENSMUSG00000003849	Nqo1
ENSMUSG00000074063	Osgin1
ENSMUSG00000049112	Oxtr
ENSMUSG00000031379	Pir
ENSMUSG00000028378	Ptgr1
ENSMUSG00000005716	Pvalb
ENSMUSG00000015846	Rxra
ENSMUSG00000050195	Scd4
ENSMUSG00000005803	Sqrdl
ENSMUSG00000050315	Synpo2
ENSMUSG00000020250	Txnrd1
ENSMUSG00000011171	Vipr2

Supplementary table 4. List of the tBHQ-induced Nrf2 target genes not upregulated by Bic/4-AP treatment of pure neuronal culture. The Ensembl ID and gene name are shown for each gene. n=3.